

**The Identification and Characterisation of Novel
Proteins and Metabolic Signalling Pathways that
Regulate TRAIL-Induced Apoptosis**

Thesis Submitted for the degree of

Doctor of Philosophy

at the

University of Leicester

By

Gemma Louise Robinson (MSc Surrey)

MRC Toxicology Unit

September 2011

The Identification and Characterisation of Novel Proteins and Metabolic Signalling Pathways that Regulate TRAIL-Induced Apoptosis

By Gemma Robinson¹

¹MRC Toxicology Unit, University of Leicester, Hodgkin Building, PO BOX 138, Lancaster Rd, Leicester, LE1 9HN

TNF-related apoptosis inducing ligand (TRAIL) is a putative anti-cancer cytokine that is relatively specific for transformed cells however Mantle Cell Lymphoma (MCL) is resistant. TRAIL induces apoptosis through formation of a Death-Inducing Signalling Complex (DISC) and the successive activation of a caspase cascade. Therefore, the aims of this thesis were two-fold: firstly to examine the known and novel protein components of the DISC through mass spectrometry analysis and second to determine how cellular metabolism, specifically glucose-deprivation, influences TRAIL-induced apoptosis.

A tagged variant of TRAIL was used to capture the DISC from a TRAIL-sensitive MCL-derived cell line (Z138) allowing for its purification and subsequent proteomic analysis by mass spectrometry. From this study, it was found that the transferrin receptor (TFR1) may interact with the DISC, specifically with the TRAIL-receptors, where it potentially modulates TRAIL-induced apoptosis and/or receptor-mediated endocytosis. In addition, it was observed that the known DISC component FADD was present in sub-stoichiometric amounts compared to caspase-8 and this permitted the identification of a novel DISC structure based on caspase-8 chain formation. In parallel to this, glucose-deprivation studies were performed, which showed that, in the absence of glucose, Z138 cells was less sensitive to TRAIL-induced apoptosis. Furthermore, these cells also showed a reduced sensitivity to both ABT-737 and x-ray radiation. As a result, proteomic, ultra-structural and gene profiling studies were performed on Z138 cells cultured in the absence of glucose, which demonstrated a switch towards an anti-apoptotic/pro-survival phenotype.

Acknowledgements

Firstly, I would like to thank my supervisors Prof. Kelvin Cain and Prof. Marion MacFarlane for giving me the opportunity to undertake this research and supporting me over the last four years. I very much appreciate all the work you have done for me.

I am also extremely grateful to all past and present colleagues and friends in lab 416 for making my time at the MRC so memorable and for all the helpful discussion and advice you have given me. I would also like to thank Mrs. Rebekah Jukes-Jones for all her work and assistance with the mass spectrometry experiments, Mrs. Kate Dudek for the much need advice and discussions on the gene profiling studies and Dr. Lindsay Law for her help with the polysome profiling.

I would especially like to thank Dr. Michael Butterworth and Dr. Nick Harper for introducing me to The Clarendon - my second but favourite home, and Dr. Ian Powley for his kind advice and friendship over the last four years. I would also like to thank all of the friends I have made during my time in Leicester for giving me some of the best memories I have of my time here.

Finally, I would like to thank my family – Mum, Dad, Kerry, Hilly, Grandad (and in loving memory of my Nan) whose love, support and laughs over the years are so gratefully received. And last, but definitely not least, my partner Steve for being my best friend and my rock. Thank you x

	Page
Abstract.....	i
Acknowledgements.....	ii
Table of Contents.....	1
List of Figures.....	5
List of Tables.....	8
Abbreviations.....	9

Chapter 1

1.0 Introduction.....	12
1.1 Cancer.....	13
1.2 Apoptosis.....	14
1.2.1 Early discoveries of apoptosis.....	15
1.3 The caspases.....	16
1.3.1 The initiator caspases.....	17
1.3.2 The executioner caspases.....	18
1.4 Apoptotic pathways.....	19
1.4.1 The intrinsic pathway.....	20
1.4.2 The extrinsic pathway.....	22
1.5 TRAIL and its DISC.....	23
1.6 Metabolism and Cancer.....	27
1.6.1 Metabolic pathways in cancer.....	27
1.6.2 Inhibitors of energy metabolism.....	31
1.6.3 Glucose-deprivation and cancer metabolism.....	32
1.6.4 The AKT Pathway.....	36
1.6.5 Additional metabolic pathways.....	37
1.6.6 Hypoxia.....	39
1.7 Aims.....	40

Chapter 2

2.0 Materials and Methods.....	41
2.1 Materials.....	42
2.2 Methods.....	42
2.2.1 Cell lines and culture conditions.....	42
2.2.2 Induction of apoptosis.....	43
2.2.3 Measurement of cell death.....	44
2.2.4 Analysis of cytochrome c release by confocal microscopy.....	45

2.2.5	Analysis of cytochrome <i>c</i> release by immunoblotting.....	45
2.2.6	Analysis of hexokinase detachment from the mitochondria.....	46
2.2.7	Preparation of cell lysates.....	46
2.2.8	Protein expression.....	46
2.2.9	TRAIL-receptor surface expression.....	46
2.2.10	Protein concentration.....	47
2.2.11	Immunoblotting.....	47
2.2.12	Coomassie-blue staining.....	48
2.2.13	Generation and purification of recombinant TRAIL.....	48
2.2.14	Biotinylation of TRAIL.....	49
2.2.15	TRAIL DISC isolation.....	49
2.2.16	Measurement of TRAIL DISC activity.....	49
2.2.17	Mass Spectrometry.....	50
2.2.18	Glycosidase treatment.....	51
2.2.19	Extracellular Flux (XF) analysis.....	51
2.2.20	ATP measurements.....	52
2.2.21	Subcellular fractionation.....	52
2.2.22	Electron microscopy.....	52
2.2.23	Microarray analysis.....	53
2.2.24	Polysome profiling.....	54

Chapter 3

3.0	Proteomic Analysis of the TRAIL Death-Inducing Signalling Complex.....	55
3.1	Introduction.....	56
3.2	Results.....	58
3.2.1	Characterisation of the mantle cell lymphoma cell line Z138....	58
(i)	Z138 cells display a concentration- and time-dependent sensitivity to TRAIL.....	58
(ii)	Z138 cells rapid cleavage of Bid and subsequent loss of mitochondrial membrane potential when treated with TRAIL.....	59
(iii)	Cytochrome <i>c</i> release from the mitochondria correlates with loss of mitochondrial membrane potential.....	60
(iv)	Cellular levels of pro- and anti-apoptotic proteins in Z138 cells.....	62
(v)	Z138 cells express both TRAIL-R1 and -R2 on their surface....	63
(vi)	Optimisation of TRAIL DISC formation in Z138 cells.....	64
(vii)	TRAIL-R1 but not TRAIL-R2 is glycosylated in Z138 cells.....	67

3.2.2 Isolation and mass spectrometry analysis of the Z138 TRAIL DISC.....	71
(i) Isolation of the Z138 TRAIL DISC.....	71
(ii) Mass spectrometry analysis of the Z138 TRAIL DISC.....	72
(iii) Label-free quantitative analysis of the mass spectrometry data.....	74
(iv) Critical analysis of the potential DISC interactors.....	77
(v) The transferrin receptor precipitates with the Z138 TRAIL DISC.....	81
(vi) Cullin-3 does not associate with the soluble TRAIL DISC in Z138 cells.....	83
(vii) Stoichiometry of the TRAIL DISC.....	83
3.3 Discussion.....	84
3.3.1 Characterisation of the Z138 cell line.....	85
3.3.2 Proteomic analysis of the Z138 TRAIL DISC.....	86

Chapter 4

4.0 The metabolic regulation of TRAIL-induced apoptosis.....	89
4.1 Introduction.....	90
4.2 Results.....	92
4.2.1 2DG reduces glycolytic flux and sensitises Z138 cells to TRAIL-induced apoptosis.....	92
4.2.2 Acute glucose-deprivation sensitises cells to TRAIL-induced apoptosis but only before they become acclimatised.....	97
4.2.3 Chronic glucose-deprivation brings about a switch in bioenergetics and reduces the sensitivity of cells to apoptotic stimuli.....	100
4.2.4 Z138 cells cultured in glucose-free media have impaired DISC signalling.....	104
4.2.5 TRAIL-receptor glycosylation is not impaired under conditions of glucose-deprivation.....	107
4.2.6 Activation of the intrinsic pathway is also impaired under glucose-free conditions.....	108
4.2.7 Isoalted mitochondria from glucose-free Z138 cells exhibit increased cytochrome c levels and cristae density.....	111
4.3 Discussion.....	113
4.3.1 2DG reduces glycolytic flux and 'primes' a cell for death.....	114

4.3.2 Chronic glucose-deprivation mediates a switch in bioenergetics and a reduction in sensitivity to apoptotic stimuli.....	115
4.3.3 The metabolic switch in glucose-free cells leads to mitochondrial proteomic and structural remodelling.....	116

Chapter 5

5.0 Transcriptional and Translational profiling of glucose-deprived Z138 cells.....	119
5.1 Introduction.....	120
5.2 Results.....	122
5.2.1 Gene expression analysis of glucose-free Z138 cells.....	122
5.2.2 Gene expression changes suggest a susceptibility toward an anti-apoptotic/pro-survival phenotype.....	127
5.2.3 Key metabolic genes are altered under conditions of glucose-deprivation.....	131
5.2.4 Evidence for the activation of the AKT signalling pathway in glucose-free cells.....	134
5.2.5 An increase in mitochondrial-bound hexokinase II appears not to correlate with the anti-apoptotic phenotype of glucose-free cells.....	137
5.2.6 Polysome profiling of glucose-free and 2DG treated Z138 cells suggest differential effects on translation efficiency.....	138
5.2.7 Profiling of mantle cell lymphoma (MCL) patients samples.....	141
5.3 Discussion.....	145

Chapter 6

6.0 Final Discussion.....	150
6.1 Overview.....	151
6.2 TRAIL and its signalling complex.....	151
6.3 Metabolic regulation of cancer.....	154
6.4 Future Work.....	157

Publications	158
Appendix 1	159
Appendix 2	160
References	161

Chapter 1 - Introduction

Figure 1.1 Morphological features of apoptosis versus necrosis.....	15
Figure 1.2 The evolutionarily conserved cell death proteins.....	16
Figure 1.3 The initiator caspases.....	17
Figure 1.4 The executioner caspases.....	19
Figure 1.5 The intrinsic pathway.....	21
Figure 1.6 The known components of the DISC.....	22
Figure 1.7 Schematic of the five TRAIL-receptors.....	24
Figure 1.8 The extrinsic pathway.....	25
Figure 1.9 The glycolytic pathway in cancer cells.....	28
Figure 1.10 An overview of the PI3K/AKT pathway.....	36
Figure 1.11 An overview of the biosynthetic pathways in tumour cells.....	38

Chapter 3 – Proteomic analysis of the TRAIL Death-Inducing Signalling Complex

Figure 3.1 Z138 cells display a concentration- and time-dependent sensitivity to TRAIL.....	59
Figure 3.2 Z138 cells display a rapid cleavage of Bid and subsequent loss of mitochondrial membrane potential when treated with TRAIL.....	60
Figure 3.3 Cytochrome c release from the mitochondria correlates with loss of mitochondrial membrane potential.....	61
Figure 3.4 The expression levels of pro- and anti-apoptotic proteins.....	62
Figure 3.5 Z138 cells express both TRAIL-R1 and -R2 on their surface.....	64
Figure 3.6 Optimisation of DISC formation using bTRAIL.....	66
Figure 3.7 Comparison of isolated TRAIL DISC complexes from BJAB, Jurkat and Z138 cells.....	67
Figure 3.8 TRAIL-R1 in Z138 cells has an additional higher molecular weight band than the expected 50 kDa band.....	68
Figure 3.9 Treatment with endoglycosidase enzymes alters the molecular weight of TRAIL-R1 but not TRAIL-R2, FADD or caspase-8.....	70
Figure 3.10 Amino acid sequence of TRAIL-R1.....	70
Figure 3.11 Isolation of the TRAIL DISC from Z138 cells for mass spectrometry analysis.....	72
Figure 3.12 Quantitative proteomic analysis of proteins identified by mass spectrometry.....	77
Figure 3.13 Peptide sequences and spectra for known TRAIL DISC components.....	78

Figure 3.14 Peptide sequences and spectra for unknown potential TRAIL DISC components.....	80
Figure 3.15 The transferrin receptor but not PP1 α / γ or DEK precipitate with the Z138 TRAIL DISC.....	82
Figure 3.16 Cullin-3 is not a component of the TRAIL DISC complex in haemopoietic cell lines.....	83
Figure 3.17 Quantitative proteomic analysis reveals a new stoichiometry of the TRAIL DISC components	84

Chapter 4 – The metabolic regulation of TRAIL-induced apoptosis

Figure 4.1 Inhibition of glucose metabolism with 2DG significantly reduces glycolytic flux and ATP levels.....	93
Figure 4.2 2DG inhibition of glycolysis sensitises Z138 cells to TRAIL-induced apoptosis.....	95
Figure 4.3 Incubation of cells with 2DG results in the down regulation of key pro- and anti-apoptotic proteins.....	96
Figure 4.4 Acute (1 h) glucose-deprivation sensitises cells to TRAIL but through necrotic cell death rather than apoptotic.....	98
Figure 4.5 Acute (20h) glucose-deprivation significantly reduces glycolytic flux whilst maintaining ATP levels concomitant with a loss in sensitivity to TRAIL-induced apoptosis.....	99
Figure 4.6 Prolonged glucose-deprivation brings about a switch in bioenergetics from aerobic glycolysis to oxidative phosphorylation.....	102
Figure 4.7 Z138 cells cultured in glucose-free media reveal a concentration- and time-dependent loss in sensitivity to TRAIL.....	103
Figure 4.8 Protein expression levels of key pro- and anti-apoptotic proteins do not display changes associated with the loss in sensitivity to TRAIL.....	104
Figure 4.9 Z138 cells cultured in the absence of glucose have reduced surface expression levels of TRAIL-R1/-R2 and form less active DISC.....	105
Figure 4.10 Z138 cells signal to apoptosis through TRAIL-R1 only.....	106
Figure 4.11 TRAIL-receptor glycosylation is not impaired under conditions of glucose deprivation.....	107
Figure 4.12 Activation of the mitochondrial amplification loop is impaired under glucose-free conditions.....	108
Figure 4.13 Key pro- and anti-apoptotic proteins involved in the mitochondrial amplification loop.....	109

Figure 4.14 Z138 cells cultured in glucose-free media are less sensitive to intrinsic death stimuli.....	110
Figure 4.15 The isolation and subcellular analysis of purified mitochondria further display the key changes observed with Bax, Bcl-2 and Cytochrome c.....	112
Figure 4.16 Z138 cells cultured in the absence of glucose have more mitochondria and increased cristae density.....	113
Figure 4.17 Scheme to show how metabolic changes induced by 2DG and glucose deprivation modulate the apoptotic proteins and TRAIL-induced cell death.....	118

Chapter 5 – Transcriptional and translational profiling of glucose-deprived Z138 cells

Figure 5.1 The gene expression profile of glucose-free Z138 cells.....	122
Figure 5.2 The relative proportion of each distinct functional group.....	126
Figure 5.3 Schematic to show how gene expression changes confer an anti-apoptotic/pro-survival phenotype in glucose-free cells.....	130
Figure 5.4 SDHA is increased under conditions of glucose-deprivation.....	131
Figure 5.5 PPM2C gene expression is reduced under glucose-free conditions.....	132
Figure 5.6 PGM3 protein expression is increased under glucose-free conditions.....	133
Figure 5.7 Protein expression analyses of the AKT pathway and its downstream targets.....	135
Figure 5.8 Pre-incubation of glucose-free cells with methyl jasmonate does not re-sensitise them to TRAIL-induced apoptosis.....	138
Figure 5.9 Polysome profiling of Z138 cells cultured with (+) or without (-) glucose.....	139
Figure 5.10 Polysome profiling of Z138 cells treated with or without 2DG.....	140
Figure 5.11 Characterisation of patient MCL samples.....	142
Figure 5.12 Subcellular fractionation analysis of an MCL patient samples.....	144

Chapter 6 – Final Discussion

Figure 6.1 Overview of research findings.....	153
---	-----

Page**Chapter 1 - Introduction**

Table 1.1 An overview of research papers examining the role of glucose deprivation in apoptotic signalling.....	35
---	----

Chapter 2 – Materials and Methods

Table 2.1 Primary antibodies used for immunoblotting.....	47
Table 2.2 Secondary antibodies used for immunoblotting.....	48

Chapter 3 – Proteomic analysis of the TRAIL Death-Inducing Signalling Complex

Table 3.1 Outline of the criteria for analysis of protein hits.....	73
Table 3.2 List of proteins identified by mass spectrometry of the Z138 TRAIL DISC...	75

Chapter 5 – Transcriptional and translational profiling of glucose-deprived Z138 cells

Table 5.1 Gene expression changes cluster into distinct functional groups.....	123
--	-----

Abbreviations

ALPS	Autoimmune Lymphoproliferative Syndrome
Annexin V	Annexin-V FITC
Apaf-1	Apoptosis Protease Activating Factor – 1
AP1	Activator protein 1
Bak	Bcl-2 homologous antagonist/killer
Bax	Bcl-2–associated X protein
Bcl-2	B-cell lymphoma 2
Bcl-X _L	Basal cell lymphoma-extra large
BH	Bcl-2 homology domains
Bid	BH3 interacting domain death agonist
BSA	Bovine Serum Albumin
bTRAIL	Soluble biotinylated TRAIL
CapLC	Micro-capillary high performance liquid chromatography
CARD	Caspase Activation and Recruitment Domain
Caspase	Cystein-dependent aspartyl specific protease
<i>C. Elegans</i>	<i>Caenorhabditis Elegans</i>
Ced	Cell Death Abnormality
cFLIP _{L/S}	Cellular Flip _{Long/Short} isoforms
CLL	Chronic Lymphocytic Leukemia
CRD	cysteine-rich domain
DD	Death Domain
DED	Death Effector Domain
DISC	Death Inducing Signalling Complex
DMEM	Dulbecco's Modified Essential Medium
DMSO	Dimethyl Sulphoxide
ECAR	Extracellular Acidification Rate
ECL	Enhanced Chemiluminescence
EDTA	Ethylenediaminetetraacetic Acid
ETR1	Mapatumumab
ETR2	Lexatumumab
FACS	Fluorescence Activated Cell Sorter
FADD	Fas-associated Death Domain protein
FAO	Fatty Acid Oxidation
FCCP	Carbonyl cyanide-p-trifluoromethoxyphenylhydrazone
FITC	Fluorescein isothiocyanate
FSC	Forward Scatter Channel

HRP	Horseradish peroxidase
IAP	Inhibitor of Apoptosis Protein
ICE	Interleukin-1- β -Converting Enzyme
IETD.afc	Acetyl-Lle-Glu-Thr-Asp-7-amino-4-trifluoromethylcoumarin
IPTG	Isopropyl β -D-1-thiogalactopyranoside
HEPES	(4-(2-hydroxyethyl)-1-piperazineethanesulfonic acid)
LC-MS/MS	Liquid chromatography tandem mass spectrometry
MCL	Mantle Cell Lymphoma
MOMP	Mitochondrial Outer Membrane Permeabilisation
mg	milligram
NF- κ B	nuclear factor kappa-light-chain-enhancer of activated B cells
ng	nanogram
NOXA	Phorbol-12-myristate-13-acetate-induced protein 1
NSAF	Normalised spectral abundance factor
OCR	Oxygen Consumption Rate
OMM	Outer Mitochondrial Membrane
OPG	Osteoprotegerin
p53	Tumor Protein 53
PAGE	Polyacrylamide Gel Electrophoresis
PBS	Phosphate Buffered Saline
PE	Phycoerythrin
PI	Propidium Iodide
PS	Phosphatidylserine
PUMA	p53 Up regulated Modulator of Apoptosis
Q-TOF	Quadrupole time of flight
RIP	Receptor Interacting Protein
RPMI	Roswell Park Memorial Institute
SAF	Spectral abundance factor
SDS	Sodium Dodecyl Sulphate
SEM	Standard Error of Mean
tBID	truncated BID
TEMED	Tetramethylethylenediamine
TNF	Tumor Necrosis Factor
TNF-R1	Tumor Necrosis Factor Receptor 1
TRAF	TNF receptor-associated factor
TRAIL	TNF-related Apoptosis Inducing Ligand
TRAIL-R1	TRAIL Receptor 1 (DR4)

TRAIL-R2	TRAIL Receptor 2 (DR5)
TRAIL-R3	TRAIL Receptor 3 (DcR1)
TRAIL-R4	TRAIL Receptor 4 (DcR2)
TMRE	Tetramethylrhodamine, ethyl ester, perchlorate
Z138	Mantle Cell Lymphoma cell line
UT	Untreated
µg	microgram
µl	microlitre
WT	Wildtype
zVAD.fmk	Carbobenzoxy-Val-Ala-Asp-(O-methyl)-fluoromethylketone

1. Introduction

1.1 Cancer

Cancer, an abnormal growth of cells, is the second leading cause of death worldwide and is projected to affect greater than 11 million people in 2030 (WHO, 2008). It is evident, therefore, that the global burden of cancer is increasing and, thus, improvements are required in both the prevention and treatment of cancer (reviewed in Jemal *et al*, 2011). Cancers originate from alterations in a single cell as a result of exposure to external agents and/or inherited genetic factors. These cells exhibit uncontrolled proliferation and thus grow beyond their usual cellular boundaries, invading adjacent cells and sometimes metastasising to other areas of the body. The term cancer is broadly used for a collection of diseases, which are classified according to the type of cell from which the cancer originates. One type of cancer, termed lymphoma or lymphoid leukaemia, originates from haematopoietic cells and covers a broad range of cancers of the blood. The World Health Organisation (WHO) classification of more than 43 different types of lymphoma attempts to group these cancers according to their cell type i.e. B, T or NK cells (Jaffe *et al*, 2001; Swerdlow *et al*, 2008). A subtype of B-cell lymphoma known as Mantle Cell Lymphoma (MCL) accounts for approximately 5% of all non-hodgkin lymphomas (Goy and Kahl, 2010) and is one of the most difficult incurable B-cell lymphomas with a patient's life expectancy of only 5-7 years (Pérez-Galán *et al*, 2010). MCL is proposed to originate from naïve, pre-germinal centre lymphocytes in the mantle zone of lymph nodes (Pérez-Galán *et al*, 2010) although some studies suggest that a small subset of MCL show evidence of exposure to a germinal-centre environment (Thelander and Rosenquist, 2008). MCL is also associated with, and characterised by, the presence of a gene translocation specifically t(11;14)(q13;q32) (Weisenburger and Armitage, 1996; Thelander *et al*, 2008). This translocation involves the movement of the cyclin D1 gene, on chromosome 11, to the enhancer region of the immunoglobulin (Ig) heavy-chain locus (14q32), which leads to the over expression of cyclin D1 (Thelander *et al*, 2008). Cyclin D1 is a key regulator of the cell cycle and its over expression facilitates the progression of cells through G1 to S phase and thus has been linked to the development of cancer (reviewed in Jares *et al*, 2007). This translocation distinguishes it from other types of lymphoma, which also exhibit gene translocations. For example, follicular lymphoma is caused by a translocation between the bcl-2 gene and Ig heavy locus resulting in a significant loss in sensitivity to apoptotic stimuli (Tsujiimoto *et al*, 1984). Burkitt's lymphoma is also characterised by a gene translocation involving c-myc and the Ig heavy locus (Yustein and Dang, 2007).

MCL is incurable with current frontline chemotherapy therapies (aside from stem cell transplantation), which includes CHOP (high-dose cyclophosphamide, vincristine, doxorubicin and prednisone), hyper-CVAD (hyperfractionated cyclophosphamide, vincristine, doxorubicin and dexamethasone) and Ara-C (cytarabine) combined with rituximab (Jares *et al*, 2007; Ogura, 2010). Despite these aggressive treatment approaches, there is still no cure and, therefore, there is clearly a requirement for a more novel targeted treatment approach. Although new treatment regimens are emerging, including proteasome, mTOR and HDAC inhibitors (Goy and Kahl, 2010), current opinions suggest that these will only improve long-term outcomes and will not cure the disease (Williams *et al*, 2011). Therefore, understanding the pathways that promote and/or regulate MCL could aid in establishing more successful therapeutic agents for targeting this disease. Similarly, determining the underlying cause of the resistance of these cells to primary treatments would also aid this process.

1.2 Apoptosis

The term apoptosis was first introduced by Kerr and colleagues who described a form of cell death that differed notably from the previously accepted form of cell death known as necrosis (Kerr *et al*, 1972). Cells were observed to die in a distinct morphological manner, which unlike necrosis did not result in an inflammatory response (Fig. 1.1). In contrast, apoptotic cells advance through an active, orderly sequence of structural changes that demonstrate a form of cell suicide through which embryonic development (Brill *et al*, 1999), the immune system (Feig and Peter, 2007) and normal cell turnover (Ellis *et al*, 1991) are regulated. Apoptotic cells are characterised morphologically by a number of recognisable features including nuclear condensation and fragmentation, membrane blebbing and the formation of apoptotic bodies (Fig. 1.1) (Kerr *et al*, 1972).

Apoptosis allows for the elimination of a large number of cells that are no longer required without affecting adjacent cells/tissues. The number of cells in a multi-cellular organism are therefore tightly regulated by both the rate of cell division (mitosis) and the rate of cell death (apoptosis). Thus, it is not surprising that since its discovery, apoptosis has been at the forefront of scientific research since a deregulation in this equilibrium can lead to the development of a number of pathological conditions including neurodegeneration, autoimmune disease and cancer.

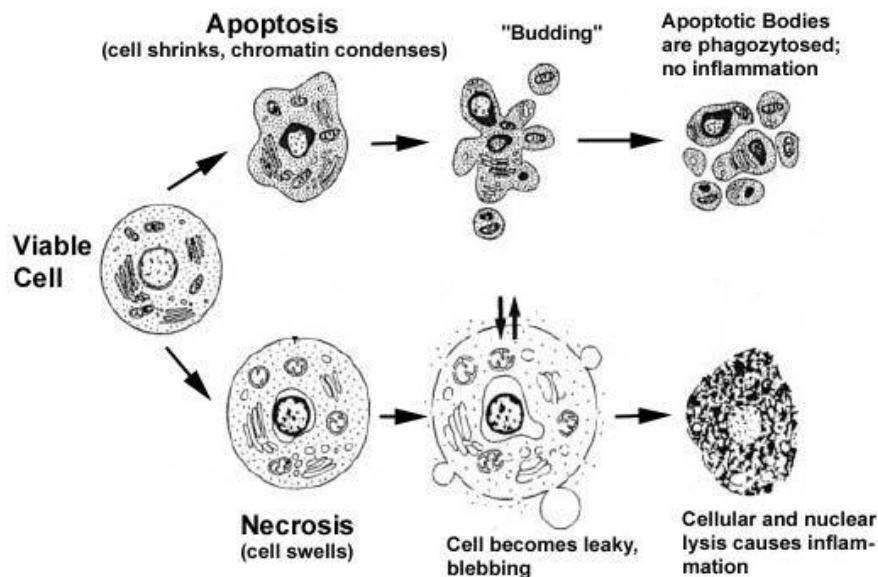


Figure 1.1 Morphological features of apoptosis versus necrosis. Apoptotic cells are characterised morphologically by a number of recognisable features including cell shrinkage, nuclear condensation and membrane blebbing ('budding'). Necrosis, on the other hand, is a passive form of uncontrolled degradation characterised by cellular swelling and rupture. Necrosis does not, unlike apoptosis, result from a predetermined pro-enzyme pathway. Image taken from Cruchten and Van Den Broeck, 2002.

1.2.1 Early discoveries of apoptosis

Major insights into the understanding of apoptosis stem from the study of programmed cell death (PCD) in less complex organisms such as the nematode worm, *Caenorhabditis Elegans* (reviewed in Ellis *et al*, 1991 and Lettre and Hengartner, 2006). Sulston and colleagues explored how 131 of the worm's 1090 cells died by PCD as it matured and further observed that these specific cells always die (Sulston and Horvitz, 1977; Kimble and Hirsh, 1979; Sulston *et al*, 1983). Therefore, in order to identify genes regulating the controlled cell death observed in these cells, mutational studies were subsequently carried out. These studies identified the absolute requirement of two genes, *ced-3* and *ced-4*, for successful PCD (Ellis and Horvitz, 1986). Successive studies found a further two genes: *ced-9*, which acts to prevent cell death (Hengartner *et al*, 1991) and *egl-1*, which acts as an inhibitor of inhibitors by blocking the function of the *ced-9* protein (Conradt and Horvitz, 1998) (Fig. 1.2). The controlled cellular deletion observed in *C. Elegans* demonstrated similar characteristics to the structured cell death observed in their mammalian counterparts and hence the function of these genes can and have been extrapolated in order to identify their evolution into more complex, higher order animals (Fig. 1.2). Sequence comparison of the *ced-3* protein found similarities to the human interleukin-1 β (IL-1 β)-converting enzyme (ICE) (Yuan *et al*, 1993); a previously identified cysteine protease (Cerretti *et al*, 1992; Thornberry *et al*, 1992) later noted to have apoptotic inducing properties when over-expressed (Gagliardini *et al*, 1994). These observations prompted the

search for other ICE-like proteases leading to the identification of a further ten related human proteins subsequently designated the ‘caspases’ (reviewed in Cohen, 1997; Pop and Salvesen, 2009). Similarly, the *ced-4* homolog Dark (also known as dAPAF) and the *ced-3* homologs Dronc and Drice in the fruitfly (*Drosophila melanogaster*) correlate with cell death pathways in both the nematode and mammals (Fig. 1.2) and thus the fruitfly is also used as a model for examining PCD (reviewed in Ryoo and Baehrecke, 2010).

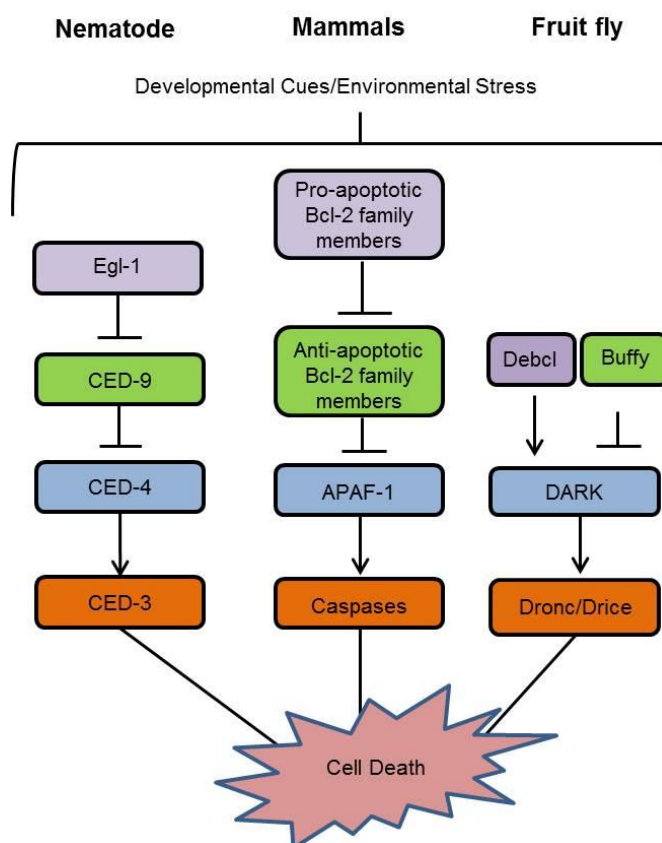


Figure 1.2 The evolutionarily conserved cell death proteins. The nematode shows direct homology with several human cell death pathway proteins including BH3-only proteins (Egl-1), Bcl-2 (Ced-9), Apaf-1 (Ced-4) and the proteolytic caspases (Ced-3). The homology with drosophila is less clear nevertheless they express key variants of Bcl-2 family members (Debc1/Buffy), Apaf-1 (DARK) and caspases (Dronc/Drice). Image modified from Riedl and Shi, 2004.

1.3 The Caspases

The majority of morphological changes observed during apoptosis are initiated by a large family of protein mediators known as the caspases: aspartate-specific cysteine proteases (Alnemri *et al*, 1996; reviewed in Fuentes-Prior and Salvesen, 2004). To date at least ten human caspases have been identified seven of which are likely to be directly involved in apoptosis (Cohen, 1997). All human caspases comprise a common pentapeptide active-site motif: QACXG (where X is R, Q or G) (Fig. 1.3), which

contains the 'active' cysteine residue at its centre (Wilson *et al*, 1994; Fuentes-Prior and Salvesen, 2004). Once activated, the caspases cleave cellular substrates by recognising a specific tetrapeptide sequence site denoted P_4 , P_3 , P_2 , P_1 where P_1 represents a highly conserved aspartate residue (Talanian *et al*, 1997; Thornberry *et al*, 1997; Stennicke *et al*, 2000). Thus, aside from their gene family similarities, caspases can be further defined by, for example, their conserved catalytic domains and/or substrate recognition patterns. Accordingly, subsequent work divided the apoptotic-inducing caspases into two distinct families: the initiator caspases and the effector caspases, depending on their *in vivo* role and sequence similarities.

1.3.1 The initiator caspases

The initiator caspases-8, -9 and -10 contain long pro-domains (Fig. 1.3) and exist in the cell as inactive monomers, which require recruitment to adaptor molecules, dimerisation and, in the case of caspase-8, cleavage to become activated (Boatright *et al*, 2003; Boatright and Salvesen, 2003; Hughes *et al*, 2009). Depending on the stimulus, activation occurs firstly through proximity-driven dimerisation at specific multi-protein activating complexes followed by proteolytic cleavage (reviewed in Boatright and Salvesen, 2003).

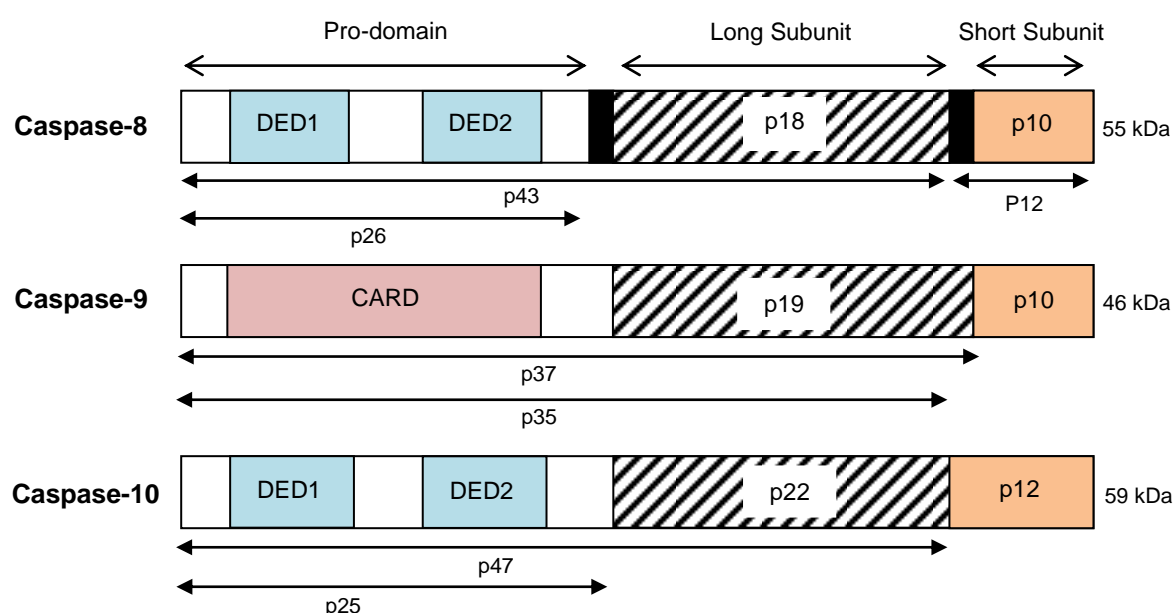


Figure 1.3 The Initiator Caspases. Caspases-8, -9 and -10 exist in the cell as single chain proenzymes comprising an N-terminal peptide (pro-domain), a long subunit (striped fill) and a small subunit (orange fill), which are occasionally separated by a linker (black fill). The N-terminal domain contains the sequence of amino acid that are paramount for activation at signalling complexes, which include the DED's (blue) in caspase-8 and -10 and the CARD (pink) in caspase-9. These caspases require dimerisation and cleavage at specific multi-protein complexes to become active.

The initiator caspase: caspase-8 was first identified through its association with the TNF-death receptor family member CD95 and is present within the cell as pro-enzyme monomers (Fig. 1.3) (Kischkel *et al*, 1995; Muzio *et al*, 1996). At least eight different isoforms of caspase-8 have been identified, the most abundant being caspase-8a (55 kDa) and caspase-8b (53 kDa) (Scaffidi *et al*, 1997). Both of these isoforms are recruited to and activated at the Death Inducing Signalling Complex (DISC) following activation of the extrinsic pathway of apoptosis (see section 1.4). In addition to the recruitment of caspase-8, it has been observed that the initiator caspase: procaspase-10, an ortholog of caspase-8, can also be recruited into the DISC and is able to process the executioner caspases (reviewed in Boatright and Salvesen, 2003). Caspase-10 was first identified through its sequence similarity to the executioner caspase: caspase-3 (see section 1.3.2) and encodes a 479-amino acid protein of approximately 59 kDa (Fig. 1.3) (Fernandes-Alnemri *et al*, 1996). Similar to caspase-8 in structure, it exists as single chain proenzyme containing two *N*-terminal DEDs, which allow for its recruitment to the DISC. However, the ability of caspase-10 to functionally substitute for caspase-8 in the DISC is controversial (Kischkel *et al*, 2001; Sprick *et al*, 2002). Humans containing a mutant version of caspase-10 have, however, been shown to exhibit autoimmune lymphoproliferative syndrome (ALPS) indicative of a vital role of functional caspase-10 in apoptotic signalling (Wang *et al*, 1999).

The initiator caspase: caspase-9, similar to caspase-8 and -10, contains a long pro-domain and was originally identified through sequence comparison to the executioner caspase: caspase-7 (Fig. 1.3) (Duan *et al*, 1996). It is synthesised as a 46 kDa procaspase monomer and contains, in its *N*-terminal domain, a caspase recruitment domain (CARD) as opposed to DEDs (Fig. 1.3). The CARD allows for the recruitment and activation of caspase-9 at a multi-protein activating complex known as the apoptosome (see section 1.4) (Acehan *et al*, 2002; Cain *et al*, 2002).

1.3.2 The executioner caspases

In contrast to the initiator caspases, the executioner caspases have short pro-domains and exist in the cell as dimeric zymogens, which require limited proteolytic cleavage by the initiator caspases to become active (Fig. 1.4) (reviewed in Boatright and Salvesen, 2003). Similar to previously discussed caspases, caspase-3 was first identified through its sequence homology to the nematode 'caspase' Ced-3 (Fernandes-Alnemri *et al*, 1994) and was later identified as a key apoptotic protease involved in the dismantling of a cell (Nicholson *et al*, 1995). It is present as a 32 kDa protein comprised of a short pro-domain along with p17 and p12 long and short subunits respectively (Fig. 1.4)

(Kumar, 1997). Caspase-3, unlike the initiator caspases, exists as a proenzyme dimer, which requires only limited proteolytic processing in the linker-region followed by rearrangement to become active (reviewed in Pop and Salvesen, 2009). This is in stark contrast to the initiator caspases, which require recruitment to adaptor molecules, dimerisation and, in some cases, cleavage to become activated. Once activated caspase-3 cleaves key cellular substrates to bring about a cell's demise.

Caspase-7 was first identified due to its similarity to caspase-3 (Fernandes-Alnemri *et al*, 1995; Duan *et al*, 1996; Lippke *et al*, 1996) and exists as a 34 kDa proenzyme containing two subunits, which at physiological levels are also dimeric (Fig. 1.4) (Chai *et al*, 2001; Reidl *et al*, 2001). Caspase-7 shares several target substrate specificities with caspase-3 however it has recently been suggested that their roles, in some instances, are quite distinct (reviewed in Lamkanfi and Kanneganti, 2010). Nevertheless, the activation of both caspase-3 and -7 by upstream initiator caspases is fundamental to the process of apoptosis and it is the inherent simplicity of executioner caspase activation that allows for a rapid response following detection of apoptotic stimuli.

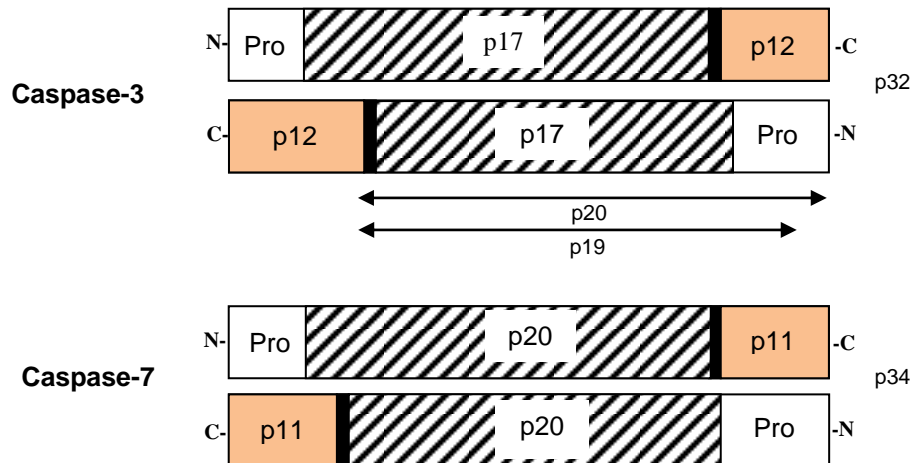


Figure 1.4 The Executioner Caspases. Caspase-3 and -7 exist as proenzyme dimers that require limited proteolytic cleavage between the linker-region (black fill) to become activated. Unlike initiator caspases, they have short pro-domains (Pro) but are similarly made up of a long (striped fill) and short subunit (orange fill).

1.4 Apoptotic Pathways

Cytotoxic T lymphocytes (CTLs) and Natural Killer (NK) cells can remove infected or cancerous cells by releasing cytotoxic granules that contain perforin and granzyme B. Perforin forms channels in the cell membrane, which permits the entry of granzyme B –

a proteolytic enzyme that cleaves and activates caspases, specifically caspase-3, to initiate cell death (reviewed in Creagh *et al*, 2003; Taylor *et al*, 2008). However, aside from this pathway (known as the granzyme B pathway), two main pathways leading to apoptosis are known; the intrinsic pathway and the extrinsic pathway.

1.4.1 The intrinsic pathway

The intrinsic pathway, or mitochondrial pathway, of apoptosis is activated from signals within the cell primarily originating from the detection of cytotoxic stress initiated by, for example, chemotherapeutic drugs, cytokine withdrawal and/or DNA damage (reviewed in Hale *et al*, 1996; Kaufmann and Earnshaw, 2000; Norbury and Zhivotovsky, 2004). Upon detection of cellular stress, alterations occur which disrupt the balance between survival signals and death signals favouring a cell's demise. In some instances these alterations are brought about through activation of the tumour suppressor transcription factor p53. The p53 protein is particularly significant because it acts as a tumour suppressor gene, which detects cellular stress and temporarily inhibits DNA synthesis and thus proliferation whilst activating target genes (reviewed in Vogelstein *et al*, 2000; Vousden, 2002). Unsurprisingly therefore, the mutation or loss of functional p53, as found in the majority of cancers, allows for tumour formation and progression (reviewed in Lozano and Zambetti, 2005).

In cells with functional p53, detection of cellular stress leads to, among other things, the up-regulation of pro-apoptotic members of the Bcl-2 family of apoptotic regulators (Vousden, 2005). Bcl-2, the founding member of this family of proteins, was first identified as an oncogene in follicular lymphoma present as a result of a chromosomal translocation (Tsujimoto *et al*, 1984) and was later found to play an important role in apoptosis (Vaux *et al*, 1988). Since its discovery a number of other proteins have been identified, through sequence similarity to Bcl-2, which lead to the classification of so-called Bcl-2 family members (Chao and Korsmeyer, 1998; Danial and Korsmeyer, 2004). These family members can be divided into pro-apoptotic (Bid, Bax, Bak) or anti-apoptotic (Bcl-2, Bcl-X_L, Mcl-1) depending on their central role in apoptosis. p53, in particular, up regulates the Bcl-2 pro-apoptotic family members PUMA (p53-upregulated modulator of apoptosis) and NOXA (Nakano and Vousden, 2001; Jeffers *et al*, 2003; Oda *et al*, 2000), which allows for the inactivation of anti-apoptotic Bcl-2 family members and activation of pro-apoptotic members such as Bax and Bak (Fig. 1.5) (Vousden, 2002). Bax and Bak are fundamental to the intrinsic apoptotic pathway (Wei *et al*, 2001). Their activation and ensuing oligomerisation in the mitochondrial outer membrane triggers the permeabilisation of the outer mitochondrial membrane

(MOMP) allowing for the release of cytochrome *c* normally confined, in healthy cells, to the inter-membrane space (Fig. 1.5) (reviewed in Yan and Shi, 2005; Hutteman *et al*, 2011). Once released into the cytosol, cytochrome *c* initiates the energy-dependent oligomerisation of 'apoptosis protease activating factor-1' (APAF-1); a pro-apoptotic adaptor protein found to be highly homologous to the Ced-4 protein (reviewed in Adrain and Martin, 2001), resulting in the formation of the apoptosome (reviewed in Cain *et al*, 2002). APAF-1 binds and processes procaspase-9 monomers to form a holoenzyme complex allowing for the activation of caspase-9 through dimer formation (Renatus *et al*, 2001). It is the role of active caspase-9, in the intrinsic pathway, to generate the active forms of the effector caspases-3 and -7, which brings about a cell's demise (Fig. 1.5). In addition to the release of cytochrome *c*, MOMP permits the release of other mitochondrial apoptogenic factors such as Smac/Diablo and Omi/HtrA2, which act to regulate the inhibitor of apoptosis (IAP) proteins whose role is to negatively regulate cell death by binding and inhibiting caspases (Fig. 1.5) (Martins *et al*, 2002; Twiddy *et al*, 2004; Gyrd-Hansen and Meier, 2010).

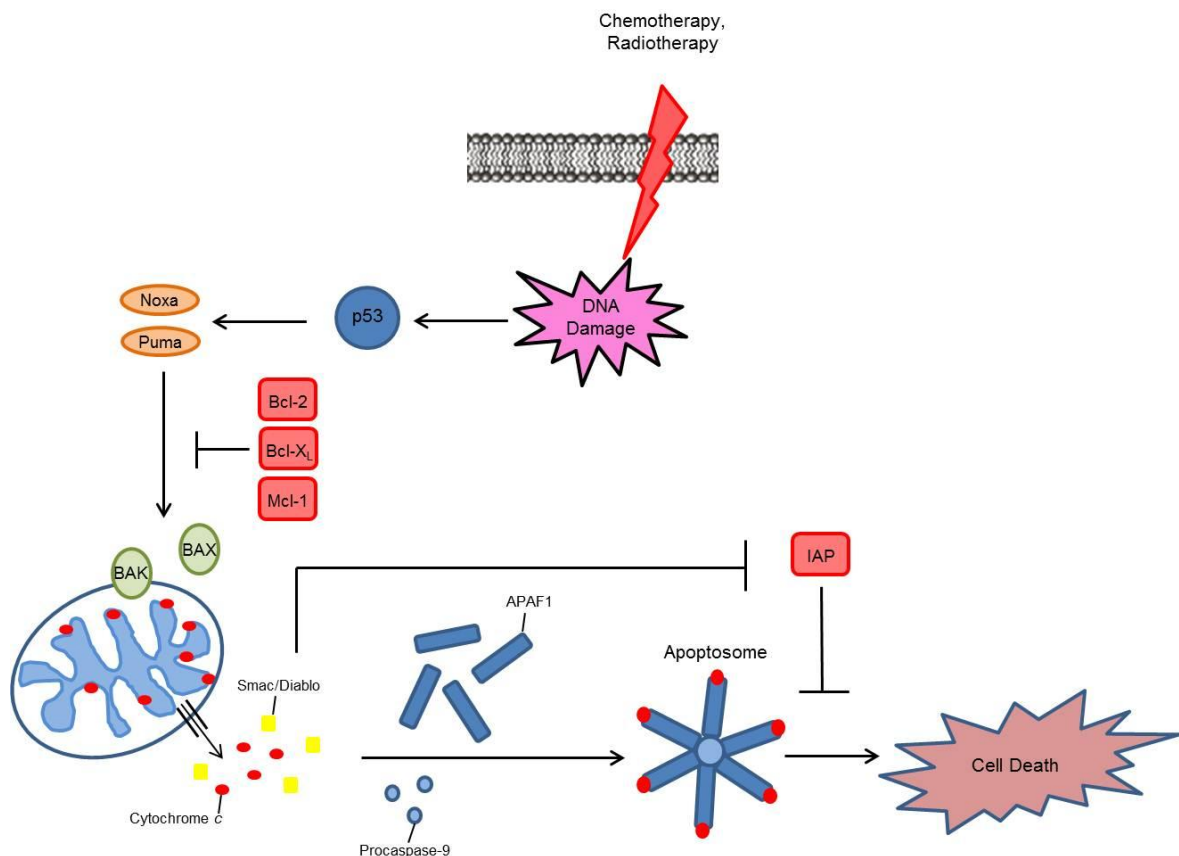


Figure 1.5 The intrinsic pathway. The intrinsic apoptotic pathway is activated by signals originating from outside the cell leading to, for example, the activation of p53, which up regulates pro-apoptotic Bcl-2 family members such as NOXA and PUMA. The ensuing permeabilisation of the outer mitochondrial member allows for the release of cytochrome *c* and thus formation of the apoptosome leading to cell death.

1.4.2 The extrinsic pathway

In contrast to the intrinsic apoptotic pathway, the extrinsic pathway is initiated by the extracellular binding of a ligand, such as Tumor Necrosis Factor (TNF), CD95L or TNF-related apoptosis inducing ligand (TRAIL), to its cognate transmembrane death receptor of the TNF-receptor superfamily (reviewed in Ashkenazi, 2002). These death receptors are characterised by the presence of numerous extracellular cysteine-rich domains (CRD's) and an intracellular death domain (DD) motif, which are central to the induction of apoptosis (reviewed in Ashkenazi, 2002). Similar to the apoptosome in the intrinsic pathway, the extrinsic pathway also requires formation of a multi-protein activating complex to initiate apoptosis.

The most characterised death-receptor pathway is that of CD95L and its death receptor CD95, which has served as a prototype for elucidating the initial signalling events of the extrinsic pathway (reviewed in Peter and Krammer, 2003). Extensive research found that the activation of pre-associated death-receptor homotrimers, by the binding of their cognate ligands, resulted in a conformational change that reveals the intracellular death domain of the receptor (Fig. 1.6).

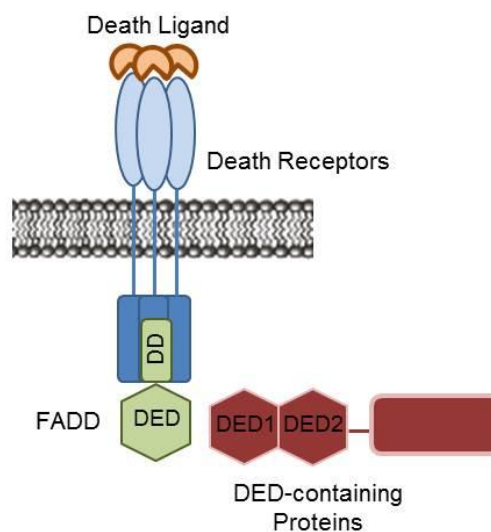


Figure 1.6 The known components of the DISC. The extrinsic pathway is activated by ligation of a death ligand to its cognate transmembrane death receptor of the TNF-receptor superfamily. Following ligand-receptor binding, the adaptor molecule FADD is recruited, which in turn allows for the recruitment of DED-containing caspases forming a multi-protein activating complex termed the DISC.

As a result, the bipartite adaptor molecule: Fas-associated death domain (FADD) is able to bind through homotypic interaction of their respective death domains (Fig. 1.6). Recruitment of caspase-8 monomers to the DISC then occurs through homophilic interaction of the death effector domain (DED), present in the *N*-terminal domain of caspase-8 (Fig. 1.3), with the *N*-terminal DED of the adaptor molecule FADD present

at the DISC (Boldin *et al*, 1996) resulting in formation of a multi-protein activating complex designated the Death-inducing Signalling Complex or DISC (Fig. 1.6) (Kischkel *et al*, 1995; Peter *et al*, 1996; Algeciras-Schimmich *et al*, 2002). It is at the DISC that the initiator caspase-8 is activated by recruitment, dimerisation and cleavage of caspase-8 monomers (Hughes *et al*, 2009). Thus, following removal of the pro-domains, active caspase-8 dimers are released from the DISC where they proceed to cleave the executioner caspases -3, -7 and/or Bid (see section 1.3.2) to bring about cell death (Chang *et al*, 2003; Boatright and Salvesen, 2003).

Although CD95L and its receptor are the best characterised, the TNF-ligand was actually the founding member of what was to become a superfamily of transmembrane proteins and their receptors (reviewed in Locksley *et al*, 2001). TNF and its receptors, however, proved slightly more complicated than its fellow family members. The discovery of two sequential TNF-receptor signalling complexes (Micheau and Tschopp, 2003) and the discovery that its adaptor molecule TNF-receptor associated death domain (TRADD) can recruit a DD-containing kinase, termed receptor-interacting protein (RIP), and TNF receptor-associated factor 2 (TRAF2), which permit activation of survival signalling pathways such as NF κ B and JNK, demonstrated a potential limitation in the induction of apoptosis via this pathway (Hsu *et al*, 1996a; Hsu *et al*, 1996b; Shu *et al*, 1996). Furthermore, it was soon discovered that upon systemic administration, TNF and CD95L were associated with a variety of unfavourable side effects, including liver toxicity, thus rendering them unsuitable for use as anticancer therapies (Ashkenazi *et al*, 1999). As a result, a novel TNF-superfamily death ligand, termed TRAIL, was subsequently identified through sequence homology to TNF and CD95L (Wiley *et al*, 1995). Unlike TNF or CD95L, numerous derived human tumour cell lines, but not the majority of normal cells, displayed marked sensitivity to TRAIL-mediated apoptosis (Pitti *et al*, 1996; Walczak *et al*, 1999; Pasquini *et al*, 2006). As a result, TRAIL gained intense interest as a prospective cancer therapeutic agent because of its potentially selective anti-tumour properties.

1.5 TRAIL and its DISC

TRAIL is expressed as a type II transmembrane protein, which can be cleaved from the cell membrane by metalloproteases to produce a soluble form of the ligand (reviewed in Walczak and Haas, 2008). The extracellular domain of TRAIL forms a homotrimer that engages with three molecules of its cognate transmembrane TRAIL death receptors. Unlike TNF and CD95L, TRAIL can bind to any one of five different

receptors: TRAIL-R1 (DR4), -R2 (DR5), -R3 (DcR1), -R4 (DcR2) and Osteoprotegerin (OPG) (Fig. 1.7) (reviewed in Ashkenazi, 2002; Kimberley and Screaton, 2004; Falschlehner *et al*, 2007). TRAIL-R1 was the first receptor to be cloned (Pan *et al*, 1997) followed closely by TRAIL-R2 and TRAIL-R3 (MacFarlane *et al*, 1997), TRAIL-R4 (Marsters *et al*, 1997) and OPG (Emery *et al*, 1998). However, it soon became apparent that not all of these receptors were capable of promoting apoptosis upon ligation of TRAIL (Fig. 1.7).

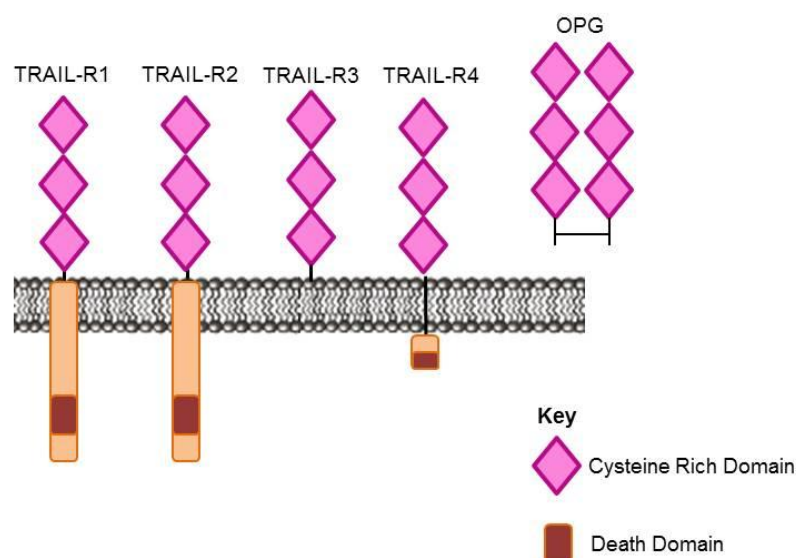


Figure 1.7 Schematic of the five TRAIL-receptors. TRAIL-R1 and -R2 possess cysteine-rich extracellular domains (CRDs) and an ~80 amino acid death domain motif in the cytoplasmic region, which is essential for transmitting the apoptotic signal upon binding of TRAIL. TRAIL-R2 (DcR1) is a 'so-called' decoy receptor, which does not contain a death domain and therefore cannot transmit an apoptotic signal. TRAIL-R4 (DcR2) is another decoy receptor, which contains a truncated non-functional death domain and therefore also cannot transmit an apoptotic signal. OPG is a soluble receptor that binds TRAIL and thus prevents its interaction with TRAIL-R1 or -R2 (reviewed in Gonzalez and Ashkenazi, 2010).

TRAIL-R1 and -R2 are both type I transmembrane receptors containing complete intracellular death domains and thus are able to transmit an apoptotic signal upon ligation of TRAIL through formation of a DISC (Fig. 1.7) (reviewed in Degli-Esposti, 1999; Ashkenazi, 2002). TRAIL-R3, on the other hand, lacks a death domain (MacFarlane *et al*, 1997) whilst TRAIL-R4 comprises a truncated death domain (Marsters *et al*, 1997) and, as a result, both of these receptors are unable to activate subsequent events that would primarily lead to apoptosis (Fig. 1.7). In addition, OPG, despite having a lower affinity for TRAIL, is able to act as a soluble antagonist counteracting signalling through TRAIL-R1 or -R2 (Emery *et al*, 1998; Vitovski *et al*, 2007).

The binding of TRAIL to TRAIL-R1 or -R2 brings about formation of the DISC (Fig. 1.6 and 1.8), which is essential for initiation of an apoptotic signalling cascade. Any deregulation at the level of the DISC can completely abrogate the apoptotic signal. For example, the cellular FLICE-like Inhibitory protein (cFLIP), a protease-deficient caspase-8 homolog, can interfere with the recruitment and activation of procaspase-8 through heterodimerisation potentially inhibiting its activation (Scaffidi *et al*, 1999; Micheau, 2003). cFLIP is expressed mainly in a long (cFLIP_L) and short (cFLIP_s) splice form. The latter contains *N*-terminal DED domains only and hence completely blocks procaspase-8 activation (Fig. 1.8) (Krueger *et al*, 2001). cFLIP_L, on the other hand, although enzymatically inactive, shows high homology to caspase-8 and has demonstrated, at endogenously expressed levels, to facilitate in the transduction of the apoptotic signal by interacting with the DISC to promote apoptosis (Fig. 1.8) (Chang *et al*, 2002; Fricker *et al*, 2010).

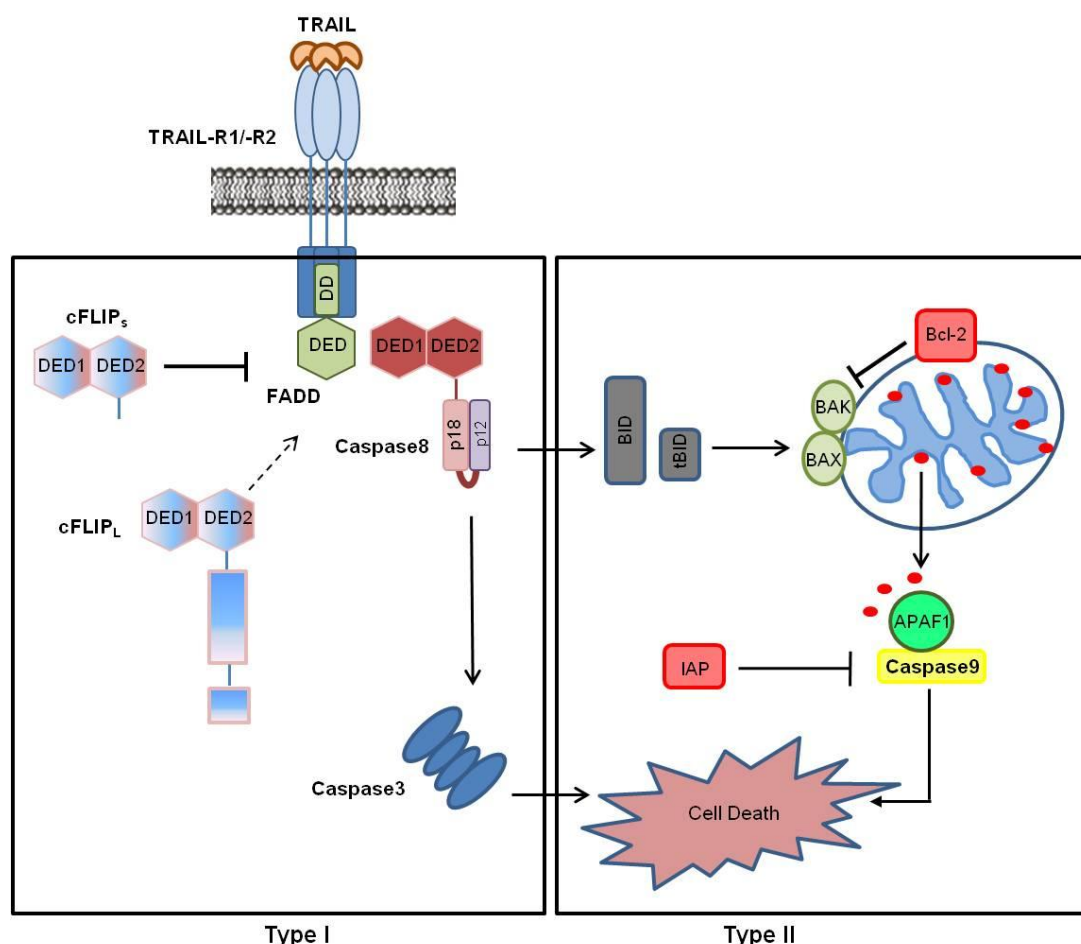


Figure 1.8 The extrinsic pathway. TRAIL-induced signalling is activated by ligation of TRAIL to its cognate transmembrane death receptors TRAIL-R1/-R2. Following ligand-receptor binding, the adaptor molecule FADD is recruited, which allows for the recruitment of procaspase-8 monomers forming a multi-protein activating complex termed the TRAIL-DISC. It is at the DISC that caspase-8 is activated which, in Type I cells, directly cleaves caspase-3 resulting in cell death. In Type II cells active caspase-8 preferentially cleaves the pro-apoptotic Bcl-2 family member Bid allowing for cross-talk and thus stimulation of the intrinsic pathway also resulting in cell death. Numerous regulators of the TRAIL signalling pathway have also been identified including cFLIP, Bcl-2 and IAPs. Image modified from Wang and El-Diery, 2003.

Further studies into death-receptor signalling found that in certain cell types initiation of apoptosis through the death receptor pathway also involved the loss of mitochondrial membrane transmembrane potential as observed upon activation of the intrinsic pathway (Scaffidi *et al*, 1998; reviewed in Barnhart *et al*, 2003). In so-called Type I cells, for example, the activation of caspase-8 at the DISC is sufficient to directly cleave the executioner caspase: caspase-3 and the apoptotic signal is not blocked by over-expression of anti-apoptotic Bcl-2 family members (Fig. 1.8) (Rudner *et al*, 2005). However, in other cell types, termed Type II, the apoptotic signal is amplified by involvement of the mitochondrial pathway and thus can be inhibited by over expression of anti-apoptotic Bcl-2 family members (Fig. 1.8) (Lacronique *et al*, 1996; Rudner *et al*, 2005). The crosstalk observed in the latter cell type was found to be mediated by the pro-apoptotic Bcl-2 family member, Bid (Luo *et al*, 1998; Li *et al*, 1998). Bid is a substrate of activated caspase-8 and is cleaved into its truncated form (tBID), which subsequently translocates to the mitochondria triggering permeabilisation of the mitochondrial outer membrane through activation of Bax and Bak (Fig. 1.8). Thus, as described previously, this permits the release of cytochrome *c* from the mitochondria resulting in the indirect activation of the intrinsic pathway by death receptor signalling (Fig. 1.8). However, it should be noted that Type I cells can also signal to cell death through the mitochondrial amplification loop. Thus, the key difference being that apoptotic signalling is not inhibited in Type I cells by the over expression of an anti-apoptotic Bcl-2 family member whereas in Type II cells signalling is inhibited.

Alternative signalling pathways, induced by TRAIL, may also modulate the apoptotic signal. For example, it has been shown that TNF and its death receptor TNFR1 requires formation of a secondary signalling complex to promote cell death and that binding of TNF to TNFR1 primarily induces activation of NF- κ B (Harper *et al*, 2003; Micheau and Tschopp, 2003). NF- κ B is a transcription factor that is found constitutively activated in the majority of cancer cells where it regulates the expression of a multitude of genes to promote cell survival (Chaturvedi *et al*, 2011). Similarly, both TRAIL and CD95 have been shown to form secondary cytoplasmic complexes however these are thought to activate survival pathways (Varfolomeev *et al*, 2005; Lavrik *et al*, 2008). In line with this, caspase-8 has also been found to be present in a complex at the mitochondria where it cleaves Bid and thus initiates cell death (Gonzalvez and Gottlieb, 2007; Gonzalvez *et al*, 2008; Schug *et al*, 2011). These 'novel' signalling complexes provide evidence for the existence of alternative death-inducing complexes. Nevertheless, it is evident that TRAIL DISC formation is fundamental to the initiation of the extrinsic pathway and therefore a more detailed analysis of TRAIL-induced cell

death might aid in understanding the potential of this death ligand and/or its derivatives as a cancer therapeutic.

1.6 Metabolism and Cancer

In the early 1920's, Otto Warburg described how cancer cells prefer to undergo cellular respiration by glycolysis rather than by oxidative phosphorylation, an observation subsequently termed the 'Warburg effect' (Warburg *et al* , 1927; Warburg, 1956). Warburg proposed that, in cancer cells, there is an increase in the conversion of glucose to lactate along with a decrease in mitochondrial respiration. This phenomenon occurs even in the presence of oxygen and is known as aerobic glycolysis (reviewed in Gatenby and Gillies, 2004). Although the fundamental cause of this switch is still unclear, the alteration in energy metabolism became the basis of the diagnostic test FDG-PET, which has been used as a tool to identify tumours for a number of years (Hawkins and Phelps, 1988; Weber *et al*, 1999). 2-Fluoro-2-deoxy-D-Glucose (FDG) is a glucose analogue taken up by high-glucose consuming cells where it can be detected using positron emission tomography (PET) and thus provides a way of examining for the presence of tumours in the body (reviewed in Gambhir, 2002). Thus, the metabolic phenotype of cancer cells has been exploited to aid in the detection of the disease. However, in parallel, the increased glucose uptake observed in these tumours often correlates with a more aggressive cancer phenotype and thus poor prognosis. Nevertheless, since glucose metabolism is vital for providing energy to rapidly dividing cancer cells, research into the relationship between energy metabolism and evasion from apoptosis have expanded over recent years and a number of concepts have been proposed to provide a link between the two.

1.6.1 Metabolic pathways in cancer

Metabolism comprises a complex set of reactions that are central to the formation of ATP and paramount for cell growth, reproduction and maintenance of multiple cellular functions (Erecinska and Wilson, 1982; Alberts *et al*, 2002). Glucose is the main energy supply of this process and is facilitated into cell through specific membrane-bound transporters (Gluts) (Medina and Owen, 2002). A number of isoforms of Glut have been identified and their expression is often tissue-specific. For example, Glut-3 and -4, which have a high affinity for glucose, are primarily found in brain and muscle cells where the requirement for glucose is particularly important even when glucose concentrations are low. Interestingly, these glucose transporters are often found over expressed in cancer cells and this is thought to be one contributing factor influencing

the high aerobic glycolysis of cancer cells (Fig. 1.9) (reviewed in Macheda *et al*, 2005). Although at first energetically unfavourable, glycolysis results in a net yield of two ATPs per glucose molecule and does not require oxygen to proceed. Notably, this results in a relatively low yield of ATP especially when compared to mitochondrial respiration (36 ATPs). However, the rate at which glycolysis occurs in cancer cells means that they can efficiently compensate for this seemingly inadequate generation of ATP. The specific stages of glycolysis are outlined in Figure 1.9 along with the key regulators of this pathway that are proposed to bring about the altered metabolic phenotype found in cancer cells (Fig. 1.9). It is evident from this that there are multiple stages at which glycolysis can be regulated as well as numerous modulators of this pathway and thus only a selection of these changes are discussed.

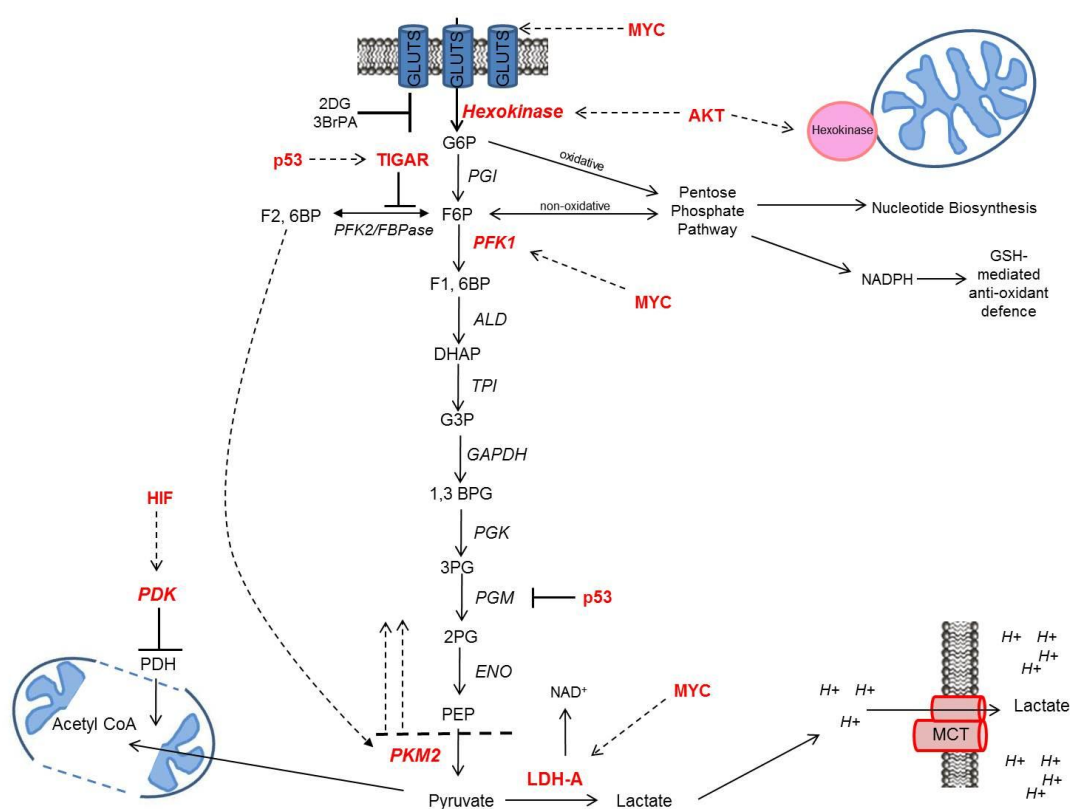


Figure 1.9 The glycolytic pathway in cancer cells. Glucose is transported into cells via specific glucose transporters (Gluts), which are highly expressed on the surface of cancer cells. Upon entering the cell, glucose is rapidly phosphorylated by hexokinase to form glucose-6-phosphate (G6P). G6P is then converted to fructose-6-phosphate (F6P) by phosphoglucosomerase (PGI) in the glycolytic pathway or diverted to the oxidative arm of the pentose phosphate pathway (PPP) where it is used to generate nucleic acids and NADPH. In the glycolytic pathway, F6P is converted to Fructose 1,6-bisphosphate (F1,6BP) by phosphofructokinase 1 (PFK1) or alternatively to Fructose 2,6-bisphosphate (F2,6BP) by PFK2. F2,6BP is a major activator of PFK1 and thus enhances the glycolytic flux. Similarly, the inhibition of PFK1 diverts F6P into the non-oxidative arm of the PPP. TIGAR, a p53 target gene, was identified as an inhibitor of the conversion of F6P to F2,6BP thus favouring the 'shunting' of glycolysis into the PPP. Similarly, p53 is an inhibitor of phosphoglycerate mutase (PGM), which converts 3-phosphoglycerate (3PG) to 2-phosphoglycerate (2PG). The last stage of glycolysis converts Phosphoenolpyruvate (PEP) to pyruvate by pyruvate kinase (PK) specifically the M2 form (PKM2). This enzyme is activated by F2,6BP and inhibited by tyrosine phosphorylation, which is thought to be the predominant form in tumours where it reversed glycolysis to favour anabolic processes. In cancer cells, pyruvate is largely converted to lactate and exported out of the cell by specific monocarboxylate transporters (MCT) since the pyruvate dehydrogenase complex (PDH) that is required to convert pyruvate to acetyl-CoA in the mitochondria is inhibited by an increased expression of pyruvate dehydrogenase kinase (PDK). Reviewed in Tennant *et al*, 2009.

The first step of glycolysis is the rapid irreversible phosphorylation of glucose, catalysed by hexokinase, to form glucose 6-phosphate (G6P) (Fig. 1.9). Hexokinase activity is one of the main controlling steps in the glycolytic pathway and, to date, four human isoforms are known to exist – HKI, II, III and Glucokinase (or IV) (Wilson, 2003). Two of these isoforms, HKI and II, contain hydrophilic N-terminal segments meaning that they can exist free in the cytosol or bound to the mitochondria (Fig. 1.9). The specific binding site of hexokinase on mitochondria has been shown to be the voltage-dependent anion channel (VDAC). Here, it has been implicated as exerting an anti-apoptotic role through the prevention of Bax-induced cytochrome *c* release (Pastorino *et al*, 2002) and thus, unsurprisingly, expression levels of hexokinase are significantly increased in transformed cells (reviewed in Pedersen *et al*, 2002). Mitochondrial-bound hexokinase has also been found to exert an anti-oxidant defence mechanism through the prevention of ROS formation (Seixas da-Silva *et al*, 2004). In line with these findings, the detachment of hexokinase from the mitochondria has been shown to promote cell death (Goldin *et al*, 2008) and thus much work is being carried out with pharmacological compounds that target this process (reviewed in Mathupala *et al*, 2009).

Following the conversion of G6P to F6P by phosphoglucosomerase (PGI), phosphofructokinase 1 (PFK1) converts F6P to F1, 6BP (Fig. 1.9). PFK1 was found to be a key metabolic target of the myc oncogene; a transcription factor that regulates a number of genes that control cell metabolism particularly those involved in glycolysis (reviewed in Kim *et al*, 2005), and thus its expression levels are elevated in cancer cells. In addition to the glycolytic pathway, PFK1 is also important in regulating glycolytic flux into the pentose phosphate pathway (PPP) and is therefore highly regulated by cellular conditions. One such regulator is F2, 6BP, which, under the control of PFK2, is a major activator of PFK1, and thus both PFK1 and PFK2 are often found increased in tumours (reviewed in Tennant *et al*, 2009). In line with this, more recently, a gene target for p53 was also found to regulate energy metabolism suggesting that p53 could influence the metabolism of cancer cells (reviewed in Bensaad and Vousden, 2007). TP53-induced glycolysis and apoptosis regulator (TIGAR) was specifically found to regulate PFK1 by inhibiting the conversion of F6P to F1, 6BP and thus reducing PFK1 activity as well as diverting glucose into the pentose phosphate pathway (Fig. 1.9) (Bensaad *et al*, 2006). The pentose phosphate pathway is essential for nucleotide biosynthesis and the generation of NADPH and thus the up regulation of TIGAR by p53 is thought to regulate ROS production in response to transient stress by directing glucose metabolism through the pentose phosphate

pathway (Fig. 1.9). Interestingly, TIGAR was found to be active even in the absence of functional p53, which suggests a role for this protein in transformed cells in the absence of p53 (Bensaad *et al*, 2006). Furthermore, p53 has also been shown to regulate mitochondrial respiration following the identification of Synthesis of Cytochrome c Oxidase 2 (SCO2); a key regulator of the cytochrome c oxidase complex (complex IV) in the electron transport chain (Matoba *et al*, 2006). Cells with mutated p53 show defects in mitochondrial respiration, associated with decreased expression of SCO2, and a shift toward glycolytic respiration, a response which can be reversed following addition of viable p53 (Matoba *et al*, 2006). Furthermore, the loss or mutated version of p53, common to most tumours, is also associated with an increase in glycolytic enzymes such as phosphoglycerate mutase (PGM), which could be contributing to the Warburg effect observed in cancer cells (Fig. 1.9) (Kondoh *et al*, 2005).

The final enzyme in the glycolytic pathway is pyruvate kinase (PK), which converts phosphoenolpyruvate (PEP) into pyruvate (Fig. 1.9). There are four known isoforms of pyruvate kinase; L, R, M1 and M2 (Yamada *et al*, 1999). Isoforms L and R are largely associated with liver and blood cells, whilst PKM1 is found expressed in most adult tissues and PKM2 is largely expressed in foetal tissue (Yamada and Noguchi, 1999). Interestingly, PKM2 was also found to be the form highly expressed in tumour cells and is important for the altered metabolic phenotype in cancer cells (Christofk *et al*, 2008a; reviewed in Israel and Schwartz, 2011). PKM2 is the low activity version of pyruvate kinase and is inhibited by tyrosine phosphorylation, which displaces its allosteric activator F2, 6BP (Fig. 1.9) (Christofk *et al*, 2008b; Hitosugi *et al*, 2009). This reduces the conversion of PEP to pyruvate and thus promotes anabolic processes for the synthesis of nucleotides and lipids rather than catabolic processes (reviewed in Gupta and Bamezai, 2010).

Pyruvate is the end product of glycolysis and in normal cells this is largely transported into the mitochondria where it is converted in to acetyl-coA by the pyruvate dehydrogenase complex (PDH) (Fig. 1.9). This permits metabolism through the TCA cycle and oxidative phosphorylation to generate substantially more ATP than glycolysis and also intermediates for fatty and amino acid synthesis. However, in cancer cells pyruvate is largely converted to lactate and exported from the cell (Fig. 1.9) largely due to the increase in pyruvate dehydrogenase kinase, which ensures the constitutive phosphorylation, and thus inactivation, of the pyruvate dehydrogenase complex (Fig. 1.9) (reviewed in Feron, 2009). In addition, under the regulation of the myc oncogene,

lactate dehydrogenase A (LDH-A) expression is increased and this allows for the rapid conversion of pyruvate to lactate, and thus the recycling of nicotinamide adenine dinucleotide (NAD⁺), to maximise the glycolytic pathway and replenish intermediates (Fig. 1.9) (Feron, 2009). Interestingly, the suppression of LDH-A, apart from promoting oxidative phosphorylation, reduced the proliferation of cancer cells *in vitro* and enhanced cancer survival rates *in vivo* (Fantin *et al*, 2006). This suggests that LDH-A in tumour cells has a significant influence on the glycolytic status of these cells. In line with this, to prevent a build-up of cellular lactate and to maintain intracellular pH, lactate is exported from the cell via mono-carboxylate transporters (MCT), which contributes to the acidic tumour microenvironment (Fig.1.9) (reviewed in Kennedy and Dewhurst, 2010). MCT4, in particular, is often found over-expressed in cancers and thus represents a potential therapeutic target (reviewed in Izumi *et al*, 2003).

In addition, aside from myc and p53, the oncogenes H-RAS and v-SRC also contribute to alterations in metabolism the latter of which was found to phosphorylate and thus inhibit PKM2 (Presek *et al*, 1988; Dang and Semenza, 1999). Furthermore, a study by Ramanathan *et al* examined the response of immortalised human cells to progressive transformation with several known oncogenes and observed that cells exhibited a greater reliance on glycolysis following these transformations, which was prevented when inhibitors of glycolysis were introduced (Ramanathan *et al*, 2005). More recently, a Ras-dependent oncogenic transformation has been described indicating a role for Signal Transducers and Activators of Transcription (STATs) - transcription factors normally thought to be associated with the nucleus that were found to mediate with the mitochondria where they induce key metabolism changes in response to Ras activation (Gough *et al*, 2009).

1.6.2 Inhibitors of energy metabolism

Energy metabolism involves a complex set of reactions that can clearly be affected by a number of factors at different stages of the process. Intracellular conditions and even mediators of energy metabolism itself, through feedback mechanisms, control the synthesis of ATP at different points of the pathway and a number of specific inhibitors have also been identified.

2-Deoxy-D-Glucose (2DG) is a glucose analogue, which has the 2-hydroxyl group replaced by hydrogen and as a result cannot undergo glycolysis (Pelicano *et al*, 2006). It is taken up into cells through the same receptors as glucose and rapidly phosphorylated by hexokinase (2DG-P). High levels of 2DG-P allosterically and

competitively inhibit hexokinase and thus inhibit glycolysis at the first step (Aft *et al*, 2002). In addition, hexokinase itself can be inhibited by a build-up of G6P, which acts through a feedback mechanism from the inhibition of PFK. Similarly, regulation of the citric acid cycle is primarily driven by substrate availability.

The electron transport chain has several known inhibitors, an example of one being Rotenone. Rotenone inhibits the electron transport chain at complex I, preventing the re-oxidation of NADH by inhibiting the iron-sulphur clusters from transferring electrons to ubiquinone. However, the transfer of electron from FADH₂ in complex II can still continue since the inhibition is upstream of the ubiquinone-binding site (Hames and Hooper, 2005). In cells, the electron transport chain is tightly regulated to ATP synthesis by oxidative phosphorylation and therefore inhibition of one will directly affect the other. Oligomycin can bind and block the F_o subunit of ATP synthase (complex V), which inhibits the oxidative phosphorylation of ADP to ATP and thus prevent the flow of electrons (Devenish *et al*, 2000). However, uncoupling agents such as Carbonyl cyanide-p-trifluoromethoxyphenylhydrazone (FCCP) can prevent ATP synthesis whilst allowing electron transport to continue. Uncoupling agents are lipid soluble molecules that prevent ATP synthesis by providing an alternative pathway for hydrogen ions to re-enter the mitochondrial matrix thus preventing formation of a proton gradient. However, electron transport still proceeds, usually at an accelerated rate, in an attempt to rectify the loss in membrane potential generated by the uncoupling agent (Hames and Hooper, 2005).

1.6.3 Glucose deprivation and cancer metabolism

Since most cancer cells exhibit an increase, and thus dependence, on glycolysis to fuel proliferation and growth, the potential to target this adaptation as a novel cancer therapeutic strategy is a key line of current research. One aspect of such studies is to essentially block glycolysis through pharmacological or physiological means, the latter being through the deprivation of glucose from culture media. As a result, a large number of studies have been performed to investigate potential mediators of the apoptotic signalling pathway brought about through deprivation of glucose, some of which have conflicted results and are discussed below.

Thakkar and Potten studied the effects of the anti-glycolytic 2-deoxyglucose (2DG) on Doxorubicin-induced apoptosis *in vivo* and found that tumour cells were protected against death under these conditions (see Table 1.1) (Thakkar and Potten, 1993). They concluded that a depletion in cellular ATP, caused by the administration of 2DG,

prevented the cleavage of DNA induced by doxorubicin and thus prevented the induction of apoptosis (Thakkar and Potten, 1993). Similarly, Ferrari and co-workers studied the effects of ATP depletion on apoptosis and found that the intrinsic pathway, induced by chemotherapeutic drugs, was completely inhibited under these conditions whilst the receptor mediated pathway, induced by CD95L, was not affected (Ferrari *et al*, 1998). More recently, Zamaraeva *et al* observed that cells undergoing apoptosis had elevated levels of cytosolic ATP compared to their control cells and concluded that cytosolic ATP is a necessity for apoptosis (Zamaraeva *et al*, 2005). These findings correspond with previous work by Leist and co-workers, who observed that ATP was a prerequisite for the successful signalling of apoptosis, including CD95-induced apoptosis, and that when cytosolic ATP levels were depleted, the form of cell death switched from apoptosis to necrosis (Leist *et al*, 1997). However, a number of studies (Halicka *et al*, 1995; Nam *et al*, 2002; Munoz-Pinedo *et al*, 2003; Wood *et al*, 2008; Pradelli *et al*, 2009) have described the opposite, whereby cells have become sensitised to death-receptor mediated apoptosis under conditions of glucose deprivation (Table 1.1).

Halicka and colleagues observed that following treatment with TNF α and 2DG, signalling to apoptosis was greatly enhanced in U937 cells through an unknown mechanism (Halicka *et al*, 1995). More recently, Wood *et al*, using a cell-based high-throughput screen, identified a number of compounds that selectively sensitised resistant tumour cells to death-receptor mediated apoptosis (Wood *et al*, 2008). One compound, Fasentin, was observed to alter the regulation of a number of genes associated with glucose metabolism and resulted in the sensitisation of cells to death ligands through its interaction with glucose transporters and the inhibition of glucose uptake (Wood *et al*, 2008).

Table 1.1 An overview of research papers examining the role of glucose deprivation in apoptotic signalling.

Inhibitor	Pathway	Outcome	Cell Line(s)	Reference
2DG	Intrinsic	Inhibited	<i>In vivo</i> (Mice)	Thakkar and Potten, 1993
2DG	Extrinsic	Sensitised	U937	Halicka <i>et al</i> , 1995

↓ ATP (Media)	Intrinsic Extrinsic	Inhibited Inhibited	JURKAT	Leist <i>et al</i> , 1997
↓ ATP (Media)	Intrinsic Extrinsic	Inhibited No Effect	Jurkat	Ferrari <i>et al</i> , 1998
Glucose Deprivation (Media)	Extrinsic	Sensitised	DU145 CX1	Nam <i>et al</i> , 2002
2DG and Glucose deprivation (Media)	Extrinsic Extrinsic	Sensitised Inhibited	U973, HeLa, MCF7 MCF7 ^{bcl2}	Munoz-Pinedo <i>et al</i> , 2003
Glucose Inhibitor	Extrinsic	Sensitised	PPC1, DU145, U937	Wood <i>et al</i> , 2008

Previous to this, Muñoz-Pinedo, utilizing both 2DG and glucose withdrawal from media, similarly found that tumour cells become sensitised to death receptor-triggered apoptosis induced by TNF α , CD95L and TRAIL when cells were deprived of glucose. Under these conditions, they observed that DISC formation, caspase activation and mitochondrial depolarisation were all increased (Muñoz-Pinedo *et al*, 2003). However, they also observed that over-expression of Bcl-2 in MCF-7 cells, alongside glucose deprivation, caused the complete abrogation of death-receptor triggered apoptosis (Muñoz-Pinedo *et al*, 2003). MCF-7 cells do not express caspase-3 and therefore, to successively signal to cell death, via the extrinsic pathway, they require input from the mitochondrial amplification loop. Thus, over expression of the anti-apoptotic protein Bcl-2 would prevent apoptotic signalling through the mitochondrial amplification and this would occur irrespective of culture conditions. From these studies, Muñoz-Pinedo and colleagues concluded that an alteration in the processing of caspase-8 is the primary step regulated by glucose metabolism and this occurs through a currently unknown mechanism. Further experimental investigations ruled out changes in the expression levels of a number of pro- and anti-apoptotic proteins including cFLIP; a protein thought to interact with the DISC altering caspase 8 processing (Scaffidi *et al*, 1999; Muñoz-Pinedo *et al*, 2003). However Nam *et al*, who also examined the relationship between low glucose and death-receptor mediated apoptosis, concluded from their results that enhanced TRAIL cytotoxicity mediated by glucose deprivation

was a result of the down regulation of cFLIP through the PI3K/Akt pathway (Nam *et al*, 2002). Following glucose deprivation, they observed an increase in ceramide levels along with a decrease in the expression levels of cFLIP. From this, they concluded that glucose deprivation was causing the dephosphorylation of Akt through the up regulation of ceramide, which resulted in the down regulation of cFLIP thus sensitising cells to death-receptor stimuli (Nam *et al*, 2002).

Further analysis into glucose deprivation and apoptotic signalling by Yang and colleagues illustrated how the molecular chaperone; glucose-regulated protein 75 (Grp75) a member of the heat shock 70 (Hsp70) family, could actually protect rather than sensitise cells to glucose deprivation-induced apoptosis through the inhibition of BAX conformational changes and alteration of the Bax/Bcl-2 expression ratio (Yang *et al*, 2008). In addition, the molecular chaperone GRP78 has also been found to prevent cell death under conditions of stress (Park *et al*, 2007).

Substrate availability and altered protein expression following glucose deprivation can also influence the apoptotic response. Cui *et al*, similar to Wood and colleagues, found a number of genes whose expression was enhanced following glucose deprivation one of which, asparagine synthetase (ASNS), was studied in detail (Cui *et al*, 2007; Wood *et al*, 2008). ASNS encodes an enzyme that catalyses the conversion of aspartic acid to asparagine and it has been suggested, by Cui and colleagues, that as a secondary role it suppresses apoptosis through inhibition of SAPK/JNK activation (Cui *et al*, 2007). The Jun N-Terminal Kinases (JNK)/ Stress-Activated Protein Kinases (SAPK) pathway is activated by stress stimuli, such as glucose withdrawal, leading to the phosphorylation of c-Jun: an early response transcription factor, which among other things promotes pro-apoptotic signalling (Stalheim and Johnson, 2007). However, the actual process by which ASNS can inhibit the JNK/SAPK pathway is still unclear (Cui *et al*, 2007).

Another important pathway that responds to cellular energy status is the AMP-Activated Protein Kinase (AMPK) cascade, which responds to depletions in ATP by switching on pathways that generate ATP whilst switching off processes that consume ATP (Hardie, 2011). The first identified substrates of the AMPK pathway were those involved in suppressing cholesterol and fatty acid synthesis thus driving the synthesis of ATP (Shaw, 2006). In addition, activated AMPK promotes cell cycle arrest through activation of the tumour suppressor gene p53 whose activation is required for survival under conditions of short-term glucose deprivation (Jones *et al*, 2005). However, a

deregulation in this pathway could easily be manipulated by cancer cells whose aim is to survive under conditions of extreme stress. As a result, mutations that drive the AMPK pathway could provide cancer cells with an alternative route to obtain energy, which restores intracellular ATP levels and prevents its inhibitory role at the cell cycle (Shaw, 2006).

1.6.4 The Akt pathway

Another important regulator of cellular metabolism in both normal and cancerous cells is the PI3K/Akt signalling pathway. PI3Ks (phosphatidylinositol 3-kinase) are a family of signal transducer enzymes, which activate Akt (or Protein Kinase B) through phosphorylation of PIP₂ (phosphatidylinositol (4,5)-bisphosphate) producing PIP₃ (phosphatidylinositol (3,4,5)-Trisphosphate). PIP₃ binds Akt where it becomes activated by phosphorylation and functions as a regulator of cell survival and metabolism by activating and inhibiting numerous downstream targets such as mdm2 – an inhibitor of p53, and GSK3 β – an inhibitor of glycogen synthase (Fig. 1.10) (reviewed in Vivanco and Sawyers, 2002; Arcaro and Guerreiro, 2007; Manning and Cantley, 2007; Liu *et al*, 2009).

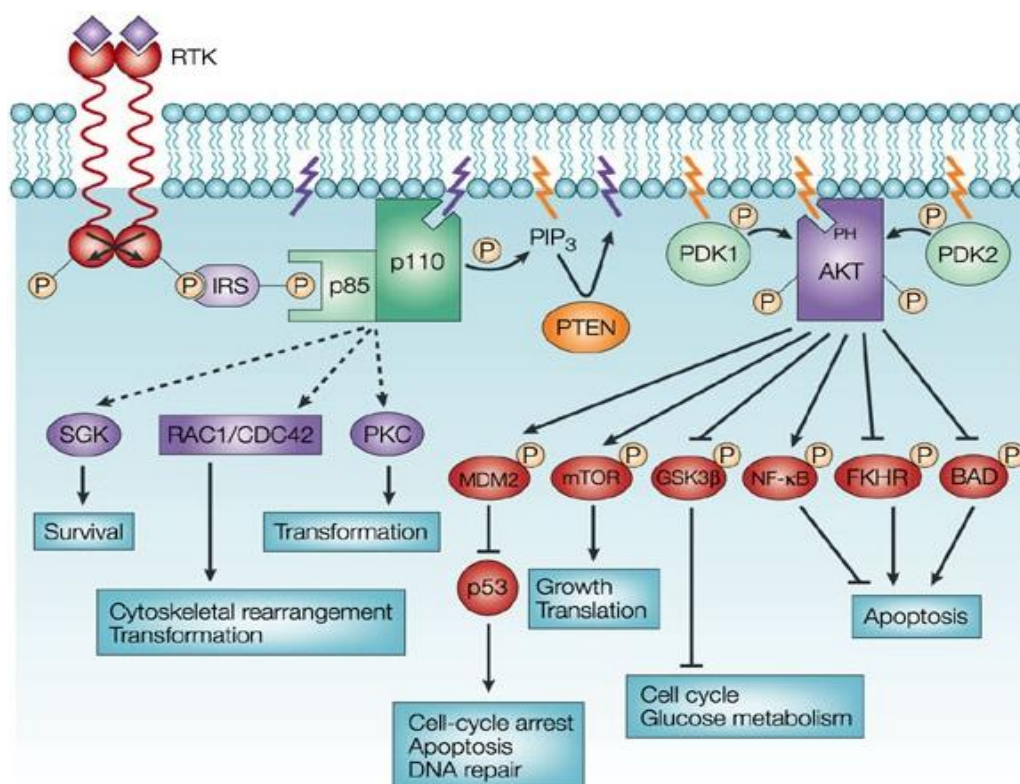


Figure 1.10 An overview of PI3K/Akt pathway PI3K, activated by receptor tyrosine kinases (RTK), phosphorylates the phospholipid PIP₂ forming PIP₃, which recruits Akt allowing for its activation by PDK1 and 2. Activation of Akt promotes cell survival by activating and inhibiting downstream regulators of numerous signalling pathways. Image taken from Vivanco and Sawyers, 2002.

In normal cells, growth-factor dependent activation of PI3K is tightly controlled by the potent tumour suppressor phosphatase: PTEN (Jones and Thompson, 2009). However, deregulation of this pathway is often found in cancer cells, largely as a result of constitutively activated PI3K/Akt and also mutated PTEN, thus allowing for sustained metabolic transformation and proliferation (Vivanco and Sawyers, 2002; Jones and Thompson, 2009). Constitutively activated Akt regulates glycolysis through a number of approaches including the maintenance of surface transporters, following growth factor withdrawal, through an mTOR-dependent mechanism and by increasing the expression of glycolytic enzymes (Edinger and Thompson, 2002). Another downstream target of activated Akt is thought to contribute to the up-regulation of mitochondrial-associated hexokinase, which interferes with Bax-translocation to the mitochondria and thus inhibits apoptosis (Gottlob *et al*, 2001; Edinger and Thompson, 2002; Pelicano *et al*, 2006). Further research into Akt signalling, and its role in apoptosis, suggest that activated Akt requires glucose for its pro-survival function and that limitations in glucose availability decrease this role especially in situations where deregulation of the pathway is not a contributing factor (Gottlob *et al*, 2001; Edinger and Thompson, 2002).

1.6.5 Additional metabolic pathways

Tumour cells need to sustain activities, including protein and lipid metabolism, to allow them to exist as normal cells and therefore two pathways important for proliferating tumour cells are nucleotide biosynthesis and lipid biosynthesis both of which use glucose (or glutamine) as a carbon source (DeBerardinis *et al*, 2008). For nucleotide biosynthesis, glucose metabolism is diverted through the pentose phosphate pathway, influenced by oncogenes and tumor suppressors including p53 inducible TIGAR, in order to generate NADP⁺ and ribose 5-phosphates (Fig. 1.11) (DeBerardinis *et al*, 2008). Also influenced by oncogenes, such as the PI3K/Akt pathway, is fatty acid synthesis, which is regulated by the citric acid cycle (Fig. 1.11) (DeBerardinis, *et al*, 2008). The citric acid cycle is often found to be truncated in tumour cells due to the inhibition of enzymes such as aconitase, which catalyses the conversion of citrate to isocitrate (Fig.1.11) (Dajani *et al*, 1961). Since citrate cannot progress through the remaining citric acid cycle, it is transported from the mitochondria into the cytosol where it can be used for fatty acid synthesis (Fig. 1.11). In addition, a heterozygous point mutation in isocitrate dehydrogenase (IDH), which catalyses the conversion of isocitrate to α -ketoglutarate, has been observed in glioblastoma patients (Parsons *et al*, 2008). This point mutation confers a gain-of-function to the enzyme, which results in the conversion of isocitrate to 2-hydroxyglutarate, a metabolic enzyme later to found to

be a potential “onco-metabolite” (Dang *et al*, 2009; reviewed in Frezza *et al*, 2010; Yen *et al*, 2010). In addition, the amino acid glutamine, found in high levels in tumour cells, can be used as an additional energy source when glycolytic production is decreased. Glutamate can be converted to a number of substrates including aspartate, lactate and citrate, which can be utilised by the numerous biosynthetic pathways in a cell. Recent data has implicated a significant role for glutamine levels in apoptotic signalling, specifically through changes in sensitivity to death-receptor mediated triggers (Mates *et al*, 2006). Glutamine starved cells were more sensitive to CD95L whilst they were desensitised to the effects of TNF α (Oehler and Roth, 2003). Cells deprived of glutamine show a decrease in levels of HSP70, which is important for cell survival (Mates *et al*, 2006; Park *et al*, 2007; Yang *et al*, 2008). However, glutamine deprivation *in vitro* brought about rapid cell cycle arrest and subsequent apoptosis even in the absence of an extracellular trigger (Mates *et al*, 2006). The regulation of apoptosis by glutamine levels is still relatively unclear although suggestions have been made as to where in the apoptotic pathway it may act to regulate cell death (Fig. 1.11) (Mates *et al*, 2006).

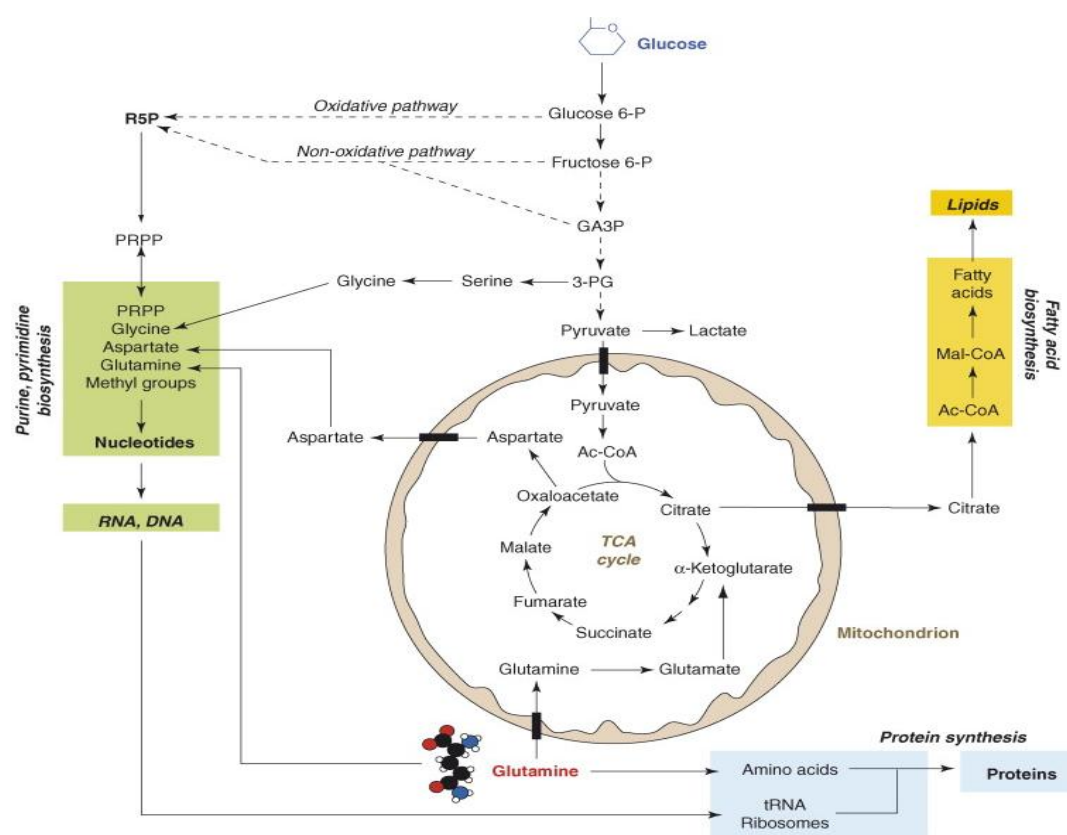


Figure 1.11 An overview of the biosynthetic pathways in tumour cells. Metabolic re-profiling in tumour cells has been found to assist in their growth, proliferation and survival under conditions of nutrient stress. Image taken from DeBerardinis *et al*, 2008.

1.6.6 Hypoxia

Hypoxia, a condition whereby cells are deprived of an adequate oxygen supply, is an environment usually associated with tumour cells and has been implicated in poor treatment responses (Fulda and Debatin, 2007). Tumours have adapted accordingly to survive under these conditions primarily through the activation of signalling pathways that allow for their survival. The lack of tumour vascularisation during early tumourigenesis is thought to contribute this state of hypoxia and the changes associated with this transition appear to constitute a cancer phenotype that remains even when oxygen is available.

The identification of hypoxia-inducible factor (HIF1), a transcription factor that activates the transcription of various genes in response to low levels of oxygen, was a principal finding in the understanding of how hypoxic tumours can survive under such conditions. HIF1, under normal oxygen tension, is targeted for degradation through a post-translational modification by prolyl hydroxylation. This promotes its association with the von Hippel-Lindau (VHL) tumour suppressor, targeting it for ubiquitination and thus proteosomal degradation (DeBerardinis *et al*, 2008; Jones and Thompson, 2009). However, during conditions of hypoxia, prolyl hydroxylation is inhibited and as a result the HIF1 complex is stabilised and able to up regulate a number of genes involved in energy metabolism and apoptosis including lactate dehydrogenase A (LDHA), pyruvate dehydrogenase kinase 1 (PDK1) and bcl2/adenovirus E1B 19kDa interacting protein 3 (BNIP3) (DeBerardinis *et al*, 2008; Lu *et al*, 2008; Jones and Thompson, 2009; reviewed in Semenza, 2010). The increased expression of LDHA, in response to HIF-1 activation, promotes the conversion of pyruvate to lactate and similarly the activation of PDK1 protein prevents the oxidation of pyruvate to acetyl CoA, which taken together increase glycolysis and decrease oxidative phosphorylation respectively (Fig. 1.9). Furthermore, the expression of BNIP3 has been associated with the induction of autophagy of mitochondria through disruption of the interaction of Beclin-1 (an autophagy related gene) with Bcl-2 (Zhang *et al*, 2008) and thus could be a survival mechanism for the tumours under such extreme conditions. In line with this, a recent study by Frezza and colleagues examined the metabolic profile of cancer cells under hypoxic conditions in an attempt to identify the exact effects of hypoxia on metabolism (Frezza *et al*, 2011). Here, they demonstrate an absolute requirement of autophagy for cell survival under hypoxic conditions and further demonstrated how cancer cells can survive under such extreme conditions (Frezza *et al*, 2011). These findings are significant for the identification of novel therapeutic cancer targets and, taken together, the hypoxic conditions encountered during the early stages of solid tumour cell

development have been regarded as the underlying cause of the metabolic switch (Wilson and Hay, 2011).

1.7 Aims

Since its discovery more than a decade ago, TRAIL has been at the forefront of scientific research largely because of its selectivity toward tumorigenic cells. The biological function of TRAIL and its selectivity, however, are still not completely understood and thus the research carried out in this thesis was designed to investigate the complex and dynamic TRAIL signalling cascade(s) by identifying and functionally characterising novel regulators and modulators of this pathway

The first results chapter (Chapter 3) of this thesis was performed to investigate known and novel TRAIL DISC components by mass spectrometry in order to identify any previously unidentified protein interactors that might regulate TRAIL-induced apoptosis. The mantle cell lymphoma cell line Z138 was characterised for its potential as a model for TRAIL DISC analyses and a tagged variant of TRAIL employed to capture the DISC. Potential interactors identified by mass spectrometry were examined by immunoblotting to confirm their interaction at the DISC and their potential to regulate TRAIL-induced apoptosis discussed. In the second results chapter (Chapter 4), the metabolic regulation of TRAIL-induced apoptosis was investigated using glucose-deprivation as a model system to inhibit glycolysis. Here, using Z138 cells, 2DG treatment and acute/chronic glucose-deprivation were assessed for their sensitising capabilities and comparisons between the different approaches made. Chronic glucose-deprivation was examined in more detail and the changes associated with this metabolic modulation were examined by bioenergetic, proteomic and ultra-structural examination and the role of glucose metabolism in modulating TRAIL-induced apoptosis discussed. The final results chapter (Chapter 5) aimed to investigate the modulated glucose metabolism from Chapter 4 in more detail, in particular by examining the gene and protein expression changes associated with this phenotype. These findings were then extended to determine their relevance in a clinical setting by examining patient samples of mantle cell lymphoma.

Together these aims permit two lines of parallel research in investigating novel regulators of TRAIL-induced apoptosis. The first being the examination of the TRAIL DISC directly through proteomic analyses and the second by analysing how changes in metabolic status can modulate TRAIL-induced apoptosis.

2. Materials and Methods

2.1 Materials

Unless otherwise stated, all materials were obtained from Fisher Scientific Ltd (Loughborough, UK). 2-deoxyglucose (2DG), albumin serum from bovine, ammonium persulfate, β -mercaptoethanol, bromophenol blue, digitonin, DMSO, FCCP, formaldehyde, glycerol, glycine, HEPES, imidazole, Kodak biomax XAR Film, *N*-acetylglucosamine (NAG), magnesium chloride, oligomycin, ponceau S, propidium iodide (PI), rotenone, saponin, sera from goat, sucrose, SDS, TEMED, triton-X-100 and tween 20 were all obtained from Sigma-Aldrich (Poole, UK). Acrylamide and protoblu safe Coomassie were obtained from Geneflow (Staffordshire, UK). Bio-Rad protein assay reagent and precision plus protein standard were both obtained from Bio-Rad (Herts, UK). ECL was obtained from GE Healthcare (Buckinghamshire, UK). FITC conjugated annexin V was obtained from Bender Medsystems (Vienna, Austria) and nitrocellulose membrane (Hybond C) from Amersham (Buckinghamshire, UK). *E. coli* (BL21-DE3) competent cells, IPTG, S.O.C media, kanamycin-sulphate, TMRE, RPMI 1640, DMEM, sodium pyruvate, dyna-M280 streptavidin beads, Mitotracker® Red, goat anti-mouse Alexa-488 antibody and Novex® TRIS-glycine gels were obtained from Invitrogen (Paisley, UK). Phycoerythrin (PE)-conjugated anti-human TRAIL-R1 and -R2 and PE-Mouse IgG1, κ isotope control were obtained from EBioscience (San Diego, USA). Tris, complete™ protease Inhibitor with/without EDTA and D-Biotinoyl- ϵ -amidocaproic acid-*N*-hydroxysuccinimide ester were obtained from Roche (Sussex, UK). Ni-NTA agarose beads were obtained from Qiagen (Sussex, UK). PNGase F/Endo H glycosidases were purchased from NEB (Hertfordshire, UK). The caspase-8 substrate ac-IETD.afc and the pan-caspase inhibitor zVAD.fmk were obtained from MP Biomedicals (Illkirch, France). BD cell-tak™ was obtained from BD Biosciences (Lutterworth, UK) and the ATP bioluminescence assay was purchased from Promega (Madison, WI). Cytochrome *c* antibodies for confocal were purchased from Pharmingen (San Jose, USA). Hoechst-33342 and Poly-L-Lysine slides were made-in house. ABT-737 was a kind gift from Dr. Ken Young (MRC Toxicology Unit). Recombinant TRAIL and TRAIL-R1/-R2 specific mutants were made in-house (MacFarlane *et al*, 1997; MacFarlane *et al*, 2005; Harper and MacFarlane, 2008).

2.2 Methods

2.2.1 Cell lines and culture conditions

The mantle cell lymphoma cell line Z138 (passage 2), a kind gift from Prof. Martin J.S Dyer (University of Leicester) (Estrov *et al*, 1998), was cultured in RPMI 1640 media supplemented with 10% FCS and 2 mM Glutamax and incubated at 37 °C under 5%

CO₂ in a humidified atmosphere. Cells were seeded at 0.1×10^6 /ml and passaged every 3 to 4 days.

The B-cell lymphoma cell line BJAB (passage 35) was generously provided by Dr Andrew Thorburn (University of Colorado Health Science Centre, USA) (Thomas *et al*, 2004) and was cultured in RPMI 1640 media supplemented with 10% FCS and 2 mM Glutamax and incubated at 37 °C under 5% CO₂ in a humidified atmosphere. The Jurkat cell line (Clone E6.1) (passage 20) was obtained from the ECACC and cultured as described for the BJAB cell line. The human cervical carcinoma cell line HeLa (passage 18) was obtained from the ATCC and cultured in Dulbecco's Modified Eagle's Medium containing 4.5g/litre glucose and supplemented with 10% FCS and 2 mM Glutamax. All cells were seeded at $0.1\text{-}0.2 \times 10^6$ /ml and passaged every 3 to 4 days

For glucose deprivation studies, glucose-containing Z138 cells were cultured in RPMI 1640 media (11 mM Glucose) supplemented with 10% FCS, 2 mM glutamax and 1 mM sodium pyruvate and incubated at 37 °C under 5% CO₂ in a humidified atmosphere. Glucose-free Z138 cells were cultured in RPMI 1640 (without D-Glucose) containing L-Glutamine supplemented with 10% FCS and 1 mM sodium pyruvate. Treatment with 2DG was performed in Z138 cells cultured in glucose-containing media supplemented with 5 mM 2DG for 20 h. FCS stock contained 0.52 mg/ml of glucose, which when diluted in its appropriate media gave a final glucose content of 0.047 mg/ml. These glucose deprivation models could, therefore, also be referred to as low glucose. However, the glucose provided by the FCS would be metabolised rapidly and thus may not have such an influence on the chronic glucose deprivation studies discussed in this thesis.

Primary mantle cell lymphoma cells were obtained from patients during routine diagnosis at the Leicester Royal Infirmary (UK) and were purified as described previously (MacFarlane *et al*, 2002). Samples were obtained with patient consent and local ethical committee approval (see Appendix 1).

2.2.2 Induction of apoptosis

Cells were seeded up to 48 h prior to treatment and harvested at a concentration of 1×10^6 cells/ml. Cells were then treated with various preparations of recombinant WT-TRAIL (Chapters 3, 4 and 5), R1-TRAIL (Chapter 4), R2-TRAIL (Chapter 4), ABT-737 Chapter 4 and 5) or methyl jasmonate (Chapter 5) as indicated in figure legends and

assessed for apoptosis induction. Alternatively, cells were irradiated using a Pantak X-ray unit at a dose of 35 GY and assessed for apoptosis induction at the indicated times post-radiation. Aliquots from apoptosis-induced cells were retained for analysis of caspase cleavage by immunoblotting (see 2.2.9 Immunoblotting). Briefly, control and treated cells (1×10^6) were centrifuged for 3 min at 200 g (4 °C), media removed and pellets washed twice in ice-cold PBS. Pellets were frozen and stored in -80 °C freezer until required or resuspended in 100 µl of SDS-sample buffer and analysed by immunoblotting.

2.2.3 Measurement of cell death

Apoptotic cells undergo a number of morphological changes that allow them to be distinguished easily from healthy cells. One such distinguishing feature is the externalisation of phosphatidylserine (PS) to the outer leaflet of the plasma membrane during apoptosis (Fadok *et al*, 1992; Martin *et al*, 1996). Annexin V is a naturally occurring protein with high binding affinity for PS and, thus, recombinant annexin V can be conjugated to the fluorescent dye Fluorescein Isothiocyanate (FITC) to label apoptotic cells (King *et al*, 1998; Brumatti *et al*, 2008). In addition, the membrane impermeable intercalating agent Propidium Iodide (PI) can be incorporated alongside annexin V-FITC staining to assess membrane integrity and hence the stage of apoptosis. Thus, externalisation of PS to the outer leaflet of the plasma membrane and PI incorporation were used as a measure of cell death following apoptotic stimulation as previously described (MacFarlane *et al*, 2002). Briefly, control and treated samples (approximately 0.2×10^6 cells) were transferred to annexin V-buffer (10 mM Hepes (pH 7.4), 150 mM NaCl, 5 mM KCl, 1mM MgCl₂, 1.8 mM CaCl₂) and incubated with 1.5 µl of appropriately diluted annexin V-FITC. Samples were then incubated at room temperature in the dark for between 10-30 min (depending on the cell line) followed by addition of PI (50 µg/ml). Samples were then incubated on ice for 2 min and PS⁺/PI⁺ cells analysed by flow cytometry on a FACSCalibur using the CellQuest Pro™ software version 5.2.1

Activation of the intrinsic pathway, and mitochondrial amplification loop of the extrinsic pathway, leads to mitochondrial membrane permeabilisation. Thus, loss of mitochondrial membrane potential (MMP) can be used as another distinguishing hallmark of apoptosis and this can be measured using the fluorescent dye Tetramethylrhodamine, ethyl ester, perchlorate (TMRE). In healthy cells, the membrane potential drives accumulation of TMRE in the mitochondria resulting in a punctate fluorescent signal. During apoptosis, mitochondria depolarise resulting in the

loss of TMRE to the cytoplasm where it becomes diffuse. This change in fluorescence intensity can be measured by flow cytometry. Thus, the loss of MMP was also used as a measure of cell death following apoptotic stimuli and was performed as described previously (Sun *et al*, 1999). Briefly, control and treated samples (approximately 0.2×10^6 cells) were transferred to pre-warmed media and incubated with 1 μ l of TMRE (50 μ M) for 10 min at 37 °C. Samples were then analysed by flow cytometry as described above.

2.2.4 Analysis of cytochrome c release by confocal microscopy

Z138 cells (1.5×10^6) treated for 0 to 6 h with 400 ng/ml TRAIL, were prepared for confocal microscopy analysis in order to visualise the loss of cytochrome c from the mitochondria. To identify the mitochondria, 25 nm of Mitotracker® Red was incubated with Z138 cells 15 min prior to the end of the treatment time. Cell suspensions were washed four times in PBS and resuspended in 250 μ l of PBS, a sample of which was transferred to poly-L-lysine coated slides and cells allowed to settle by incubating at room temperature for 30 min. Cells were fixed in 3.8 % formaldehyde for 10 min and washed with PBS before permeabilising in 3 % BSA and 0.1 % Saponin for 5 min at room temperature. The samples were then blocked for 1 h in 3 % BSA at room temperature before incubating with cytochrome c antibody for 1 h. After washing with PBS, secondary Alexa-Fluoro 488 goat anti-mouse antibody was incubated with the samples for 1 h at room temperature followed by washing with PBS. The cells were then stained with the DNA specific dye Hoechst-33342 for 10 min at room temperature in the dark. Slides were mounted with cover slips and stored at 4 °C in the dark before analysing with a Zeiss Axiovert LSM 510 microscope and images analysed on the LSM Image Browser Software.

2.2.5 Analysis of cytochrome c release by immunoblotting

Cytochrome c release was performed essentially as previously described (Bossy-Wetzel *et al*, 1998; Sun *et al*, 1999). Briefly, cells (10×10^6) were washed in ice-cold PBS and resuspended in cytochrome c lysis buffer (250 mM sucrose, 20 mM HEPES (pH 7.4), 5 mM $MgCl_2$, 10 mM KCl, 1 mM EDTA and 1 mM EGTA) containing 0.05 % digitonin and protease inhibitors. Cells were left on ice for 10 min followed by centrifugation at 18,000 g for 3 min, 4 °C. Supernatant and pellets were separated and analysed for cytochrome c by immunoblotting (see 2.2.10 Immunoblotting).

2.2.6 Analysis of hexokinase detachment from the mitochondria

Methyl jasmonate was used to bind and detach mitochondrial-bound hexokinase. For this, 10×10^6 Z138 cells cultured in glucose-free media were incubated with varying concentrations (0-9 mM) methyl jasmonate for 60 min. Samples were then separated into supernatant and mitochondrial fractions and the latter probed for the loss of hexokinase II by immunoblotting.

2.2.7 Preparation of cell lysates

Cells (5.0×10^6) were centrifuged at 200 g for 3 min at 4 °C, the media discarded and cell pellets washed three times in ice-cold PBS by repeated centrifugation and resuspension. The washed cells were lysed in lysis buffer (30 mM Tris/HCl (pH 7.5), 150 mM NaCl, 10% Glycerol, 1% Triton-X-100) containing Complete™ Protease Inhibitor with EDTA for 30 min on ice. The samples were centrifuged at 18,000 g for 20 min at 4°C and the resulting supernatant assessed for protein concentration using the Bradford Assay (see 2.2.10 Protein Concentration). Pellets were resuspended in 100 µl lysis buffer, snap-frozen on dry ice and stored at -80°C until analysis.

2.2.8 Protein expression

Glucose-containing, glucose-free, 2DG-untreated and 2DG-treated Z138 cells (5.0×10^6) were centrifuged at 200 g for 3 min at 4 °C and washed three times in ice cold PBS. Cell pellets were then resuspended in SDS-PAGE sample buffer, sonicated and analysed by immunoblotting.

2.2.9 TRAIL-receptor surface expression

TRAIL-R1 and -R2 surface receptor expression was examined as previously described (MacFarlane *et al*, 2002). Briefly, cell aliquots (1×10^6) were pelleted at 200 g for 3min (4°C), resuspended in 10% goat sera and incubated for 5 min at room temperature. PE-conjugated human antibodies for TRAIL-R1, TRAIL-R2 or IgG control were added to the respective cell suspensions and incubated on ice for 1 h in the dark. Cells were then washed twice in ice-cold PBS and centrifuged at 200 g for 3 min at 4°C. After washing, pellets were resuspended in 500 µl PBS and analysed by flow cytometry on a FACSCalibur using the CellQuest Pro™ Software. Antibody binding was assessed using a single-parameter histogram with 'cell count' on the y-axis and a log scale of the FL2-channel fluorescence on the x-axis.

2.2.10 Protein concentration

Protein concentration of cell lysates was determined using the Bio-Rad Protein Assay (Bradford, 1976). A standard curve using BSA (1-8 µg/ml) was prepared in triplicate and test samples analysed by transferring 10 µl of appropriately diluted sample into 990 µl of diluted dye reagent. Absorbance was measured on a spectrophotometer (Beckman Coulter) at 595 nm and compared against the standard curve.

2.2.11 Immunoblotting

Immunoblotting was performed as previously described (Harper *et al*, 2001). Briefly, samples were separated by SDS-PAGE using a TRIS/Glycine buffer system in a mini-protean tetra cell kit (Bio-Rad). After electrophoresis, gels were transferred to nitrocellulose membranes and stained with Ponceau S to assess for protein loading. Membranes were then probed with the indicated primary antibodies (Table 2.1) using standard protocols followed by incubation with the appropriate secondary antibody (Table 2.2). Antibody dilutions were selected as outlined in the data sheets provided by the manufacturer and/or indicated references (Table 2.1). Where the dilution does not match this information, subsequent antibody dilutions were made according to the quality of the western blot obtained at the time of analysis. Immunostained membranes were then visualised on X-ray film using the enhanced chemiluminescence (ECL) detection system as outlined in the manufacturer's protocol. Films were developed on a Compact X4 Xograph imaging system and scanned using Photoshop Elements version 7.

Table 2.1 Primary antibodies used for immunoblotting.

Antibody	Source	Dilution	Host	Catalogue/Reference
Caspase-8	In-house	1:2000	Rabbit	Sun <i>et al</i> , 1999
Caspase-3	Gift (Merck)	1:10,000	Rabbit	Chandler <i>et al</i> , 1998
Caspase-9	MBL	1:1000	Mouse	M054-3
TRAIL-R1 (DR4)	ProSci	1:1000	Rabbit	1139
TRAIL-R2 (DR5)	Cell Signalling	1:1000	Rabbit	3696
FADD	BD	1:250	Mouse	610400
cFLIP	Gift (Merck)	1:3000	Rabbit	Rasper <i>et al</i> , 1998
Bid	Gift (X.Wang)	1:1000	Rabbit	Luo <i>et al</i> , 1998
Bax	Upstate	1:500	Rabbit	06-499
Bak	Upstate	1:1000	Rabbit	06-536
Cytochrome <i>c</i>	BD	1:2000	Mouse	556433
Bad p-Bad (S136)	Cell Signalling	1:1000	Rabbit	9105
PUMA	ProSci	1:1000	Rabbit	3043
Noxa	Calbiochem	1:1000	Mouse	OP180
PARP	Alexis	1:2500	Mouse	804210
RIP	BD	1:500	Mouse	6559
Bcl-2	Dako	1:1000	Mouse	0887

Mdm2 (D7)	Santa Cruz	1:1000	Mouse	13161
Bcl-x _L	BD	1:1000	Rabbit	556361
Mcl-1	Santa Cruz	1:500	Rabbit	819
Bfl-A1	Gift (J.Borst)	1:2000	Rabbit	Werner <i>et al</i> , 2002
XIAP	BD	1:2000	Mouse	610716
p53	BD	1:1000	Mouse	554294
PPI α	Millipore	1:500	Rabbit	06-221
PP1 γ	Santa Cruz	1:500	Goat	6108
DEK	BD	1:1000	Mouse	610948
TFR1	BD	1:500	Mouse	612124
Cullin-3	Abcam	1:1000	Rabbit	72187
SOD2	Abcam	1:2000	Mouse	16956
Cox IV	Cell Signalling	1:1000	Rabbit	4844
VDAC2	Imgenex	1:1000	Goat	3279
SDHA	Cell Signalling	1:1000	Rabbit	5839
Hexokinase I	Santa Cruz	1:1000	Goat	6517
Hexokinase II	Santa Cruz	1:1000	Rabbit	2106
p-AKT	Cell Signalling	1:1000	Mouse	4051
GSK3 β	Cell Signalling	1:1000	Rabbit	9369
pGSK3 β	Cell Signalling	1:1000	Rabbit	9369
p-P70S6K	Cell Signalling	1:1000	Mouse	9206
IRS2	Cell Signalling	1:1000	Rabbit	4502
PGM3	Santa Cruz	1:1000	Mouse	100410
GAPDH	Abcam	1:5000	Mouse	2118
α -Tubulin	Calbiochem	1:1000	Mouse	CP06

Table 2.2 Secondary Antibodies used for immunoblotting

Antibody	Host	Source	Dilution
Anti-Rabbit	Goat	Dako	1:2000
Anti-Mouse	Goat	Sigma	1:2000
Anti-Goat	Rabbit	Dako	1:2000

2.2.12 Coomassie-blue Staining

Following electrophoresis, polyacrylamide gels were briefly deionised with water and incubated with a solution of the ProtobluTM/Ethanol mixture overnight at room temperature with gentle agitation. Gels were then destained in water or destain (400 ml Methanol and 100 ml Acetic Acid) and either analysed by mass spectrometry (see section 2.2.16) or briefly incubated in gel conserving buffer and stored accordingly.

2.2.13 Generation and purification of recombinant TRAIL

Recombinant TRAIL was generated in-house as previously described (MacFarlane *et al*, 1997). Briefly, competent cells were transformed with 200-400 ng of pET28b-TRAIL (residues 95-281) by incubating the mixture on ice for 30 min followed by heat shock treatment at 42 °C for 45 s. Cells were then incubated on ice for 2 min before adding 200 μ l S.O.C media and shaking at 37 °C for 45 – 60 min. Transformed bacteria were plated on LB-Agar plates containing 25 μ g/ml Kanamycin and incubated overnight at 37 °C. Single colonies were picked and used to inoculate 10 ml LB-media, which was

cultured overnight at 37 °C with constant shaking. Cultures were sub-cultured into 400 ml LB-media and grown at 37 °C for 3 h with constant shaking until cultures reached an OD ($\lambda 600$ nm) of between 0.6-0.8. Cultures were then induced with 1 mM IPTG for a further 3 h at 37 °C with constant shaking after which bacterial suspensions were centrifuged at 5000 rpm for 15 min. Pellets were washed once in ice cold PBS, snap frozen and stored at -80 °C until required. His-tagged TRAIL was then purified using nickel affinity purification as required.

2.2.14 Biotinylation of TRAIL

Recombinant TRAIL was biotinylated (bTRAIL) using D-Biotinoyl- ϵ -Amidocaproic Acid-N-Hydroxysuccinimide ester according to the manufacturer's instructions and as previously described (Harper and MacFarlane, 2008). Briefly, nickel-purified HIS-tagged TRAIL was washed resuspended in PBS and labelled with 2.5 μ l of D-Biotinoyl- ϵ -Amidocaproic Acid-N-Hydroxysuccinimide ester (20 mg/ml) (Roche) on an end-to-end shaker for 1 h at 4 °C. Beads were then washed in lysis buffer (see below) and eluted with 150 mM EDTA. Biotinylated TRAIL is then aliquoted and stored at -80 °C.

2.2.15 TRAIL DISC isolation

Isolation of TRAIL signalling complexes were performed essentially as previously described (Sprick *et al*, 2000; Harper *et al*, 2001; Harper and MacFarlane, 2008). Briefly, cells (60×10^6 - 1×10^9) were pre-treated with bTRAIL (500 ng/ml) for 1 h on ice followed by incubation at 37 °C for the indicated time. Cells were then washed three times with ice-cold PBS and lysed in DISC lysis buffer (30 mM TRIS/HCl (pH 7.5), 150 mM NaCl, 10% glycerol, 1% Triton X-100) containing Complete™ protease inhibitor on ice for 30 min. Lysates were cleared by centrifugation (15, 000 x g for 30 min at 4 °C) and bTRAIL complexes precipitated overnight at 4 °C using Dyna-M280 Streptavidin beads. bTRAIL complexes were then eluted from the beads by boiling at 95 °C for 5 min in 1 x sample buffer and the complex examined by immunoblotting or mass spectrometry analysis.

2.2.16 Measurement of DISC activity

Isolated TRAIL DISC complexes from Z138 cells cultured with or without glucose were examined for caspase-8 activity using ac.IETD.afc as previously described (Hughes *et al*, 2009). Briefly, Dyna beads containing DISC complexes were resuspended in caspase assay buffer (100 mM HEPES, 10 % Sucrose, 0.1% CHAPS and 10 mM DTT, pH 7.0) and cleavage of the fluorogenic substrate ac-IETD.afc was measured at 37 °C

on a Wallac Victor fluorometer at excitation and emission wavelengths of 400 nm and 505 nm, respectively.

2.2.17 Mass spectrometry

Shotgun proteomics using liquid chromatography tandem mass spectrometry (LC-MS/MS) was carried out by Ms. Rebekah Jukes-Jones of the protein profiling group, MRC Toxicology Unit and as described previously (Boyd *et al*, 2009).

(i) In-gel protein digestion

Gel slices (approximately 1-1.5 mm) were cut sequentially from the SDS-PAGE gel lanes and in-gel protein digestion was completed by one of two methods. Gel slices were either processed using the Montage In-Gel Digest_{ZP} kit (Millipore) (Pluskal *et al*, 2002) or using PCR plates (Axygen Scientific Inc.). Individual gel slices were destained in the destain buffers provided (Montage In-Gel Digest_{ZP} kit) or in 25 mM ammonium bicarbonate with 5 - 50 % acetonitrile. Destained gel slices were then dehydrated using 100 % acetonitrile and subsequently rehydrated with porcine trypsin solution (Promega, sequencing grade). With the Montage In-Gel Digest_{ZP} kit, the dehydrated gel piece and trypsin were incubated for 3 hr at 37 °C whilst incubation was completed overnight at 30 °C when the samples were processed in PCR plates. Tryptic peptides were extracted using either the extraction and elution buffers provided (Montage In-Gel Digest_{ZP} kit) or 0.2 % trifluoroacetic acid. Extracted tryptic peptides were concentrated to dryness and then solubilised in 5 % formic acid.

(ii) Mass spectrometry of tryptic peptides

Tryptic peptides were separated using a micro-capillary high-performance liquid chromatography nanoLC system (CapLC, Waters, Elstree, UK). The separated peptides were loaded onto an Atlantis[™] dC₁₈, 5 µm OPTI-PAK[™] trap column (Waters) in 0.1 % formic acid for pre-concentration. The peptides were eluted using a linear gradient of acetonitrile (7 - 80 %) over 50 min and directly loaded onto an Atlantis[™] dC₁₈, 3 µm analytical column (Waters). Eluate from the analytical column was loaded into the Q-TOF (quadrupole time of flight) mass spectrometer (Waters) through a nanospray Z ion source. The mass-to-charge ratio (*m/z*) of the ionized peptides was analyzed and, based on the ion signal intensity, peptides were selected for fragmentation and sequencing by tandem mass (MS/MS) spectrometry. The peptide spectra generated were used for protein identification through comparison to the non-redundant SwissProt database (<ftp://us.expasy.org/databases/>) using the MASCOT

program (Matrix Science, London, UK). Protein and peptide identification was validated using Scaffold (Proteome Software Inc.).

(iii) Quantitative proteomic analysis

To analyse quantitatively the abundance of a protein in the isolated bTRAIL DISC we calculated the spectral abundance factor (or SAF) of each individually identified protein and normalised to TRAIL-R2 to calculate the protein's normalised spectral abundance factor (or NSAF) (modified from Paoletti *et al*, 2006 and Zybaylov *et al*, 2006). The mathematical formulas for these are shown below:

$$SAF_K = (SpC/L)_K$$

$$NSAF_K = (SAF)_K / (SAF)_{TRAIL-R2}$$

The SAF for a protein *K* is its spectral count (*SpC*) divided by its length (*L*). The NSAF is then calculated by dividing the SAF of protein *K* by the SAF of TRAIL-R2 for all identified proteins.

2.2.18 Glycosidase treatment

Endoglycosidases can be used to determine whether or not a protein contains *N*-linked glycans. Thus, glycosylation of TRAIL DISC components was examined by digestion using Endoglycosidase H (Endo H) and N-Glycosidase F (PNGase F) following the manufacturer's protocol. Briefly, isolated DISC complexes were incubated with 1000 U of either EndoH or PNGase F for 2 h at 37 °C. After incubation, samples were diluted with SDS-PAGE sample buffer, heated to 95 °C for 5 minutes and analysed by immunoblotting.

Treatment of glucose-free Z138 cells to test for all types of glycosylation was carried out by incubating cells with 5 mM *N*-acetylglucosamine (NAG) for 2h followed by various concentrations of TRAIL (0-1000 ng/ml) for 4 h in the same media. Apoptotic cell death was then assessed as described previously.

2.2.19 Extracellular flux (XF) analysis

For bioenergetic analysis, measurements were made using the Seahorse XF24 Extracellular flux (XF) analyser essentially as previously described (Wu *et al*, 2007; Capasso *et al*, 2010) and following the manufacturer's instructions. Briefly, 4.0×10^5 Z138 cells/well were adhered to XF 24-well cell culture microplates (Seahorse

Biosciences) using BD Cell-Tak™ and plates incubated at 37 °C for 1 h prior to XF analysis. FCCP, rotenone and oligomycin were loaded into drug delivery ports and added sequentially at the indicated time points. XF assay medium was low-buffered bicarbonate-free DMEM (pH 7.4) containing either: 11 mM Glucose, 1 mM pyruvate, 2 mM Glutamax (glucose-containing cells); 1 mM pyruvate, 2 mM Glutamax only (glucose-free cells); 11 mM Glucose, 2 mM glutamax without (-) or with (+) 2-deoxyglucose for control and treated 2DG samples, respectively. Assays were initiated by washing cells in their respective assay media (described above) twice followed by incubation at 37 °C for 1 h to allow media temperature and pH to equilibrate prior to analysis.

2.2.20 ATP measurements

Cellular ATP content was determined using a bioluminescence assay as outlined in the manufacturer's protocol. Essentially, Z138 cells were transferred to opaque-walled 96 well plates and allowed to equilibrate for 30 min at room temperature. CellTiter-Glo® reagent, equal to the volume of cell culture media, was added and the contents mixed on an orbital shaker for 2 min followed by 10 min incubation at room temperature. ATP content was measured using a luminometer.

2.2.21 Subcellular fractionation

1.5×10^9 cells were washed in PBS, pelleted and resuspended in homogenisation buffer (10 mM KCl, 1.5 mM $MgCl_2$, and 10 mM HEPES-KOH, pH 7.5) and left on ice for 10 min. Cells were homogenised using a glass dounce homogeniser (50 strokes) and diluted in 2.5 x volume of concentrated mannitol/sucrose buffer (525 mM mannitol, 174 mM sucrose, 2.5 mM EDTA, 12.5 mM Hepes-KOH [pH 7.5]). The cell suspension was centrifuged (3500g/10 min) to remove nuclei and then centrifuged at 11000g for 10 min to pellet mitochondria and remove the cytosolic (supernatant) fraction. Mitochondria were resuspended in mannitol/sucrose resuspension buffer (200 mM mannitol, 70 mM sucrose, 1 mM EGTA, 10 mM HEPES-KOH [pH 7.5] containing protease inhibitors. Samples were then assayed for the indicated proteins by immunoblotting.

2.2.22 Electron microscopy

Electron microscopy was carried out by Dr. D Dinsdale at the MRC Toxicology Unit. Briefly, Z138 cells were fixed in 2% glutaraldehyde in 0.1 M sodium cacodylate buffer [pH 7.4] at 4° C overnight and postfixed with 1% osmium tetroxide/1% potassium ferrocyanide for 1 h at room temperature. After fixation, cells were stained en bloc with

5% aqueous uranyl acetate overnight at room temperature, dehydrated, and embedded in Taab epoxy resin (Taab Laboratories Equipment Ltd., Aldermaston, UK). Electron micrographs of ultrathin sections were recorded using an ES1000W CCD camera and Digital Micrograph software (Gatan, Abingdon, UK) in a Zeiss 902A electron microscope

2.2.23 Microarray Analysis

Microarray analysis of glucose-containing and glucose-free Z138 cells was performed in collaboration with the Systems Toxicology Group, MRC Toxicology Unit and as previously described (Pointon *et al*, 2010). Briefly, two colour microarrays with reverse labelling were carried out using a full-genome human oligo array (70mer) with exon centred probes (Human Exonic Evidence Based Oligonucleotide) (Invitrogen). A total of 49, 000 probes were covered, including various spike-ins, non-coding RNA and control spots, and were printed in-house using an Inkjet style ArrayJet Printer (AJ120 Ultra-Marathon) over two aldehyde slides (Genetix). Total RNA was extracted from glucose-containing or glucose-free cells using a miRNeasy Mini Kit (Qiagen), as outlined in the manufacturers protocol, and labelled using the Low Input Quick AMP Labelling Kit (Agilent), also as described by the manufacturer. Labelled cRNA was then purified using an RNeasy MiniElute Clean-up Kit (Qiagen) and dye incorporation assessed using a nanodrop ND-1000 UV Spectrophotometer (Nanodrop Technologies). cRNA was then fragmented using fragmentation reagent (Ambion) and samples hybridised on to the microarray slides overnight at 42 °C. Following hybridisation, slides were washed three times under increasingly stringent buffer conditions containing Saline-Sodium Citrate (SSC), the first of which also contained SDS, followed by centrifugation at 200 g for 4 min to dry. Slides were scanned using an Axon 4200A scanner with Genepix 6.0 software. For each analysis three biological repeats were used each with two technical repeats (reverse labelling). Raw data files from each scanned image underwent lowness normalisation followed by one sample, two labelling *T*-test to generate a list of significantly altered genes. This list was refined using a *p* value of ≤ 0.05 (statistical significance threshold) and a fold-change of ≥ 1.45 for up regulated genes and ≥ 0.75 for down regulated genes (biologically significant difference). This gave a final list of potentially interesting candidates. The analysis programmes applied to this study were StatsOR and NorTT, both in-house programmes generated developed by Dr Shu-Dong Zhang.

2.2.24 Polysome Profiling

Polysome profiles were performed in collaboration with the Gene Expression Profiling Group at the MRC Toxicology Unit and as previously described (Johannes and Sarnow, 1998; Powley *et al*, 2009).

(i) Sucrose Density Gradients

10-60 % sucrose density gradients were prepared in 12 ml polyallomer centrifuge tubes (Sorvall, USA). Seven different sucrose solutions were prepared containing 300 mM NaCl, 15 mM MgCl₂, 15 mM TRIS/HCl (pH 7.5), 0.1 mg/ml cyclohexamide, 1 mg/ml heparin and sucrose concentrations of 10%, 18%, 26%, 34%, 42%, 50% and 60%. 0.5 ml of 60 % sucrose solution was added to a gradient tube and frozen at -80 °C. 1.6 ml additions of the remaining sucrose solutions were added sequentially allowing each layer to freeze before addition of the next. Sucrose gradients were stored at -80 °C and allowed to thaw slowly before use.

(ii) Polysome Profiling

Briefly, cyclohexamide was added to cells at a final concentration of 100 µg/ml and samples incubated at 37 °C for 3 min. Cells were then washed twice in PBS containing 100 µg/ml Cyclohexamide. Pellets were resuspended in 1 ml polysome lysis buffer (15 mM TRIS/HCl (pH 7.5), 300 mM NaCl, 15 mM MgCl₂, 0.1 mg/ml Cyclohexamide, 1% Triton X-100 and 1 mg/ml Heparin) and centrifuged at 4000 rpm for 4 min at 4 °C. The supernatants were then gently loaded onto 10-60 % sucrose density gradients and centrifuged at 38,000 rpm for 2 h at 4 °C. Gradients were then fractionated through a Teledyne ISCO Foxy R1 Fractionator and continuously measured at 254 nm by a Teledyne ISCO UA-6 UV detector. The gradient solutions were collected in 1 ml fractions and stored at -80 °C in 50 % ethanol and 7.7 M guanidine HCl.

3. Proteomic Analysis of the TRAIL Death-Inducing Signalling Complex

3.1 Introduction

TNF-Related Apoptosis Inducing Ligand (TRAIL) has, since its discovery, undergone extensive scientific research into its biological function and mode of action largely because of its ability to induce apoptosis in transformed cells whilst sparing most normal cells. TRAIL mRNA is found constitutively expressed in a number of tissues (Wiley *et al*, 1995) although its protein expression is largely associated with cells of the immune system, such as Natural Killer (NK) and Cytotoxic T cells, where it is induced in response to various stimuli (reviewed in Falschlehner *et al*, 2009). TRAIL-deficient mice, however, are viable and show no obvious developmental defects (Cretney *et al*, 2002; Sedger *et al*, 2002). Instead they show increased susceptibility to tumour development and metastasis (Cretney *et al*, 2002). Thus, TRAIL appears to play an important role in immuno-surveillance against tumours. It is important to note, however, that mice only express one form of TRAIL-receptor, termed mDR5, and thus the physiological role of TRAIL in humans may differ somewhat (Wu *et al*, 1999). Nevertheless, studies carried out in cell lines, patient samples and clinical trials have provided valuable evidence as to the potential cancer therapeutic properties of TRAIL in humans. For example, numerous human tumour derived cell lines (such as Glioma LN18, Breast MDA-MB-231 and prostate DU145 cells), tumour xenografts and human tumour cells transplanted into mice, have displayed marked sensitivity to TRAIL-mediated apoptosis (reviewed in Ashkenazi, 2002). Studies carried out in primary tumour cells, however, have not been so clear and rather early findings suggest resistance of these cells to TRAIL-induced apoptosis (MacFarlane *et al*, 2002; Pasquini *et al*, 2006; Dyer *et al*, 2007). Despite this, TRAIL remains as a potential cancer therapeutic agent because of its distinct and potentially selective anti-tumour properties. Thus, clinical trials involving TRAIL and several agonistic antibodies against TRAIL-R1 and -R2, termed Pro-Apoptotic Receptor Agonists (or PARA's), have been tested with varying successes (reviewed in Ashkenazi, 2008 and discussed in Chapter 6).

The underlying cause for TRAIL selectivity has not yet been determined and key questions about this death ligand remain unanswered, such as why are some cancer cells sensitive to TRAIL and others not? And how does the formation and activation of the Death-Inducing Signalling Complex (DISC) influence this? Finding the answers to these questions could prove insightful in determining key regulators of TRAIL-induced apoptosis and ascertain the underlying cause for the resistance of some primary tumours to TRAIL. Therefore, based on this, the research carried out in this chapter

aimed to identify and functionally characterise novel protein components involved in the formation and/or activation of the TRAIL DISC.

Studies into the absolute composition of both the CD95 and TRAIL DISC have been reported previously. For example, Harper *et al* identified Receptor Interacting Protein 1 (RIP1) as a component of the TRAIL DISC in HeLa and HEK293 cells (Harper *et al*, 2001) although it was found not to be present in TRAIL DISC isolated from BJAB cells (Kischkel *et al*, 2000). Similarly, additional studies over the years have provided evidence for other novel DISC interactors, the majority of which have been linked to CD95L and its receptor complex (Yang *et al*, 1997; Imai *et al*, 1999; Ryu *et al*, 2003; Lavrik *et al*, 2006) although some reports have examined the TRAIL DISC (Miyazaki *et al*, 2001). Many of these findings are based on yeast-two hybrid and immunoprecipitation experiments and, interestingly, the actual involvement of the majority of these interactors has subsequently been disputed (Koonin *et al*, 1999; Villunger *et al*, 2000; Berger and Kretzler, 2002). As a result, to date only the TRAIL-receptors, FADD, caspases-8/-10 and cFLIP have been confirmed as consistently identified DISC components. A more recent study, however, using a tandem affinity purification approach linked with mass spectrometry analysis, identified two novel components of the TNF-R1 signalling complex (Haas *et al*, 2009). These novel components, termed HOIL-1 and HOIP, were shown to ensure stability of the TNF-R1 complex through formation of ubiquitin chains and are proposed to be key novel regulators of this signalling pathway (Haas *et al*, 2009). This shows that the use of mass spectrometry in analysing known and identifying novel protein components of a signalling complex can identify new protein interactors. Thus, the research carried out in this chapter is based on a similar hypothesis whereby mass spectrometry analyses were performed to examine protein components of the TRAIL DISC. Previous work in the laboratory had identified the mantle cell lymphoma line (MCL) Z138 as a particularly sensitive model for TRAIL-induced apoptosis. Therefore, in line with this, the Z138 cell line was used as a model for investigating known and novel TRAIL DISC interactors.

Initially, the Z138 cell line was characterised with respect to TRAIL-signalling including analysis of caspase-8/-3 cleavage and cell death; Bid cleavage, the loss of mitochondrial membrane potential (MMP) and release of cytochrome c from the mitochondria; TRAIL-receptor surface expression, optimal TRAIL DISC formation and analysis of TRAIL-receptor glycosylation. Following this, the TRAIL DISC was isolated from cells for mass spectrometry analysis and label-free quantitative analysis applied

to determine significant protein 'hits' to follow up. These were then examined by immunoblotting of isolated TRAIL DISC components and their potential role as regulators of this pathway explored.

3.2 Results

3.2.1 Characterisation of the Mantle Cell Lymphoma Cell Line, Z138

The Z138 cell line was originally derived from a patient initially diagnosed as having B-cell chronic lymphocytic leukaemia (CLL) but was later redefined, as a result of improvements in lymphoma classification, as a form of mantle cell lymphoma (MCL) (Estrov *et al*, 1998; Medeiros *et al*, 2006). MCL is an aggressive subtype of B-cell lymphoma characterised by the presence of the t(11;14)(q13;q32) translocation and consequently the over-expression of cyclin-D1 (Drexler, 2002; Tucker *et al*, 2006). Cyclin-D1 is a regulator of the cell cycle and its over-expression has been linked to the development of cancers (Alao, 2007). Other MCL cell lines, in order of decreasing TRAIL sensitivity, have been described and include UPN-1, HBL-2, Jeko-1, REC-1, GRANT 519 and JVM-2 (Roué *et al*, 2007). In addition, varying responses to TRAIL-induced apoptosis have been identified in other lymphoma cell line models such as the Burkitt's Lymphoma cell line BJAB, which is sensitive (Sprick *et al*, 2000), and the T cell leukaemia cell line Jurkat, which is relatively insensitive (MacFarlane *et al*, 2002).

(i) Z138 cells display a concentration- and time-dependent sensitivity to TRAIL

To characterise the sensitivity of Z138 cells to TRAIL-induced apoptosis, cells were incubated with various concentrations of recombinant TRAIL for 4 h or 400 ng/ml of TRAIL for various times and assessed for cell death and caspase-8 and -3 cleavage (Fig. 3.1). Procaspase-8 (p55/53) processing to p43/41 was detected with 100 ng/ml TRAIL followed by processing to the p18 subunit with 200 ng/ml (Fig 3.1a). Procaspase-3 (p32) processing was apparent between 100-200 ng/ml TRAIL with formation of active caspase-3 (p20), and its further cleavage to p17, clearly evident with 200 ng/ml TRAIL (Fig. 3.1a). An increase in cell death, in TRAIL treated cells, was observed between 50-100 ng/ml of TRAIL (Fig. 3.1a). Subsequently, Z138 cells were incubated with 400 ng/ml of TRAIL for various times and the rate of caspase-8 and -3 cleavage assessed (Fig. 3.1b).

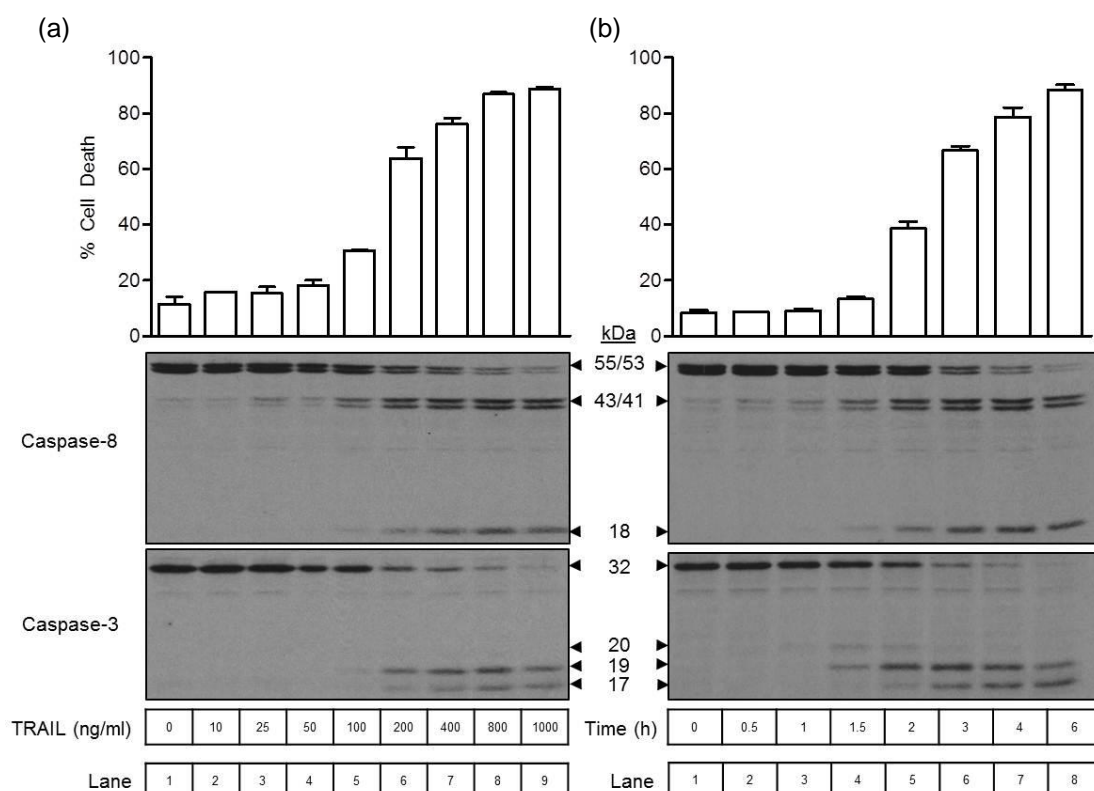


Figure 3.1 Z138 cells display a concentration- and time-dependent sensitivity to TRAIL. (a) Z138 cells were incubated with 0-1000 ng/ml TRAIL for 4 h and assessed for % cell death and cleavage of caspase-8 and -3 as outlined in Materials and Methods. (b) Z138 cells were incubated with 400 ng/ml TRAIL for the indicated times (0-6 h) and assessed for % cell death and processing of caspase-8 and -3. % cell death data represents mean \pm SEM (n=3). Immunoblots are representative of three independent experiments.

Procaspase-8 processing to p43/41, followed by the generation of p18, was evident at 1.5 h after TRAIL treatment with reduced full length caspase-3 evident between 1.5 and 2 h incubation and its cleavage to the p20/19/17 subunits thereafter (Fig. 3.1b). The amount of cell death clearly increased following a 1.5 h incubation period with TRAIL (Fig. 3.1b). Taken together, these results showed that Z138 cells were sensitive to TRAIL in a concentration- and time-dependent manner.

(ii) Z138 cells display rapid cleavage of Bid and subsequent loss of mitochondrial membrane potential when treated with TRAIL

As described Chapter 1, death receptor-mediated apoptosis can induce cell death via a Type I caspase-8 mediated caspase-3/7 cleavage route or alternatively through a Type II mitochondrial amplification loop involving cleavage of Bid (Scaffidi *et al*, 1998; Luo *et al*, 1998). Therefore, in order to determine the involvement of the mitochondrial amplification loop in TRAIL-induced apoptosis in Z138 cells, cells were incubated with 400 ng/ml TRAIL for various times and assessed for Bid cleavage and loss of mitochondrial membrane potential (MMP) – two key markers for activation of the mitochondrial cell death pathway (Heiskanen *et al*, 1999) (Fig. 3.2). Loss of full-length

Bid in Z138 cells, which is expressed as a 22 kDa protein, was observed after 1 h incubation with TRAIL (Fig. 3.2a, lane 2 and 3). An increase in the loss of MMP was also evident after 1 h of TRAIL treatment and reached a peak after 4 h incubation, which was reflected in the near complete loss of full length Bid at this time point (Fig. 3.2a, lane 5).

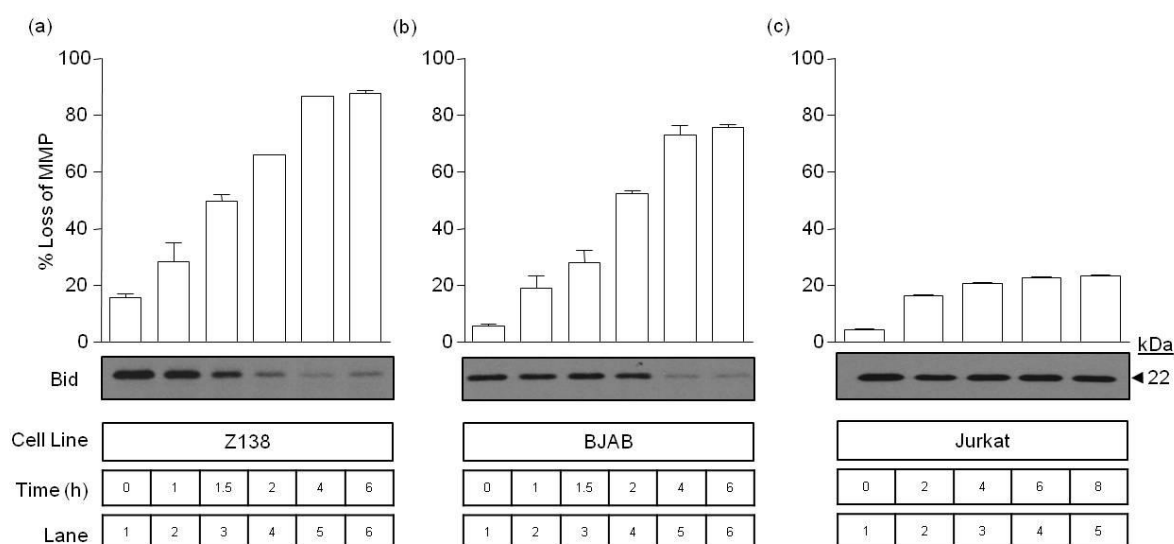


Figure 3.2 Z138 cells display rapid cleavage of Bid and subsequent loss of mitochondrial membrane potential when treated with TRAIL. Z138 (a), BJAB (b) and Jurkat (c) cell lines were incubated with 400 ng/ml TRAIL for the indicated times (Z138 and BJAB 0-6 h; Jurkat 0-8 h) and assessed for both loss of mitochondrial membrane potential (MMP) and loss of full-length Bid. % loss of MMP represent mean \pm SEM (n=3) where immunoblots are representative of three independent experiments.

When compared to known Type I and II cells - BJAB and Jurkat cell lines, respectively (Scaffidi *et al*, 1998), Z138 cells show more rapid loss of Bid than the BJAB cell line suggesting more prominent Type II behaviour (Fig. 3.2a-b). However, the Jurkat cell line appeared relatively resistant to TRAIL with both minimal Bid cleavage and loss of mitochondrial membrane potential (Fig. 3.2c). As a result, this does not show Type II signalling to its full extent. Furthermore, in Z138 cells, the loss of full length Bid occurred concomitantly with cleavage of caspase-3 (Fig. 3.1b and Fig. 3.2a), thus demonstrating a significant role for both the extrinsic and mitochondrial-mediated apoptotic pathways. Therefore, these data show that Z138 cells can signal to apoptosis through both a Type I and II mechanism.

(iii) Cytochrome c release from the mitochondria correlates with loss of mitochondrial membrane potential

The cleavage of Bid and its subsequent translocation to the mitochondria induces loss of MMP and triggers the release of pro-apoptotic mediators such as cytochrome c (Desagher *et al*, 1999). Cytochrome c release from the mitochondria can therefore also

be used to provide further evidence for activation of the mitochondrial-mediated cell death pathway. For this, fixed and permeabilised Z138 cells were incubated with an antibody to cytochrome *c* to enable its subcellular localisation to be determined by confocal microscopy in response to TRAIL-treatment (Fig. 3.3).

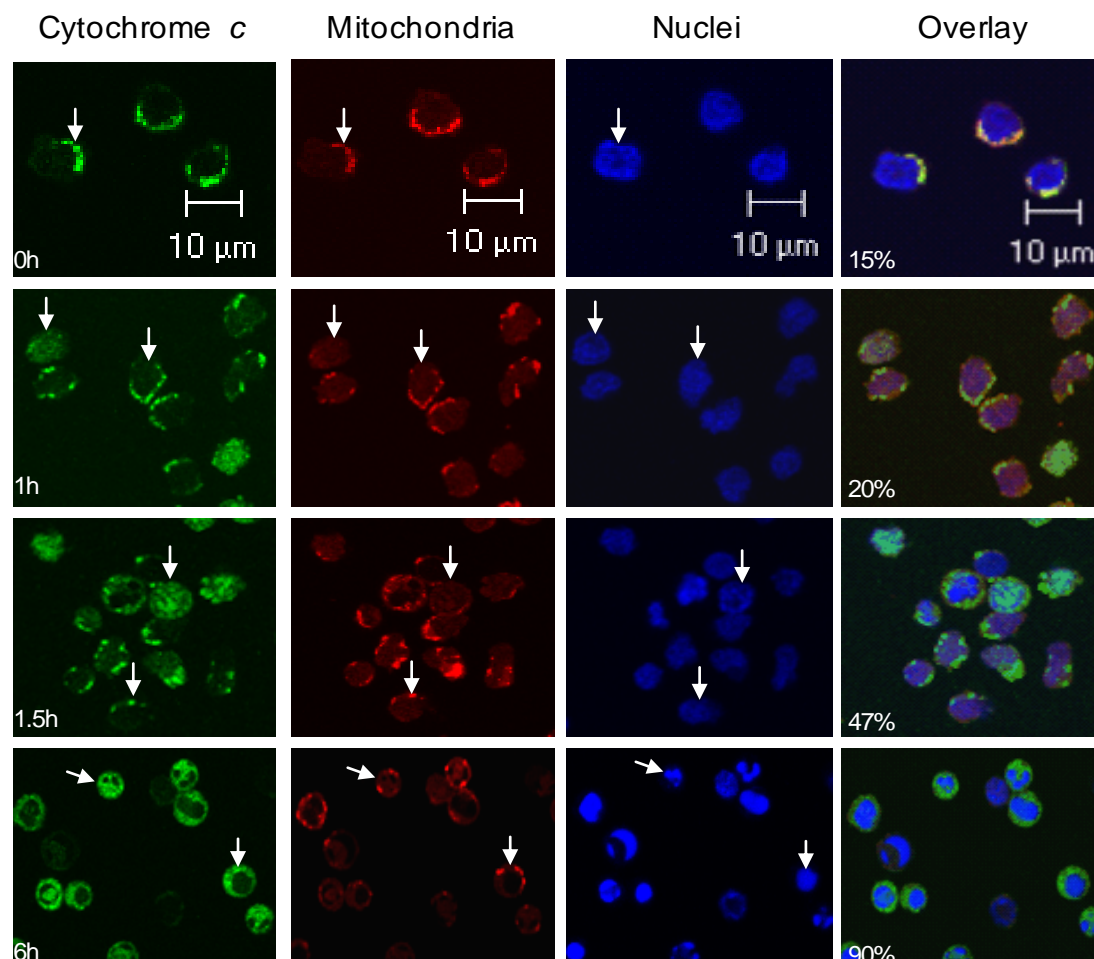


Figure 3.3 Cytochrome *c* release from the mitochondria correlates with loss of mitochondrial membrane potential. Z138 cells were treated for 0–6 h with 400 ng/ml TRAIL and incubated with Mitotracker® Red 15 min prior to the end of treatment. Cells were washed in PBS and fixed in 3.8 % formaldehyde for 10 min. Cells were permeabilised and incubated with cytochrome *c* antibody for 1 h followed by 1 h incubation with secondary goat anti-mouse Alexa-fluoro-488 antibody. Excess antibody was removed by washing in PBS followed by staining with Hoechst-33342 for 10 min. Data shown are from one of three experiments. Results shown are representative of several images. Only selected time points are shown. Indented values on the right represent % cells with loss of MMP as measured by flow cytometry using TMRE and indented values on the left represent time-point of TRAIL treatment. Arrows indicate the position of cytochrome *c*, mitochondria and nuclei in control (0 h) cells.

Control Z138 cells (0 h) display punctuate cytochrome *c* fluorescence in areas where Mitotracker® red is visible (Fig. 3.3 – 0 h arrows), which is indicative of cytochrome *c* retained within the mitochondria. Hoechst staining demonstrated large, slightly indented nuclei reminiscent of viable cells (Fig. 3.3 – 0 h arrows). After 1h incubation with TRAIL, a number of cells displayed diffuse areas of cytochrome *c* fluorescence suggesting that mitochondria are beginning to become permeabilised (Fig. 3.3 – 1 h

arrows). However, the majority of the cells are similar to control cells and this coincides with the minimal changes observed earlier in the loss of MMP (Fig. 3.2).

Following 1.5 h incubation with TRAIL most of the cells showed diffuse areas of cytochrome *c* fluorescence concurrent with both a 47 % loss in MMP and a release of cytochrome *c* from mitochondria (Fig. 3.2 and Fig. 3.3 – 1.5 h arrows). At 6 h, however, Z138 cells displayed a near complete loss of mitochondrial cytochrome *c* and, furthermore, these cells had visibly condensed fragmented nuclei indicative of cells undergoing apoptosis (Fig. 3.3 – 6 h arrows). Similarly, there was a 90 % loss of MMP at this time point (Fig. 3.2) and this was reflected in the confocal images (Fig. 3.3). Thus, TRAIL induced a time-dependent loss of cytochrome *c* from the mitochondria further demonstrating that Z138 cells actively signal to apoptosis through the mitochondrial amplification loop.

(iv) Cellular levels of pro- and anti-apoptotic proteins in Z138 cells

The cellular levels of pro- and anti-apoptotic proteins can influence the sensitivity of cancer cells to TRAIL-induced apoptosis. Therefore, to examine the protein expression levels of key apoptotic proteins in Z138 cells, lysate samples from unstimulated cells were analysed by immunoblotting for the expression levels of the indicated proteins and compared to those found in the prototype Type I and II BJAB and Jurkat cell lines (Fig. 3.4).

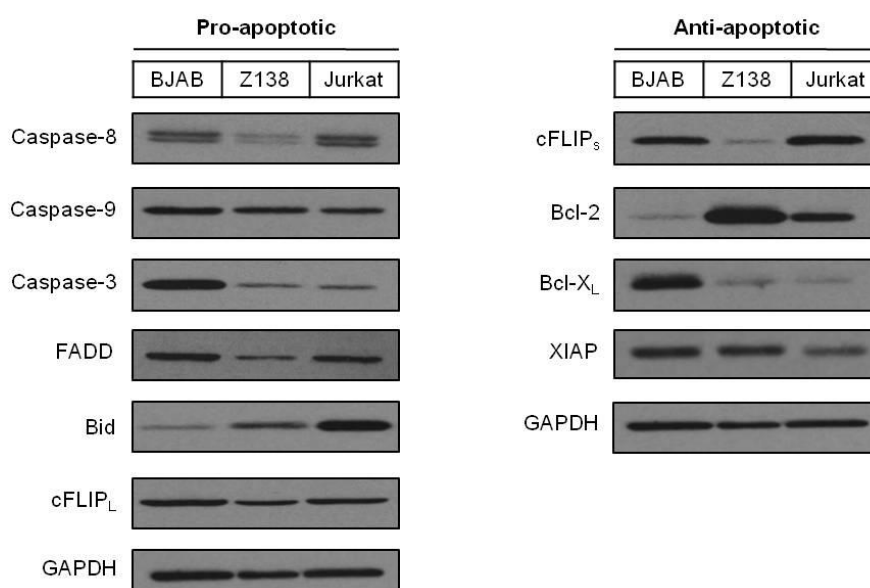


Figure 3.4 The expression levels of key pro- and anti-apoptotic proteins. 20 µg of unstimulated lysates from BJAB, Z138 and Jurkat cells were analysed for the protein expression levels of the indicated proteins. Immunoblots are from one experiment and are representative of at least three independent experiments.

In comparison to the BJAB and Jurkat cell lines, Z138 cells display marked differences in the cellular levels of Bid and Bcl-2 (Fig. 3.4). Z138 cells have significantly elevated levels of Bcl-2 and it has been previously suggested that Z138 cells are a Bcl-2 over-expressing cell line (Tucker *et al*, 2008). Elevated levels of Bcl-2 have been linked to the inhibition of cell death signalling through the mitochondrial amplification loop and this is often a feature of Type II cells (Scaffidi *et al*, 1998). However, the data discussed earlier indicates that Z138 cells can signal efficiently to cell death through the mitochondrial amplification loop despite their constitutively high levels of Bcl-2.

The expression level of Bid in Z138 cells was less than that observed in the Jurkat cell line but more than the levels observed in the BJAB cell line (Fig. 3.4). Thus, the relative levels of Bid (and caspase-3) in BJAB and Jurkat cells could in part explain their propensity for Type I and II status, respectively. Z138 cells have relatively similar levels of caspase-3 and Bid (Fig. 3.4) and this, in part, may explain their ability to signal to cell death through both pathways.

Similar to the data shown in Figure 3.4, Roué and colleagues examined the protein expression levels of key apoptotic regulators in a range of MCL cell lines, excluding Z138 cells (Roué *et al*, 2007). They observed that both the long (cFlip_L) and short (cFlip_S) isoforms of cFLIP were over-expressed in the MCL cell lines that demonstrated resistance to TRAIL-induced apoptosis (Roué *et al*, 2007). Z138 cells, however, were sensitive to TRAIL-induced apoptosis and expressed both cFLIP_L and cFLIP_S (Fig. 3.1 and Fig. 3.4). Thus, cFLIP expression in Z138 cells does not appear to confer resistance to TRAIL; on the contrary it should be noted that cFLIP_S levels in Z138 cells are considerably lower than those observed in the BJAB and Jurkat cell lines (Fig. 3.4). In these analyses I have categorised cFLIP_L as pro-apoptotic and cFLIP_S as anti-apoptotic (Fig. 3.4). However, it should be noted that cFLIP_L is only pro-apoptotic up to a threshold since saturation of this protein, in the DISC, inhibits caspase-8 activation due to its lack of inherent enzymatic activity (see 3.3 Discussion). This also remains true for the subsequent chapters.

(v) Z138 cells express both TRAIL-R1 and -R2 on their surface

As discussed in Chapter 1, unlike other death-ligands, TRAIL can bind to any one of five different receptors – TRAIL-R1 (DR4), -R2 (DR5), -R3 (DcR1), -R4 (DcR2) and Osteoprotegerin (OPG) (reviewed in Ashkenazi, 2002). However, not all of these receptors are capable of promoting apoptosis upon ligation of TRAIL and rather TRAIL-R3, -R4 and OPG, act as decoy receptors to prevent apoptotic signalling (Ashkenazi

and Dixit, 1998; Kimberley and Screaton, 2004). Initially, altered levels of these decoy receptors were thought to contribute to the marked sensitivity to TRAIL displayed in tumour cell lines but not the majority of normal cells. However later studies disproved this hypothesis (Kim *et al*, 2000; MacFarlane *et al*, 2002) and rather TRAIL signals to cell death predominantly through either TRAIL-R1 or TRAIL-R2 depending on the cell type (MacFarlane *et al*, 2005). Accordingly, I therefore determined the relative abundance of TRAIL-R1 and -R2 on the surface of unstimulated Z138 cells (Fig. 3.5). As shown in Figure 3.5, Z138 cells express both TRAIL-R1 and TRAIL-R2 on their surface (Fig. 3.5). In contrast to the Type I BJAB cell line, Z138 cells express considerably less TRAIL-R1 and -R2 on their surface (Appendix 2) (Sprick *et al*, 2000) but have similar levels of TRAIL-R2 to that of the Type II Jurkat cell line (Appendix 2) (MacFarlane *et al*, 2002). Despite these differences, the data confirm that Z138 cells express both TRAIL-R1 and -R2 on their surface. Taken together, these data show that Z138 cells contain all of the essential components (receptors, FADD, caspase-8) required for DISC formation and can therefore successfully signal to cell death when exposed to TRAIL.

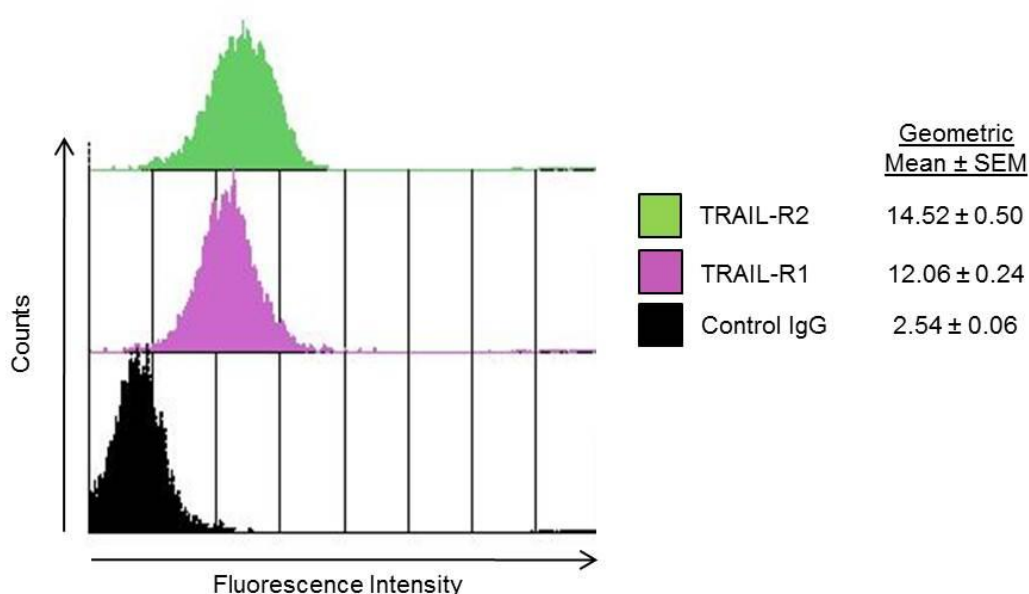


Figure 3.5 Z138 cells express both TRAIL-R1 and -R2 on their surface. Z138 cells were labelled with PE-conjugated TRAIL-R1, -R2 or IgG antibodies as described in Materials and Methods. The black fill represents isotype control, the purple fill represents surface expression of TRAIL-R1 and the green fill represents surface expression of TRAIL-R2. The numbers to the right are the geometric mean \pm SEM (n=3). Graph shown is representative of three independent experiments.

(vi) Optimisation of TRAIL DISC formation in Z138 cells

DISC formation is a key step in the extrinsic pathway of apoptosis. Briefly, ligation of a TRAIL homotrimer induces trimerisation of TRAIL-R1 and/or -R2 leading to the

recruitment of the adaptor molecule: Fas-associated death domain (FADD). Subsequently, FADD recruits the death effector domain (DED)-containing initiator caspase: procaspase-8, resulting in formation of the DISC (reviewed in MacFarlane, 2003). Formation of the DISC primarily allows for the activation of caspase-8, which in turn instigates a caspase cascade involving activation of the executioner caspases and thus cell death.

TRAIL DISC can be isolated and examined using recombinant affinity tagged versions of soluble TRAIL (Wiley *et al*, 1995). For this study, a biotinylated variant of soluble TRAIL (bTRAIL) was used to affinity purify the DISC, in accordance with previously published reports, and streptavidin coated beads, with high affinity for biotin, were used to efficiently recover the captured TRAIL DISC (Sprick *et al*, 2000; Harper *et al*, 2001; Drakas *et al*, 2005; Harper and MacFarlane, 2008). Initial experiments were performed to optimise the time required for maximal DISC formation in Z138 cells (Fig. 3.6).

Z138 cells were incubated with or without (Untreated - UT) bTRAIL for 1 h at 4 °C to prevent internalization and enable maximal interaction of TRAIL, with its receptors, at the cell membrane (Algeciras-Schimmich *et al*, 2002; Kohlhaas *et al*, 2007). Following this, cells were incubated at 37 °C for the times indicated to induce maximal DISC formation (Fig. 3.6). Although TRAIL DISC can be detected following 1 h at 4°C (Fig. 3.6 lane 2), that is DISC formation without full activation, it is evident that Z138 cells require a further incubation at 37 °C to ensure optimal DISC formation/activation (Fig. 3.6 lanes 3-6,). Thus, the results show that with increasing time of incubation (0 - 30 min) at 37 °C the amount of captured DISC increases (Fig. 3.6 lanes 3-6). Binding of TRAIL-R1 and -R2, together with the recruitment of FADD and caspase-8, were detected after ~10 min incubation at 37 °C and were accompanied by the partial processing of caspase-8 to the p43/41 fragment. Maximal DISC formation was achieved in Z138 cells with incubation of TRAIL for 25 min at 37 °C (Fig. 3.6 lane 5). Interestingly, analysis of the Z138 TRAIL DISC components revealed accumulation of cFLIP_L (and its respective cleaved version, p43) but not cFLIP_S (Fig. 3.6 and data not shown). Previous work carried out in this laboratory established that the optimal formation of TRAIL DISC in the BJAB and Jurkat cell lines was 10 min and 25 min, respectively (L. Dickens, PhD Thesis 2009). Therefore, to directly compare DISC formation, BJAB, Jurkat and Z138 TRAIL DISCs were isolated following incubation with TRAIL for their optimal times at 37 °C and assayed by immunoblotting for the recruitment of DISC components (Fig. 3.7).

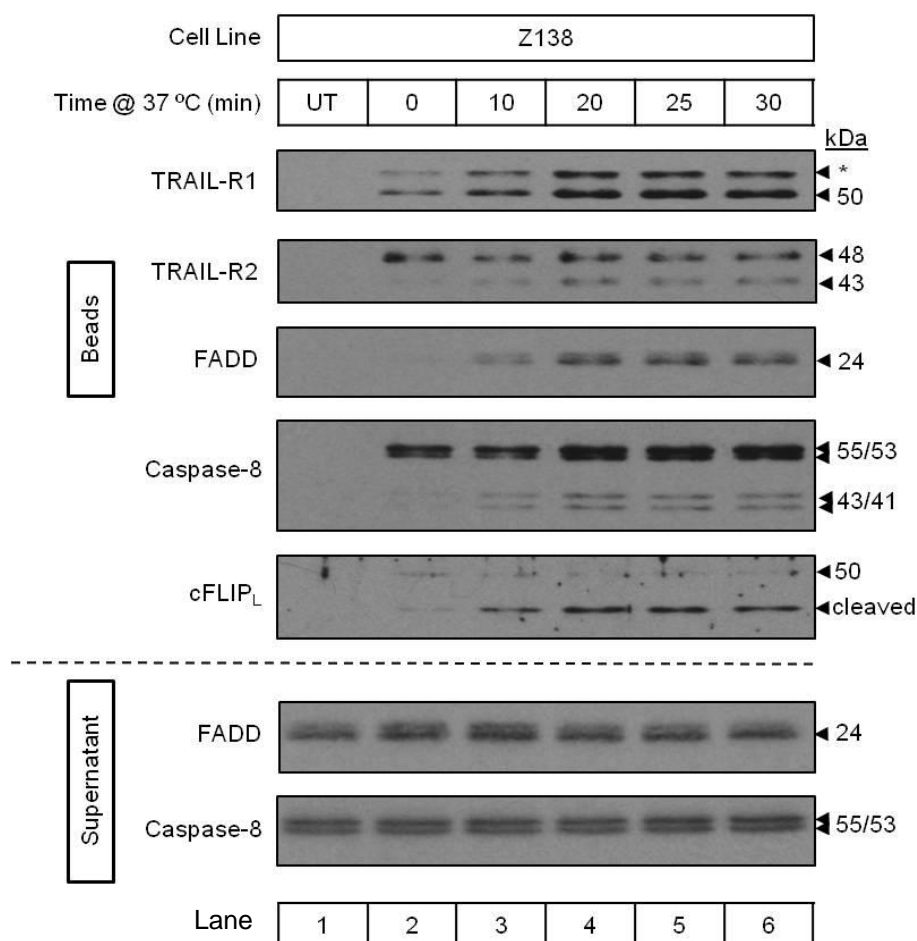


Figure 3.6 Optimisation of DISC formation using bTRAIL. Z138 cells were analysed for DISC formation from 0-30 min at 37 °C following a 1 h pre-chill at 4 °C as described in Materials and Methods. UT refers to untreated sample. * indicates unknown higher molecular weight immuno-responsive TRAIL-R1 band. 18 µl of bead sample and 30 µl of supernatant were loaded onto each SDS-PAGE gel. Immunoblots are representative of three experiments.

The data show that TRAIL DISC isolated from the three cell types differs somewhat in the amount of known components present (Fig. 3.7). BJAB cells form optimal DISC at 37 °C more rapidly than the Jurkat or Z138 cell lines and incorporate more FADD into the complex (Fig. 3.7, lane 3, 6 and 9). Jurkat cells do not express TRAIL-R1 and incorporate significantly less FADD into the complex compared to the other two cell lines (lane 6, Fig. 3.7). Z138 cells appear to incorporate higher levels of TRAIL-R1 and -R2 than BJAB cells but similar levels of TRAIL-R2 to Jurkat cells (Fig. 3.7). Furthermore, the amount of FADD and caspase-8 isolated from Z138 cells is higher than Jurkat cells but less than in BJAB cells (Fig. 3.7). Thus, DISC formation in Z138 cells was extensive and complete within 25 min. Subsequent experiments were therefore designed to scale-up the purification of the Z138 DISC to enable proteomic analysis of its components.

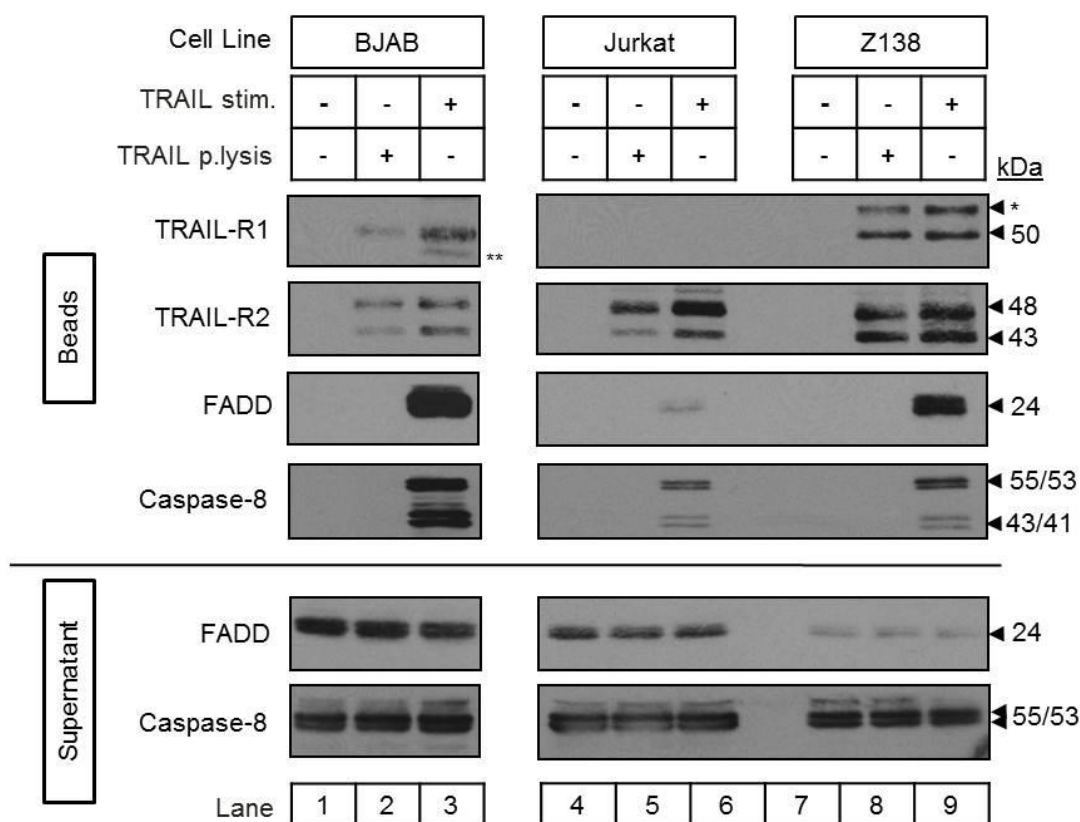


Figure 3.7 Comparison of isolated TRAIL DISC complexes from BJAB, Jurkat and Z138 cells. TRAIL DISC complexes were isolated from 60×10^6 BJAB, Jurkat and Z138 cells after 10, 25 or 25 min, respectively at 37 °C as outlined in Materials and Methods. Equal volumes (18 μ l) were loaded on to gels and exposure times are the same for all blots. * indicates unknown higher molecular weight TRAIL-R1 band. ** indicates residual TRAIL-R2 band from re-probing the same blot.

(vii) TRAIL-R1, but not TRAIL-R2, is glycosylated in Z138 cells

Interestingly, analysis of the TRAIL-R1 death receptor in Z138 cells by immunoblotting revealed an additional immuno-responsive band higher than the expected/predicted 50 kDa band (Fig. 3.6 and 3.7, indicated by asterisk). Further experiments demonstrated that this band was not present in HeLa, BJAB or Jurkat cells (Fig. 3.8a). In addition, mass spectrometry analysis of the Z138 TRAIL DISC detected two distinct clusters of TRAIL-R1 peptides in four different slices of a Coomassie-stained gel (analysed as outlined in Materials and Methods) (Fig. 3.8b). This confirmed that the higher molecular weight band detected by immunoblotting was TRAIL-R1. In addition, it suggests that the TRAIL-R1 receptor in Z138 cells is present in two distinct forms; the 50 kDa predicted band and a ~ 55 kDa unknown band.

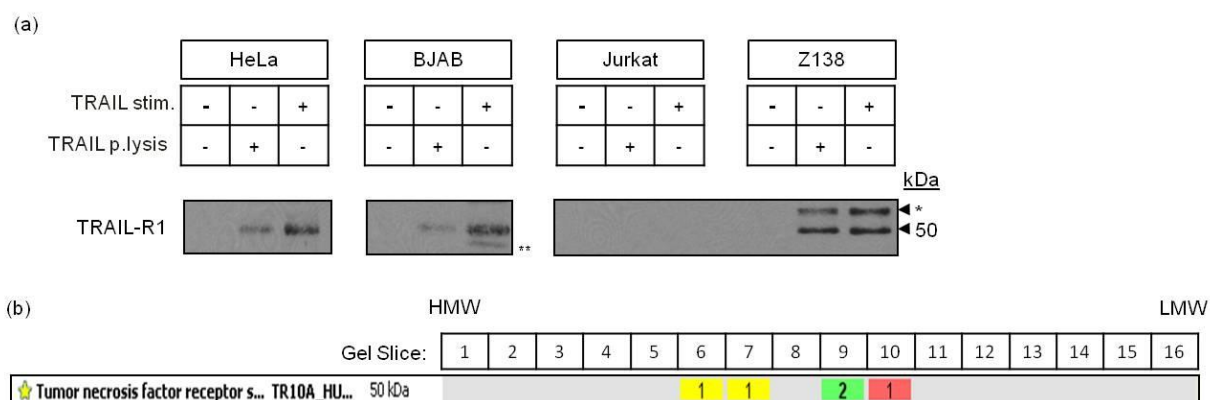


Figure 3.8 TRAIL-R1 in Z138 cells has an additional higher molecular weight band than the expected 50 kDa band. (a) TRAIL DISCs were isolated from 60×10^6 HeLa, BJAB, Jurkat and Z138 cells as outlined in materials and methods. Equal volumes of each were loaded on to SDS-PAGE gels and analysed for TRAIL-R1 by immunoblotting. Blots are representative of one experiment. (b) TRAIL DISC isolated from Z138 cells was analysed by mass spectrometry for the detection of TRAIL-R1 as outlined in materials and methods. Graphic shows screen shot of the Scaffold Software used to analyse the proteins identified by mass spectrometry. Gel slices are as indicated.

SDS-PAGE separates proteins based on their size and thus suggest that TRAIL-R1, in Z138 cells, is being modified in such a way that its molecular weight increases. There are a number of possibilities as to why the actual band size may differ than the predicted size one of which is alternative splicing of mRNA transcripts. TRAIL-R1 mRNA, examined by northern blotting, detected three major transcripts suggesting alternative splicing of this receptor (Pan *et al*, 1997). However, unlike TRAIL-R2 (Screaton *et al*, 1997), there is no further evidence in the literature to suggest that TRAIL-R1 protein exists as spliced variants and, to date, this higher molecular weight band has only been identified in Z138 cells. Furthermore, the size difference is too small to represent dimerisation of the receptor and it is also present when the samples are analysed under reducing conditions (Fig. 3.8a). Thus, one possibility is that, in Z138 cells, TRAIL-R1 is undergoing a post-translational modification, which would increase the molecular weight of the protein. However, the data suggest that not all of the receptor is being modified since the 50 kDa expected band is present in addition to the unknown band (Fig. 3.8).

A recent study by Wagner and colleagues discussed the role of death receptor O-glycosylation in determining the sensitivity of tumour cells to TRAIL (Wagner *et al*, 2007). Using whole-genome profiling to identify genes that were differentially expressed between TRAIL-sensitive and -resistant cells, they identified a number of glycosylation enzymes that were significantly over-expressed in TRAIL-sensitive cells (Wagner *et al*, 2007). Subsequently, by inhibiting these over-expressed glycosylation enzymes, using the general inhibitor: benzyl- α -GalNAc (bGalNAc) and siRNA, it was

observed that TRAIL-mediated apoptosis was suppressed (Wagner *et al*, 2007). This led to the assumption that TRAIL-receptor glycosylation was important in distinguishing between sensitive and resistance cells. However, Z138 cells, when treated with benzyl- α -GalNAc did not show any reduction in sensitivity to TRAIL (data not shown).

To examine for the presence *N*-glycosylation, endoglycosidase enzymes, which can be used to characterise protein *N*-linked glycosylation, were employed (reviewed in Marino *et al*, 2010). Upon treatment with Peptide *N*-Glycosidase F (PNGase F), which cleaves between the glycan modification and the asparagine residue of all *N*-glycosylated proteins (Marino *et al*, 2010), I observed a decrease in the molecular weight of both TRAIL-R1 bands (Fig. 3.9, Lane 4). This would suggest that both TRAIL-R1 species are *N*-glycosylated. However, PNGase F had no observable effect on the remaining DISC components including TRAIL-R2, FADD and caspase-8 (Fig. 3.9). Thus, these DISC components do not appear to undergo *N*-glycosylation modification and, in line with this finding, it has been reported previously that TRAIL-R2, unlike TRAIL-R1, does not contain any potential *N*-glycosylation sites in its sequence (Walczak *et al*, 1997).

Next, I employed the *N*-glycosylation specific enzyme endoglycosidase H (Endo H) to further deduce the type of *N*-glycosylation occurring on TRAIL-R1 (reviewed in Hossler *et al*, 2009). Endo H acts slightly different to PNGase F in that it specifically cleaves between the two glycan residues directly proximal to the asparagine and targets high mannose and some hybrid type *N*-glycosylation modifications only (Hossler *et al*, 2009; Marino *et al*, 2010). The data show that none of the examined DISC components, including TRAIL-R1, underwent a mobility shift upon treatment with Endo H (Fig. 3.9, Lane 3). Taken together the data suggest that both species of TRAIL-R1 undergo complex *N*-glycosylation but this is not a high mannose structure since it is cleavable by PNGase F but not Endo H (Fig. 3.9). Since the evidence presented above suggests that both of the detectable TRAIL-R1 bands undergo post-translation modification this could not explain the observed size difference. However, the sensitivity of Z138 cells to TRAIL-induced apoptosis following treatment with the Endoglycoside enzymes was not investigated and thus the experiments described above only show that TRAIL-R1 is potentially *N*-terminally glycosylation and does not describe how this could affect signalling to cell death.

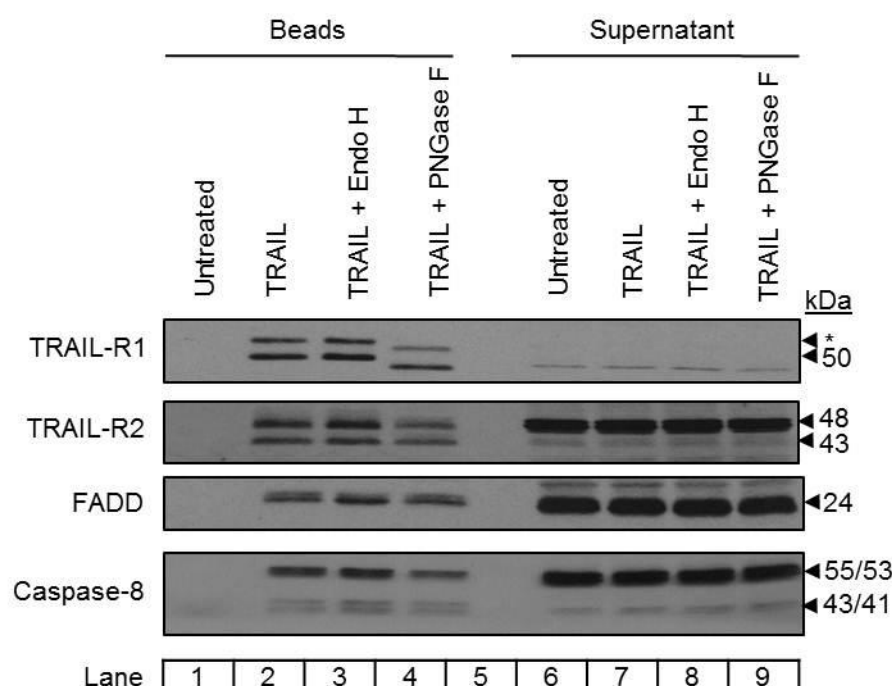


Figure 3.9 Treatment with endoglycosidase enzymes alters the molecular weight of TRAIL-R1 but not TRAIL-R2, FADD or caspase-8. Isolated DISC from bTRAIL-treated Z138 cells were incubated in the presence or absence of Endo H and PNGase F for 2 h at 37 °C. Complexes were then denatured and analysed by immunoblotting for the indicated DISC components. A mobility shift of the examined protein was determined when compared to control (TRAIL) sample. Immunoblots shown are representative of three independent experiments.

TRAIL-R1 is expressed as a protein of 468 amino acids (Pan *et al*, 1997) and contains a putative signal peptide (Fig. 3.10), which is cleaved off at alanine 24 during processing through the endoplasmic reticulum (ER) to generate the mature (445 amino acids) protein (Pan *et al*, 1997) (Fig. 3.10). It is, therefore, possible that in Z138 cells the putative signal peptide might not be cleaved from some of the translated TRAIL-R1 protein and this may explain why a higher molecular weight band is detected. Z138 cells could therefore generate a ~49 kDa mature TRAIL-R1 protein (445 amino acid) and a ~52 kDa full-length form of TRAIL-R1 (468 amino acid).

```

-23 MAPPPARVHLGAFLAVTPNPGSAASGTEAAAATPSKVWGSSAGRIEPRGGGRGALPTSMGQHGPSARARAGRA 50
51 PGPRPAREASPRLRVHKTFKFVVVGVLQVVPSSAATIKLHDQSIGTQQWEHSPLGELCPPGSHRSERPGACN 123
124 RCTEGVGYTNASNNLFACLPCTACKSDEEERSPCTTTTRNTACQCKPGTFRNDNSAEMCRKCSTGCPRGMVKVK 196
197 DCTPWSDIECVHKESGNGHNIWVILVVTLLVPLLLVAVLIVCCCIGSGCGGDPKCMDRVCFWRLGLLRGPAGAE 269
270 DNAHNEILSNADSLSTFVSEQQMESQEPADLTGVTVQSPGEAQCLLGPAEAEQSQRRLVLPANGADPTETLM 342
343 LFFDKFANIVPPD[SWDQLMRQLDLTKNEIDVVVRAGTAGPGDALYAMLKWKVNKTGRNASIHTLLDALERMEER 415
416 HAKEKIQDLLVDSGKFIYLEDGTGSAVSLE 445

```

Figure 3.10 Amino acid sequence of TRAIL-R1. TRAIL-R1 is generated as protein of 468 amino acids with the mature protein predicted to start at amino acid 24 (alanine – indicated by black triangle). The putative signal peptide (underlined) is cleaved off during processing to generate the mature 445 amino acid protein. Red line indicates the transmembrane domain and the intracellular death domain is boxed. Image taken from Pan *et al*, 1997.

However, further evidence to confirm this hypothesis, such as sequence analysis experiments, would be required. Nevertheless, these data show that both detectable bands of TRAIL-R1 undergo *N*-glycosylation, but not any of the other DISC proteins examined, and that both bands are constitutively expressed in Z138 cells.

3.2.2 Isolation and mass spectrometry analysis of the Z138 TRAIL DISC

As described earlier, the formation of the TRAIL DISC is essential for signalling to apoptosis. Deregulation at the level of the DISC, such as low expression of TRAIL-R1 and/or TRAIL-R2 (MacFarlane *et al*, 2002), deletions in FADD (Kuang *et al*, 2000) or mutations in caspase-8 (Chun *et al*, 2002; Hughes *et al*, 2009) can completely abrogate the apoptotic signal. Ligand, receptors, FADD and caspase-8 together make-up the core known components of the TRAIL DISC. However, there are a number of reports that suggest the initiator caspase; caspase-10 and the pro/anti-apoptotic molecule cFLIP as additional components of the TRAIL DISC (Kischkel *et al*, 2001; Micheau, 2003); although the absolute contributions of these in TRAIL signalling are somewhat contradictory (reviewed in Zhang and Fang, 2005). I, therefore, sought to examine core components and novel interactors of the TRAIL DISC using the Z138 cell line described above. Previous studies to examine components of the CD95, TNF α and TRAIL-signalling complexes have employed immunoprecipitation and/or mass spectrometric approaches to successfully identify core and novel protein interactors (Kischkel *et al*, 1995; Haas *et al*, 2009; Jin *et al*, 2009). In addition, proteomic profiling has been used successfully to identify plasma membrane and lipid raft proteins in mantle cell lymphoma and B cell lymphoma lines (Boyd *et al*, 2009; Capasso *et al*, 2010). Thus, using affinity purification and shotgun proteomics, it should be possible to characterise the protein composition of the Z138 TRAIL DISC and further elucidate its signalling role in apoptosis.

(i) Isolation of the Z138 TRAIL DISC

The large scale isolation of a Z138 TRAIL DISC is required to obtain enough protein for mass spectrometry analysis. Both small and large scale isolations of the DISC, in various cell lines, have been optimised extensively and successfully within our laboratory. In the case of Z138 cells, a large scale DISC preparation from 1.0×10^9 cells was performed as described in Materials and Methods (Chapter 2). Small (5%) aliquots of control and TRAIL-treated samples were first fractionated by SDS-PAGE and immunoblotted for the known TRAIL DISC components to confirm successful isolation of the complex (Fig. 3.11a). The remaining sample was then separated by SDS-PAGE and the resulting gel Coomassie-stained to visualise the proteins isolated

from the purified DISC (Fig. 3.11b). Comparison of the control and treated lanes on the stained gel, surprisingly, did not show any detectable differences except for the presence of a protein band indicative of recombinant biotinylated TRAIL in the treated lane only (Fig. 3.11b – labelled arrow). The bands that are visible in both lanes of the stained gel largely correspond with carboxylases and cytoskeletal proteins, which are contaminants frequently identified in large scale DISC IP experiments (Fig. 3.11b – unlabelled arrows). Importantly, subsequent studies/repeat experiments found the absence of any major differences to be a common observation in TRAIL DISC purifications for mass spectrometry analysis. Despite being unable to visualise any overt differences, I proceeded with mass spectrometry analysis.

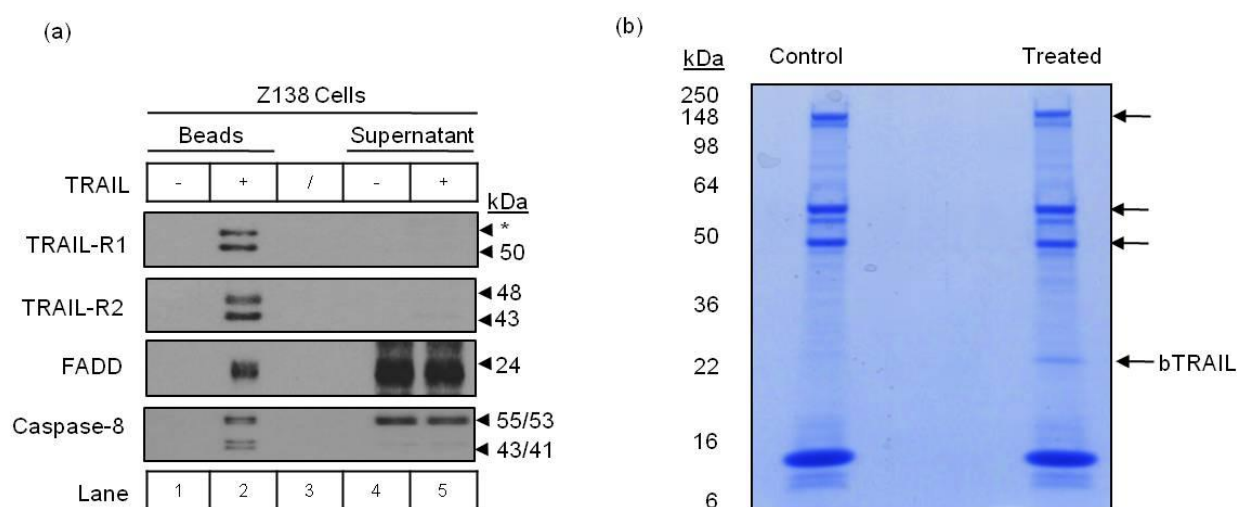


Figure 3.11 Isolation of the TRAIL DISC from Z138 cells for mass spectrometry analysis. TRAIL DISC from 1×10^9 Z138 cells was isolated for mass spectrometry analysis as outlined in Materials and Methods. (a) 5 % of the isolated DISC was examined by immunoblotting for confirmation of DISC formation prior to mass spectrometry. (b) Remaining DISC was separated by SDS-PAGE and the gel stained with Coomassie blue for visualisation of proteins. Coomassie stained gel is representative of three independent experiments.

(ii) Mass spectrometry analysis of the Z138 TRAIL DISC

Briefly, gel slices were sequentially cut from control and treated lanes (Fig. 3.11b) and subjected to in-gel protein digestion. Tryptic peptides were then separated by HPLC and applied to a Q-TOF (quadrupole time-of-flight) mass spectrometer followed by tandem mass (MS/MS) spectrometry. The generated spectra were then used for protein identification using the search engine Mascot and the data generated uploaded into the proteome software Scaffold to validate protein hits. The scaffold proteome software allows users to then dissect and interpret the large amounts of mass spectrometry data received from Mascot. Due to the vast amount of data uploaded from the Mascot search engine to the scaffold proteome software, it is essential to set up criteria that could positively exclude any redundant proteins. To do this, criteria

were devised with specific standards that the identified protein had to meet in order to be considered a viable hit; these criteria are outlined in Table 3.1.

Table 3.1 Outline of the criteria for analysis of protein hits. The list of identified proteins uploaded into the Scaffold software was subjected to the above criteria in order to ensure rigorous validation as potential TRAIL DISC interactors. Protein probability - minimum probability that a given protein has been identified correctly; Peptide probability - minimum required certainty that the peptide identified is correct from at least one spectrum; Number of peptides: number of unique peptides that must be found from one protein; mascot ion score – a measure of how certain the observed spectrum matches the stated peptide. * Proteins were also included if the protein probability in the treated sample was greater than that observed in the control sample.

Criteria	Standard
Min. Protein Probability	≥ 50 %
Min. Peptide Probability	≥ 50 %
Number of Peptides	≥ 1
Mascot Ion Score	≥ 30
Keep <i>known</i> proteins	TRAIL, TRAIL-R1/R2, FADD, Caspase-8, cFLIP
Species specific	Human
Are not identified as any of the following known contaminants:	Keratin, Tubulin, Actin, Histones, Carboxylases, Ribosomal, Heterogeneous, Splicing factor, Histocompatibility antigen, 26S protease subunits.
Exclude proteins identified in a previously published contaminant protein list:	Trinkle-mulcahy <i>et al</i> , 2008
In treated sample only	Exclude proteins identified in control sample*

Three independent large scale Z138 TRAIL DISC isolation experiments were performed and analysed by mass spectrometry. Following data analysis (outlined in

Table 3.1), a final combined list of identified proteins was produced, which identified 25 proteins that met or exceeded the criteria outlined in Table 3.1. These 25 proteins (listed in Table 3.2) include both known TRAIL DISC components and novel previously unidentified proteins.

The known TRAIL DISC components - TRAIL (*TNF10*), TRAIL-R1 (*TR10A*), TRAIL-R2 (*TR10B*) and caspase-8 (*CASP8*), were each identified in all three TRAIL DISC isolations and thus show significant protein identification probability, number of unique peptides and sequence coverage (Table 3.2). Interestingly, FADD (*FADD*) and cFLIP (*cFLAR*) were only identified in two out of the three experiments. This implied that these latter proteins were less abundant in the Z138 TRAIL DISC compared to the other known components. The number of assigned spectra, supplied from the scaffold proteome software, provides an indication of the protein abundance and, in line with the above findings, the number of spectra identified for FADD and cFLIP was low compared to other known DISC components (data not shown). This is, potentially, not surprising for cFLIP due to its exact role in the DISC being debatable and possibly more dynamic. However, considering its importance, the low detection of FADD was rather unexpected. Nevertheless, all known TRAIL DISC components were successfully identified in at least two out of the three DISC isolation experiments (Table. 3.2). The remaining 19 proteins were made up of previously unidentified proteins that have no previous known role in TRAIL DISC formation or apoptotic cell death. These are listed in Table 3.2 in order of highest to lowest protein probability and represent potential novel TRAIL DISC interactors.

(iii) Label-free quantitative analysis of the mass spectrometry data

To justify further examining the remaining unknown proteins (Table 3.2) as potential TRAIL DISC interactors all identified proteins, including the known components, were subjected to quantitative proteomic analysis (Paoletti *et al*, 2006). The actual relationship between these known and novel proteins is hard to decipher in the lists shown above. Therefore, applying label-free quantitative analysis allowed me to establish the relative abundance of a specific protein in the complex. This approach, outlined in Materials and Methods, takes into account both the protein size and spectral counts obtained for each identified protein thereby generating the spectral abundance factor (SAF) (Paoletti *et al*, 2006; Zybaylov *et al*, 2006).

Number	Accession Number	Identified Protein	Molecular Weight (kDa)	Protein Identification Probability (%)	Unique Peptides	Sequence Coverage (%)
1	TNF10	<i>Tumor Necrosis Factor Ligand Superfamily member 10</i>	55	100 100 100	10 9 7	30
2	TR10A	<i>Tumor Necrosis Factor Receptor Superfamily member 10A</i>	50	100 100 100	5	12
3	TR10B	<i>Tumor Necrosis Factor Superfamily 10B</i>	48	100 87 93	3	11
4	FADD	<i>Protein FADD</i>	23	99 93	1	9
5	CASP8	<i>Caspase-8</i>	55	100 100 100	4	9
6	CFLAR	<i>Casp8 and FADD-like apoptosis regulator</i>	55	100 74	4 2	5
7	PP1 α/γ	Serine/Threonine Protein Phosphatase α/γ catalytic subunit	38	100	2	7
8	DEK	Protein DEK	43	100	2	6
9	TFR1	Transferrin Receptor Protein 1	85	98	2	1
10	MYPT1	Protein Phosphatase 1 regulatory (inhibitor) subunit 12A	115	98	2	2
11	ECH1	Delta(3,5)-Delta(2,4)-Dienoyl-CoA Isomerase, Mitochondrial Precursor	36	90	1	4
12	EFHD2	EF-hand Domain Containing Protein D2	27	90	1	4
13	AT1A1	Sodium/Potassium Transporting ATPase Subunit Alpha_1	113	82	1	1
14	STAG3	Cohesin Subunit SA_3	139	82	1	1

Number	Accession Number	Identified Protein	Molecular Weight (kDa)	Protein Identification Probability (%)	Unique Peptides	Sequence Coverage (%)
15	DCA15	DDB1- and CUL4 associated factor 15	66	58 76 79	1 1 1	1
16	FA20A	Protein FAM20A	61	77	1	5
17	IL25	Interleukin-25	20	76 80	1 1	6
18	LUZP1	Leucine Zipper Protein 1	120	75	1	1
19	K1841	Uncharacterised Protein KIAA1841	82	69	1	2
20	QRIC2	Glutamine-Rich Protein 2	181	62	1	1
21	CLCF1	Cardiotrophin-like Cytokine Factor 1	25	62	1	4
22	NR1I3	Nuclear Receptor Subfamily 1 Group I Member 3	40	61	1	3
23	LRC59	Leucine Rich Repeat-containing Protein 59	35	54	1	3
24	ASPP2	Apo-Stimulating p53 Protein 2	126	52	1	1
25	C1GLT	Glycoprotein-N-Acetylgalactosamine 3- β Galactosyltransferase 1	42	51	1	1

Table 3.2 List of proteins identified by mass spectrometry of the Z138 TRAIL DISC. Mass spectrometry data from Z138 bTRAIL DISC experiments (N=3) were analysed as outlined in materials and methods and table 3.1. Protein identification probability (%) and unique peptides show values obtained from each run. Sequence coverage (%) were taken from the 'best' hit where proteins were identified in >1 experiment. Proteins identified in red are known TRAIL DISC components. Unknown proteins are ranked according to protein identification probability (%).

For this study, SAF was then normalised to a consistently identified protein, in our case TRAIL-R2, to account for run to run variation and is termed 'normalised spectral abundance factor' or NSAF (modified from Paoletti *et al*, 2006; Zybailov *et al*, 2006). The NSAF value for each identified protein was then plotted against its respective 'highest' protein identification probability to determine identified proteins that should be further investigated (Fig. 3.12). The proteins with the highest protein identification probability versus NSAF value were identified as potential targets for further investigation (Fig. 3.12). Thus, from the analyses carried out in Table 3.2 and Figure 3.12, I selected the serine/threonine protein phosphatase α/γ catalytic subunit (PP1 α/γ), protein DEK (DEK), EF-hand domain containing protein D2 (EFHD2), Delta(3,5)-Delta(2,4)-Dienoyl-CoA Isomerase Mitochondrial Precursor (ECH1), Protein Phosphatase 1 regulatory (inhibitor) subunit 12A (MYPT1) and Transferrin Receptor Protein 1 (TFR1) as proteins that justified further investigation.

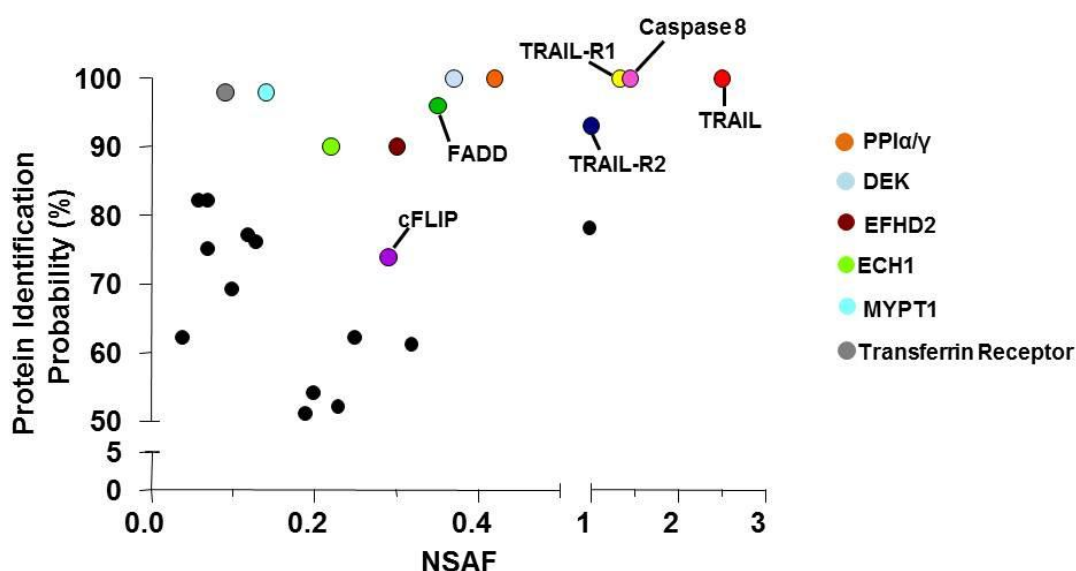
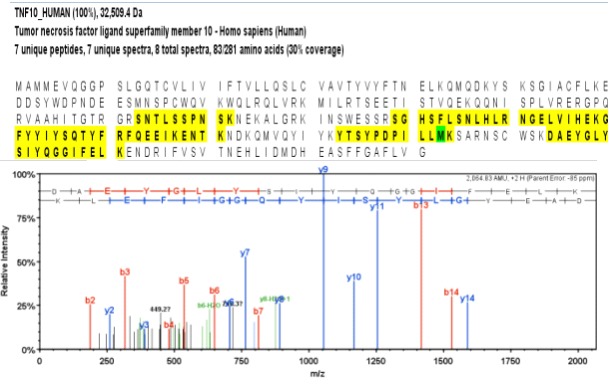


Figure 3.12 Quantitative proteomic analyses of proteins identified by mass spectrometry. 'Highest' protein identification probability (%) for each protein was plotted against its normalised spectral abundance factor (NSAF) calculated as described in Materials and Methods. Proteins identified as potential novel interactors that require further investigation are indicated by colour and corresponding legend.

(iv) Critical analysis of the potential DISC interactors

Every database generates false positives and therefore, in addition to setting criteria and using quantitative proteomic analysis, mass spectrometry data can be further examined for accuracy by observing the identified peptides of an individual protein sequence and their corresponding spectra. These data are provided by the Scaffold proteome software and illustrated in Figure 3.13 for the known TRAIL DISC components.

TRAIL



The data shows the Scaffold protein view of TRAIL, TRAIL-R1, TRAIL-R2, FADD, caspase-8 and cFLIP along with their representative spectra (Fig. 3.13). The areas highlighted in yellow represent the actual peptides identified by mass spectrometry (upper panel) along with the corresponding spectrum for a given peptide (lower panel) (Fig. 3.13). Visible on the individual spectra of each protein are the detected *b*- and *y*-type ions, which correspond to specific fragments of the dissociated peptide. For example, *y*-type ions represent the fragmentation profile of a peptide with the charge retained on the C-terminal end as appose to the N-terminal, which represents *b*-type ions. Taken together, these *b*- and *y*-type ions can be used to deduce the corresponding peptide sequence and, in our case, the search engine Mascot was used to match the associated spectrum peaks with known peptide sequences. Ideally, the *b* and *y* ion fragmentation would make up a full peptide sequence. However, the fewer breaks present and thus the more of a given peptide identified, the greater the confidence in the identified peptide (reviewed in Jonscher, 2005). The data show that the spectra obtained for the known DISC components are of good quality (Fig. 3.13) and the known DISC proteins identified by mass spectrometry have been correctly assigned (Fig. 3.13).

I next wanted to examine the identified peptides and corresponding spectra of the selected potential DISC interactors, which include PP1 α/γ , DEK, EFHD2, ECH1, MYPT1 and the transferrin receptor. PP1 α/γ had the highest protein identification probability, number of unique peptides identified and percentage sequence coverage of all unknown proteins identified (Table 3.2). In addition, in the quantitative analysis of the PP1 α/γ protein (Fig. 3.12) it ranked among the known DISC components. The representative spectra show large *y*-ion fragmentation identification (Fig. 3.14). Importantly, the identified peptide sequence is homologous to both PP1 α and PP1 γ . Since the amino acid residues detected by mass spectrometry are conserved in both isoforms of PP1, this could suggest that either or both of these isoforms are potentially present in the TRAIL DISC. Protein DEK was the next 'best' identified novel protein and, similar to PP1 α/γ , was largely detected through *y*-ion fragmentation (Fig. 3.14). EFHD2 and ECH1 both had lower (90%) protein identification probabilities than PP1 α/γ and DEK but, out of the novel proteins identified, were two of the highest protein hits upon quantitative analysis (Fig. 3.12).

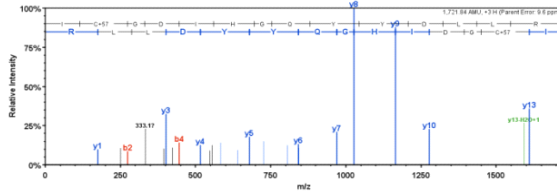
PP1 α/γ

PP1A_HUMAN (100%), 37,813.0 Da

Serine/threonine-protein phosphatase PP1-alpha catalytic subunit - Homo sapiens (Human)

2 unique peptides, 2 unique spectra, 2 total spectra, 23,000 amino acids (7% coverage)

MSDSKLNLD SIIGRLLEVO GSRPGKNVQL TENEIRGLCL KSREIFLSOP ILLELEAPLK
LDLIDQGY **DL**LLRLFEYGG FPESNYLFL GQYVDRGQS LETICLLAY KIK**YFENFF**L
 LSNHCEASL KRIQFYDEG KRRYINLWK TFTOCFNCP IAAIVDEKIF CCHGLSPDL
 QSWGIRIM RPTDVPDGL LQDLLWSPD KQVQGWEND RGVSTFGAE VVAKFLKHD
 LQICRAHOV VEDGYEFAK RQLVTLFSP NYDGEFDNAG AMMSVDETLW OSFOILKPAD
 KKKGYGDFS GLNPGGRIT PPRNSAKAK



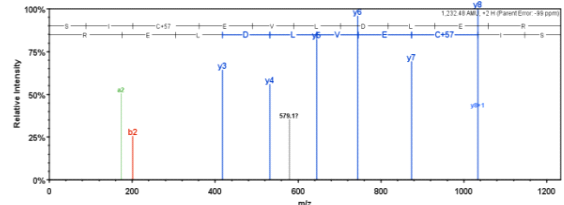
DEK

DEK_HUMAN (100%), 42,675.9 Da

Protein DEK - Homo sapiens (Human)

2 unique peptides, 2 unique spectra, 2 total spectra, 22,075 amino acids (6% coverage)

MSASAPAEQ EGTPTQPAE KEPEMPGPRE ESEEEEDD EEEEEEEK SLIVEGKREK
 KKVERLTMOV SSLOREPFTI AOGKGKLOE IERIHFFLSK KKTDELRNLH KLYNRPQTV
 SLLK**NYGQF** **SGFPFENG**SV QYKKKEMLK KFRNAMLK**S1** **REVLDLEN**SG VNSVELVKRIL
 NFLMHPKPSG KPLPKSKKTC SKGSKKEKNS SGMARKAKRT KOPEILSDS SSDEDEKKNK
 EESDDDEKE SEEEPPKTA KREPKQKAT SKSKSKVSA NVKKADSSIT KKNQSSKKE
 SESESSDE PLIKLKKPP TDEELKETIK KLLASANLEE VTMQICKVKV YENPTYDIT
 ERDPIKTTV KELIS



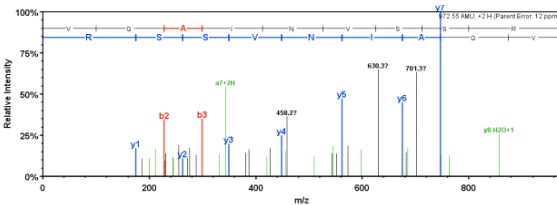
EFHD2

EFHD2_HUMAN (90%), 26,698.4 Da

EF-hand domain-containing protein D2 - Homo sapiens (Human)

1 unique peptides, 1 unique spectra, 1 total spectra, 9,240 amino acids (4% coverage)

MATDELATKL SRRLOMEGEG GGETPEQPLG NGAAAAAAGA PDEAAEALGS
 ADCELSAKLL RRAOLNQGIG EPSPSRRVF NYITEFKEFS RKQIKDMEKM
 FKQYDAGRDG FIDLMELKML MEKLGAPQTH LGLKNMKEV DEDFDSKLSF
 REFLLIFRKA AAGELQEDSG LCVLARLSEI DVSSEGKGA KSFFFAK**YQA**
INVSRRFEFE IKAQEERKK QAEMKQKA AFKELQSTFK



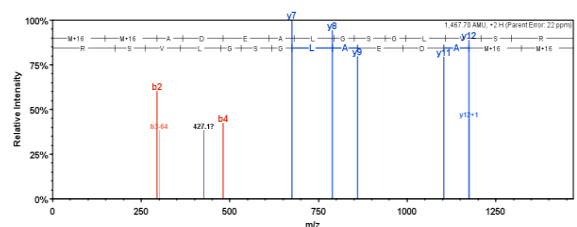
ECH1

ECH1_HUMAN (90%), 35,816.2 Da

Delta(2,5)-Delta(2,4)-dienoyl-CoA isomerase, mitochondrial precursor - Homo sapiens (Human)

1 unique peptides, 1 unique spectra, 1 total spectra, 14,328 amino acids (4% coverage)

MAAGIVASRR LRDLTLRLT GSNNYPLSLIS LRLTGSSAQE EASGVALGEA
 PCHSVESLRV TSAQKHVLHV QLNRPKNRNA MNKVFWREMY ECFNKISRDA
 DCRAYVISGA GKMFTAGIDL MDMASDILQP KGDDVARISW YLRDIITRYQ
 EFTNVIERC KPIVIAVHQB CIGGGDLVT AGDRIYDAD AFFQVKEDVD
 GLAADVGTLO RLPKVIQNGDS LVMELAFAT **KMADEALGS** **GLVSR**VFPDK
 EVMDLAALAL AAEISSKSPV AVOSTKVNLL YSRDHSVAES LNYVASWNMS
 MLQGTDLVKS VQATTENKEL KTVTFSKL



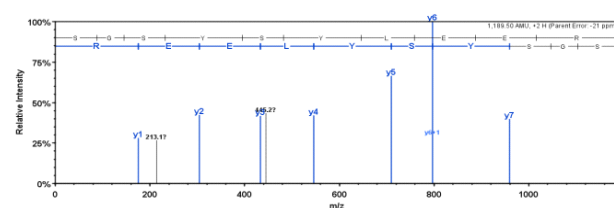
MYPT1

MYPT1_HUMAN (98%), 115,283.4 Da

Protein phosphatase 1 regulatory subunit 12A - Homo sapiens (Human)

2 unique peptides, 2 unique spectra, 2 total spectra, 31,100 amino acids (2% coverage)

MKMADAKQR NEGLKRWIGS ETDLEPPYVK RQITKVFYDD GAVFLAACS GDTDEVLLKL
 HEGADINYN VOGLTALHQA CDDNVDMVK FLVENGAIN QDNEGWIPL HAAASCGYLLD
 IAEFLIQGA HVGAVNSEG TPLDIAEEA MELQLNEYN RQVDIEAAR KEERIMLRD
 ARQWLNQHI NDYVRAKSGG TALVVAAGQ YTEVKKLLID AGDYVNIKDY GQWTFPLHAA
 HWGKEACRI LVNLCODEM VHKVGOTAFD VAEDDILGV LELQKKQLH HSEKROKKSP
 LIESTAMDN NOBQTFKNK ETLIIEPEK ASPIESLEGE KYDEEEGKK DESSCSESD
 EDDSEAE TQTKPLASV THAITSITGA APYAVTPTV SGGATPTSP IKKFTTATH
 ISPKERKD SPATWRGLG RITQSYGALA EITASKEDQK EKDAGVTRS ASPPRLSSSL
 DNKEKQSK OTRLAVAPT IPRPLASTD IEKENRDS SLRTSSSYR RKWEDDLKK
 SSVNEGISTH KSCSFGRRQD DLSSVSPST TSTPTVTSAA GLQKSLSSST STTKITGGS
 SSSADTQSTL NRIWAEDSTE KEKDSVPTAV TIPVAPTIVN AASTITLLT TTAGVSSST
 EVERRSYL TPVDESES QRKASROAR QSRSTQDVT LTDLQEAET IGRSSTSTR
 DEEKEKEKE EKEKQDKEQ EKKKESSTSR EDEYKQKYSR TYDETYQYVR PVSTSSSTTP
 SLSLTMBSL LVASQLRRP NLSLVITISAY SRGIITNEER EGEREEKKE GEDKQPKSI
 SRRRPPREB SSTGVSPWTO DSDENEQEQ DTEEGSNKK ETQDSISRY ETSSTAGDR
 YDSSLGR **SGS** **YSYLER**KPY SRRLEKDDST DFKK**LYEGL** **AENK**LKQAL HDTHMELTDL
 KLOLEKATOR GERFADRLL ESKERRRAL ERRISEMEEE LMLPLDLKAD NQRLKDNGA
 LRVISKLSK



TFR1

TFR1_HUMAN (98%), 84,873.6 Da

Transformin receptor protein 1 - Homo sapiens (Human)

1 unique peptides, 1 unique spectra, 1 total spectra, 10,780 amino acids (1% coverage)

MMDAQSAFSL HLFQGEPLSY TRFLARQVD GDNHVMKLV AVDEENADN NTKANVTXPK
 RCGSICQYOT IAVIVFFLIQ FMIGLYGCK GVEPHTECR LAQTESPVRE EPGEFPAAR
 RLYWDLKRR LSEKLDSTDF TOTI**HLNEN** **SYVPR**EAGSG KQENALYVE KQREFPLSK
 VWRDDQFVKI QVDSQNSV IIVDQGLRLL EYVPGGVY AYSAATVTD KLVHAFSTK
 KQFEDLYTPV NGSIIVIRAG KIFTAEKAN AESLNAIGVL IYMDQTFPI VNAELSPFGH
 AHLQDGPYT PQPSPNTO FPFSSSLQIP NIPVQTSRA AAEKLFQME GDCPSWKT
 STCRMVTSR KNVCLTVSNV LKEKILNIF GVIQGFVED RYVYVQARD AWGPGAKSO
 VGTALLKLA QMFSDMLVND GQPPRSII FASWAGDQGS VGATEWLEDY LSSHLKAPT
 YINLQKAVLD TSNFVVSAP LVLTLKTM QNVHPTYSO FLYQSNWAS KVELTLDNA
 APFFLAYSGI PAVSFCFCD TDYPLQTTM DTYKELIERI PELNKVAVAA AEVAGQVIK
 LTHVDENLD YERYNSQLS FVRLDQYRA DTKEMGLSG WLISAKGDFP RATSRLTDP
 QNAETDRFV MNKLDQVMP VEYHFLSPV SPKESPRVY FWGSSHTLP ALLENKLRK
 QNNGAFNETL FRNQLALATW TIGGAANALS GDVWDIDNEF

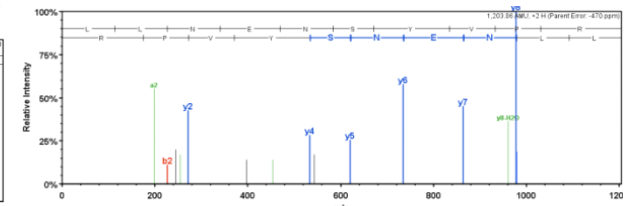


Figure 3.14 Peptide sequences, coverage and spectra for unknown potential TRAIL DISC components. Scaffold protein view of protein sequences including identified peptides (highlight in yellow) and % protein coverage (upper panel) with an example spectra (lower panel) for each of the selected unknown potential TRAIL DISC interactors. Scaffold shows y ions in blue and b ions in red. Black lines represent unidentified ions and green represent ions minus water.

However, the spectra for EFHD2 indicates increased signal to noise ratio, which represents a poor quality spectra (Fig. 3.14) whilst ECH1 represents a relatively weak spectra with regards to the fragmentation profile especially when compared to the known DISC components (Fig. 3.13 and Fig. 3.14).

Protein MYPT1 is a large 115 kDa protein, which was identified by 2 unique peptides (Table 3.2 and Fig. 3.14). It is reasonable to assume that the longer the protein the more peptides hits you might expect to observe and, therefore, it is surprising that more peptides were not identified for this protein. The transferrin receptor was also identified as a good 'hit' with regard to protein identification probability (Table 3.2) and quantitative analysis (Fig. 3.12). Similar to MYPT1, it is a relatively large protein (89 kDa) and, therefore, more numerous peptide identifications might have been expected. Nevertheless, the spectra obtained for the transferrin receptor was better quality than some of the other unknown proteins identified (Fig. 3.14). Thus, from the analysis and observations carried out above, PP1 α/γ , Protein DEK and the transferrin receptor were investigate further as potential TRAIL DISC interactors.

(v) The transferrin receptor precipitates with the Z138 TRAIL DISC

PP1 α and γ are serine/threonine protein phosphatase catalytic subunits, which remove phosphate groups from proteins and thus alter the function of the protein (Cohen, 2002). They have been shown to be involved in numerous cellular processes including, but not limited to, cell proliferation and apoptosis (Cohen, 2002; Xiao *et al*, 2010). Protein DEK, a nuclear phosphoprotein, has also been implicated as a regulator of apoptosis (Vinnedge *et al*, 2011) and was largely found to be over-expressed in tumours (Kondoh *et al*, 1999). In addition, the transferrin receptor, a transmembrane protein involved in the cellular transport of iron (Testa *et al*, 1993), has been implicated as a receptor for triggering apoptosis (Kasibhatla *et al*, 2005) and is overexpressed in cancer (Gatter *et al*, 1983) where it potentially regulates proliferation (Jones *et al*, 2006). Therefore, I performed TRAIL DISC isolation experiments and immunoblots to determine the interaction of these novel proteins with the TRAIL DISC (Fig. 3.15). The results show that the transferrin receptor, but not PP1 α/γ or DEK, were present in a Z138 TRAIL DISC (Fig. 3.15). Interestingly, the transferrin receptor also seems to be pre-associated with the TRAIL-receptors, which suggests that it interacts with the receptors independently of FADD and caspase-8 recruitment (Fig. 3.15).

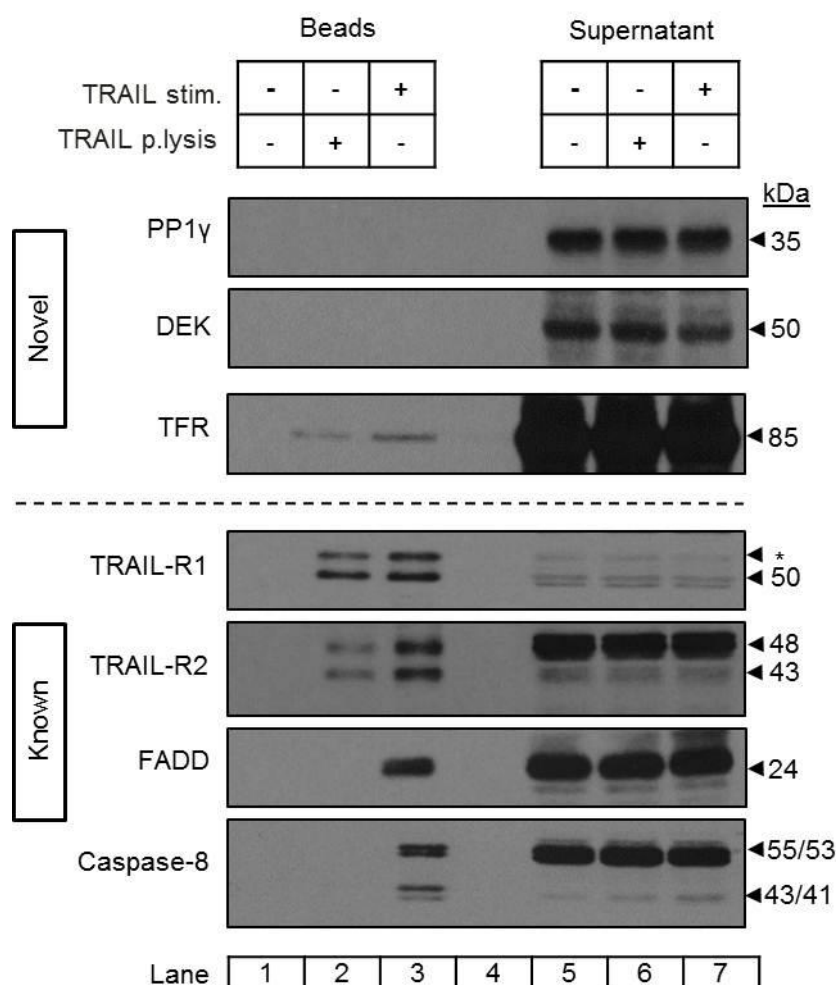


Figure 3.15 The transferrin receptor but not PP1α/γ or DEK precipitates with the Z138-TRAIL DISC. Z138 cells were analysed for the presence of PP1α/γ, protein DEK and transferrin receptor from isolated TRAIL DISC samples. Cells were either left untreated or treated with 500 ng/ml bTRAIL for 1 h at 4 °C followed by 25 min at 37 °C. TRAIL-receptors were isolated post-lysis using 1 µg of bTRAIL and represent bTRAIL-receptor complex only. All samples were then processed as outlined in materials and methods. Immunoblots are representative of 3-5 experiments. PP1γ is representative of both PP1α and γ isoforms.

Unfortunately, despite repeated experiments, PP1α/γ and DEK could not be detected with the DISC at the protein level (Fig. 3.16 and data not shown). The PP1α antibody cross-reacts strongly with the secondary antibody, which resulted in a fairly 'dirty' immunoblot, thus a representative PP1γ immunoblot is shown. To investigate the role of the transferrin receptor in the Z138 TRAIL DISC I performed RNA interference (RNAi) experiments to determine the effect of its knockdown on TRAIL-induced apoptosis. However, the data obtained from these experiments was not reproducible and thus, at present, its role in the Z138 TRAIL DISC is still unknown (see 3.3 Discussion).

(vi) Cullin-3 does not associate with the soluble TRAIL DISC in Z138 cells

A recent study identified Cullin-3 (an E3 ubiquitin ligase) as a novel TRAIL DISC interactor, which mediates caspase-8 polyubiquitination (Jin *et al*, 2009). Although Cullin-3 was not identified in the mass spectrometry assays described above, I investigated whether Cullin-3 could be identified at the protein level in TRAIL DISC isolated from HeLa, BJAB and Z138 cells. Therefore, TRAIL DISC was isolated from these cell lines and immunoblotted for Cullin-3 (Fig. 3.16). These data show that Cullin-3 was only detected in TRAIL DISC isolated from the epithelial cell line HeLa and not the haematopoietic cell lines tested here (Fig. 3.6). Jin and colleagues further claimed that Cullin-3 interacted with the DISC in lipid rafts (Jin *et al*, 2009). However, work carried out in our laboratory found that only a small fraction of the Z138 (and BJAB) TRAIL DISC associated with lipid rafts (Dickens *et al*, 2011). Therefore, these results suggest that Cullin-3 only associates with the TRAIL DISC in certain cell lines (such as epithelial cell lines) and does not appear to play a role in the TRAIL DISC isolated from haematopoietic cells.

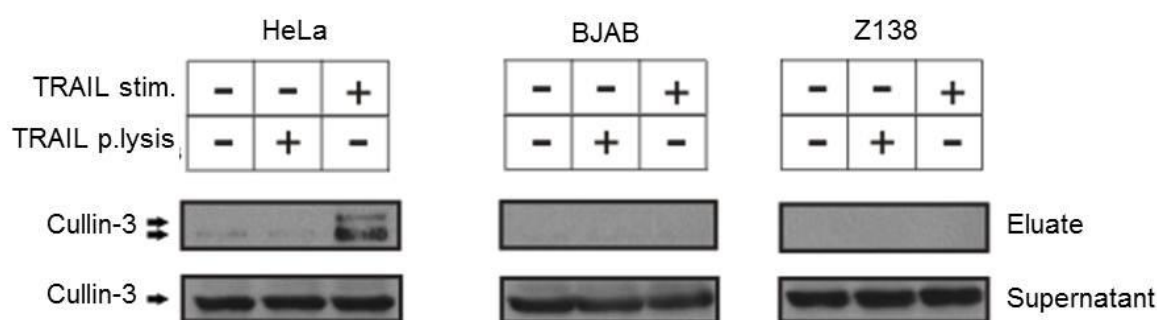


Figure 3.16 Cullin-3 is not a component of the TRAIL DISC in haemopoietic cell lines but is present in an epithelial cell line. HeLa, BJAB and Z138 cells were stimulated with TRAIL for 1 hour at 4 °C and further incubated at 37 °C for 10 min (BJAB) or 25 min (Z138 and HeLa) and the TRAIL DISC isolated. DISC-containing eluates were separated by SDS-PAGE for immunoblotting and probed for Cullin-3. Exposure times for Cullin 3 are the same across the three cell lines.

(vii) Stoichiometry of the TRAIL DISC

The proteomic data presented above primarily examined for the existence of novel TRAIL DISC proteins by mass spectrometry. However, whilst conducting these studies, we performed label-free spectral counting techniques (Paoletti *et al*, 2006; Zybailov *et al*, 2006) to determine the relative stoichiometry of the known TRAIL DISC components (Fig. 3.17). The current model for the ratio of DISC components is 1:1 however, using normalised spectral abundance factor (NSAF), we show that FADD is present in the complex at sub-stoichiometric amounts compared to either the TRAIL-receptors or caspase-8/cFLIP (Fig. 3.17a and b). Taken together, these data suggests that there is

~2.5-fold more caspase-8 in the complex than FADD (Fig. 3.17a). These observations are even more evident when the DISC components are grouped according to their recruitment into the complex (Fig. 3.17b). Thus, based on these findings, research is currently being performed to determine how this novel TRAIL DISC stoichiometry affects complex formation and structure (Dickens *et al*, 2011).

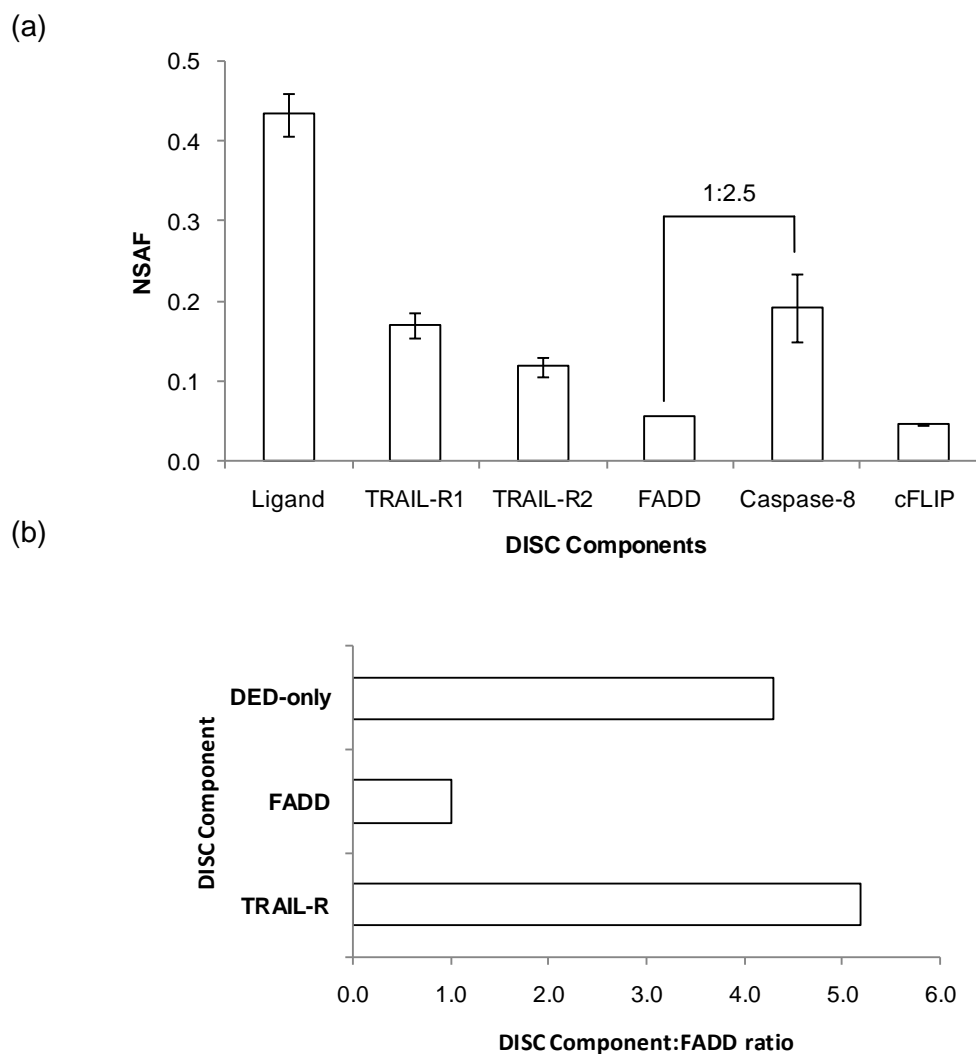


Figure 3.17 Quantitative proteomic analysis reveals a new stoichiometry of the TRAIL DISC components. (a) Normalised spectral abundance factor (NSAF) for the TRAIL DISC isolated from Z138 cell lysate. Data represents mean \pm SEM, N3). (b) Known DISC components were assigned a category (receptor, FADD, DED-only) and the NSAF values for each combined and corrected to FADD to examine stoichiometry of components.

3.3 Discussion

Although TRAIL is believed to be selective for tumor cells, there are some malignancies that are resistance. Primary CLL and MCL, in particular, are resistant to TRAIL-induced apoptosis and they form low amounts of TRAIL DISC (MacFarlane *et*

et al, 2002). It is therefore important to find mechanisms of resistance and overcome these by analysing sensitive cell lines. The Z138 cell line is MCL-derived and preliminary experiments showed it to be sensitive to TRAIL. It is therefore an ideal cell line to investigate TRAIL DISC composition and function.

3.3.1 Characterisation of the Z138 cell line

Initial experiments were performed to characterise the Z138 cell line with respect to TRAIL-signalling. It is evident that there is a significant decrease in the number of viable cells in TRAIL-treated samples with both increasing concentration of TRAIL and treatment time (Fig. 3.1). In accordance, there is also evidence of early caspase-8 and -3 cleavage at relatively low doses of TRAIL (Fig. 3.1). Analysis of Bid cleavage and mitochondrial cytochrome *c* release, following TRAIL treatment, demonstrates a significant input from the mitochondrial amplification loop in signalling to cell death (Fig. 3.2 and 3.3). Together, the caspase-8, -3 and Bid cleavage data suggest that Z138 cells can signal via the extrinsic and mitochondrial-mediated pathways following TRAIL stimulation. However, the requirement, or not, of the mitochondrial-amplification loop in signalling to cell death requires confirmation by over-expression of a Bcl-2 anti-apoptotic family member (Scaffidi *et al*, 1998). Furthermore, it is important to note that the majority of research carried out on the Type I and II signalling theory have used the CD95-induced pathway as a model. The few studies that have examined TRAIL-receptor induced cell death and Type I/II signalling found that Type I cells can induce a Type I and II response simultaneously (Yamada *et al*, 1999) and furthermore the inhibitory effects of over-expressed Bcl-2 can be overcome with high doses of TRAIL (Rudner *et al*, 2005). In addition, the difference in DISC strength observed in Type I and II cells (Scaffidi *et al*, 1998) has been suggested to be as a result of receptor clustering in lipid rafts. Muppidi and colleagues discussed how receptor localisation in lipid rafts can determine the proximal signalling events induced by the TNF-family of receptors (Muppidi *et al*, 2004). CD95-induced apoptosis in Type I cells has been shown to be associated with the involvement of lipid rafts whilst, in Type II cells, the receptor is found to be excluded from lipid rafts (reviewed in Muppidi *et al*, 2004). Similarly, it has been suggested that TRAIL-signalling to apoptosis requires DISC assembly in lipid rafts and that non-lipid raft DISC assembly inhibits TRAIL-induced apoptosis (Song *et al*, 2007). Lipid rafts are membrane micro-domains consisting of sphingolipids and cholesterol, which have low fluidity and high rigidity, and are critical for some cellular processes including ligand-receptor interactions and endocytosis (Mattson, 2005). However, work carried out in our laboratory found that in Z138 cells

only a small fraction of TRAIL DISC associates with lipid rafts and the majority of TRAIL DISC generated is in a 'soluble' non-lipid raft fraction despite Z138 cells successfully signalling to apoptosis (Dickens *et al*, 2011).

The protein expression levels of key pro- and anti-apoptotic proteins can influence the sensitivity of cells to apoptotic stimuli. For example, Inhibitor of Apoptosis (IAP) proteins can modulate the activity of caspases activated by both the intrinsic and extrinsic pathway to prevent apoptosis (reviewed in Deveraux and Reed, 1999). Thus, the balance of pro- and anti-apoptotic proteins is also important for successful signalling to apoptosis. Similarly, a high cFLIP to caspase-8 ratio at the DISC can prevent activation of the extrinsic pathway (MacFarlane *et al*, 2002; Micheau, 2003). Thus, the balance of pro- and anti-proteins in a cell must favour a pro-apoptotic phenotype in order to successfully signal to cell death.

TRAIL surface-receptor expression is also paramount for successful signalling to cell death. A study by MacFarlane *et al* found that primary Chronic Lymphocytic Leukaemia (CLL) is largely resistant to TRAIL due to low surface receptor expression of TRAIL-R1 and -R2 (MacFarlane *et al*, 2002). Thus, analysis of TRAIL surface-receptor expression is clearly key in predicting if cancer cells are going to be sensitive to TRAIL-induced apoptosis. Interestingly, research with TRAIL-receptor selective mutants found that cancer cells largely signal to death through TRAIL-R1 only (MacFarlane *et al*, 2005). Despite these observations, the majority of PARA's, to date, target TRAIL-R2 (Ashkenazi, 2008) and thus may explain the low response of some primary cancer cells to these treatment approaches. Taken together, these data suggest that specific cancer types need to undergo in-depth functional characterisation to determine if they are likely to be responsive to TRAIL and only then should this be considered a suitable cancer therapeutic strategy.

3.3.2 Proteomic Analysis of the Z138 TRAIL DISC

It is apparent, from the comparisons made in this chapter, that the TRAIL DISC is a dynamic-system dependent on tumour type and, therefore, questions still remain regarding the specific mode of action, and thus successful signalling to apoptosis, by this death ligand. The formation of the DISC in death receptor signalling is vital for initiation of the apoptotic pathway and any deregulation at the level of the DISC completely abrogates the apoptotic signal. cFLIP, a catalytically inactive caspase-8 homolog, is suggested as one such deregulator, which interferes with the recruitment

and activation of pro-caspase-8 through heterodimerisation. cFLIP is expressed as either a long (cFLIP_L) or short (cFLIP_s) isoform, the latter of which contains the *N*-terminal DED's only and thus completely blocks caspase-8 activation (Chang *et al*, 2002). Conversely cFLIP_L, although enzymatically inactive, shows high homology to caspase-8 and at endogenously expressed levels demonstrates the ability to facilitate the apoptotic signal through its hetero-interaction with caspase-8 (Chang *et al*, 2002). Analysis of the Z138 TRAIL DISC revealed the accumulation of cFLIP_L but not cFLIP_s (Fig. 3.6) thus suggesting that the absence of cFLIP_s and the low levels of cFLIP_L could be facilitating TRAIL-signalling.

Prototype death ligands, such as TNF α and CD95L, have been essential in elucidating the role and formation of the TRAIL DISC, both of which form TRAIL DISC-like complexes. More recently, novel components of the TNF-R1 signalling complex have been identified using affinity purification along with mass spectrometry (Haas *et al*, 2009). Similarly, the aim of the research performed in this chapter was to successfully isolate a large scale Z138 TRAIL DISC to detect and analyse known and novel components by mass spectrometry analysis (Fig. 3.11). From this analysis PP1 α/γ , protein DEK and the transferrin receptor were investigated as potential novel DISC interactors. Out of these proteins, the transferrin receptor was the only identified protein that was successfully found to be present in an isolated Z138 TRAIL DISC (Fig. 3.15). Follow-up experiments to determine the role of this protein in TRAIL-signalling were unsuccessful (data not shown). RNAi-based experiments were performed but either the transferrin receptor protein was still expressed or the results were not reproducible despite successive attempts. Thus, this approach needs further optimisation to determine the role of the transferrin receptor in TRAIL-induced apoptosis.

Interestingly FADD, one of the most important TRAIL DISC components, had a relatively poor identification with respect to both the number of unique peptides identified (Table 3.2) and quality of spectra obtained (Fig. 3.3). However, quantitative proteomic analysis resulted in a high protein identification probability versus NSAF score and, based on its known role in the DISC, our confidence that it had been correctly identified was increased. However, the reason for the low abundance of FADD was still unclear. Thus, based on this observation, research in our laboratory was performed to investigate the actual structural formation of known DISC components on the premise that FADD appears to be present in sub-stoichiometric amounts to other known DISC components.

It is currently accepted that the known DISC components are present in a 1:1:1 ratio that is one TRAIL-receptor, recruits one molecule of FADD, which in turn recruits one DED-containing protein. However, this structure does not account for dimerisation of caspase-8 molecules, which is an absolute requirement activation and cleavage of caspase-8 (Hughes *et al*, 2009). Thus, using both the mass spectrometry data discussed in this chapter and data generated by colleagues in BJAB and Jurkat cells, we were able to show that the adaptor molecule FADD is present in sub-stoichiometric amounts compared to caspase-8 in a range of haematopoietic cell lines (Dickens *et al*, 2011). Using label-free quantitative counting, we were then able to show that the accepted 1:1:1 ratio does not agree with our observations and that caspase-8 is instead in excess relative to FADD (Dickens *et al*, 2011). These findings have resulted in a new structural model of the DISC, which takes in to account the low levels of FADD, and is based on formation of a DED-chain (Dickens *et al*, 2011). These findings have significant implications into how the known DISC components interact and could aid in our understanding of how TRAIL successfully signals to cell death.

To conclude, the use of mass spectrometry-based analysis in this study of the TRAIL DISC has provided two significant findings. Firstly, this approach permitted the identification of the transferrin receptor as a novel component of the TRAIL DISC where it was found to specifically interact with the TRAIL-receptors. Although preliminary RNAi experiments against the transferrin receptor were unsuccessful in the Z138 cell line, further experiments need to be performed to elucidate its role in TRAIL-induced apoptosis in Z138 cells. Secondly, the observation and determination that FADD is sub-stoichiometric in the TRAIL DISC permitted a line of research that suggests the formation of the DISC differs significantly from the currently accepted complex structure. These results provide important previously unidentified findings that could aid in interpreting how TRAIL DISC formation and its absolute components differ between sensitive and resistant cell lines. Thus, these findings should be used as a bench-mark for future research into the analysis of the TRAIL DISC and, potentially, the analysis of other apoptotic signalling complexes such as the CD95 DISC. In the final discussion (Chapter 6) I have outlined the experiments that could be performed to follow-up the research carried out in this chapter.

4. Metabolic Regulation of TRAIL-induced Apoptosis

4.1 Introduction

There is increasing evidence to support the view that during neoplasia there is extensive metabolic reprogramming to support tumour cell growth and proliferation (DeBerardinis *et al*, 2008). Glycolysis, although more rapid than oxidative phosphorylation, is an essentially inefficient method of producing ATP and is thought to predominate in tumours as a direct result of hypoxia during early stage tumorigenesis (Cairns *et al*, 2011). However, the rate at which glycolysis occurs in cancer cells means that their energy demands are sufficiently met. Furthermore, in addition to ATP, glycolysis can provide the intermediates necessary for the pentose phosphate pathway, which is used to produce ribose sugars (nucleotide synthesis), reducing equivalents (fatty acid synthesis), and non-essential amino acids. Thus, since the switch from mitochondrial respiration to glycolysis appears to be a hallmark of cancer cells (Warburg, 1956), there is increasing interest in using and developing glycolytic inhibitors to target cancer cells (Pelicano *et al*, 2006).

2-Deoxyglucose (as discussed in Chapter 1) is a glucose analogue, which inhibits the phosphorylation of glucose by hexokinase and as a result competitively inhibits glucose metabolism (Parniak and Kalant, 1988). Its inhibitory role in glycolysis has long been known (Brown, 1962) as has the altered metabolic phenotype of cancer cells (Warburg, 1956). Thus, the potential for 2DG, and other glucose analogues, as cancer therapeutic agents has been examined extensively (reviewed in Pelicano *et al*, 2006). For example, cell killing by 2DG has been described in several human cancer cell lines (Jain *et al*, 1985; Kaplan *et al*, 1990; Ko *et al*, 2001; Muñoz-Pinedo *et al*, 2003; Dwarakanath *et al*, 2005; Coleman *et al*, 2008), animal models (Kern and Norton, 1987; Mjiyad *et al*, 2011) and phase I/II clinical trials (reviewed in Dwarakanath *et al*, 2009; Mjiyad *et al*, 2011). It is important to note, however, that the majority of these studies employ 2DG in combination with other treatments rather than as a single-agent. In addition, 2DG shows evidence of cytotoxicity *in vitro* and *in vivo* and thus its potential as a cancer therapeutic appears limited (Aft *et al*, 2002; reviewed in Dwarakanath, 2009). Nevertheless, exploiting the metabolic phenotype of cancer cells for diagnostic purposes offers a promising line of novel research because of its potential as a targeted therapy.

An alternative approach to targeting cancer cell metabolism, in contrast to glucose analogues, is the notion that depriving cancer cells of glucose may also have the same effect but without the cytotoxicity or undesirable side-effects. Glucose-deprivation

studies have intensified over the last decade, the majority of which have had varying successes in sensitising cancer cells to apoptotic stimuli following glucose-deprivation. This is thought largely to be a direct result of glycolysis inhibition and the changes associated with targeting this pathway. However, these studies appear not to examine mitochondrial respiration in addition to glycolysis, presumably on the premise that inhibiting glycolysis would also prevent metabolism through the citric acid cycle and oxidative phosphorylation. However, it has long been known that some cancer cells display signs of excess glutamate metabolism and fatty acid oxidation (Lawrence *et al*, 1979; Newsholme *et al*, 1983; DeBerardinis and Cheng, 2010; Pike *et al*, 2011) and thus could compensate for any loss through glycolysis. Furthermore, the centres of solid tumours have often been associated with hypoxic (or even anoxic) conditions along with significantly low glucose levels and thus, although slower growing, these cells are able to survive and proliferate even under such extreme conditions. This suggests that glucose metabolism may not be their only means of obtaining energy. Therefore, in line with this, the research carried out in this chapter aims to investigate how glycolytic and oxidative phosphorylation status, following 2DG treatment or glucose-deprivation, affects TRAIL-induced apoptosis. Furthermore, the ability of cells to survive and proliferate under conditions of extreme low glucose are examined.

Firstly, the metabolic phenotype of 2DG treated cells was assessed using Extracellular Flux (XF) analysis along with analysis of cellular ATP levels. The apoptotic response of these cells to TRAIL-induced apoptosis was then determined in addition to the effect of 2DG on protein expression levels. As a direct comparison, the response of cells to short-term (acute) glucose deprivation (1 and 20 h) was examined, also by extracellular flux analysis and cellular ATP level measurements. The response of these cells to TRAIL-induced apoptosis was determined and the balance between apoptotic cell death and necrotic cell death discussed. Finally, the long-term (chronic) glucose-deprivation of Z138 cells was assessed including metabolic phenotyping, ATP level assessment, analysis of responses to apoptotic stimuli and signalling through the mitochondrial amplification loop. This was followed by the assessment of proteomic and ultra-structural changes at the mitochondria. These results show that in Z138 cells, the anti-glycolytic effects of 2DG and glucose restriction produced opposite effects on TRAIL-induced cell death. Furthermore, these results demonstrate that mitochondrial metabolism can enable both survival and proliferation under conditions of glucose-deprivation, but not when incubated with 2DG, and that this effect appears to modulate apoptosis.

4.2 Results

4.2.1 2DG reduces glycolytic flux and sensitises Z138 cells to TRAIL-induced apoptosis

Initially, studies to determine the effect(s) of the anti-glycolytic 2-deoxyglucose (2DG) on the metabolism of Z138 cells were performed. Using a Seahorse Extracellular Flux (XF) Analyser, real-time measurements of oxygen consumption (OCR) and extracellular acidification (ECAR), indicative of oxidative phosphorylation and glycolysis respectively, were measured in Z138 cells maintained on glucose, pyruvate and glutamine in the absence (-) or presence (+) of 5 mM 2DG for 20 h (Fig. 4.1a - e).

In the absence of 2DG, Z138 cells exhibited basal OCR levels of ~ 600 pmol/min/ 10^6 cells (Fig. 4.1a and c) coupled with high ECAR values of ~ 200 mpH/min/ 10^6 cells (Fig. 4.1b and d). In comparison, incubating Z138 cells with 5 mM 2DG for 20 h reduced basal OCR by 35% to ~ 400 pmol/min/ 10^6 cells (Fig. 4.1a and c) demonstrating that $\sim 1/3^{\text{rd}}$ of the basal OCR was due to glucose-derived metabolism. Notably, this decrease was not significant. The remaining respiratory capacity is likely to be derived from pyruvate and glutamine through the TCA cycle. Since 2DG cannot be metabolised by the glycolytic or pentose phosphate pathways (Parniak and Kalant, 1988), incubating Z138 cells with 2DG had profound effects on the glycolytic rate of these cells (Fig. 1b and d). Basal ECAR of 2DG treated Z138 cells decreased by around 80% to ~ 40 mpH/min/ 10^6 cells compared to control (-2DG) cells (Fig. 4.1b and d). These results show that 2DG inhibition of glycolysis alters the OCR/ECAR ratio of the cells, diminishing glycolysis and reducing oxidative phosphorylation capacity (Fig. 4.1e). Significantly, this reduction in glycolytic capacity resulted in a 50% reduction in cellular ATP levels (Fig. 4.1f).

Inhibitors of mitochondrial respiration were utilised to further define the metabolic profile of 2DG-treated cells. FCCP and rotenone, as discussed in the Introduction (Chapter 1), were added to the cells as indicated (Fig. 4.1a and b). FCCP is a protonophore which, in coupled mitochondria, depolarises the mitochondrial membrane and thus stimulates oxygen consumption via the electron transport chain. Upon injection, FCCP induced a small increase ($\sim 20\%$) in OCR regardless of whether the cells had been incubated with or without 2DG (Fig. 4.1a).

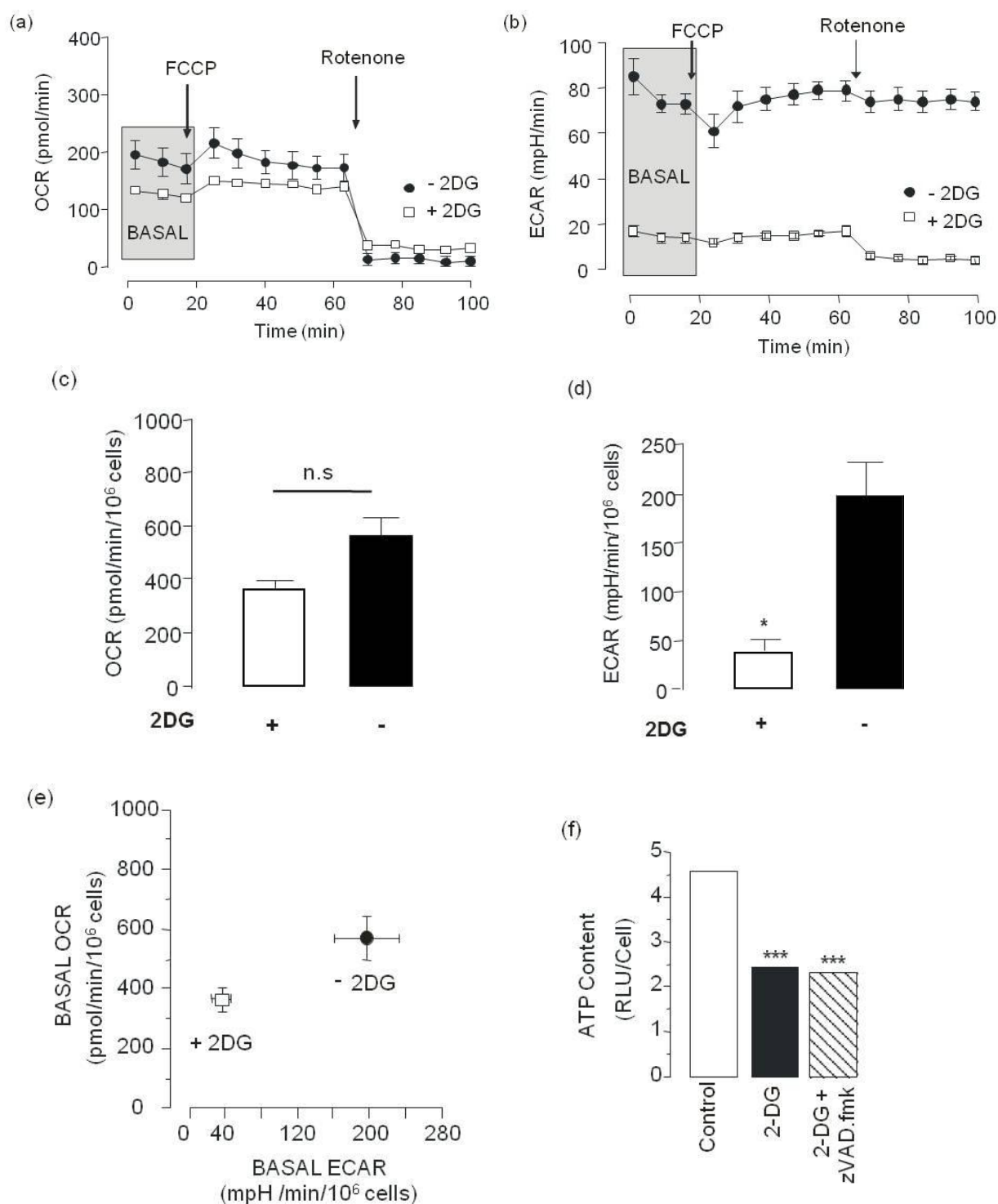


Figure 4.1 Inhibition of glucose metabolism with 2DG significantly reduces glycolytic flux and ATP levels. Z138 cells were cultured for 20 h in 11 mM glucose, 1 mM pyruvate and 2 mM glutamax supplemented media in the absence (●) or presence (□) of 5 mM 2DG. Real-time measurements of (a) OCR and (b) ECAR were measured in 24 well Seahorse assay plates (mean ± SEM, n=3). Graphs are representative of three independent experiments and display the effects of the mitochondrial inhibitors: FCCP (400 nM) and rotenone (1 μM). Basal OCR (c) and ECAR (d) values were calculated from the mean basal values of each real-time run and normalised to cell number (mean± SEM, n=3). (e) The effect of 2DG on the balance between glycolysis (ECAR) and oxidative phosphorylation (OCR). (f) ATP levels of Z138 cells incubated without 2DG (open bar), with 2DG (black bar) or with 2DG plus zVAD.fmk (hatched bar) were assayed as described in Materials and Methods. Where indicated, cumulative data were analysed by Students *t*-test where n.s - not significant, **P*<0.05 and ****P*<0.001.

Upon injection of rotenone, an electron transport chain complex I inhibitor, the OCR in both cell types was inhibited by >95% demonstrating that the observed respiration was largely derived from oxidative phosphorylation. Interestingly, rotenone had very little effect on the ECAR in control (-2DG) cells but it further abrogated the ECAR in 2DG treated cells (Fig. 4.1b). This suggests that, under these conditions, the residual ECAR levels observed in 2DG treated cells were likely due to a rotenone-sensitive, electron transport chain-dependent, proton leak from the mitochondria. These data show that incubating Z138 cells with 2DG significantly reduces glycolytic flux and, as a secondary effect, reduces (the glycolysis-dependent) oxidative phosphorylation capacity, which results in a significant decrease in cellular ATP levels.

Next, the effect of 2DG on the sensitivity of Z138 cells to TRAIL-induced apoptosis was examined. Previous findings have shown that 2DG potentiates TNF α killing in U937 cells (Halicka *et al*, 1995) and CD95 and TRAIL-induced apoptosis in HeLa, MCF-7 and melanoma cell lines (Muñoz-Pinedo *et al*, 2003; Liu *et al*, 2009). Therefore, Z138 cells were treated with (\square) or without (\bullet) 5 mM 2DG for 20 h followed by induction of cell death with varying concentrations of TRAIL (0-1000 ng/ml) for 4 h (Fig. 4.2a). The data show that Z138 cells treated with 2DG were 6-8 fold more sensitive to TRAIL-induced killing (EC_{50} = 25-30 ng/ml) compared to control cells (EC_{50} = 180-200 ng/ml) (Fig. 4.2a). 2DG treatment alone would presumably, given time, cause the cells to die as a direct result of the loss of ATP. Nevertheless, 2DG pre-treatment appears to exert a synergistic effect on TRAIL-induced apoptosis since the response of cells to TRAIL is enhanced when cells are pre-incubated with 2DG (Fig. 4.2a and c).

Cleavage of caspases-8, -3 and PARP (a caspase-3/-7 substrate) was detectable with concentrations as low as 25 ng/ml TRAIL in 2DG-treated cells compared to 100 ng/ml for control cells (Fig. 4.2b). TRAIL-induced caspase-mediated apoptosis was inhibited by pre-incubation with zVAD.fmk (Fig. 4.2a) but, significantly, this did not abrogate the effects of 2DG on cellular ATP levels (Fig. 4.1f). Thus the metabolic effects of 2DG on ATP production were not due to caspase activity. However, it was also evident that incubating Z138 cells with 2DG alone considerably stressed the cells as basal levels of cell death, prior to incubation with TRAIL and in the presence of zVAD.fmk, were ~20% compared to control cells where basal cell death was ~10% (Fig. 4.2a). Thus, the addition of 2DG alone appeared to confer some toxicity to the cells, which in part could be due to the significant reduction in ATP levels (Fig. 4.1d and f).

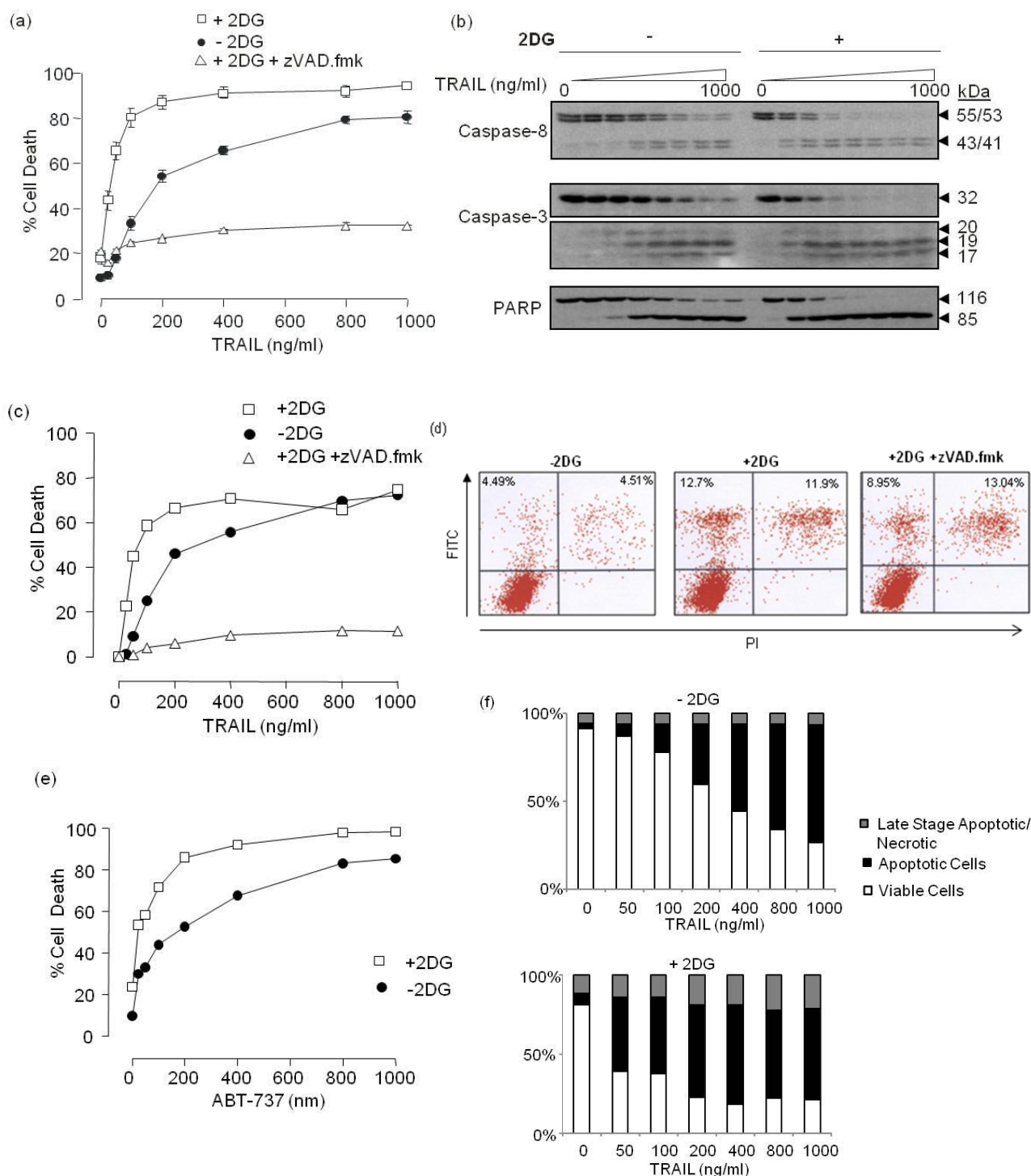


Figure 4.2 2DG inhibition of glycolysis sensitises Z138 cells to TRAIL-induced apoptosis. Z138 cells were cultured for 20 h in 11 mM glucose, 1 mM pyruvate and 2 mM Glutamax supplemented media in the absence (●) or presence (□) of 5 mM 2DG ± zVAD.fmk and further incubated with varying concentrations of TRAIL (0-1000 ng/ml) for 4 h. (a) Cells were analysed for % cell death as outlined in Materials and Methods (mean ± SEM, n=3). (b) Whole cell pellets from (a) were analysed for caspase-8, caspase-3 and PARP cleavage by immunoblotting. (c) Data obtained in (a) were normalised to '0' to account for background cell death. (d) Dot plots generated by the CellQuest-Pro software for the measurement of apoptosis show control (-), 2DG (+) and 2DG + zVAD.fmk treated Z138 cells at 0 ng/ml. Apoptotic cells are annexin V-FITC positive (upper left quadrant) and late stage apoptotic/necrotic are annexin V-FITC and PI positive (upper right quadrant). (e) Control (-) and 2DG treated (+) Z138 cells were treated with various concentrations of ABT-737 (0-1000 nM) for 4 h and assessed for loss of MMP. Results are from one experiment. The relative distribution of apoptotic and late apoptotic/necrotic with increasing TRAIL-treatment are shown in (f)

Similarly, if these cells were 'normalised' to basal levels then the increase in sensitivity is less significant (Fig. 4.2c). Furthermore, it is evident using FACS analysis that 2DG induces causes necrotic rather than apoptotic cell death (Fig. 4.2d), as a single agent, since basal death is occurring even in the presence of the pan-caspase inhibitor zVAD.fmk (Fig. 4.2a). Thus, a clear distinction between cell death that is apoptotic versus that which is necrotic is essential, especially when examining its potential as a cancer therapeutic.

The effect of 2DG on the cellular content of selected pro- and anti-apoptotic proteins was also investigated in order to determine the underlying cause of the observed increase in sensitivity to TRAIL (Fig. 4.3). Interestingly, following 2DG treatment, the majority of proteins examined were down-regulated (Fig. 4.3). In particular, Mcl-1 was significantly depleted in 2DG treated cells and this is in agreement with a recently published study (Pradelli *et al*, 2009). The pro-apoptotic protein cFLIP_L appeared to be the only protein examined that has maintained its cellular levels (Fig. 4.3). These data show that 2DG-treatment significantly alters the ratio of pro- and anti-apoptotic proteins prior to treatment with a death ligand. Thus, the down-regulation of key anti-apoptotic proteins and the stabilised levels of cFLIP_L, taken together, could explain the increase in sensitivity to TRAIL and other death stimuli (Fig. 4.2a and Fig. 4.2e).

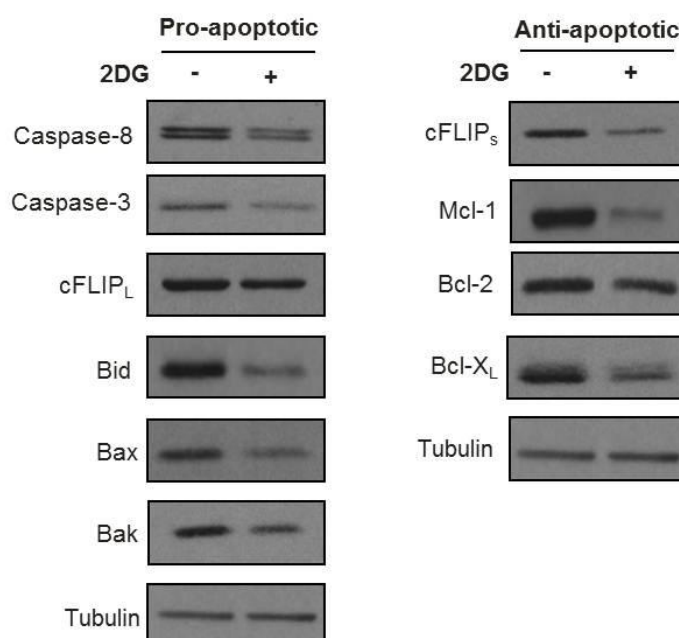


Figure 4.3 Incubation of cells with 2DG results in the down regulation of key pro- and anti-apoptotic proteins. Whole cell pellet samples from Z138 cells incubated in the absence (-) or presence (+) of 2DG for 20 h were immunoblotted for the indicated pro- and anti-apoptotic proteins. Tubulin was used as a loading control. Results are representative of three independent experiments.

4.2.2 Acute glucose-deprivation sensitises Z138 cells to TRAIL-induced apoptosis but only before they become acclimatised

Although 2DG clearly sensitises cells to apoptotic stimuli, it is evident that as a single agent it is cytotoxic and furthermore there are increasing reports to suggest that it is no longer merely a low glucose mimetic (Kang and Hwang, 2006). This is largely due to the off-target effects 2DG has on protein glycosylation and protein folding (Zhang and Kaufman, 2004; Kurtoglu *et al*, 2007; Mjiyad *et al*, 2011). Similarly, despite a number of clinical trials, the potential of 2DG as a cancer therapeutic appears to be limited to a sensitising agent for other commonly used therapeutics. Thus, an alternative approach to the use of glycolytic inhibitors to prevent glycolysis is to deprive a tumour of glucose and thus abrogate glycolysis through a more physiological route. Glucose-deprivation could then be used as a way to 'prime' a cell for death before treatment with a chemotherapeutic agent. To date, the majority of studies investigating glucose deprivation and chemotherapeutics have largely carried out short-term deprivation studies (Nam *et al*, 2002; Muñoz-Pinedo *et al*, 2003; Pradelli *et al*, 2009; Caro-Maldonado *et al*, 2010). Therefore, initially I performed glucose-deprivation experiments for 1 h followed by incubation with TRAIL for 4 h, in the same media, to assess for cell death (Fig. 4.4). It should be noted, however, that the glucose deprivation models discussed below include incubating the cells with fetal calf serum (FCS), which contains 0.52 mg/ml of glucose. This could, therefore, provide the cells with some residual glucose and thus these experiments could also be referred to as low glucose rather than glucose deprivation.

The results show that, similar to pre-treatment with 2DG, glucose-deprivation for 1 h sensitised cells to TRAIL-induced apoptosis (Fig. 4.4a). However, when performing FACS analysis on these cells it was evident that (i) the basal cell death under both conditions was elevated to ~20 % (Fig. 4.4a) and (ii) there was a significant input from necrotic cell death in the 'sensitisation' of glucose-free cells (Fig. 4.4b). Thus, these data indicate that the mode of cell death has switched from apoptotic to necrotic cell death under conditions of glucose-deprivation and therefore might not be representative of a sensitising agent.

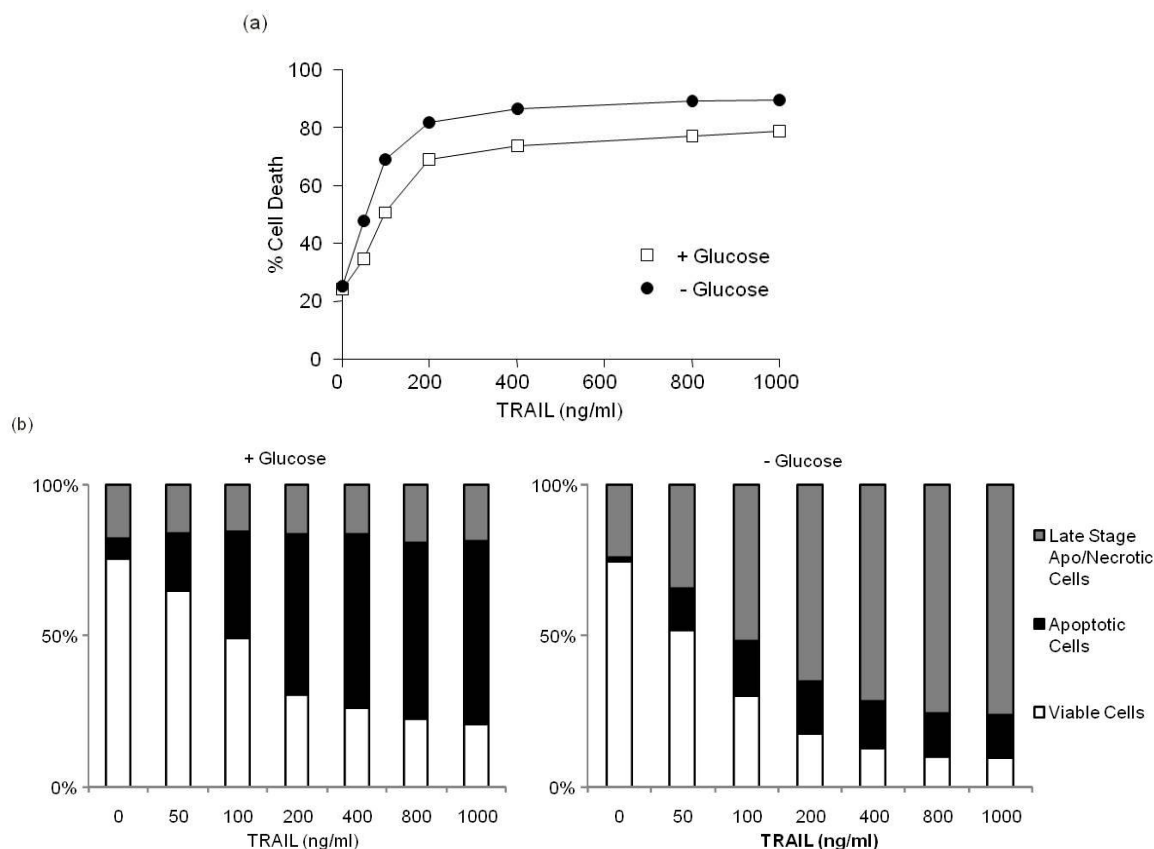


Figure 4.4 Acute (1 h) glucose-deprivation sensitises cells to TRAIL but through necrotic rather than apoptotic cell death. (a) Z138 cells cultured with (□) or without (●) glucose for 1 h were treated with 0-1000 ng/ml TRAIL for 4 h and assessed for cell death (n=1). (b) The relative input from the 'healthy', 'apoptotic' or 'late stage apoptotic/necrotic' quadrants from FACS analysis were examined from the experiment shown in (a) and as outlined in Materials and Methods.

I next determined if 20 h glucose-deprivation would enable the cells to acclimatise to the loss of glucose and thus become sensitised to TRAIL-mediated apoptosis without necrosis. Therefore, to begin, I determined the metabolic status of cells deprived of glucose for 20 h using extracellular flux analysis (Fig. 4.5a) to ensure that, similar to 2DG, the glycolytic capacity of these cells was hindered through the lack of glucose for this length of time. Interestingly, the results show that Z138 cells cultured in the absence of glucose for 20 h, unlike 2DG treated cells, had an approximately 30% increase in basal OCR (Fig. 4.5a). This was accompanied by a more significant (> 85%) decrease in glycolysis and/or extracellular acidification as measured by ECAR (Fig. 4.5b). Thus, in comparison to 2DG, 20 h glucose-deprivation had similar effects on the glycolytic capacity of these cells (Fig. 4.1b and Fig. 4.5 b) but had opposing effects on the mitochondrial capacity of these cells (Fig. 4.1a and Fig. 4.5a). Thus, similar to 2DG, mitochondrial inhibitors were employed to further define the metabolic status of these cells (Fig. 4.5a and b). In addition to FCCP and rotenone, the ATP synthase inhibitor oligomycin was utilised to determine if the OCR increase, under conditions of acute (20 h) glucose-deprivation, was directly associated with an increase

in mitochondrial respiration. Upon addition of oligomycin, the OCR of both + and – glucose cells were inhibited (Fig. 4.5a). The addition of FCCP uncoupled mitochondria and allowed maximal respiratory chain activity (OCR), the response of which did not differ between conditions, and was inhibited by the addition of rotenone (Fig. 4.5a). The effects discussed above on OCR differ from those obtained with 2DG and suggest that mitochondrial respiration can be increased under conditions of acute (20 h) glucose deprivation but not with 2DG (Fig. 4.1a and 4.5a). However, glucose-deprivation and 2DG appear to exert the same effects on glycolysis; that is a complete inhibition (Fig. 4.1b and Fig. 4.2b).

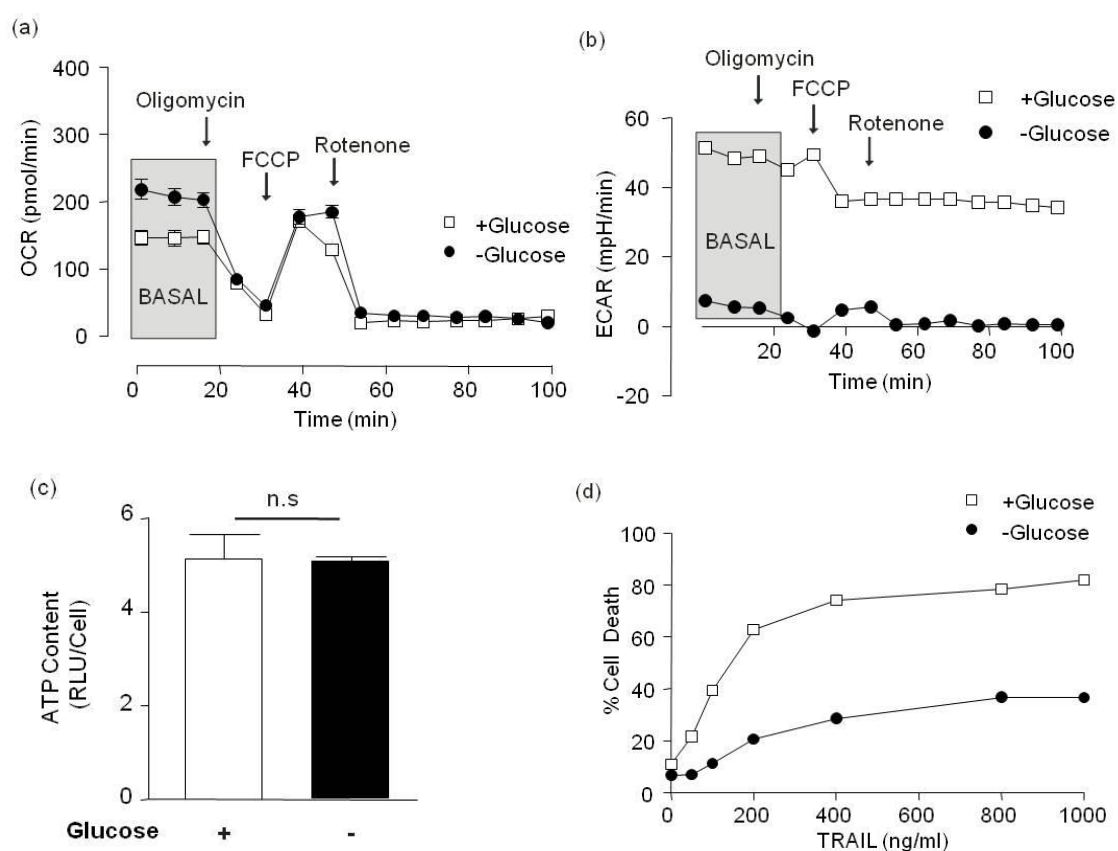


Figure 4.5 Acute (20 h) glucose-deprivation significantly reduces glycolytic flux whilst maintaining ATP levels concomitant with a loss in sensitivity to TRAIL-induced apoptosis. Z138 cells were cultured for 20 h in glutamax- and pyruvate-supplemented media with or without glucose. Real-time measurements of OCR (a) and ECAR (b) were taken from + (□) and – (●) glucose cells (n=2). Graphs are from one experiment and display the effects of the mitochondrial inhibitors: Oligomycin (400 nM), FCCP (400 nM) and Rotenone (1 μM). (c) Cellular ATP levels were measured in glucose-cultured (open bar) and glucose-deprived (black bar) as described in Materials and Methods. Where indicated, cumulative data were analysed by students *t*-test where n.s – not significant. (d) Z138 cells cultured with (□) or without (●) glucose for 20 h were treated with 0-1000 ng/ml TRAIL for 4 h and assessed for cell death (n=2).

Due to the glucose-deprivation effects on OCR, cellular ATP levels were examined following 20 h glucose-deprivation (Fig. 4.5c). The results show that under these conditions, ATP levels can be maintained (Fig. 4.5c), which might be a direct result of the increase in mitochondrial-respiration (Fig. 4.5a). Thus, taken together, these results differ from those obtained from 2DG treated cells and also to previous studies that have reported a reduction in ATP levels upon glucose limitation (Muñoz-Pinedo *et al*, 2003).

Next, the effect of acute (20 h) glucose-deprivation on the sensitivity of cells to TRAIL-induced apoptosis was examined. Therefore, similar to 2DG, control (□) and glucose-deprived (●) Z138 cells were incubated with varying concentrations (0-1000 ng/ml) of TRAIL for 4 h and assessed for cell death (Fig. 4.5d). The results show that under conditions of glucose-deprivation, Z138 cells display a concentration-dependent loss in sensitivity to TRAIL (Fig. 4.5d). These findings further differ to those observed with 2DG (Fig. 4.2) and together suggest that Z138 cells can up-regulate mitochondrial respiration in the absence of glycolysis (Fig. 4.5a and b), which maintains ATP levels (Fig. 4.5c) and brings about a loss in sensitivity to TRAIL (Fig. 4.5d). Furthermore, the cytotoxic effects observed with 20 h 2DG treatment were not reciprocated following 20 h glucose-deprivation (Fig. 4.5d).

4.2.3 Chronic glucose-deprivation brings about a switch in bioenergetics and reduces the sensitivity of cells to apoptotic stimuli

The results discussed above suggest that cancer cells (or specifically Z138 cells) can be sensitised to apoptotic stimuli but only up to a threshold whereby they become acclimatised to these conditions and develop resistance to apoptotic stimuli. These results differ considerably from recently published papers (see Chapter 1). Therefore, in line with these findings, I sought to examine the effect(s) of chronic glucose deprivation (>7 days) on the cellular metabolism and apoptotic-response of Z138 cells, which was proposed to mimic a more physiological model of glucose-deprivation. Initial studies showed that Z138 cells could be maintained on glucose-free, pyruvate- and glutamine-supplemented media. Under these conditions, the glucose-free Z138 cells continued to proliferate, albeit more slowly, with a doubling time of 35-39 h compared to glucose-maintained cells which have a doubling time of 24-26 h. Thus, these slower growing, glucose-deprived cells could potentially mimic primary cancer cells at the centre of a solid tumour, which are known to be highly resistant to multiple cancer therapeutics.

Firstly, the metabolic competence of glucose-free (- glucose) Z138 cells against Z138 cells cultured with glucose (+ glucose) was compared. XF analysis showed that cells cultured in glucose-free media had increased levels of oxidative phosphorylation with basal OCR ~60% higher than in control cells (+ glucose) (Fig. 4.6a and c). Conversely, ECAR activity in glucose-maintained Z138 cells was ~6-fold higher than cells cultured in the absence of glucose (Fig. 4.6b and d) demonstrating that glycolytic flux had been almost completely abolished. In the absence of glucose, Z138 cells exhibited a higher OCR/ECAR ratio demonstrating a metabolic dependency, or switch, to oxidative phosphorylation (Fig. 4.6e). Interestingly, this switch in metabolism was not accompanied by changes in the cellular ATP content (Fig. 4.6f). Thus, under glucose-free conditions, pyruvate- and glutamine-metabolism via the respiratory chain and oxidative phosphorylation were sufficient to maintain cellular ATP levels. This also appears true for rescuing ATP levels after 20 h glucose-deprivation (Fig. 4.5c) but not when treated with the anti-glycolytic 2DG (Fig. 4.1f)

To further characterise the metabolic profile of glucose-free Z138 cells and to determine the mitochondrial coupling status of the cells, FCCP, rotenone, and oligomycin were employed. Upon addition of oligomycin, the OCR of both + and – glucose cells was inhibited by approximately 80% (Fig. 4.6a). This suggests that in Z138 cells, under both conditions, respiratory chain activity is tightly coupled to the ATP synthase complex. Subsequent addition of FCCP uncoupled mitochondria, bypassed the oligomycin block and allowed maximal respiratory chain activity (OCR), which could be inhibited by addition of rotenone (Fig. 4.6a). The addition of oligomycin and FCCP had minimal effects on the ECAR under either culture conditions (Fig. 4.6b). However, the addition of rotenone further abrogated the ECAR of glucose-free Z138 cells and thus residual ECAR was also likely to be derived from proton leakage at the mitochondria (Fig. 4.6b). Thus, in comparison to acute (20 h) glucose-deprivation, chronic (> 7days) glucose-deprivation further enhanced the observed increase in basal OCR but, similarly, maintained ATP levels and significantly inhibited glycolysis.

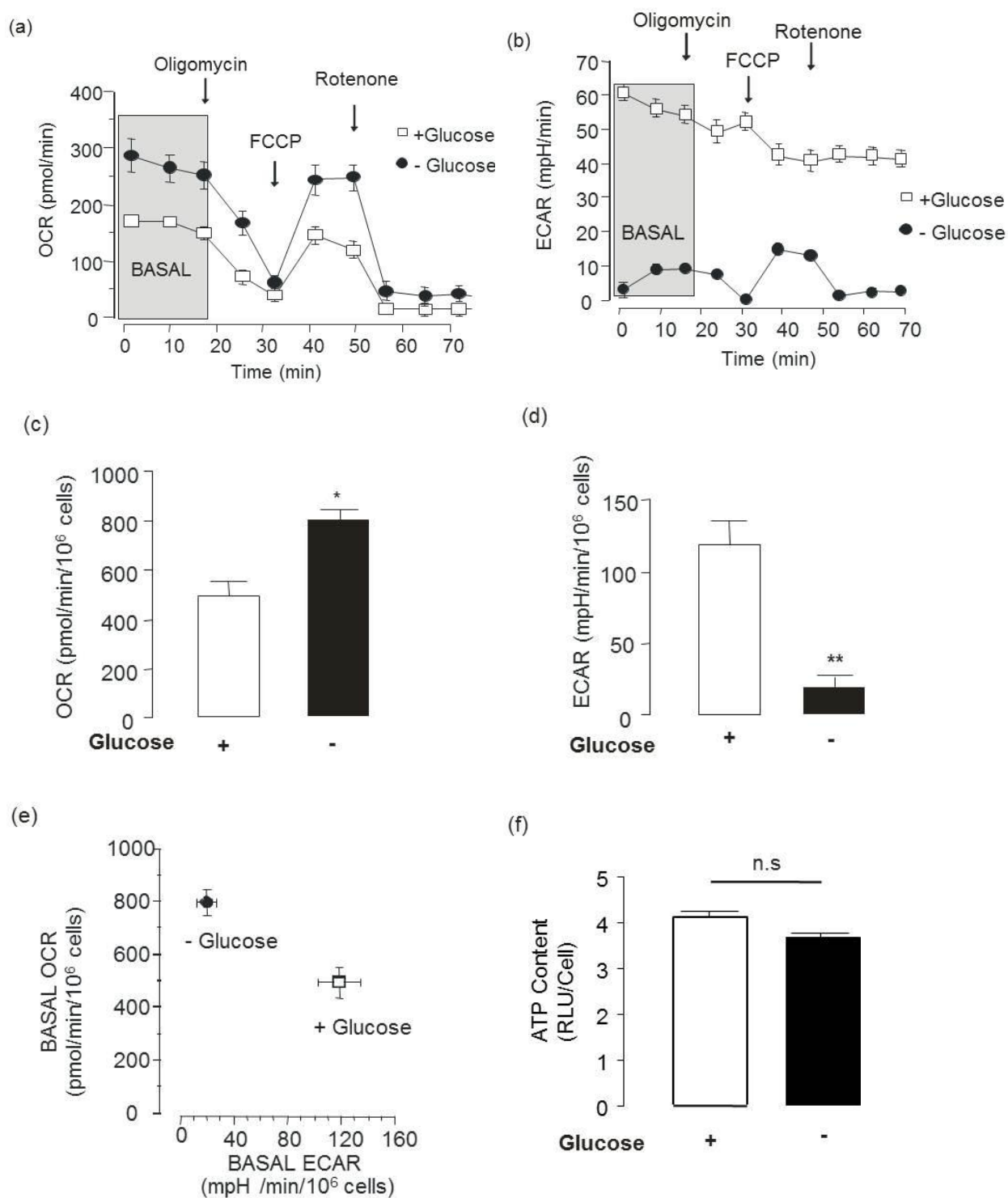


Figure 4.6 Prolonged glucose deprivation brings about a switch in bioenergetics from aerobic glycolysis to oxidative phosphorylation. Z138 cells were cultured for a minimum of 7 days in glutamax- and pyruvate-supplemented media with or without glucose. Real-time measurements of OCR (a) and ECAR (b) were measured in + (□) and – (●) glucose cells (mean ± SEM, n=3). Graphs are representative of three independent experiments and display the effects of the mitochondrial inhibitors: oligomycin (400 nM), FCCP (400 nM) and rotenone (1 μM). Basal OCR (c) and ECAR (d) values were calculated from the mean basal values of each real-time run and normalised to cell number (mean ± SEM). (e) The effect of 2DG on the balance between glycolysis (ECAR) and oxidative phosphorylation (OCR). (f) Cellular ATP levels were measured in + glucose (open bar) and – glucose (black bar) as described in Materials and Methods. Where indicated, cumulative data were analysed by Students *t*-test where n.s - not significant and **P*<0.05, ***P*<0.01.

To examine the effects of chronic glucose-deprivation on TRAIL-induced apoptosis, cells were incubated with various concentrations (0-1000 ng/ml) of TRAIL for 4 h or 400 ng/ml of TRAIL for various time points (0-6 h) and assessed for cell death and caspase-8 and -3 cleavage (Fig. 4.7). Similar to the findings observed with 20 h glucose-deprivation, chronic glucose-deprivation brought about a concentration- and time-dependent loss in sensitivity to TRAIL-induced apoptosis (Fig. 4.7). Z138 cells cultured in glucose-free media (●) were less sensitive to TRAIL (EC_{50} = 350-400 ng/ml) (Fig. 4.7a) and produced a slower onset of cell death (Fig. 4.7b) compared to Z138 cells cultured with glucose (□) (Fig. 4.7a-b). Thus, acute (20 h) and chronic (> 7 days) glucose-deprivation together confer a phenotype that was resistant to TRAIL-induced apoptosis and thus, in the following, I investigate the possibly mechanisms for this using chronic glucose deprivation as a representative model.

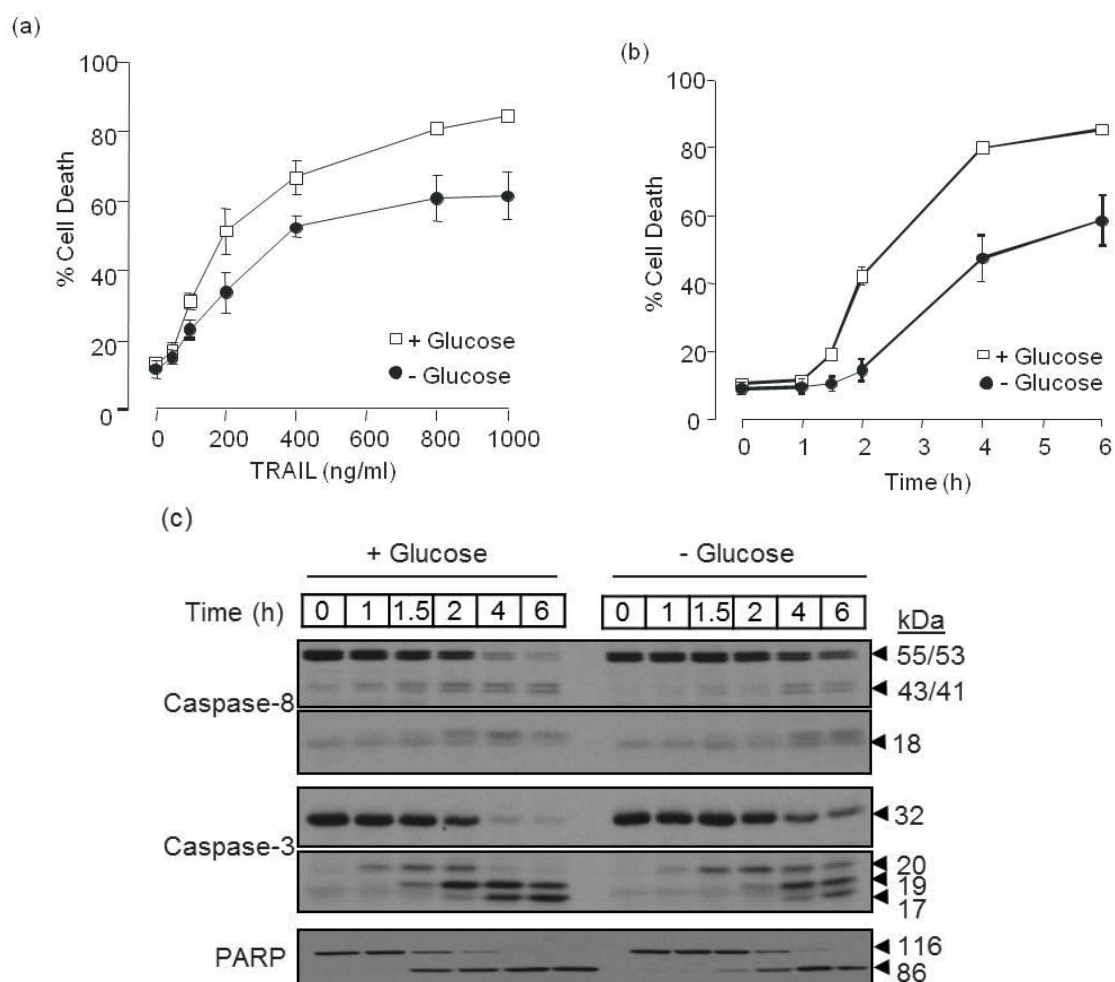


Figure 4.7 Z138 cells cultured in glucose-free media reveal a concentration- and time-dependent loss in sensitivity to TRAIL. (a) Z138 cells cultured with (□) or without (●) glucose were treated with 0-1000 ng/ml TRAIL for 4 h and assessed for cell death (mean ± SEM, n=3). (b) Z138 cells cultured with (□) or without (●) glucose were treated with 400 ng/ml TRAIL and assayed for cell death at the indicated times (0-6 h) (mean ± SEM). (c) Cell pellets taken from (b) were examined for caspase-8, caspase-3 and PARP cleavage. Immunoblots are representative of three independent experiments.

Due to the profound effects of 2DG on protein expression, the effects of glucose-deprivation on protein expression were also examined (Fig. 4.8). Initially, the cellular levels of proteins directly involved with DISC formation and/or activation and the cell death effector caspase – caspase-3, were examined. Interestingly, the data show that Z138 cells cultured in glucose-free media have increased basal levels of key pro-apoptotic proteins namely FADD, caspase-8 and caspase-3 (Fig. 4.8). However, there were no observed changes in the protein expression levels of cFLIP_L, cFLIP_S or RIP (Fig 4.8). Taken together, these changes in protein expression levels do not account for the loss of sensitivity to TRAIL-induced apoptosis observed in glucose-free Z138 cells. Rather, taken on its own, these data would suggest that glucose deprivation should enhance TRAIL-mediated cell death.

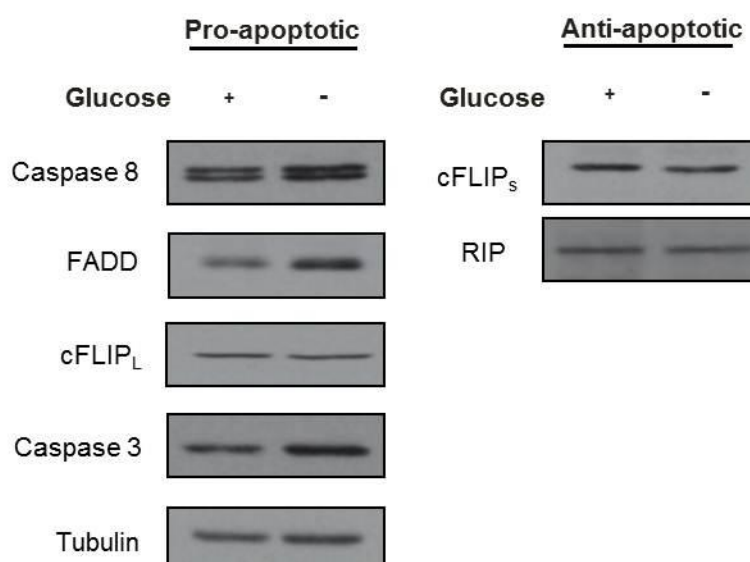


Figure 4.8 Protein expression levels of key pro- and anti-apoptotic proteins do not display changes associated with a loss in sensitivity to TRAIL-induced apoptosis. Whole cell pellet samples from Z138 cells incubated in the presence (+) or absence (-) of glucose were immunoblotted for the indicated pro- and anti-apoptotic proteins. Tubulin has been used as a loading control. Results are representative of three independent experiments.

4.2.4 Z138 cells cultured in glucose-free media have impaired DISC signalling

Since Z138 cells conditioned on glucose-free media were less sensitive to TRAIL, I investigated whether the key steps involved in triggering TRAIL-induced apoptosis, namely DISC formation and activity, were functional. I had already established that basal levels of FADD and caspase-8 were increased (Fig. 4.8) but this does not reflect how much protein is being recruited to the DISC. Therefore, TRAIL-receptor surface

expression levels, DISC formation and DISC activity were examined in Z138 cells cultured with (+) or without (-) glucose (Fig. 4.9).

Cell surface receptor expression analysis of TRAIL-R1 and TRAIL-R2 in glucose-free Z138 cells showed a slight decrease in basal levels compared to control (+ glucose) cells (Fig. 4.9a). Therefore, to determine whether this decrease in TRAIL-receptor expression conferred a reduction in DISC formation, the time course of DISC formation (0-60 min) was analysed in + and - glucose cells (Fig. 4.9b). In cells maintained on glucose, maximal DISC formation (determined by receptor, FADD and caspase-8 recruitment) was detected within ~20 min of TRAIL treatment whilst in the absence of glucose the rate of maximal DISC formation was slower (~50 min) (Fig. 4.9b).

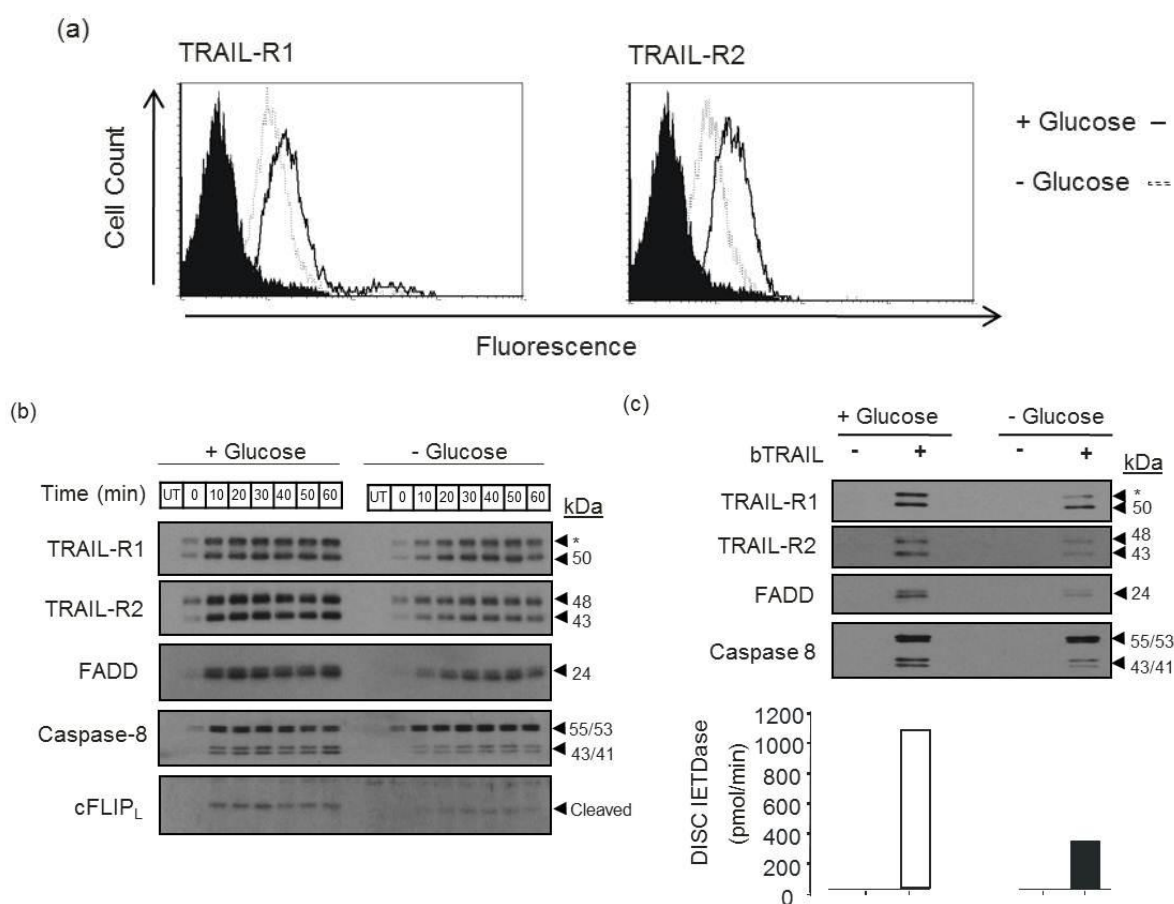


Figure 4.9 Z138 cells cultured in the absence of glucose have reduced surface expression levels of TRAIL-R1/R2 and form less active DISC (a) Glucose-containing (solid line) and glucose-free (broken line) Z138 cells were labelled with PE-conjugated TRAIL-R1, TRAIL-R2 or IgG (black fill) antibodies and assessed for receptor expression as outlined in Materials and Methods. Results are representative of three independent experiments. (b) Time-dependent DISC formation (0-60min) was assayed in (+) and (-) glucose cells using biotinylated WT-TRAIL (500 ng/ml). (c) DISC complexes were prepared from cells treated with TRAIL for 30 min and immunoblotted for TRAIL-R1/R2, FADD and caspase-8 (upper-panel). DISC preparations were then assayed for catalytic activity using ac.IETD.afc – a fluorimetric tetra-peptide substrate for caspase-8 (lower-panel). DISC activity is representative of two independent experiments.

Recruitment of FADD and processing of caspase-8 at the DISC were clearly reduced in glucose-free Z138 cells and this could be reflected in part by the decreased TRAIL-receptor surface expression levels (Fig. 4.9a-b). In addition, the initiator caspase activity of the isolated DISC, as measured by IETD.afc cleavage, was significantly reduced (~3-fold lower) when Z138 cells were cultured in the absence of glucose (Fig. 4.9c).

Based on the above findings, I decided to determine the relative significance of the observed TRAIL-R1/R2 receptor expression changes with respect to cell death and, therefore, employed TRAIL-specific ligands to identify which receptor(s) were signalling to cell death in Z138 cells. Previous studies in our laboratory have shown that receptor-selective mutants can be used to determine the relative contribution of TRAIL-R1 and/or -R2 in signalling to cell death (MacFarlane *et al*, 2005). Similarly, Human Genome Sciences (HGS) have generated humanised monoclonal TRAIL-R1 and TRAIL-R2 antibodies termed ETR1 and ETR2, respectively, both of which are currently undergoing clinical trials for use in the treatment of cancers (Georgakis *et al*, 2005). The results show that the TRAIL-R1 specific ligand signalled to apoptosis as efficiently as WT-TRAIL and there was a corresponding loss in sensitivity to the TRAIL-R1 specific ligand when cells were maintained on glucose-free media (Fig. 4.10).

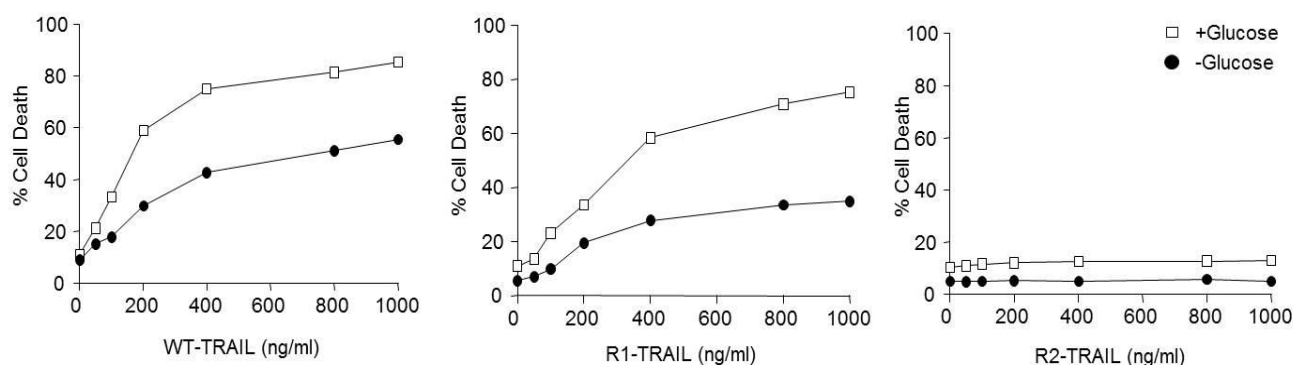


Figure 4.10 Z138 cells signal to apoptosis through TRAIL-R1 only. Z138 cells cultured with (•) or without (□) glucose were incubated for 4 h with varying concentrations (0-1000 ng/ml) of WT-TRAIL, R1-TRAIL or R2-TRAIL and analysed for cell death. Results are from two independent experiments.

Interestingly, treatment with the TRAIL-R2 specific ligand did not induce apoptosis, irrespective of whether the cells were maintained with (+) or without (-) glucose (Figure 4.10). This corresponds with earlier studies which found that primary lymphoid malignancies (MacFarlane *et al*, 2005) and pancreatic carcinomas (Stadel *et al*, 2010)

also signalled to apoptosis primarily via TRAIL-R1. Therefore, in Z138 cells cultured in the absence of glucose, down-regulation of TRAIL-R1 but not TRAIL-R2, in part, could explain the decrease in TRAIL DISC formation and the loss in sensitivity to TRAIL. However, heterotrimerisation of the TRAIL receptors could also be important for signalling to cell death and thus a decrease in TRAIL-R2 may confer a reduction in trimerisation, which itself could affect the propensity of TRAIL signalling.

4.2.5 TRAIL-Receptor glycosylation is not impaired under conditions of glucose deprivation

As described in Chapter 3, a recent study discussed the potential role of death receptor glycosylation in determining the sensitivity of tumour cells to TRAIL (Wagner *et al*, 2007). TRAIL-R1, but not any of the other known DISC components, is *N*-glycosylated and was reduced in size on SDS-PAGE gels when incubated with PNGase F (Fig. 3.9). Therefore, I investigated whether glycosylation of TRAIL-R1 was impaired under conditions of glucose deprivation and thus altering the sensitivity of Z138 cells to TRAIL (Fig. 4.11). Isolated DISCs from + and – glucose Z138 cells were treated with the endoglycosidase enzymes; Endo H and PNGase F to examine for changes in *N*-glycosylation (Fig. 4.11a). The data show that TRAIL-R1 undergoes deglycosylation upon treatment with PNGase F but not Endo H and this occurs irrespective of culture conditions (Fig. 4.11a).

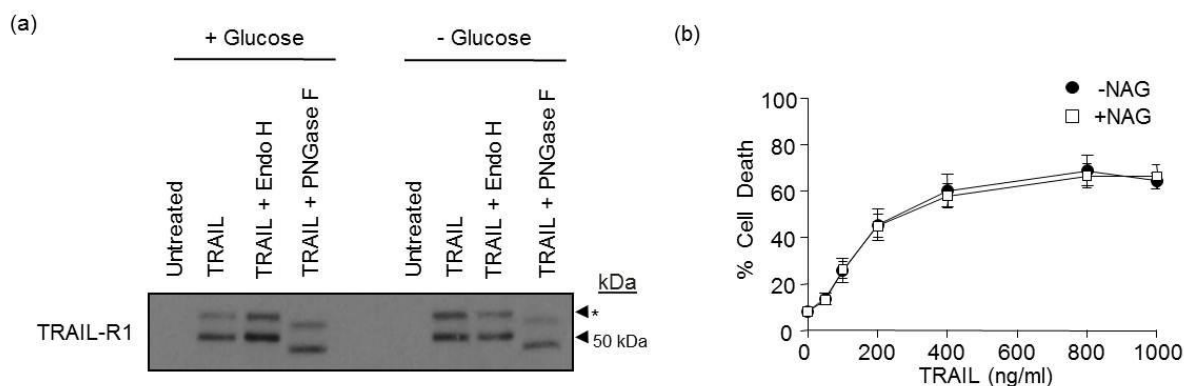


Figure 4.11 TRAIL-receptor glycosylation is not impaired under conditions of glucose-deprivation (a) DISC isolated TRAIL-R1 (DR4) from + and – glucose Z138 cells were treated with the endoglycoside enzymes Endo H and PNGase F to examine for *N*-glycosylation. Immunoblots are representative of three independent experiments. (b) Glucose-free Z138 cells were pre-incubated with (□) or without (●) *N*-acetylglucosamine (NAG) for 2 h followed by 4 h with various concentrations of TRAIL (0-1000 ng/ml) and assessed for cell death (mean ± SEM).

To confirm that *O*-glycosylation was also still functional under glucose-free conditions, Z138 cells were pre-incubated cells with *N*-acetylglucosamine (NAG), which promotes glycosylation (Kuo *et al*, 2008), to determine if the loss in sensitivity could be reversed

(Fig. 4.11b). The results show that the loss in sensitivity to TRAIL still occurs in glucose-free cells irrespective of incubation with NAG (Fig. 4.11b). Taken together, these data show that Z138 cells cultured in glucose-free media have functional glycosylation since TRAIL-R1 is still glycosylated (Fig. 4.11a) and incubation with NAG could not re-sensitise these cells (Fig. 4.11b). Therefore, lack of glycosylation, through deprivation of glucose, appears not to be the cause of the observed loss in sensitivity.

4.2.6 Activation of the intrinsic pathway is also impaired under conditions of glucose-deprivation

As previously discussed in Chapter 1, death receptor-mediated apoptosis can occur through a Type I or Type II mechanism (Scaffidi *et al*, 1998; Scaffidi *et al*, 1999). Type I cells are characterised by strong DISC formation and direct caspase-8 activation whereas Type II cells have weaker DISC formation and require generation of tBID to engage the intrinsic mitochondrially-mediated cell death pathway. Loss of mitochondrial membrane potential (MMP) accompanies cytochrome *c* release and initiates mitochondrial-dependent apoptosis (Heiskanen *et al*, 1999). It has already been shown (Chapter 3) that Z138 cells make significant use of the mitochondrial-mediated cell death pathway when treated with TRAIL (Fig. 3.2). Therefore, the time-dependent loss of MMP in TRAIL treated + and – glucose Z138 cells was also examined (Fig. 4.12a).

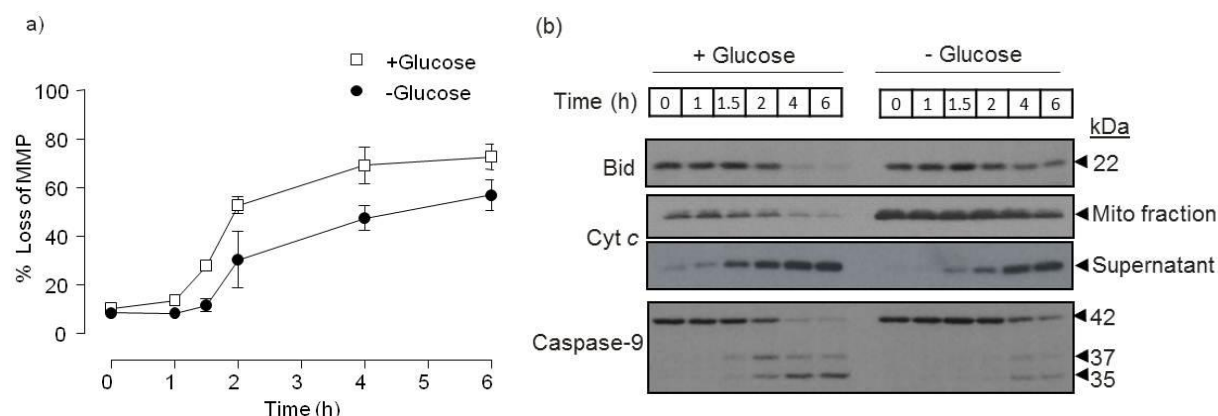


Figure 4.12 Activation of the mitochondrial-amplification loop is impaired under glucose-free conditions (a) Z138 cells cultured with (□) or without (●) glucose were treated with TRAIL (0-1000 ng/ml) for 4 h and assessed for loss of mitochondrial membrane potential (MMP) as outlined in Materials and Methods. (b) Cell pellets taken from (a) were analysed for loss of full-length BID, release of cytochrome *c* from the mitochondria and cleavage of caspase-9. Immunoblots are representative of three independent experiments.

A decrease in MMP was observed in both control (□) and glucose-free (●) Z138 cells (Fig. 4.12a), which closely followed the cell death response as shown earlier (Fig.

4.5b). The results showed that the activation of the mitochondrial intrinsic pathway was also reduced in cells maintained on glucose-free media (Fig. 4.12a). Since the loss of MMP after TRAIL treatment was delayed in cells maintained on glucose-free media, I analysed cells for BID cleavage, cytochrome *c* release from the mitochondria and caspase-9 cleavage (Fig. 4.12b). In parallel to the loss of MMP; BID cleavage, cytochrome *c* release and caspase-9 activation were also delayed in under glucose-free conditions (Fig. 4.12a and b). The delay in BID cleavage in glucose-free cells is likely to be a result of the reduced initiator caspase activity at the DISC (Fig. 4.7c). Similarly, this could have a direct effect on the release of cytochrome *c* from the mitochondria and the subsequent activation of caspase-9 at the apoptosome. Interestingly, the mitochondrial levels of cytochrome *c* were significantly increased in glucose-free Z138 cells (Fig. 4.12b – ‘Mito Fraction’). However, despite this increase, release of cytochrome *c* into the cytosol was clearly attenuated (Fig. 4.12b – ‘Supernatant’) suggesting that permeabilisation in the outer mitochondrial membrane (OMM) might be impaired.

Due to the impaired cytochrome *c* release from the mitochondria, the total cell content of pro- and anti-apoptotic proteins associated with the mitochondrial pathway were analysed (Fig. 4.13). The results show that the cellular levels of the majority of proteins examined were unchanged under conditions of glucose-free media. However, most notably, Bax levels were decreased and Bcl-2 levels were increased in the absence of glucose thus altering the Bax/Bcl-2 ratio to a more anti-apoptotic phenotype (Fig. 4.13).

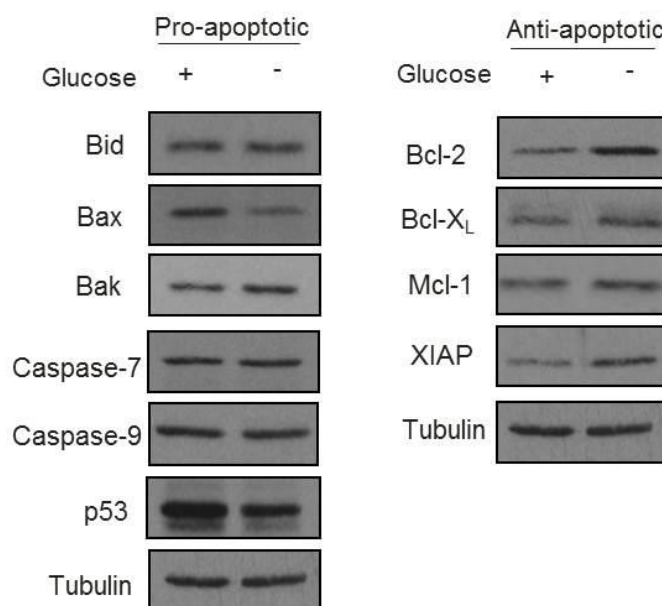


Figure 4.13 Key pro- and anti-apoptotic proteins involved in the mitochondrial-amplification loop. Whole cell pellets taken from Z138 cells cultured with (+) or without (-) glucose were analysed for pro- and anti-apoptotic proteins by immunoblotting for the indicated proteins. Tubulin was used as a loading control. Immunoblots are representative of three independent experiments.

XIAP levels were also found to be slightly increased under conditions of glucose-removal (Fig. 4.13). Thus, culturing Z138 cells in glucose-free media alters the ratio of pro- and anti-apoptotic proteins, which could prevent OMM pore formation and thus signalling to death.

The changes observed at the mitochondria suggested that, in glucose-free cells, the intrinsic cell death pathway was also likely to be attenuated. Therefore, to examine the response of glucose-free cells to intrinsic death stimuli, ABT-737 and X-ray radiation were used as specific activators of the mitochondrial cell death pathway (Fig. 4.14).

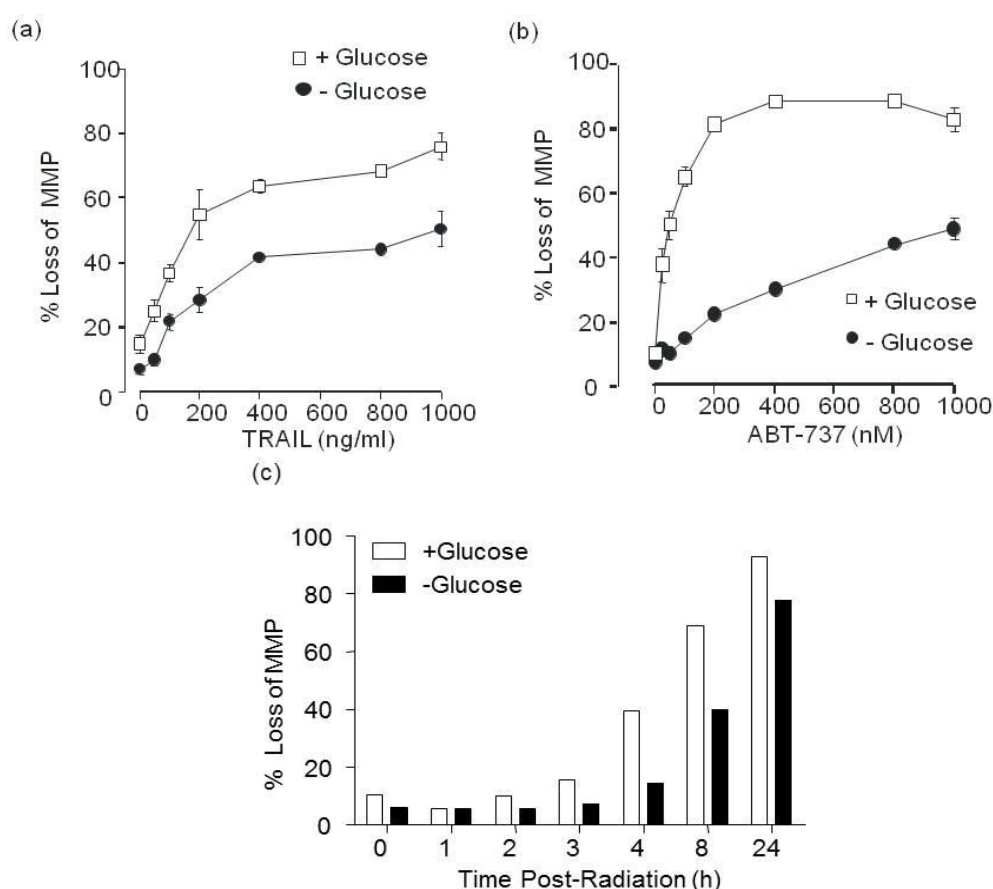


Figure 4.14 Z138 cells cultured in glucose-free media are less sensitive to intrinsic death stimuli (a) Z138 cells cultured with (□) or without (●) glucose were treated with various concentrations of TRAIL (0-1000 ng/ml) for 4 h and assessed for loss of mitochondrial membrane potential (MMP) (mean \pm SEM, $n=3$). (b) Z138 cells cultured with (□) or without (●) glucose were treated with various concentrations of ABT-737 (0-1000 nM) for 4 h and assessed for loss of MMP (mean \pm SEM). (c) Z138 cells cultured with (no fill) or without (black fill) glucose were irradiated with 35 Gy IR and assessed for loss of MMP at the times indicated post-irradiation. Data are representative of 1-3 experiments.

ABT-737 is a small-molecule inhibitor of the anti-apoptotic proteins Bcl-2, Bcl-X_L and Bcl-w (Oltersdorf *et al*, 2005) whilst radiation works by damaging the DNA of cells and initiating the intrinsic cell death pathway through activation of p53 (Skalka *et al*, 1976).

ABT-737 induced cell death in glucose-maintained cells (data not shown) and produced a corresponding loss of MMP with an EC_{50} of ~25-30 nM (Fig. 4.14b). However, in the absence of glucose, ABT-737 was 40-fold less potent with an EC_{50} of ~1000 nM (Fig. 4.14b). Similarly, ~ 50% decrease in the response of glucose-free cells to radiation treatment compared to control cells was observed (Fig. 4.14c). However, this was only evident at the early time points (4 h post radiation) and rather at 24 h the difference was only a ~10% decrease in sensitivity (Fig. 4.14c). This suggests that, in the case of irradiation, culturing cells in glucose-free media delays rather reduces their response as an apoptotic stimulus. Thus, the observed switch in metabolism was also accompanied by a marked loss in sensitivity to intrinsic death stimuli, which is not related to formation or activation of the DISC but may be related to the changes in the Bax:Bcl-2 ratio and/or impaired cytochrome *c* release from the mitochondria.

4.2.7 Isolated mitochondria from glucose-free Z138 cells exhibit increased cytochrome *c* levels and cristae density

Thus far, key changes have been observed in apoptotic proteins associated with the mitochondria and, therefore, these were investigated further. Initially, the sub-cellular distribution of pro- and anti-apoptotic proteins was analysed in Z138 cells cultured in the presence (+) or absence (-) of glucose (Fig. 4.15). PARP was used as a nuclear protein marker and COX IV and SOD2 were used to assess mitochondrial purity and loading.

Z138 cells cultured in glucose-containing media had a higher content of Bax in all three sub-cellular fractions compared to glucose-free cells (Fig. 4.15). Bak was unchanged irrespective of culture conditions. The anti-apoptotic proteins Bfl-A1, Bcl-2, Bcl-X_L and Mcl-1 were all concentrated to the mitochondria. However, out of these, Bcl-2 was the only protein up regulated in glucose-free cells compared to control cells (Fig. 4.15). Most significant was the change in the cytochrome *c* content of mitochondria isolated from Z138 cells cultured in the absence of glucose (Fig. 4.15). The amount of mitochondrial-bound cytochrome *c* was clearly elevated in glucose-free cells compared to control cells. However, it is evident that it was not readily released upon stimulation with TRAIL (Fig. 4.12b). Although, with longer time points (2-4 h) it is apparent that a small amount of cytochrome *c* is released (Fig. 4.12b). Based on studies examining cytochrome *c* release from the mitochondria, pore opening is not selective on the amount of cytochrome *c* released and, therefore, it is presumed that once the pore is formed all cytochrome *c* is released (Goldstein *et al*, 2005).

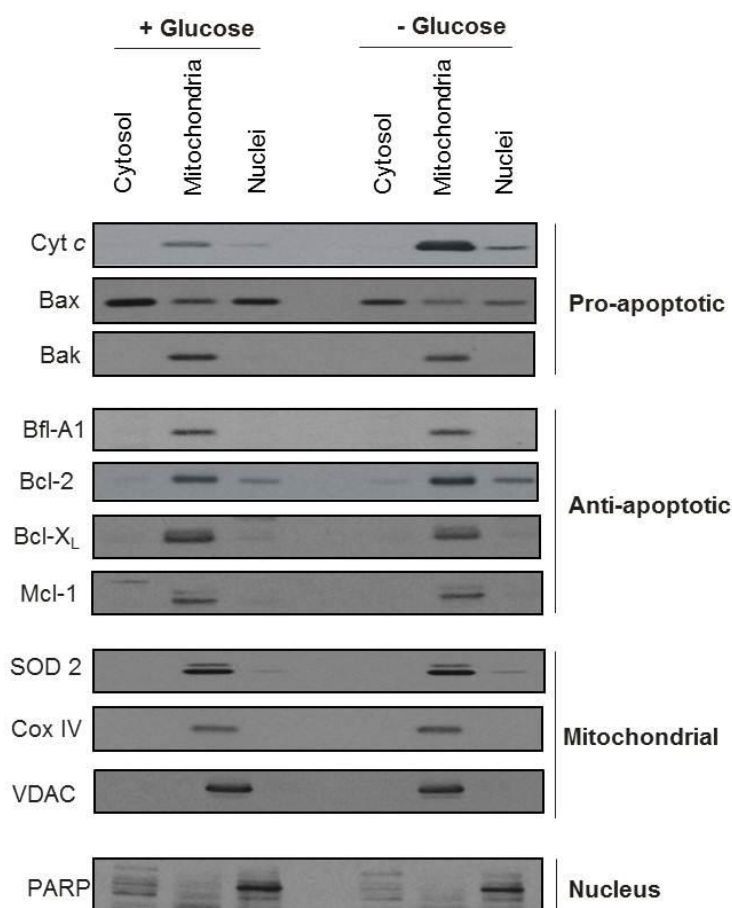


Figure 4.15 The isolation and subcellular analysis of purified mitochondria further display the key changes observed with Bax, Bcl-2 and cytochrome c. Cytosolic, mitochondrial and nuclear fractions from Z138 cells cultured in the presence (+) or absence (-) of glucose were obtained by subcellular fractionation and analysed for the indicated proteins as outlined in Materials and Methods. PARP was used as a nuclear marker whilst SOD2 and COXIV were used as mitochondrial markers.

This data clearly show that in glucose-free cells the majority of cytochrome c is retained presumably because pore formation is inhibited and thus could be trapped in the mitochondria. Since cells maintained on glucose-free media had significantly increased levels of cytochrome c, which was not readily released upon apoptotic stimulation, ultra-structural examination of the mitochondria in Z138 cells were performed (Fig. 4.16). The majority of mitochondria in glucose-maintained cells exhibited lucent matrices and sparse disorganised cristae characteristic of tumours and tumour-derived cell lines presumably reflecting their dependence on glycolytic metabolism (Fig. 4.16a; + Glucose). Glucose grown cells had an average of six mitochondria/cell (± 0.05) with a mean area of $0.51 \pm 0.127 \text{ sq } \mu\text{m}^2$ ($n=6$, S.E.M, Fig. 4.16a and b). However, mitochondria were more numerous (average of 10/cell ± 0.03) in cells maintained in glucose (-) media, with a smaller mean area of $0.31 \pm 0.057 \mu\text{m}^2$ ($n=10$, S.E.M), and contained more numerous, densely packed and regular transverse cristae than those observed in the glucose (+) cultured cells (Fig. 4.16a and b). The

ratio of IMM/OMM was significantly higher in cells grown without glucose as compared to the glucose (+) cells (Fig. 4.16b). Thus, these results show that chronically depriving cells of glucose brings about ultra-structural changes at the mitochondria that could mediate the enhanced respiration observed in these cells. Furthermore, the ultra-structural cristae changes may prevent cytochrome c release from the mitochondria and this is line with a previously published study (Gottlieb *et al*, 2003).

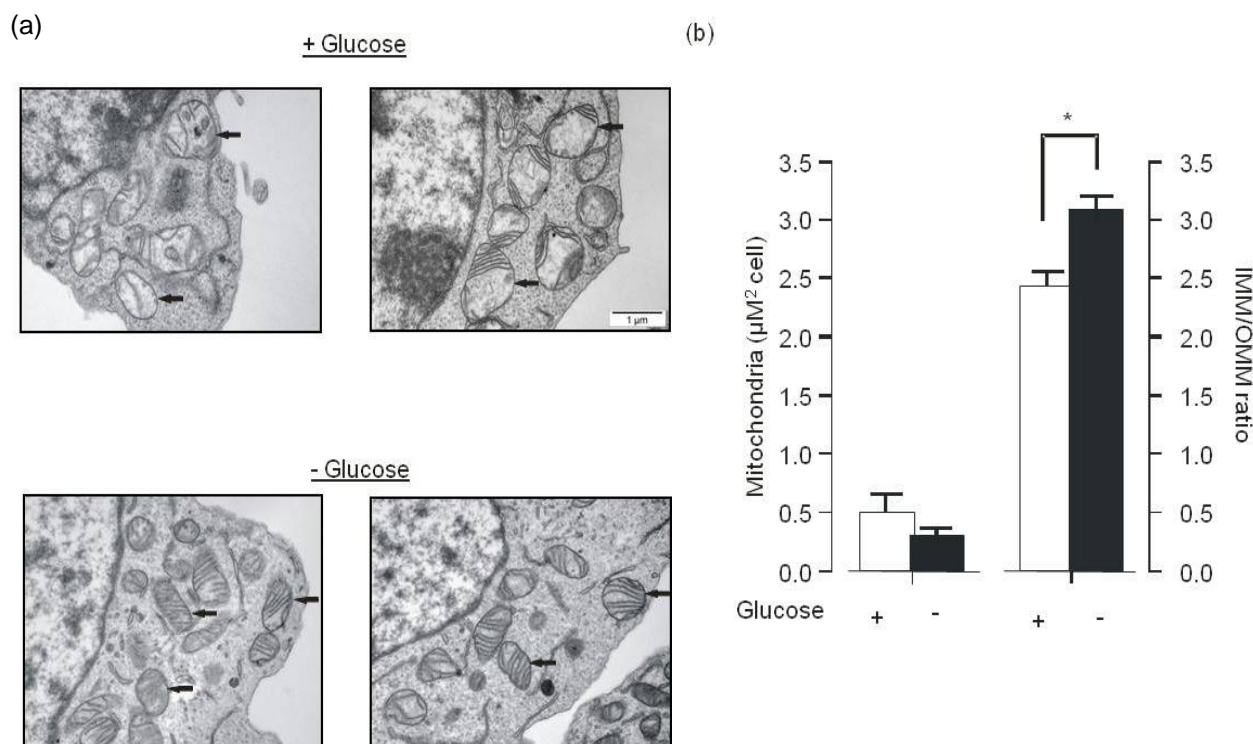


Figure 4.16 Z138 cells cultured in the absence of glucose have more mitochondria and increased cristae density (a) Z138 cells were cultured in the presence (+) or absence (-) of glucose and analysed by electron microscopy (EM) as described in Materials and Methods. Two representative images are shown from (+) and (-) glucose samples with inset dimension bars. Arrows indicate single mitochondria. (b) Mitochondria per cell and IMM/OMM ratios were determined as described in Materials and Methods.

4.3 Discussion

In this study, I have shown that the metabolic status and TRAIL-sensitivity of a mantle cell lymphoma cell line can be altered by depriving the cells of glucose. Cancer cells invariably exhibit a high rate of glycolysis, irrespective of oxygen levels, and this 'Warburg Effect' is believed to provide the transformed cell with a survival advantage. Central to this concept is the view that elevated glycolytic flux provides sufficient ATP and intermediate metabolites to support tumour growth. Consequently, there is

considerable interest in targeting glycolysis as a cancer therapeutic. The reliance of tumour cells on glycolysis could provide a weakness of the tumour to specific inhibitors of this pathway and thus conditions that prevent glycolysis could contribute to an increase in sensitivity to apoptotic stimuli. However, in Z138 cells, 2DG treatment and glucose-deprivation produced opposing effects on both metabolism and apoptotic cell death.

4.3.1 2DG reduces glycolytic flux and ‘primes’ a cell for death

Using real-time measurements of oxidative phosphorylation and glycolysis (Fig. 4.1), whole cell bioenergetics were correlated with ATP levels and their respective sensitivity to cell death. 2DG treatment of Z138 cells for 20 h produced almost complete inhibition of glycolysis and decreased cellular ATP levels by at least 50%. Therefore, pyruvate supplementation could not protect for the loss of ATP in 2DG treated cells unlike the glucose-free cells. Indirectly, this inhibition would also prevent flux through the pentose phosphate pathway and the glycosylation pathway thus shutting down all available routes that could compensate for the loss of glucose metabolism. It could be predicted, therefore, that given the above metabolic status, 2DG treatment would itself eventually bring about cell death due to the lack of ATP and glycolytic-derived intermediates.

With 2DG pre-treatment, TRAIL-induced direct caspase activation via DISC assembly is accelerated and thus cell death enhanced (Fig. 4.2). In addition, inhibition of glycolysis with 2DG results in significantly decreased cellular ATP levels, which is required for protein-translation, and consequently expression levels of pro- and anti-apoptotic proteins were significantly reduced (Fig. 4.3). With respect to the DISC, pro-apoptotic cFLIP_L levels were maintained whilst the levels of anti-apoptotic cFLIP_S were down-regulated. This change in the ratio of the long and short forms of cFLIP would be predicted to enhance DISC-mediated caspase-8 processing and thus enhance the cell death signal (Fig. 4.16). Pro- and anti-apoptotic proteins associated with the mitochondrial cell death pathway were also profoundly affected by 2DG treatment. Specifically, Mcl-1 protein levels were markedly reduced whilst Bak levels were largely unchanged (Fig. 4.3). A recent study showed that knockdown of Mcl-1 but not Bcl-X_L overcomes resistance to TRAIL, CD95L and TNF α in Bax-deficient cells (Gillissen *et al*, 2010). This indicates that the Mcl-1/Bak ratio is the major determinant of TRAIL sensitivity in the absence of Bax. Significantly, 2DG also caused a marked decrease in cellular levels of Bax but had less effect on Bcl-2 levels, which would neutralise Bax-mediated killing. Thus, these results show that 2DG enhances DISC-mediated caspase-8 activation through alterations in cFLIP_L and cFLIP_S levels as well as altering

the Mcl-1/Bak ratio to facilitate death through the mitochondrial amplification loop (Fig. 4.16). The net result is that Z138 cells treated with 2DG are sensitised to TRAIL-induced apoptosis. However, it is evident that 2DG treatment alone considerably stresses the cells (Fig. 4.2). Background necrotic cell death, following 20 h incubation with 2DG in the presence of zVAD.fmk, was elevated to around ~20 % prior to treatment with TRAIL. This suggests that incubating Z138 cells with 2DG primes a cell for death and that the mode of death can be apoptotic and/or necrotic when a death ligand is introduced. It is important, therefore, that when analysing for cell death a clear distinction between cell death which is necrotic and that which is apoptotic is made

4.3.2 Chronic glucose-deprivation mediates a switch in metabolic pathways and a reduction in sensitivity to apoptotic stimuli

A common belief is that inhibiting glycolysis with 2DG treatment or through glucose deprivation produces essentially the same effect on cellular metabolism and sensitivity to apoptotic agents. However, my data suggest that 2DG and short- and long-term glucose deprivation act through fundamentally different mechanisms. Thus, when glucose limitation (> 7 days) was used as a means of reducing glycolytic flux, Z138 cells remained viable and proliferated but were less sensitive to TRAIL-induced apoptotic cell death (Fig. 4.5). Under these conditions, TRAIL-R1/R2 receptor expression levels were marginally down-regulated and DISC formation and activity were attenuated (Fig. 4.7). This occurred despite observing an increase in the protein expression levels of FADD and caspase-8 (Fig. 4.6). In part, this could explain the slower onset of TRAIL-induced apoptosis. However, these results are in contrast to a similar study whereby glucose limitation decreased ATP levels and sensitised myeloid leukaemia U937, cervical carcinoma HeLa and breast carcinoma MCF-7 cells to death-receptor killing (Muñoz-Pinedo *et al*, 2003). A large proportion of the literature, which has investigated the effect of glucose-deprivation on cancer cell death, describe experiments where they only deprive their selected cell lines of glucose for between 2 and 24 h; a time interval that is unlikely to reflect physiological levels. Furthermore, in my initial studies, I investigated short-term (1 h) glucose deprivation and found, similar to the 2DG model, that there was an increase in both basal necrosis and death-ligand stimulated necrotic cell death suggesting the cells are already stressed (Fig. 4.15). Thus, 2DG and short-term (< 20 h) glucose-deprivation are likely 'priming' a cell for death and this can be apoptotic or necrotic.

Therefore, in this study, initial experiments were performed following both acute (20 h) and chronic (> 7 days) glucose-deprivation and it was decided that the latter model would be used as a model to condition cells and minimise cellular stress. Thus, Z138 cells were conditioned for a minimum of 7 days in glucose-free (glutamine- and pyruvate-supplemented) media prior to metabolic and cell death analyses. Using XF analysis I was able to directly compare and contrast the changes in metabolism and ATP levels following glucose-deprivation with those produced in the 2DG model. Metabolic studies showed that whilst glycolysis was almost completely inhibited, oxidative phosphorylation was up regulated and ATP levels maintained in glucose-free cells (Fig. 4.4). Thus, I propose that in certain cell types, such as Z138 cells, pyruvate and mitochondrial oxidative phosphorylation can substitute for the loss of glycolytic capacity and maintain ATP levels under conditions of chronic glucose deprivation. Mitochondria in glucose-free Z138 cells were well-coupled and functionally competent as shown by the oligomycin and FCCP data, which was analogous to tightly coupled mitochondria respiring in classical state 3 mode (Chance and Williams, 1956). Interestingly, chronic glucose deprivation had no effect on glycosylation (Fig. 4.9) whilst 2DG has been proposed to interfere with *N*-linked glycosylation (Kurtoglu *et al*, 2007) (Fig. 4.16).

4.3.3 The metabolic switch, in glucose-free cells, leads to mitochondrial proteomic and structural remodelling

A key question is why are Z138 cells, which are grown under glucose-free conditions, resistant to both intrinsic and extrinsic apoptotic stimuli? The receptor-mediated direct caspase-activation route is clearly attenuated in glucose-free conditions but the majority of the changes appear to be related to the mitochondrial pathway. In addition to the changes observed at the DISC, there was a reduction in the loss of mitochondrial membrane potential and decreased cytochrome *c* release from the mitochondria in glucose-free TRAIL-treated cells (Fig. 4.10). Therefore, I examined the expression levels of key pro- and anti-apoptotic mitochondrial proteins and observed a shift in the ratio of Bax/Bcl-2, which would correspond with anti-apoptotic phenotype regardless of stimuli (Fig. 4.11). In line with this switch, I also observed a loss in sensitivity to ABT-737 and x-ray radiation in glucose-free cells (Fig. 4.12). In trying to further explain this, isolated mitochondria from cells grown with or without glucose were immunoblotted for key proteins involved in both mitochondrial-dependent apoptosis and mitochondrial bioenergetics (Fig. 4.13). The most striking difference is the increase in cytochrome *c* levels in glucose-free cells. Ultra-structural examination

of mitochondria showed that under glucose-free conditions, Z138 cells had more mitochondria with increased cristae (Fig. 4.14). This structure is typically defined as the classical condensed configuration, which was originally described in mouse liver undergoing state 3 respiration (Hackenbrock, 1966). Electron microscopy and ultra-structural tomography studies show that this condensed state is a reversible phenomenon (reviewed in Benard and Rossignol, 2008). Interestingly, mitochondria in HeLa cells grown under glucose-free conditions have also been reported to have increased mitochondrial protein expression, enhanced oxidative phosphorylation and similar ultra-structural characteristics to glucose-free Z138 cells (Rossignol *et al*, 2008). It is possible that the observed increase in cytochrome *c* levels are a result of these structural rearrangements, which could be due to changes in the mitochondrial proteome or alternatively a dynamic phenomenon controlled by the availability of glucose and pyruvate/glutamine. Structurally cytochrome *c* is compartmentalised between the intra-cristal space (ICS) and the intermembrane space (IMS) and it has previously been shown that matrix remodelling is required for complete cytochrome *c* release (Gottlieb *et al*, 2003). Therefore, the increased mitochondrial cristae could account for the increase in cytochrome *c* and/or its retention (Fig. 4.16). In addition, the long-term adaptation of glucose-free Z138 cells to their environment may result in compensatory changes in the transcriptional and translation expression of key mitochondrial and glycolytic enzymes. Taken together, the data shows that treatment with the anti-glycolytic 2DG and chronic glucose-deprivation occurs through fundamentally different mechanisms (Fig. 4.17). With 2DG treatment, glycolysis is significantly down regulated and this results in a > 50% reduction in ATP levels, which has a direct effect on protein translation in particular Mcl-1 levels (Fig. 4.17). In comparison, glucose-deprivation significantly reduces glycolysis but increases oxidative phosphorylation and this, presumably, maintains ATP levels and thus protein translation (Fig. 4.17). I also provide evidence to suggest that 2DG inhibits glycosylation, which appears to effect TRAIL-R1 status, but this seems not be the case with glucose deprivation (Fig. 4.17). Although directly how this modulated glycosylation affects TRAIL-induced apoptosis is still unclear. cFLIP_L levels following 2DG treatment were maintained and this could, at low levels, enhance TRAIL-signalling. The down regulation of Mcl-1 could also contribute to the sensitisation of 2DG treated cells to TRAIL-induced apoptosis. Glucose-deprivation, on the other hand, inhibits TRAIL-induced apoptosis potentially as a result of both the down regulation of the TRAIL-receptors and/or the altered ratio of pro- and anti-apoptotic proteins (Fig. 4.17). In addition, the mitochondrial ultra-structural changes observed under glucose-free conditions may prevent the release of cytochrome *c* and thus reduces the response of

these cells to TRAIL. Together, the changes brought about by 2DG treatment and glucose-deprivation are illustrated in Figure 4.17.

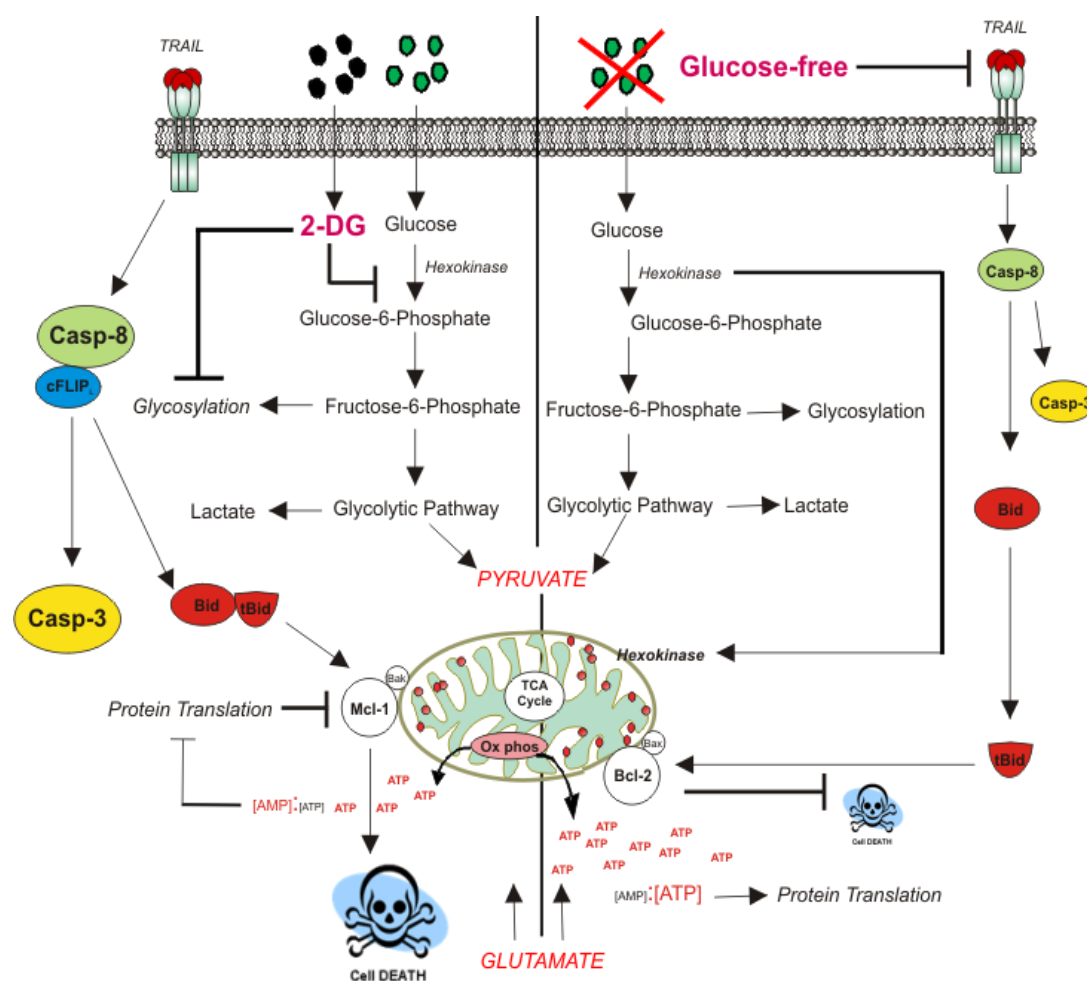


Figure 4.17 Scheme to show how metabolic changes induced by 2DG and glucose deprivation modulate apoptotic proteins and TRAIL-induced cell death. This scheme shows the effects of altered glucose-metabolism on both direct and mitochondrial-mediated cell death. In the case of 2DG, glycolysis and corresponding pathways are completely inhibited thus reducing glycolytic-dependent oxidative phosphorylation and ATP levels. Consequently, translation is inhibited because of the lack of energy (i.e. increase AMP:ATP ratio) and Mcl-1 is rapidly degraded whilst BAK levels remain the same. Similarly, the short and long isoforms of cFLIP are changed and this alters the cell to a pro-apoptotic phenotype and thus sensitises them to TRAIL-induced apoptosis. With glucose-deprivation, glycolysis is reduced but oxidative-phosphorylation is enhanced. This maintains ATP levels but alters the ratio of pro- and anti-apoptotic proteins to an anti-death phenotype. Mitochondria exhibit increased cristae and a corresponding increase in cytochrome *c* levels, which is 'trapped' inside the mitochondria and thus preventing signalling to cell death.

5. Transcriptional and Translational Changes during Glucose-Deprivation

5.1 Introduction

In early 2000, Douglas Hanahan and Robert Weinberg published a seminal paper discussing the essential 'Hallmarks of Cancer' (Hanahan and Weinberg, 2000). In this paper they introduced a collection of underlying principles that govern the transformation of normal cells into cancer cells (Hanahan and Weinberg, 2000). It is evident from these hallmarks that cancer is a complex disease. Nevertheless, rapid advances have and are being made in identifying the fundamental causes responsible for the initiation, progression and promotion of cancer. One such cause, common to all known cancers, is the presence of multiple genomic aberrations, which appear to underpin the so-called 'hallmarks of cancer' (Hanahan and Weinberg, 2000). Such genomic changes may be inherited or somatically acquired. Either way they represent a collection of cells with fundamentally diverse genomes, which allow for uncontrolled growth through alterations in gene expression levels. Together, these changes confer a specific dominant and aggressive cancer cell phenotype. Thus, researchers have sought to employ experimental techniques that allow for the large-scale analysis of these gene expression changes in cancer cells. One such approach has been the use of DNA microarrays, which are used to measure gene changes simultaneously by analysing levels of messenger RNA (mRNA) (reviewed in Brown and Botstein, 1999; Lockhart and Winzeler, 2000). DNA microarrays allow for the rapid profiling of multiple genes in a single experiment through the affinity and specificity of complementary base pairing (Duggan *et al*, 1999; Brown and Botstein, 1999). Thus, this technology has been used in a wide variety of scientific studies including drug discovery (reviewed in Bebout and Goodfellow, 1999), obesity (reviewed in Moreno-Aliaga *et al*, 2001) and inflammatory diseases (Heller *et al*, 1997). Significantly, cancer research was one of the first areas to utilise microarray technology. In 1996, Schena and colleagues reported the use of microarray analysis in the profiling of the human T-cell lymphoma cell line Jurkat based on findings reported previously on plant gene expression (Schena *et al*, 1995; Schena *et al*, 1996). As a result, since these early studies, there has been a vast array of research articles describing the use of microarray technology in the profiling of cancer cells (DeRisi *et al*, 1996; Cole *et al*, 1999; Alizadeh *et al*, 2000; Marx, 2000; Sallinen *et al*, 2000). Together these have permitted the identification of gene expression profiles for specific cancer sub-types including melanoma (Bittner *et al*, 2000), diffuse large B-cell lymphoma (Alizadeh *et al*, 2000), prostate cancer (Lapointe *et al*, 2004) and many more (reviewed in Vogelstein and Kinzler, 2002). Gene expression profiling through microarray technologies, therefore, has the potential to predict clinical outcomes based on the analysis of cancer

genomes. However, the expression of a protein from its gene is a multi-step process requiring both transcription and translation and thus the transcription of a gene does not always translate directly into the expression of its encoded protein. Therefore, in line with microarray technologies, the translation efficiency of cells can be assessed through polysome profiling (reviewed in Beilharz and Preiss, 2004; Spriggs *et al*, 2010). Polysome profiles can give a direct indication as to the amount of ribosomal-bound mRNA and thus provide evidence as to the translation of a particular mRNA sequence. As a result, polysome profiling has been used for nearly half a century to assess the translational status of mRNA and is based on velocity sedimentation in sucrose gradients (Warner *et al*, 1963). Accordingly, mRNA's are separated based on the number of ribosomes to which they are associated and the resulting gradients fractionated and measured through a continuous UV detector to record their profiles (Melamed and Arava, 2007). These profiles can then be used to assess the translational efficiency of cells under varying conditions and, furthermore, the RNA from each fraction can be extracted and assessed for the expression of an mRNA sequence of interest. Therefore, together, microarray technology and polysome profiling can provide valuable information into specific gene and protein expression changes under varying conditions. Thus, the research described in this chapter was designed to examine and identify the changes associated with the culturing of Z138 cells in the absence of glucose using DNA microarray technology and polysome profiling. However, it should be noted that the work presented in this chapter represents only preliminary findings and significantly more work is required to confirm the genomic and proteomic phenotypes described in the following. In Chapter 4, I showed that a switch in the metabolic phenotype of Z138 cells results in a reduction in sensitivity to intrinsic and extrinsic death stimuli. Following prolonged glucose deprivation both TRAIL DISC formation and activity were attenuated and, in addition, key proteomic and metabolic changes were observed at the mitochondria. These latter changes appear to induce a significant reduction in the sensitivity of cells to intrinsic death stimuli, especially ABT-737. However, the underlying cause for both the switch in metabolism and the loss in sensitivity to apoptotic stimuli is currently unknown. Therefore, in the following chapter I employed genomic analyses, namely DNA microarrays, in an attempt to identify and characterise gene expression changes that could be associated with the altered phenotype identified in Chapter 4. To begin, gene expression changes identified through DNA microarray analyses were investigated followed by the confirmation of a selection of these changes at the protein level along with their downstream targets. Following this, I used translational profiling of metabolically challenged Z138 cells to examine the second stage of gene expression

namely translation. Finally, I sought to examine primary samples from patients with mantle cell lymphoma in an effort to establish the relevance of these findings in a clinical setting.

5.2 Results

5.2.1 Gene expression analysis of glucose-free Z138 cells

In order to determine the specific changes associated with the glucose-free phenotype identified earlier (Chapter 4), gene expression profiles using DNA microarray technology were performed. This work was carried out in collaboration with the Systems Toxicology Group at the MRC Toxicology Unit. For this, two-colour microarrays with reverse labelling were performed using whole genome human oligonucleotide arrays (70mer). Total RNA extracted from glucose-containing (control) and glucose-free (test) Z138 cells were converted into cDNA through reverse transcription and labelled with Cyanine (Cy) -3 or -5 dyes. Control and test samples were then dual-hybridised overnight to in-house printed genome array slides followed by scanning using an Axon 4200A scanner (see Chapter 2 section 2.2.23). The gene expression profile generated for glucose-free Z138 cells is shown in Figure 5.1. The data shown represents three biological repeats each of which has two technical repeats (reverse labelling). In total, 174 genes were significantly altered ($p \leq 0.05$) of which 48 were up regulated (≥ 1.45 fold-change) and 126 were down regulated (≥ 0.75 fold-change) compared to the control (Fig. 5.1).

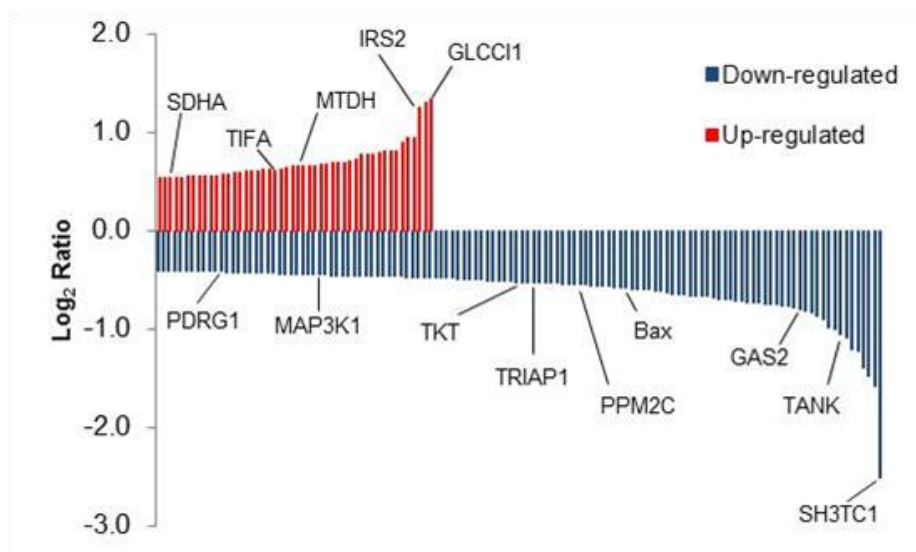


Figure 5.1 The gene expression profile of glucose-free Z138 cells. Microarray transcriptional analysis of glucose-free Z138 cells shows that, of the 174 genes identified as significantly different to the control ($p \leq 0.05$), 48 genes are up regulated (red lines) and 126 genes are down regulated (blue lines). The graph displays the \log_2 ratio of each gene in increasing order and the data represents three independent experiments each of which has two technical repeats. Selected genes changes are highlighted. Each line represents an individual gene.

Clearly, during glucose-deprivation, the majority of genes identified were down regulated (Fig. 5.1). This is seemingly not surprising since both RNA transcription and protein translation are energy-demanding process. It has long been known that general transcription and translation are inhibited during mitosis to preserve energy (Prescott and Bender, 1962; Hartl *et al*, 1993) and thus, under conditions of energy deprivation, a reduction in gene expression would also be predicted. However, it is also evident that, in this experiment, a considerable number of genes are up regulated despite the metabolically challenging environment (Fig. 5.1). Under these conditions, SH3TC1 was identified as the gene most down regulated whilst GLCCI1 was identified as the gene most up regulated gene (Fig. 5.1). Both the SH3TC1 (SH3 domain and tetratricopeptide repeats-containing protein 1) and GLCCI1 genes (glucocorticoid-induced transcript 1) encode for proteins of currently unknown function.

Microarray analysis data is largely presented in clusters or heat-maps that show gene expression changes of a data set across specific variables, such as time, dose or drug, and/or a number of comparable samples, such as different cellular states or samples from different patients (Eisen *et al*, 1998; Brown and Botstein, 1999). However, this type of data presentation was not applicable to this study since there is only one variable i.e. glucose-free versus its control. Therefore, the following table shows a selection of these gene expression changes manually clustered into distinct functional groups based on their known (current) role in the cell using the Uniprot¹, Entrez Gene² and Gene Card³ databases (Table 5.1).

Table 5.1 Gene expression changes cluster into distinct functional groups. Listed in the table below are distinct cluster groups that predominate in the microarray data. The functional group, specific gene, expression change, fold-change and known function are listed. Known function is based on admissions made to the Uniprot¹, Entrez Gene² and GeneCard³ databases. The genes underlined are described in-depth in section 5.2.2.

Functional Group	Gene	Expression Change	Fold Change	Function
Apoptosis	<u>BAX</u>	Down	0.67	Promotes apoptosis
	<u>GAS2</u>	Down	0.58	Caspase-3 substrate
	<u>TRIAP1</u>	Down	0.70	Inhibits activation of caspase-9
	<u>RNF36</u>	Down	0.72	Over-expression induces apoptosis (potential)
	<u>PDRG1</u>	Down	0.75	Cell growth regulation - p53 and DNA damage regulated

¹www.uniprot.org/ ²www.ncbi.nlm.nih.gov/gene ³www.genecards.org

	FLJ21908	Down	0.68	Potential regulator of apoptosis
	OPTN	Down	0.66	May utilize TNF-alpha or Fas-ligand pathways to mediate apoptosis
Cell Adhesion/Migration	RASGEF1A	Up	1.45	Plays a role in cell migration
	LANCL2	Up	1.5	Enhances membrane association
	COL11A2	Up	1.6	Provides instructions to produce collagen
	CLDN10	Down	0.56	Component of tight junctions
	ICAM3	Down	0.57	Type I transmembrane glycoproteins. Adhesion molecule and potent signaling molecule
	TLN1	Down	0.58	Plays a role in the assembly of actin and migration
	RASSF5	Down	0.67	Regulates lymphocyte adhesion and suppresses cell growth in response to activated Ras
	PTK2	Down	0.75	Involved in Cell Adhesion
	HGF	Down	0.68	Regulates cell growth and motility by activating a tyrosine kinase signaling cascade
	OPHN1	Down	0.70	promotes GTP hydrolysis of Rho subfamily members, which affects cell migration
	B4GALT1	Down	0.72	The cell surface form functions as a recognition molecule
Cell Survival Signalling	IRS2	Up	2.37	Activates AKT pathway
	MTDH	Up	1.58	Activates NFκB pathway
	TIFA	Up	1.54	Activates IKK
	SHOC2	Up	1.51	Participates in MAPK pathway activation
	TRIB3	Up	2.46	Negative regulator of NFκB and AKT1
	TCL1B	Down	0.47	Enhances phosphorylation and activation of AKT
	TANK	Down	0.48	Inhibits TRAF function
	MAP3K1	Down	0.73	Activates the ERK and JNK kinase pathways. Also activates IKBKB the central protein kinases of the NFκB pathway

	MAP3K3	Down	0.59	Directly regulates the SAPK and ERK pathways
	ASCC3	Down	0.64	Enhances NF κ B, SRF and AP1 transactivation
	TBC1D10C	Down	0.70	Inhibit Ras (MAPK) signalling pathway
Endoplasmic Reticulum	XBP1	Up	1.76	Transcription factor up regulated as part of the ER stress response
	ITPR1	Up	1.47	Receptor mediates calcium release from ER
	TRAM1	Up	1.53	Multi-pass ER membrane protein involved in the disposal of misfolded proteins
Glycosylation	PGM3	Up	1.86	Facilitates the conversion of G6P to G1P
	TRAM1	Up	1.53	Influences glycosylation at the ER
	ALG9	Down	0.70	Functions in lipid-linked oligosaccharide assembly
	B4GALT1	Down	0.72	Encodes a type-II membrane-bound glycoprotein
	GALNAC4S-6ST	Down	0.69	Sulfotransferase
Lipids/Fatty Acids	VLDLR	Up	1.71	Binds VLDL and transports it into the cell by endocytosis
	SMPD1	Up	1.57	Responsible for synthesis of ceramide
	ACOT2	Down	0.73	Catalyse the hydrolysis of acyl-CoA's to the free fatty acid and coenzyme A
	PLSCR3	Down	0.73	Mediates bidirectional transbilayer migration
	LRP1	Down	0.66	Involved in receptor mediated endocytosis
Metabolism (general)	SDHA	Up	1.45	Complex II of ETC and involved in TCA cycle
	PGM3	Up	1.86	Facilitates the conversion of G6P to G1P
	IRS2	Up	2.37	Activates AKT pathway

	PPM2C	Down	0.68	Pyruvate dehydrogenase (E1) is one of the three components (E1, E2, and E3) of the large pyruvate dehydrogenase complex.
	TKT	Down	0.70	Plays a role in the channeling of excess sugar phosphates to glycolysis in the pentose phosphate pathway
	ALG9	Down	0.70	Functions in lipid-linked oligosaccharide assembly
	ARL6IP5	Down	0.53	Negatively regulates glutamate transport

The majority of genes identified fall into distinct functional groups, some of which are outlined in Table 5.1. Excluding unknown and single genes, gene expression and protein trafficking/cytoskeleton are the largest functional groups with 31 and 17 genes identified in each respectively (Fig. 5.2).

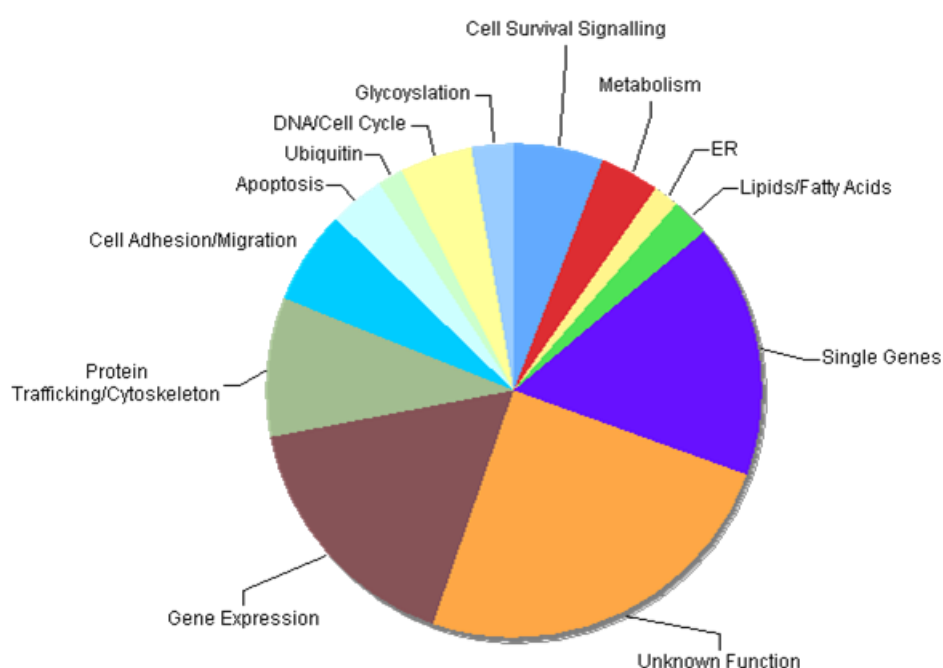


Figure 5.2 The relative proportion of each distinct functional group. The gene expression changes identified by microarray analysis can be grouped according to their functional role as determined by examining the Uniprot, Entrez Gene and GeneCard databases. The largest functional groups, excluding unknown function and single genes, are gene expression and protein trafficking/cytoskeleton. The smallest functional groups are those involving the endoplasmic reticulum (ER) and ubiquitin pathways.

Similarly, apart from the individual genes that do not 'correspond' to any of the identified functional groups, the endoplasmic reticulum (ER) and ubiquitin functional groups are the smallest clusters identified each comprising of 3 genes (Table 5.1 and Fig 5.2). Some of the genes identified appear in two or more functional groups based on both their role and effect in the cell, for example IRS2.

5.2.2 Gene expression changes suggest a switch towards an anti-apoptotic/pro-survival phenotype in glucose-free Z138 cells

With respect to the findings outlined in Chapter 4, one of the most relevant functional groups identified through microarray analysis is the cluster made up of apoptosis-related genes. Interestingly, although only made up of a small number of genes, all of the gene changes identified were down regulated (Table 5.1). One of the key genes associated with this functional group is the pro-apoptotic gene for Bax, which was previously identified as being down regulated at the protein expression level in glucose-free Z138 cells (Fig. 4.11). The down regulation of Bax at both the gene (Table 5.1) and protein level (Fig. 4.11) suggests that the pro-apoptotic role of this molecule is completely abrogated and this may facilitate the anti-apoptotic phenotype of glucose-free Z138 cells. Other identified genes belonging to this functional group include growth arrest-specific protein 2 (GAS2), p53 and DNA damage-regulated gene 1 (PDRG1) and TP53 regulated inhibitor of apoptosis 1 (TRIAP1) gene (Table 5.1).

GAS2 was originally identified as a protein member of a group of genes that are specifically expressed during growth arrest and is a component of the microfilament system (Schneider *et al*, 1988). Subsequent research also identified GAS2 as a caspase-3 and -7 substrate, which once proteolytically cleaved, induces changes in cellular shape associated with the morphological features of apoptosis (Brancolini *et al*, 1995; Sgorbissa *et al*, 1999). Interestingly, under glucose-free conditions, GAS2 is down regulated and thus its pro-apoptotic function, similar to Bax, is hindered (Fig 5.3). Likewise, the reduction of GAS2 is likely to diminish its role in arresting cell proliferation and thus have a positive effect on the growth of glucose-free Z138 cells (Brancolini *et al*, 1992). In line with this, it was recently observed that knockdown of the PDRG1 gene results in a marked reduction in tumour-cell growth suggesting that this gene also functions as a cell cycle regulator (Jiang *et al*, 2011) (Fig. 5.3). The changes identified with this gene, compared to control Z138 cells, could influence the growth of glucose-free Z138 cells by reducing their proliferation rate; a finding which has previously been observed with these cells (Chapter 4). The PDRG1 gene is also transcriptionally

regulated by both UV radiation (up regulated) and p53 (down regulated) and its expression is thought to sensitise cells to UV radiation (Luo *et al*, 2003). Thus, in glucose-free Z138 cells, PDRG1 levels are down regulated and therefore this gene expression change could contribute to the observed loss in sensitivity to apoptotic stimuli especially that seen with radiation treatment (Fig. 4.12). However, whether this down regulation is a direct effect of p53 would require further investigation. On the other hand, TRIAP1, also known as p53-inducible cell survival factor (p53-CSV), has been identified as a p53-inducible gene that enhances apoptosis when its expression is reduced and likewise, when present, can inhibit apoptosis by preventing caspase-9 cleavage (Park and Nakamura, 2005). Therefore, unlike the GAS2 and PDRG1 genes whose gene changes correlate with the anti-apoptotic phenotype identified in glucose-free cells, the reduced expression of TRIAP1 does not correlate (Fig. 5.3). Thus, further investigation into the role of this gene is required. Similarly, those genes that are p53 regulated could be altered due to the changes in p53 levels under glucose-free conditions (see later - section 5.2.4). These gene changes and their potential effects on the cell are outlined in Figure 5.3.

Comparable to the apoptotic cluster were those genes identified as regulating (positively or negatively) cell survival (Table 5.1). Notably, the majority of altered genes identified in this functional group appear to regulate the NF κ B signalling pathway and include the up regulated genes; metadherin (MTDH) and TRAF-2 binding protein (TIFA), and the down regulated genes; TRAF-family member associated NF κ B activator (TANK) and mitogen activated protein kinase kinase kinase 1 (MAP3K1) (Table 5.1). The NF κ B protein complex regulates the transcription of a multitude of target genes (Ghosh and Karin, 2002; Chaturvedi *et al*, 2011) and the activation of this pathway is largely associated with cell proliferation/survival and thus it is often found misregulated in cancers (Karin *et al*, 2002; Karin, 2006). The MTDH gene has been proposed to positively regulate this transcription factor (Emdad *et al*, 2006; Emdad *et al*, 2007) and thus the up regulation of this gene in glucose-free Z138 cells could be providing a survival advantage. Similarly, TIFA, also known as T2BP, activates NF κ B through the indirect activation of IKK; a kinase that phosphorylates IKB α , marking it for proteasomal degradation and thus releases NF κ B allowing it to enter the nucleus where it regulates gene expression levels (Kanamori *et al*, 2001; Ea *et al*, 2004). Therefore, the up regulation of these two genes in glucose-free cells could be enhancing signalling through this pathway (Fig. 5.3). Interestingly, the protein of the gene TANK can inhibit NF κ B activation by binding TRAFs – Tumour necrosis factor

receptor-associated factors (Rothe *et al*, 1996), which function as mediators of NF κ B signalling (Bradley and Pober, 2001). Thus the down regulation of this gene in glucose-free cells could, in accordance with the genes discussed above, indicate a preference toward NF κ B cell survival signalling. However, other research also found the TANK protein to be present in a complex that activates NF κ B signalling (Pomerantz and Baltimore, 1999) and therefore the actual role of this gene is somewhat contradictory. As with the apoptotic gene changes discussed above, these expression changes are shown in Figure 5.3.

MAP3K1 (also known as MEKK1) is a serine/threonine protein kinase, which is important in the regulation of a number of signalling pathways, one of which is the c-Jun activation pathway (Lee *et al*, 1997). The c-Jun N-terminal kinase (JNK) pathway, also known as the stress-activated protein kinase (SAPK) pathway, is largely activated in response to environmental stress (Weston and Davis, 2007). The JNK pathway regulates a number of target proteins, namely the transcription factor AP-1, and is involved in both cell death and survival (Ip and Davis, 1998). Its most well documented role is in apoptosis and, interestingly, it was found that apoptosis induced by the JNK pathway could be suppressed by activation of the AKT pathway (see later -section 5.2.4) (Davis, 2000). Likewise, it was observed that JNK could negatively regulate the AKT pathway through phosphorylation (and thus inhibition) of insulin receptor substrate (IRS), specifically IRS1, suggesting a regulatory role for this kinase in metabolism (Aguirre *et al*, 2000; Lee *et al*, 2003). Similarly, Tournier and colleagues observed that in the absence of JNK the apoptotic response to UV radiation was suppressed (Tournier *et al*, 2000). This suggests a pro-apoptotic role for the JNK pathway in cells and thus the down regulation of a key activator of this pathway, MAP3K1, suggests a hindrance on the JNK/SAPK pathway in glucose-free cells. Aside from its role in the JNK/SAPK pathway, more recent work found that MAP3K1 is cleaved by caspase-3 during apoptosis and thus promotes the apoptotic signal without activation of the JNK or NF κ B pathway (Schlesinger *et al*, 2002). It has been suggested that it exerts its pro-apoptotic function following cleavage by inducing mitochondrial membrane permeabilisation and thus activation of the intrinsic cell death pathway (Gibson *et al*, 2002). It is evident that MAP3K1 acts as a pro- and anti-apoptotic signalling molecule and, in the case of glucose-free Z138 cells, its down regulation is likely to prevent its pro-apoptotic function. Likewise, MAP3K3, also identified as being down regulated in glucose-free Z138 cells, has an essential role in the NF κ B pathway (Yang *et al*, 2000) although it is its over expression that been shown to confer resistance to apoptotic

stimuli (Samanta *et al*, 2004). Taken together, these changes in pro- and anti-apoptotic signalling proteins and/or regulators of this pathway suggest that these cells harbour an anti-apoptotic/pro-survival phenotype. The schematic in Figure 5.3 attempts to examine the co-ordinated effects these gene changes would exert on the cell. It is evident that the changes denote a complex network of protein interactions and signalling pathways that have the potential to contribute a cell survival phenotype. Although the protein expression of Bax has been examined extensively in the glucose-free phenotype, the remaining gene changes outlined above have not and therefore to determine if these changes contribute to this phenotype they need a more detailed analysis than what is provided above.

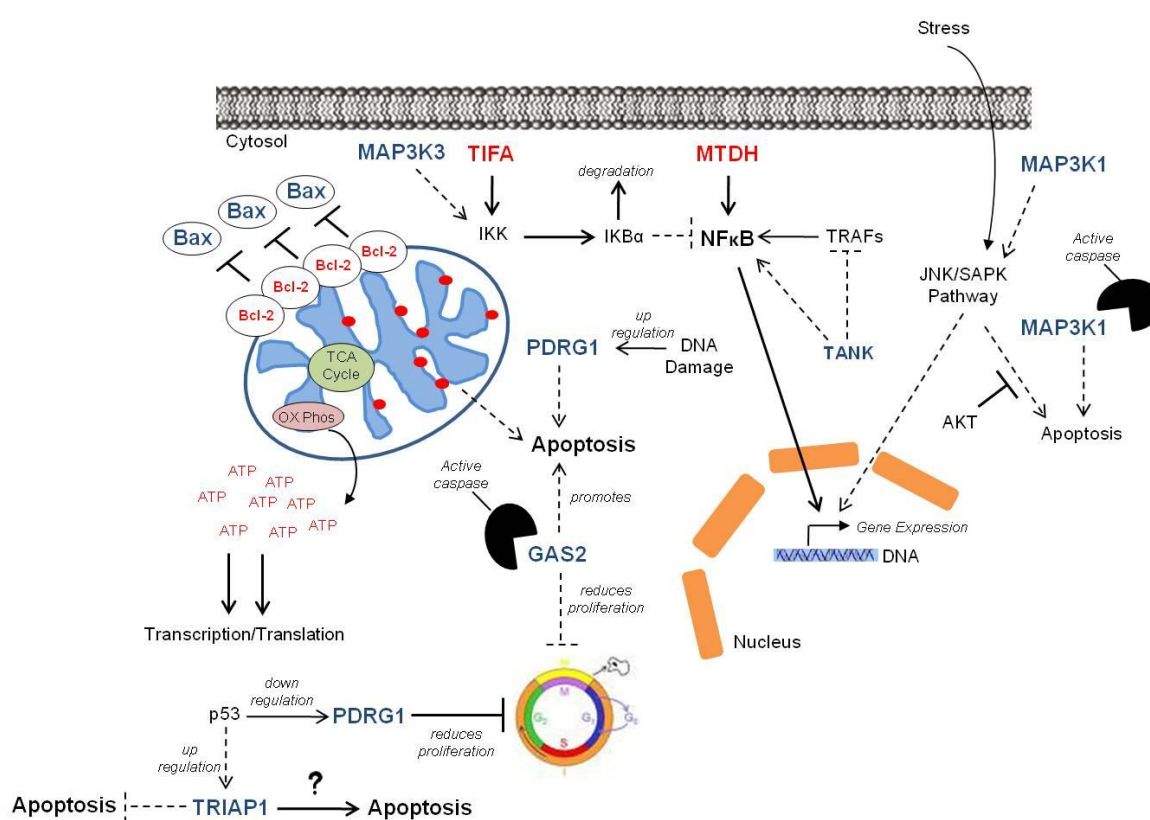


Figure 5.3 Schematic to show how gene expression changes confer an anti-apoptotic/pro-survival phenotype in glucose-free Z138 cells. Under glucose-free conditions the pro-apoptotic protein Bax is reduced whilst the anti-apoptotic protein Bcl-2 is increased, this appears to mediate resistance to apoptotic stimuli at the mitochondria. The gene for PDRG1 is down regulated and this would reduce its ability to induce cell death. Similarly, the effect of PDRG1 on proliferation is enhanced due to its down regulation potentially through direct regulation by p53. Although, the effect of p53 on TRIAP1 is not retained since this protein is down regulated, which should confer a more pro-apoptotic phenotype. The up regulation of TIFA and MTDH and the down regulation of TANK would together promote activation of the NFκB transcription factor pathway leading to alterations in gene expression levels. The down regulation of MAP3K1 would affect both signalling through the JNK/SAPK pathway and apoptotic pathway. The MAP3K1 protein is cleavable by caspase-3 and thus promotes apoptosis. MAP3K3 has been suggested to promote NFκB signalling by activating IKK and thus is down regulation suggests that this function is hindered. Key: Red is up regulated; blue is down regulated; broken lines indicate (predicted) pathway not activated; solid lines indicate (predicted) pathway activated.

5.2.3 Key metabolic genes are altered under conditions of glucose-deprivation

Unsurprisingly, a large number of the identified gene changes relate to metabolism and include the functional groups: metabolism (general), lipids/fatty acids and glycosylation (Table 5.1). Metabolism (general) is the largest of these functional groups and includes the up regulated genes: succinate dehydrogenase complex subunit A (SDHA), phosphoglucomutase 3 (PGM3) and insulin receptor substrate 2 (IRS2) along with the down regulated genes: pyruvate dehydrogenase phosphatase catalytic subunit 1 (PPM2C) and transketolase (TKT) (Table 5.1).

The up regulation of SDHA is significant in that the protein of this gene is involved in both complex II of the electron transport chain and also mediates the conversion of succinate to fumarate in the citric acid cycle (Hirawake *et al*, 1994) (Fig. 5.4a). Immunoblotting showed directly that the protein levels of SDHA were increased under conditions of glucose-deprivation (Fig. 5.4b) and this correlates with the gene expression data (Table 5.1).

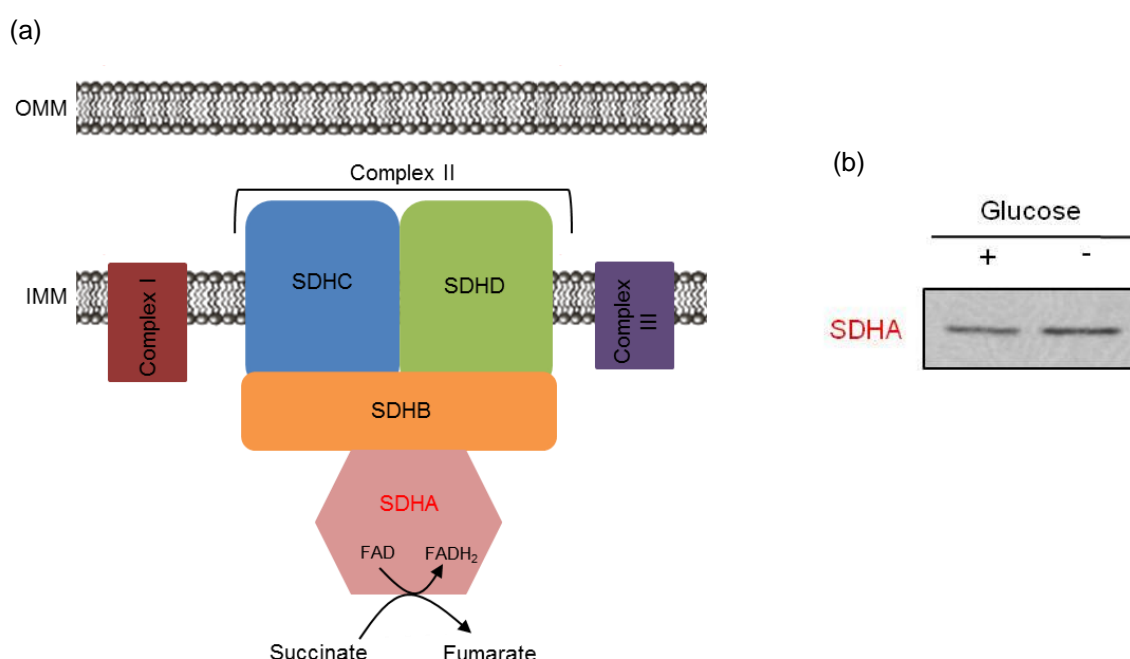


Figure 5.4 SDHA is increased under conditions of glucose deprivation. (a) Schematic to show the subunits of Complex II in the electron transport chain. SDHA (red) is up regulated under conditions of glucose-deprivation and facilitates both the conversion of succinate to fumarate in the citric acid cycle and provides the electrons for driving this complex in the electron transport chain (b) Immunoblots to show the up regulation of SDHA under glucose-free conditions. Immunoblot is from one experiment and represents whole cell lysate.

As I have previously shown, the phenotype of glucose-free Z138 cells is mediated by an increase in oxidative phosphorylation and this could be regulated by the increase in SDHA expression levels. Complex II of the electron transport chain is composed of four subunits: SDHA, SDHB, SDHC and SDHD, all of which localise to the inner mitochondrial membrane (Wang *et al*, 2008) (Fig. 5.4a). It was recently observed that mutations in the SDHB, SDHC and SDHD but not SDHA subunits cause hereditary Pheochromocytoma and Paraganglioma syndromes, the latter of which has more recently been associated with a germline loss-of-function mutation in the SDH5 gene specifically (Benn *et al*, 2006; Hao *et al*, 2009). Nevertheless, the observed increase in the gene (and protein) expression of SDHA could aid cellular respiration through its role in both the citric acid cycle and electron transport chain.

Similar to SDHA, another gene change associated with mitochondrial respiration is the PPM2C gene (Table 5.1). The down regulation of PPM2C is an interesting finding since the product of this gene, a pyruvate dehydrogenase phosphatase, is present in the mitochondrial matrix where it dephosphorylates the E1 component of the pyruvate dehydrogenase complex (PDH) reactivating it (Sugden and Holness, 1994) (Fig. 5.5). The PDH complex is responsible for the conversion of pyruvate to acetyl-CoA and thus links glycolysis to the citric acid cycle (Alberts *et al*, 2002). The down regulation of PPM2C at the gene level in glucose-free cells suggests a reduction in the dephosphorylation and thus activation of the PDH complex, reducing the conversion of pyruvate to acetyl-CoA (Fig. 5.5). It could be presumed that since glycolysis is decreased and mitochondrial respiration is increased the PDH complex and associated activating proteins would be increased since the demand for these are higher. However, the gene expression data suggests that the activation of this complex is reduced under glucose-free conditions and thus the reason for this needs to be examined in more detail.

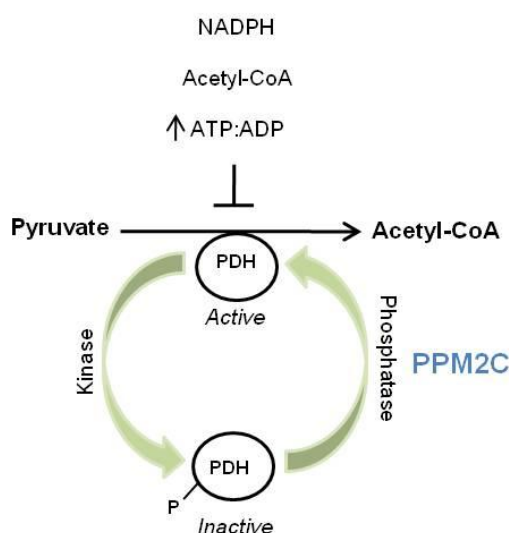


Figure 5.5 PPM2C gene expression is reduced under glucose-free conditions. Pyruvate dehydrogenase catalytic subunit 1 (PPM2C) dephosphorylates and reactivates the pyruvate dehydrogenase complex. Thus, if the down-regulation of this gene translates into the encoded protein then this suggests a decrease, under glucose-free conditions, in the reactivation of this complex and thus a reduction in the conversion of pyruvate to acetyl-CoA.

The gene encoding TKT produces a thiamine-dependent enzyme, which channels excess sugars from the pentose phosphate pathway to glycolysis (Schenk *et al*, 1997; Schenk *et al*, 1998). Therefore, the down regulation of this gene would reduce this process and thus ensure that excess sugars are kept away from the main metabolic pathway, which in glucose-free Z138 cells is completely abrogated. Similarly, PGM3 is one of a family of mutases involved in both the inter-conversion of G1P to G6P during glycogenolysis and glycogenesis (Whitehouse *et al*, 1998) and the conversion of GlcNac-6-phosphate to GlcNac-1-phosphate for glycosylation modifications (Greig *et al*, 2007). The protein expression of PGM3 correlates with its increase in gene expression levels (Fig. 5.6). PGM3 is essential for the formation of glycoprotein chains (Pang *et al*, 2002) and thus its increase under glucose-free conditions potentially maintains the glycosylation of proteins under such conditions. I have shown earlier (Chapter 4) that glycosylation is still occurring in glucose-free Z138 and therefore this could be mediated, in part, by the increase in PGM3.

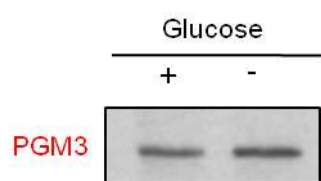


Figure 5.6 PGM3 protein expression is increased under glucose-free conditions. Immunoblot to show that under glucose-free conditions protein expression of PGM3 is increased. Image is from one experiment and represents whole cell lysate.

The product of the Insulin receptor substrate 2 (IRS2) gene is a cytoplasmic signalling molecule that mediates signalling through the AKT pathway (discussed in Chapter 1). The IRS2 gene is up regulated under conditions of glucose deprivation and, due to its role and downstream effects can be categorised into a number of identified functional groups (Table 5.1). Similarly, analysis of the protein levels of IRS2 found it to be up regulated under conditions of glucose-deprivation (Fig. 5.7). IRS2 is activated following tyrosine phosphorylation by multiple upstream targets of the receptor tyrosine kinase (RTK) family such as the insulin receptor (Sun *et al*, 1995). Following activation, IRS2 engages Phosphatidylinositol-3-OH Kinase (PI3K) and this suggests that IRS2 bridges a gap between the RTK family, PI3K and AKT signalling. As discussed in Chapter 1, there are multiple down-stream targets of activated AKT including those involved in metabolism, cellular growth and apoptosis. Therefore, since the AKT pathway appears to be a key cellular regulator of cell viability I decided to investigate this pathway further.

5.2.4 Evidence for activation of the AKT signalling pathway in glucose-free Z138 cells

Since the IRS2 gene was detected from the microarray, the protein expression levels of this gene were examined in control and glucose-free Z138 cells (Fig. 5.7). The results show that, similar to its increase in gene expression, IRS2 is increased at the protein level under glucose-free conditions. Therefore, following this, phosphorylation and thus activation of AKT (also known as protein kinase B) was examined by immunoblotting Z138 cells cultured with (+) or without (-) glucose. The data shows that in glucose-free cells, AKT phosphorylation was elevated compared to those cultured in the presence of glucose suggesting activation of this serine/threonine protein kinase (Fig. 5.7). Therefore, to confirm activation of this pathway, downstream targets of this kinase were examined (Fig. 5.7).

One of the key signalling pathways involving AKT is the PI3K/AKT/mTOR pathway, which regulates a number of key cellular processes including transcription and cell growth (LoPiccolo *et al*, 2008). To examine activation of this pathway, the phosphorylation of the mTOR target protein p70-S6 kinase was examined (Fig. 5.7). Activation of p70-S6 kinase induces protein synthesis (Fenton and Gout, 2011) and the data showed the phosphorylation and thus activation of this protein under glucose-free conditions was elevated compared to control cells (Fig. 5.7). Similarly, analysis of the cellular state of glycogen synthase kinase 3 β (GSK3 β), another downstream target of AKT, showed that the phosphorylation of this protein was increased under glucose-free conditions (Fig. 5.7). Phosphorylation of GSK3 β by AKT inactivates this multi-functional serine/threonine kinase (Rayasam *et al*, 2009). Interestingly, active GSK3 β results in the phosphorylation and inhibition of numerous downstream targets and thus the inactivation of GSK3 β by phosphorylated AKT indirectly permits activation of these GSK3 β targets. Similarly, GSK3 β has been implicated as a regulator of apoptosis where it permits outer mitochondrial membrane permeabilisation (Maurer *et al*, 2006) and has also been found to induced apoptosis through the induction of PUMA (Charvet *et al*, 2011). The phosphorylation of mdm2 was also found to be elevated in glucose-free cells (Fig. 5.7). Phosphorylated mdm2 mediates the ubiquitination and degradation of p53 (Ogawara *et al*, 2002).

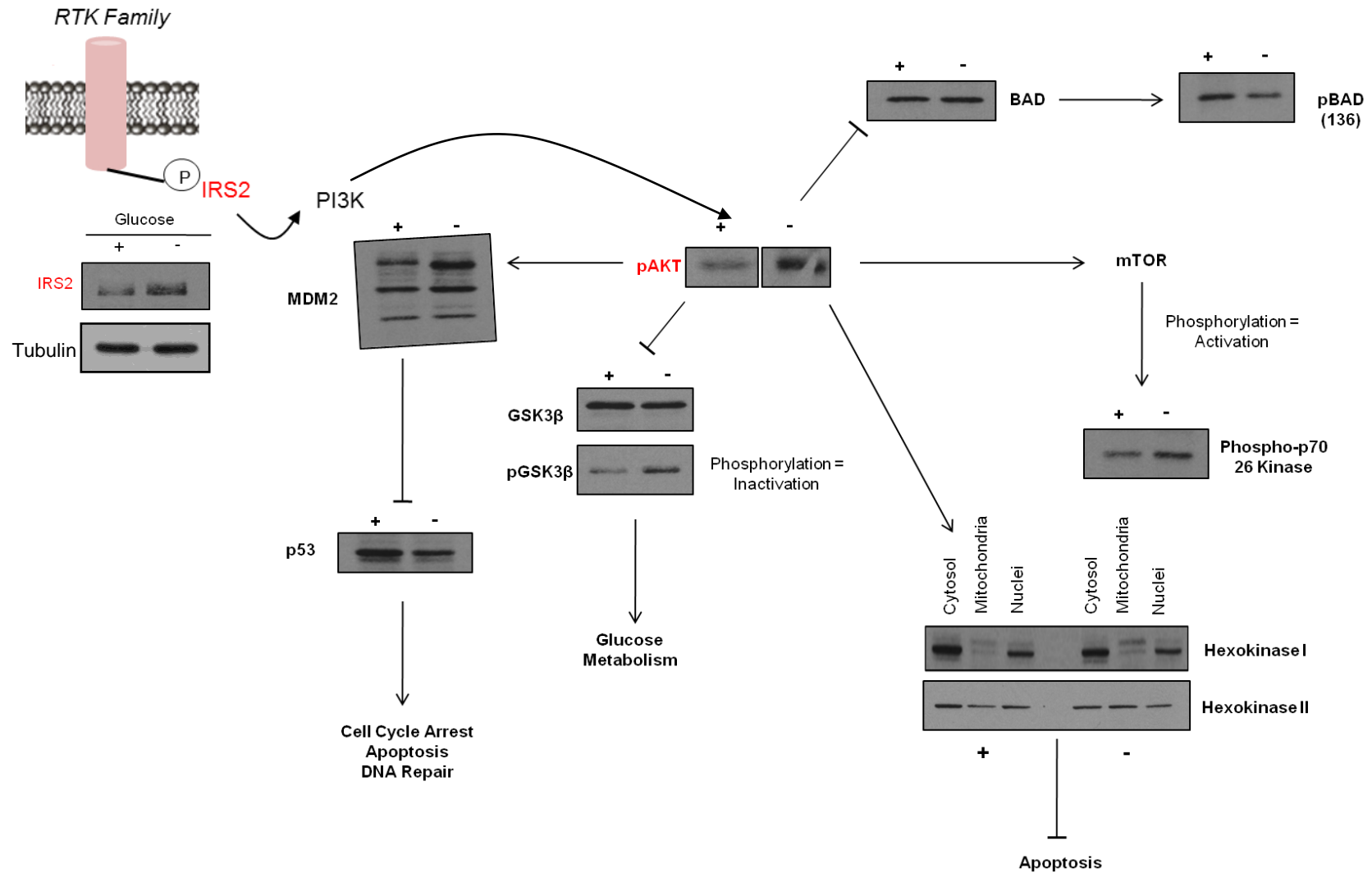


Figure 5.7 Protein expression analysis of the AKT pathway and its downstream targets. Z138 cells cultured with (+) or without (-) glucose were examined for the activation (phosphorylation) of the AKT pathway. Known downstream targets of this kinase including BAD, mTOR/p70-S6 kinase, hexokinase I and II, GSK3β and MDM2 were examined. Immunoblots are representative of 1-3 experiments and show whole cell lysates except for hexokinase, which is subcellular fractionation. Tubulin was used as a loading control.

In line with this, the degradation of p53 would indirectly regulate the target genes of this transcription factor and thus contribute to more significant downstream changes. The levels of p53 were also found to be down regulated at the protein level under glucose-free conditions (Fig. 5.7) and, in Z138 cells, both alleles of p53 are found to be wild-type (Bea *et al*, 2009; Williamson *et al*, 2010). P53 is rapidly degraded in unstressed cells and therefore the western blot data shown in Figure. 5.7 could represent basal levels of p53 in these cells, which is directly regulated by the change in MDM2 levels (Fig. 5.7). Taken together, the proteins examined thus far co-ordinate with the activation of the AKT pathway under conditions of glucose-deprivation. However, to confirm activation of the AKT pathway under glucose-free conditions, an inhibitor of this pathway, such as PI103 (Torc1 Bioscience, UK) or LY2780301 (Eli Lilly, USA), should be used. This can be used to confirm both activation of an AKT signalling cascade and also determine whether the AKT pathway, under conditions of glucose-deprivation, is modulating the sensitivity of Z138 cells to TRAIL.

Protein analysis of the AKT-mediated phosphorylation of the pro-apoptotic Bcl-2 family member BAD, however, does not correlate with these findings (Fig. 5.7). AKT phosphorylates BAD dissociating it from Bcl-2/Bcl-X_L thus permitting an anti-apoptotic phenotype (Datta *et al*, 1997). Therefore, the phosphorylation of BAD by AKT would have aided in understanding the underlying cause for the loss in sensitivity to apoptotic stimuli observed in glucose-free cells. However, the results show that the phosphorylation of BAD at serine136 by AKT in glucose-free cells is actually reduced compared to glucose-cultured cells (Fig. 5.7).

The exact mechanisms by which activated AKT prevents apoptosis are still poorly understood. However, early work by Hay and colleagues found that the physical interaction between the glycolytic enzyme hexokinase and mitochondria is vital for this function (Gottlob *et al*, 2001; Majewski *et al*, 2004a; Majewski *et al*, 2004b). As discussed in Chapter 1, hexokinase catalyses the first step of glycolysis converting glucose to glucose-6-phosphate and is often found up regulated in cancer. Its presence at the mitochondria is proposed to exert an anti-apoptotic effect and interestingly this association has been shown to be mediated by AKT activity (Gottlob *et al*, 2001; Pastorino *et al*, 2002; Majewski *et al*, 2004a; Majewski *et al*, 2004b). Therefore, to examine the differences in the levels of mitochondrial-bound hexokinase, glucose-containing (+) and glucose-free (-) Z138 cells were fractionated into cytosolic, mitochondrial and nuclear fractions and examined by immunoblotting using hexokinase I and II specific antibodies (Fig. 5.7). The data showed that, in glucose-free cells, the

levels of mitochondrial-bound hexokinase I were not significantly altered compared to the control, glucose-containing, cells (Fig. 5.7). However, protein expression analysis of mitochondrial-bound hexokinase II reveals it to be increased under conditions of glucose-deprivation (Fig. 5.7). Thus, the change in cellular location or increased expression level at the mitochondria of hexokinase II may contribute to the anti-apoptotic phenotype.

5.2.5 An increase in mitochondrial-bound hexokinase II appears not to correlate with the anti-apoptotic phenotype of glucose-free Z138 cells

To investigate further the increase in protein levels of mitochondrial-bound hexokinase II observed in Figure 5.7, methyl jasmonate - a compound found to dissociate hexokinase from the mitochondria, was utilised to assess whether glucose-free cells can be re-sensitised to TRAIL-induced apoptosis. Methyl jasmonate is a plant stress hormone whose anti-cancer effects were examined based on research carried out with salicylate – another plant stress hormone that was found to suppress the growth of a number of malignancies (reviewed in Flescher, 2005). Methyl jasmonate was found to be toxic to a number of cancer cell lines (Fingrut and Flescher, 2002) and primary cell samples (Flescher, 2005) and its mechanism of action was proposed to occur through its interaction with the mitochondria (Rotem *et al*, 2005). More specifically, it was found to bind and detach mitochondrial-bound hexokinase (Goldin *et al*, 2008). Therefore, based on these findings, glucose-free Z138 cells were incubated with varying concentrations (0-9 mM) of methyl jasmonate to investigate the ability of this compound to detach mitochondrial-bound hexokinase (Fig. 5.8a). In line with this, the response of methyl jasmonate treated cells to TRAIL-induced apoptosis was then examined (Fig. 5.8b-c). The results show that incubating glucose-free Z138 cells with 1 mM of methyl jasmonate for 1 h was sufficient to detach a proportion of mitochondrial-bound hexokinase (Fig. 5.8a). However, it is evident that incubating Z138 cells with 0-9 mM methyl jasmonate, as shown in Figure 5.8a, is insufficient in detaching all of the mitochondrial bound hexokinase and thus the remaining hexokinase could still confer an anti-apoptotic phenotype. It is also important to note, however, that methyl jasmonate was found to be extremely toxic to cells, largely through necrotic cell death (data not shown) and thus a 1 h pre-treatment with 1 mM of methyl jasmonate was also the maximum feasible dose without necrotic side-effects (data not shown). Following this, glucose-free Z138 cells were incubated with (+ MJ) or without (control) 1 mM of methyl jasmonate for 1 h followed by a 4 h dose response with 0-1000 ng/ml TRAIL (Fig.5.8b-c). The results show that detachment of hexokinase from the

mitochondria with methyl jasmonate produces only a slight increase in the sensitivity of glucose-free cells to TRAIL when examining both the loss of mitochondrial membrane potential (Fig. 5.8b) and percentage cell death (Fig. 5.8c). Thus, the increase in mitochondrial-bound hexokinase in glucose-free Z138 cells appears not to contribute significantly to the loss in sensitivity to TRAIL.

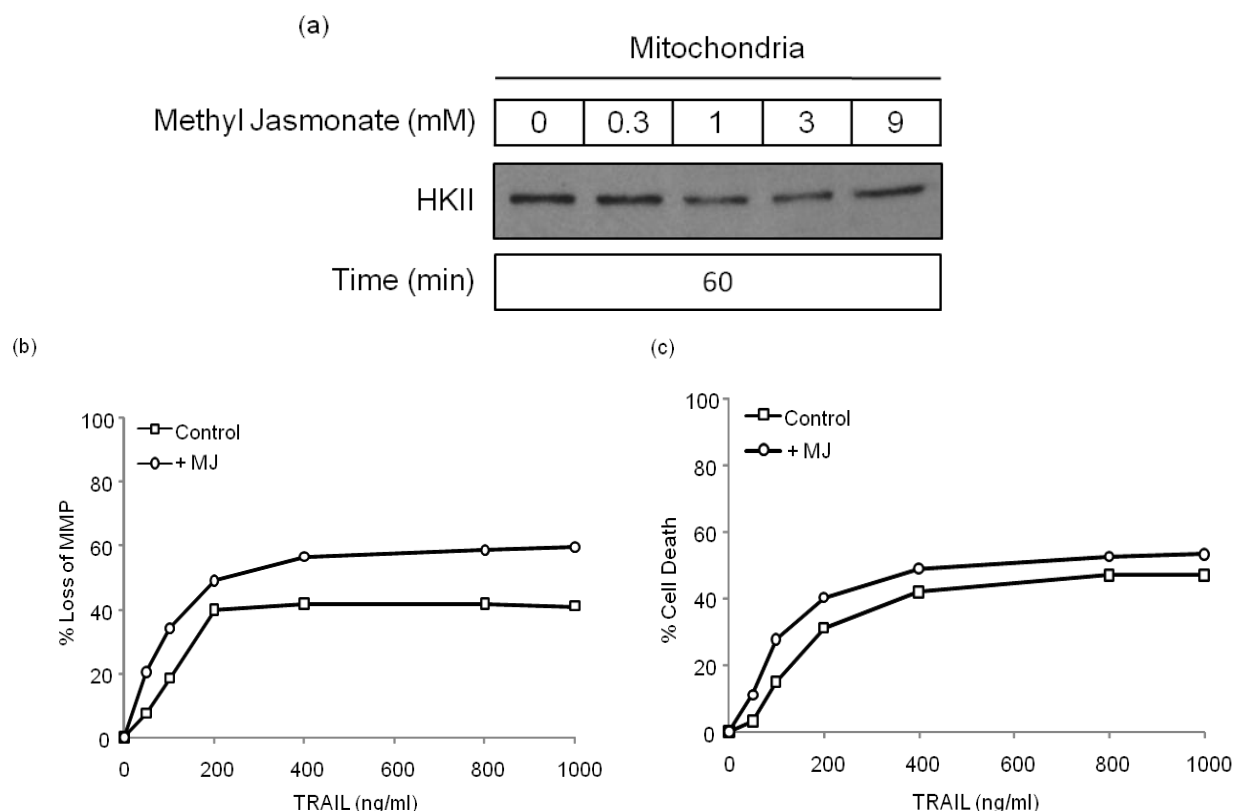


Figure 5.8 Pre-incubation of glucose-free Z138 cells with methyl jasmonate does not re-sensitise cells to TRAIL-induced apoptosis. (a) Glucose-free Z138 cells are incubated with varying concentrations (0-9 mM) of methyl jasmonate for 60 min to examine the dissociation of hexokinase from the mitochondria. Glucose-free cells are incubated without (-) or with (+) methyl jasmonate for 60 min followed by treatment with 0-1000 ng/ml TRAIL for 4 h and assessed for the loss of mitochondrial membrane potential (b) or percentage cell death (c). Results are representative of one experiment.

5.2.6 Polysome profiling of glucose-free and 2DG treated Z138 cells

From the analyses carried out above, it was apparent that some of the gene expression changes do not correlate directly with the glucose-free phenotype described in Chapter 4. Therefore, in addition to examining the transcriptional profiles of these cells, translational profiling can also be performed to examine the translation status of specific mRNA thus providing a measure of protein synthesis. The PI3K/Akt/mTOR pathway is a critical regulator of gene expression, specifically by affecting mRNA translation, and is highly regulated by the metabolic status of the cell

(reviewed in Mamane *et al*, 2006). In line with this, the data presented in Figure 5.7 of this chapter suggests that the mTOR pathway might be activated via the AKT-signalling pathway. Thus, translation, under glucose-free conditions, could be maintained as a direct result of activation of this pathway. Therefore, in the following, polysome profiling analysis was performed (a) to determine the translational status of these cells and (b) to ultimately correlate the microarray data with that of changes in ribosomal association of mRNA.

To begin, Z138 cultured with or without glucose were subjected to polysome profiling as outlined in Materials and Methods (section 2.2.24). Briefly, mRNA isolated from glucose-containing and glucose-free Z138 cells were separated on sucrose density gradients (10-60 %) according to the number of ribosomes to which they are associated. Samples were then fractionated and the absorbance of each fraction was measured at an absorbance of 254 nm and the resulting absorption profiles collected (Melamed and Arava, 2007). The polysome profiles of Z138 cells seeded 48 h prior to analysis and cultured with (+) or without (-) glucose are shown in Figure 5.9.

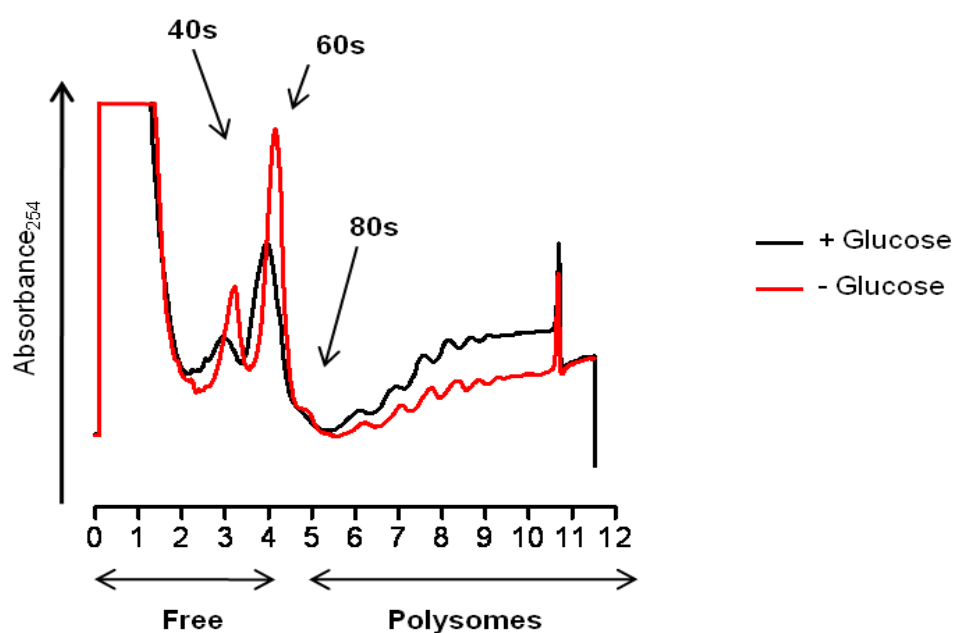


Figure 5.9 Polysome profiling of Z138 cells cultured with (+) or without (-) glucose. Cellular extracts prepared from glucose-containing (black line) and glucose-free (red line) Z138 cells were separated by centrifugation through 10-60% sucrose density gradients and the absorbance profile (260 nm) of each fraction recorded. The position of the small (40S), large (60S), monosomes (80S) and polysomes are indicated. Polysome profiles are representative of one experiments of which each sample has two technical repeats.

The results show that glucose-free Z138 cells have an enhanced association with the 'inactive' free fractions (fractions 1-4) than with those fractions attached to ribosomes (fractions 5-12) compared to Z138 cells cultured with glucose (Fig. 5.9). The polysome profile shows the position of the small (40S) and large subunits (60S), the monosomes (80S) and the polysomes (Fig. 5.9). Glucose-free cells have more free 40S and 60S subunits and less polysomes than glucose-containing cells and this suggests a reduction in translation in these cells. Thus, taken together, both transcription and translation of certain key genes are altered in glucose-free cells compared to control, glucose-containing, cells.

In the previous results chapter, the comparison between the inhibition of glycolysis using 2DG and the inhibition through glucose-deprivation was examined. It was observed that 2DG treatment had a more dramatic effect on protein expression (Fig. 4.5) than chronic glucose-deprivation (Fig. 4.6). Therefore, in line with the above findings, translational profiling of Z138 cells treated with or with 2DG was carried out. For this, Z138 cells were incubated with or without 2DG for 20 h prior to polysome profiling analysis, and the cellular extracts from these samples processed as described previously. The results show that in the absence of 2DG, mRNAs were largely present in the polysome fractions (Fig. 5.10) suggesting active translation in these cells.

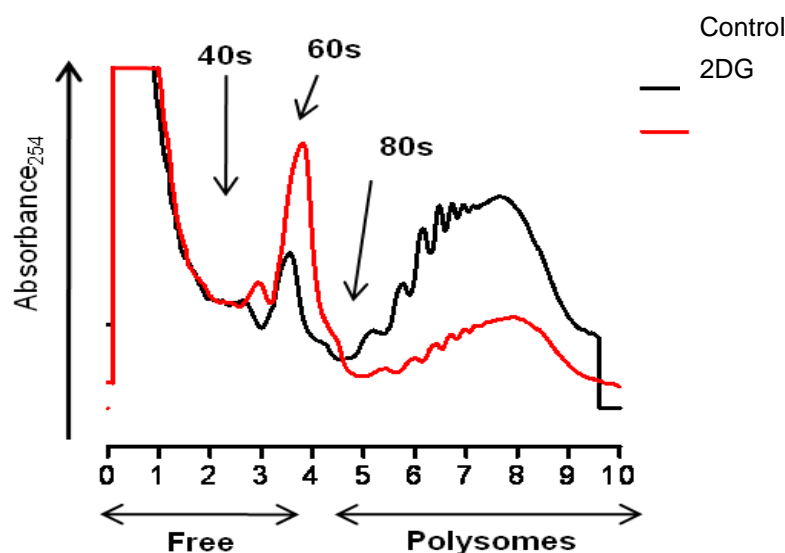


Figure 5.10 Polysome profiles of Z138 cells treated with or without 2DG. Cellular extracts prepared from Z138 cells were treated with (red line) or without (black line) 2DG for 20 h and separated by centrifugation through 10-60 % sucrose density gradients. The absorbance profiles (measure at 260 nm) of each fraction were recorded. The position of the small (40S), large (60S), monosomes (80S) and polysomes are indicated. Polysome profiles are representative of one experiment each of which has two technical repeats.

However, the treatment of these cells with 2DG for 20 h shows a significant redistribution of mRNAs from the 'active' polysome fractions to the 'inactive' small (40S) and large (60S) fractions (Fig. 5.10). This indicates that 2DG results in an inhibition in translation. Thus, incubating cells with 2DG appeared to have a more significant effect on translation (Fig. 5.10) than chronic glucose deprivation (Fig. 5.9). However, to confirm this, glucose deprivation polysome profiles would need to be examined after 20 h seeding to compare directly with the profiles of 2DG treated cells.

5.2.7 Profiling of mantle cell lymphoma (MCL) patient samples

The majority of work carried out in this thesis makes use of the mantle cell lymphoma cell line Z138. Therefore, to begin to understand the relevance of these findings in a clinical setting, MCL patient samples were characterised for their response to apoptotic stimuli, their metabolic profiles under glucose-free conditions and the subcellular localisation of key cellular proteins.

MCL cells, isolated as described in Materials and Methods, were grown in glucose-containing (+) or glucose-free (-) media for 6 h followed by incubation with varying doses (0-1000 ng/ml) of TRAIL for 4 h (Fig. 5.11a). Glucose-deprivation for 6 h was selected as the optimal time point because of the amount of spontaneous apoptosis occurring with increasing length of time. Ideally, this time-point would then be optimised based on preliminary experiments. The cells were then assessed for percentage apoptosis by FACS analysis (Figure 5.11a). After 10 h, spontaneous apoptotic cell death was elevated to around 30 % and this was irrespective of culture conditions (Fig. 5.11a). Furthermore, it was evident that the cells did not respond to increasing doses of TRAIL and this was also irrespective of the presence or absence of glucose (Fig. 5.11a). This suggested that these cells were resistant to TRAIL-induced apoptosis. Therefore, the MCL patient sample was analysed for surface receptor expression analysis of TRAIL-R1 and -R2 (Fig. 5.11b). The results show that these cells do not express TRAIL-R1 or -R2 on their surface. Thus, the resistance to TRAIL-induced apoptosis is likely due to the lack of functional cell surface TRAIL receptors. This is in accordance with previously reported findings by MacFarlane and co-workers who showed that pre-treatment with the HDAC inhibitor depsipeptide was required to sensitise MCL patient samples to TRAIL-induced apoptosis (MacFarlane *et al*, 2005) and, furthermore, this sensitisation was found to be mediated primarily by TRAIL-R1 (MacFarlane *et al*, 2005). Following on, the response of a primary MCL sample was examined for its sensitivity to the intrinsic stimuli ABT-737 (Fig. 5.11c).

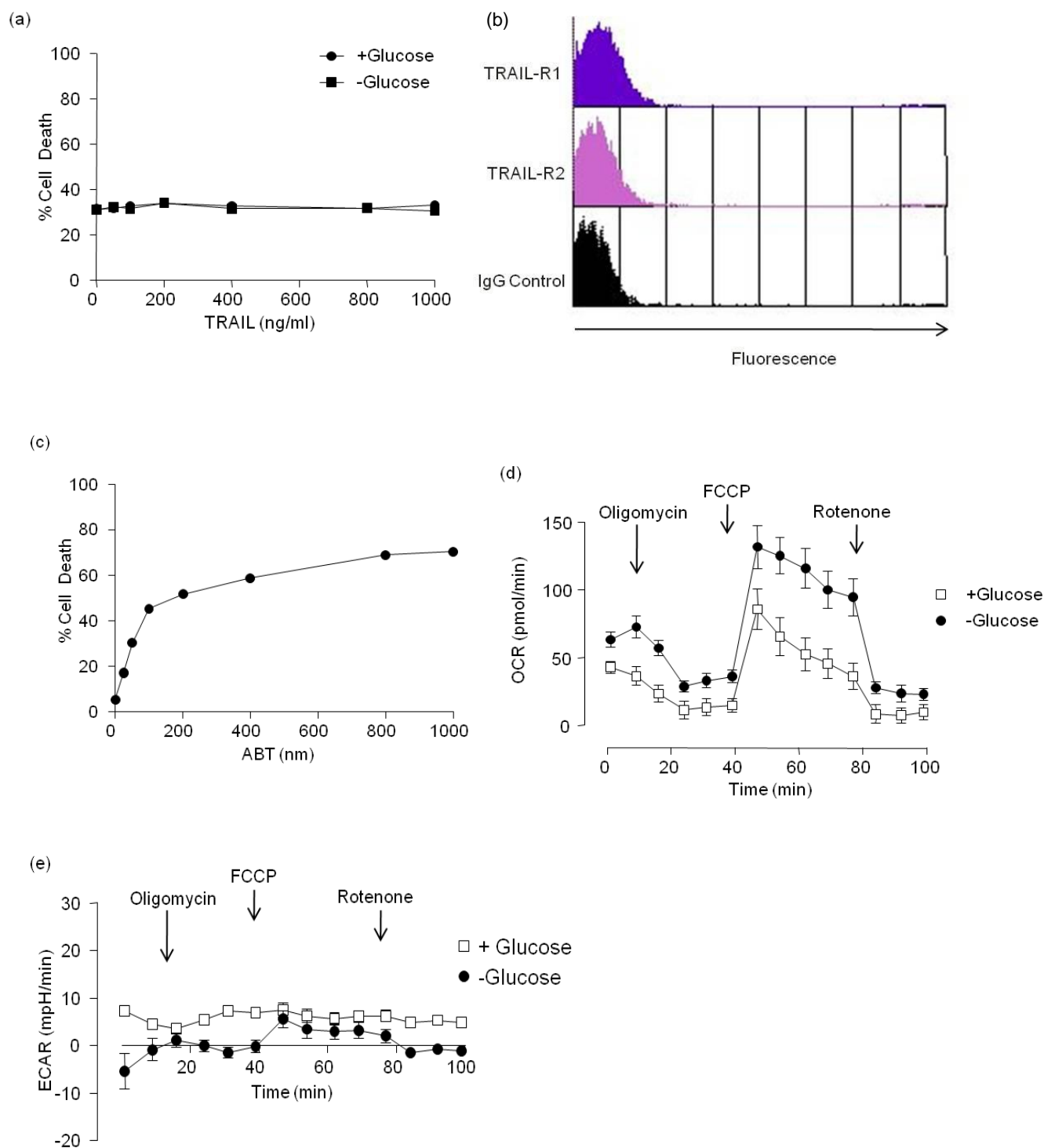


Figure 5.11 Characterisation of patient MCL samples. (a) A primary MCL patient sample (N=1) was incubated in the presence (■) or absence (●) of glucose for 6 h followed by a 4 h dose response with TRAIL (0-1000 ng/ml). Cells were then assessed for percentage apoptosis by FACS analysis. (b) Primary MCL patient sample from (a) was labelled with PE-conjugated TRAIL-R1 (solid line), TRAIL-R2 (broken line) or IgG control (black fill) antibodies and assessed for receptor expression as outlined in materials and methods. Results are representative of one experiment. (c) Primary MCL patient samples (N=1) were treated with varying concentrations of ABT-737 (0-1000 nM) for 24 h and assessed for % cell death. Real-time measurements of OCR (d) and ECAR (e) were measured in primary MCL patient samples incubated in the presence (red line) or absence (blue line) of glucose for 6 h. Graphs display the effects of the mitochondrial inhibitors: Oligomycin (400 nM), FCCP (400 nM) and Rotenone (1 μ M). Results in (d) and (e) are representative of two independent experiments.

Here I observed that cells were sensitive to ABT-737 in a dose-dependent manner (Fig. 5.11c) and this is in accordance with recently published findings (Touzeau *et al*, 2011). Thus, the response of MCL patient samples to ABT-737 under glucose-free conditions should be examined further.

Next the effects of incubating primary MCL samples with or without glucose for 6 h were examined by extracellular flux analysis (Fig. 5.11d-e). The results showed that incubating primary MCL cells without glucose for 6 h lead to an increase in basal OCR compared to patient samples incubated in glucose-containing media (Fig. 5.11d). In the absence of glucose, MCL samples exhibited elevated basal OCR levels (Fig. 5.11d) coupled with low ECAR (Fig. 5.11e) compared to those incubated in the presence of glucose (Fig. 5.11d-e). Interestingly, the ECAR of the MCL sample incubated in the presence of glucose was also relatively low (Fig. 5.11e). However, further repeats with additional patient samples would be needed to confirm this as a significant finding. The effect of oligomycin, an ATP synthase inhibitor, had a more dramatic effect on the OCR of primary samples incubated in the absence of glucose compared to those incubated in the presence of glucose (Fig. 5.11d) as did their response to the uncoupler FCCP (Fig. 5.11e). The injection of rotenone, an electron transport chain complex I inhibitor, completely inhibited the OCR of primary samples kept in the presence of glucose (Fig. 5.11d) but only reduced that of glucose-free primary samples by ~70% (Fig. 5.11e). This suggests that the electron transport chain, downstream of complex I, is still functional in these cells. Overall, the results show that primary MCL cells, similar to the Z138 cell line, incorporate a metabolic flexibility, which in the absence of glucose permits increased respiration through the mitochondria.

Lastly, the subcellular localisation of key pro- and anti-apoptotic proteins and metabolic proteins were examined in a single patient MCL sample (Fig. 5.12). 1.5×10^9 patient MCL cells were separated by differential centrifugation, as previously described (Materials and Methods), and assessed for the localisation of the pro-apoptotic proteins: Bax, Bak and cytochrome *c*, the mitochondrial proteins: SOD2, Cox IV and VDAC2, and the hexokinase enzymes type I and type II (Fig. 5.12). The results show that Bax is largely associated with both the cytosolic and mitochondrial fraction (Fig. 5.10) whilst Bak is detected only in the mitochondrial fraction (Fig. 5.12). Similarly, cytochrome *c* is largely found associated with the mitochondrial fraction (Fig. 5.12). The anti-apoptotic protein Bcl-2 is detected in all three fractions but is found primarily associated with the mitochondria (Fig. 5.12). The mitochondrial markers SOD2, Cox IV and VDAC2 all associate with the fraction designated 'mitochondria' confirming the

quality of the subcellular fractions (Fig. 5.12). Furthermore, both hexokinase I and II show evidence of being present in all three fractions examined with the majority being associated with the mitochondria (Fig. 5.12). Compared to the Z138 cell line, these primary MCL samples appear to have significantly higher levels of the hexokinase enzymes bound to their mitochondria (Fig. 4.13 and 5.12). However, notably, in these cells the hexokinase enzymes also do not appear to confer resistance to apoptotic stimuli as has been previously discussed (Fig. 5.8c). Therefore, the anti-apoptotic effects of mitochondrial-bound hexokinase appear not to correlate with the apoptotic sensitivity of cell lines or primary samples.

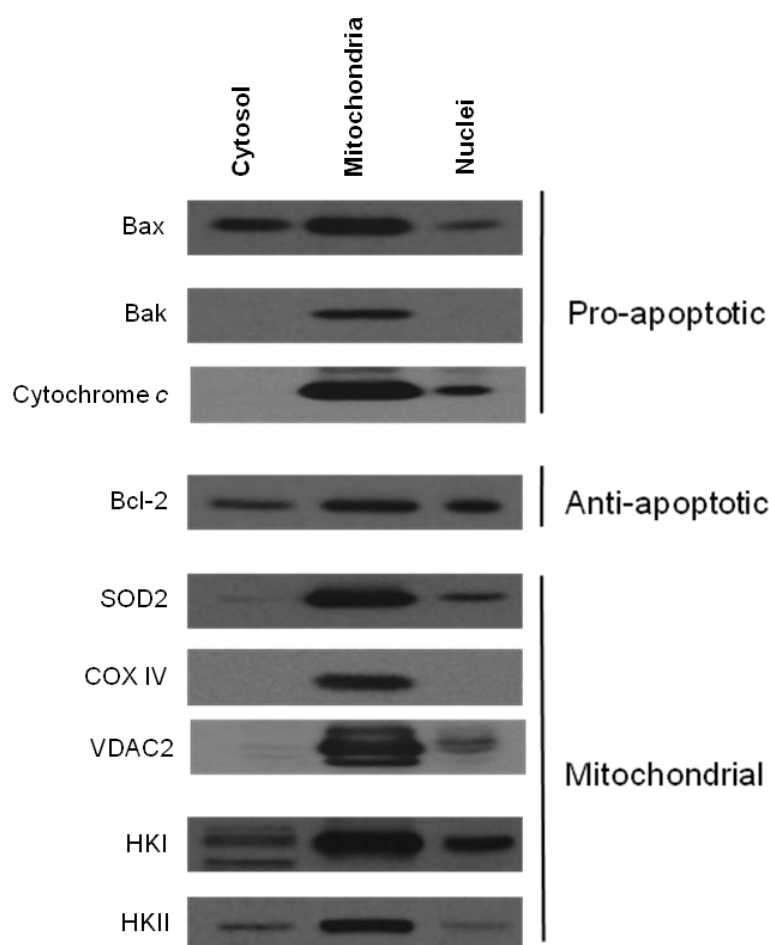


Figure 5.12 Subcellular fractionation of a MCL patient sample. Cytosolic, mitochondrial and nuclear fractions from a patient MCL sample were obtained by differential centrifugation and analysed for the presence of the indicated proteins as outlined in materials and methods. Results are from of one experiment.

5.3 Discussion

The research discussed in this chapter utilises DNA microarray technology to examine gene expression changes associated with the culturing of Z138 cells in the absence of glucose. These data shows that there are significant gene changes, both up and down

regulated, associated with this adaptation. The clustering of these genes enables a more detailed analysis of the type of effects that these gene changes might elude, some of which I have discussed above. There are clearly a number of gene changes and functional groups that have not been discussed in detail in this chapter and therefore there is more research to be done with regards to this. However, what I have attempted to highlight are the gene changes that could be associated with the apoptotic and metabolic phenotypes observed in glucose-free cells. The gene expression changes obtained are relatively small and thus, ideally, rather than examining the transcriptional changes under glucose-free conditions a more in-depth translational profiling may have provided a more accurate analysis of these cells. Future work will thus be performed to examine the translational status of specific RNA species under glucose-free conditions. Nevertheless, taking the results obtained thus far, the data shows that:

1. Chronic glucose-deprivation results in the down-regulation of 174 genes and the up-regulation of 48 genes, which can be clustered into distinct functional groups depending on their known role in the cell.
2. Together these gene expression changes suggest an anti-apoptotic/pro-survival phenotype.
3. Specifically, the PI3K/AKT pathway appears to be activated under glucose-free conditions.
4. Mitochondrial-bound hexokinase II, although increased, appears not to contribute to the reduced sensitivity observed in glucose-free cells.
5. Polysome profiling shows that, whilst 2DG treatment greatly reduces the translational capacity of cells, glucose-deprivation has less of an effect and therefore protein expression is able to proceed in the absence of glucose.
6. Preliminary experiments with patient MCL samples indicate that, although resistant to TRAIL, after 6 h glucose-deprivation they also undergo a switch in metabolism and thus modulated cellular metabolism may influence their response to alternative apoptotic stimuli.

Of the 174 altered genes identified, greater than 70% of these were down regulated (Fig. 5.1) including all of the genes clustered into the apoptotic functional group (Table

5.1). Interestingly, the gene for the anti-apoptotic protein Bcl-2 was not up regulated in the microarray study despite it being significantly up regulated at the protein level in glucose-free cells (Fig. 4.11). This suggests that the regulation of Bcl-2 protein levels in glucose-free cells is not due to a significant increase in gene expression and thus a more detailed analysis of its regulation is required. Similarly, the levels of cytochrome *c* at the mitochondria were found to be significantly increased under glucose-free conditions (Fig. 4.13) however a change in gene expression was not detected in this microarray study also suggesting an alternative regulation of this protein. Therefore, the polysome profile fractions obtained from control and glucose-free cells could be examined for the ribosomal association of Bcl-2 and cytochrome *c* mRNA. This would provide important information as to the level of expression that these proteins are being altered.

Determining the roles of the two most up/down regulated genes; GLCCI1 and SH3CT1, respectively, could prove insightful in establishing both the reason for the loss in sensitivity to apoptotic stimuli and the identification of potential novel regulators of apoptosis. An interesting gene change identified from the microarray analysis was that of the PPM2C gene whose protein regulates the pyruvate dehydrogenase complex. This gene change suggests a reduction in the conversion of pyruvate to acetyl-CoA in glucose-free cells, which would reduce the metabolic flux through the citric acid cycle and mitochondrial respiration. Therefore, the breakdown of pyruvate metabolism needs to be examined further to determine its fate within the cell. Similarly, the activity of pyruvate kinase, a HIF-1 cellular target, should be examined to confirm the activity of the pyruvate dehydrogenase (PDH) complex. In addition, since the breakdown of fatty acids can also generate acetyl-CoA, the metabolic flux through this pathway could be examined. Preliminary research to answer this question was carried out in collaboration with Prof. Atan Gross's laboratory at the Weizmann Institute of Science. Here, using extracellular flux analysis, the regulation of fatty acid oxidation (FAO) was examined in glucose-containing and glucose-free Z138 cells, however, preliminary results suggest that FAO is not increased under conditions of glucose-deprivation (data not shown). However, these results need further analysis to confirm these findings. If changes in FAO appear not to regulate levels of acetyl-CoA then the end-point of pyruvate needs further investigation including its distribution in the cell and its breakdown. This could be achieved by using radio-labelled pyruvate and tracking its processing in the cell.

Another key functional group identified by microarray analysis is the cell survival gene changes (Table 5.1). Interestingly, genes that regulate the NF κ B signalling pathway appear to be the most prevalent (Table 5.1) and a recent paper published by Mauro and colleagues demonstrated how NF κ B mediates a metabolic adaptation by up regulating mitochondrial respiration proteins (Mauro *et al*, 2011). Interestingly, they observed an increase in aerobic glycolysis when NF κ B was inhibited and thus its activation promotes oxidative phosphorylation (Mauro *et al*, 2011). Thus taken together, the potential activation of NF κ B pathways under glucose-free conditions, as observed through microarray analysis, needs to be confirmed by examining, for example, the proteosomal degradation of its inhibitor I κ B α . I κ B α is an inhibitor of the transcription factor NF κ B and its phosphorylation by I κ B kinase (IKK) dissociates it from NF κ B thereby activating the protein complex permitting transcriptional changes.

Furthermore, in this Chapter, the importance of the AKT-signalling pathway and its downstream targets has been highlighted (Fig. 5.7). The changes associated with this pathway appear to have the most influence over the glucose-free phenotype and thus, to test this theory, inhibitors of this pathway and/or specific downstream target proteins should be employed, such as the PI3K inhibitors LY-294002 and Wortmannin. However, a role for the pro-apoptotic protein Bad in the AKT pathway appears not to mediate the anti-apoptotic phenotype as might have been predicted. Rather the phosphorylation, and thus displacement of the protein from anti-apoptotic proteins, was reduced. Bad has previously been found to reside in a complex with glucokinase (or hexokinase type IV) which has been suggested to regulate mitochondrial-based glucokinase activity and thus metabolism (Daniel *et al*, 2003; Yang *et al*, 2010). However, it should be noted that this complex was primarily observed in liver cells where glucokinase is preferentially expressed. Nevertheless, the fact that Bad can reside in such a complex could implies that in certain situations the AKT-phosphorylation site of this protein could be being masked. This would clearly have implications for the activity/role of this protein in regulating apoptosis.

Another key downstream target of the AKT pathway is hexokinase and under glucose-free conditions the levels of mitochondrial-bound hexokinase II were increased (Fig. 5.7). Therefore, based on research that showed the anti-apoptotic effects of mitochondrial-bound hexokinase II, I investigated if its displacement from mitochondria in glucose-free cells could re-sensitise cells to TRAIL-induced apoptosis (Fig. 5.8). However, these results show that its displacement from the mitochondria did not re-

sensitise glucose-free cells to TRAIL-induced apoptosis. Another hypothesis was that this increase in mitochondrial bound hexokinase II was 'tethering' cytochrome *c* to the mitochondria and thus preventing its release from the mitochondria. Therefore, preliminary experiments to immunoprecipitate and perform mass spectrometry analysis of isolated complexes was performed (data not shown). The results show that cytochrome *c* was not found in a complex with hexokinase II and neither was it detected by mass spectrometry (data not shown). Further characterisation of this increase in mitochondrial bound hexokinase II, and also the increase in cytochrome *c*, needs to be investigated.

Polysome profiling was carried out to examine the translational status of glucose-free cells compared to glucose-containing cells and also 2DG treated cells versus control cells (Fig. 5.6 and Fig. 5.7). The results show that glucose-free cells exhibit a slight reduction in translation compared to glucose-containing cells (Fig. 5.7). However, to obtain a more accurate analysis of their translational status, this experiment should be repeated 24 h after seeding to ensure polysomes are analysed during the growth (and most active) phase of these cells. This would be predicated to show a greater translational profile of cells as observed with polysome profiling analysis after 2DG treatment (Fig. 5.7). Nevertheless, the effect of 2DG on translation appears to be greater than that observed with glucose-deprivation (Fig. 5.6 and Fig. 5.7). In the previous chapter the inhibition of glycolysis using 2DG was discussed. In comparison to glucose-deprivation, I proposed that the action of these conditions occur through fundamentally different mechanisms. Pradelli and colleagues show that depriving Jurkat cells of glucose for 16 h had a more dramatic effect (reduction) on translation than incubation of cells with 2DG (Pradelli *et al*, 2010). However, I show that this is not the case when comparing chronic glucose-deprivation (Fig. 5.6) and 2DG treatment (Fig. 5.7). Thus, chronically depriving cells of glucose and inhibiting glycolysis with 2DG has fundamentally different effects on translation. Importantly, analysing the translation status of cells can provide a more accurate representation of the expression of a protein than a gene expression study. As a result, the samples obtained from these experiments will be used to examine the translational profile under glucose-free conditions by microarray analysis.

The effects outlined in this chapter could prove significant in determining the response of cancers to targeted therapeutics. Gene changes associated with chronic glucose deprivation provide knowledge about novel signalling pathways and thus the relevance of these findings in a clinical setting is of up-most importance. Therefore, in an attempt

to answer some of these questions, I analysed primary MCL patient samples for their response to apoptotic stimuli (Fig. 5.8), metabolic status following glucose-deprivation (Fig. 5.8) and the subcellular distribution of key cellular proteins (Fig. 5.9). What is evident from these analyses is that primary MCL cells have a metabolic flexibility that has also been observed in the MCL line Z138. This suggests that, similar to the Z138 cell line, the metabolic status of these cells could regulate responses to apoptotic stimuli. At the least, these findings show that MCL cells can modulate their metabolism based on the surrounding environment and thus attempting to sensitise these cells to apoptotic stimuli by glucose-deprivation as a chemotherapeutic approach would not be advantageous. However, more research into the role of cancer cell metabolic status on the response of cells to apoptotic stimuli is required before further conclusions can be made. Importantly, one of the limitations of this study is the availability of patient samples in particular those diagnosed with MCL. Therefore, to overcome this, preliminary studies to investigate cancer metabolism could be performed with Chronic Lymphocytic Leukaemia (CLL) patient samples, which are more prevalent and obtainable.

6.0 Final Discussion

6.1 Overview

The fundamental reason for carrying out the research in this thesis was to investigate the complex and dynamic TRAIL signalling cascade by identifying and characterising novel regulators of this pathway. These aims were met through performing proteomic, metabolic and gene expression profiling studies and together have provided evidence for previously unidentified regulators and modulators of both the TRAIL signalling pathway and the intrinsic pathway initiated by ABT-737 and radiation. Taken together, the findings from this research are outlined in Figure 6.1. Here, I attempt to demonstrate how, despite the extensive research that has been conducted on TRAIL, there is still much to be learnt about how this death ligand exerts its effect(s) and how these are modulated to prevent or promote its signalling pathways. Furthermore, these findings have the potential to provide insight into the how other death ligands or apoptotic pathways may be modulated and thus this research can be used as a basis to explore these findings in other cancer cell models. Similarly, for close to half a century defects in cancer cell metabolism have been known however it is only more recently that research has identified some interesting changes in metabolism that facilitate tumour growth and prevent apoptosis. These findings have the potential to aid the design of novel cancer therapeutics based on metabolic abnormalities and thus represent an important line of current scientific research.

6.2 TRAIL and its signalling complex

Over the last decade, the use of TRAIL as a potential cancer therapeutic has been investigated extensively. Numerous human derived cell lines, animal models and clinical trials have been tested/conducted for their response to TRAIL-induced apoptosis. Preclinical studies have enabled the identification of sensitive and resistant cell lines (reviewed in Ashkenazi, 2002) whilst studies in mice have been paramount in elucidating the physiological role of TRAIL, where it was found to elicit an immune response against cancerous cells (Takeda *et al*, 2002). Together, these studies have provided further evidence as to the importance of TRAIL as a potential cancer therapeutic. Clinical trials, however, have proved to be the most informative but not without their complications. Initial clinical studies with tagged-variants of recombinant human TRAIL (rhTRAIL) were halted after they were found to be toxic to normal human cells (reviewed in Nagata, 2000). However, a non-tagged variant of rhTRAIL was subsequently generated, which was found to be non-toxic to normal human cells (Lawrence *et al*, 2001; Hao *et al*, 2004). rhTRAIL activates its pathway through the binding of both TRAIL-R1 and -R2 whilst human monoclonal antibodies, generated by

a number of pharmaceutical companies including Human Genome Sciences (ETR1/Mapatumumab and ETR2/Lexatumumab), Genentech (Apomad) and Novartis (LBY-135), target either TRAIL-R1 or -R2 specifically (reviewed in Ashkenazi, 2008). Interestingly, the majority of these monoclonal antibodies appear to target TRAIL-R2 specifically. This is surprising since the data generated in this thesis and other studies (MacFarlane *et al*, 2005; Dyer *et al*, 2008) demonstrate that the majority of cell lines and patient tumour samples signal to death primarily through TRAIL-R1. Therefore, in these cell lines/primary tumours there is no logical reason to employ TRAIL-R2 specific monoclonal antibodies. Furthermore, to date, primary tumours that have demonstrated resistance to TRAIL appear to mediate this response through genomic alterations of key regulators of this pathway such as the loss of the TRAIL-receptors, caspase-8 or Bax expression (Hopkins-Donaldson *et al*, 2000; Li *et al*, 2006; reviewed in Bellail *et al*, 2009). In line with this, the research carried out in this thesis observed that patient MCL samples were inherently resistant to TRAIL, but not ABT-737, presumably due to the lack of surface expression of TRAIL-R1/-R2. Taken together, it is evident that a full characterisation of patient cancer tissues needs to be performed in order to distinguish between tumours that will be sensitive to TRAIL and those that will be resistant.

The proteomic research carried out in Chapter 3 provides evidence for both a previously unidentified TRAIL DISC interactor, specifically the transferrin receptor (Fig. 6.1 – boxed (a)), and a novel stoichiometry of the known DISC components (Fig. 6.1 – boxed (b)). The transferrin receptor, in normal cells, is a transmembrane receptor involved in the internalisation of iron-laden transferrin by endocytosis (reviewed in Thorstensen and Romslo, 1990; Wang and Pantopoulos, 2011). In Z138 cells, however, it was also found to precipitate with the TRAIL DISC both in a ligand-receptor only complex and following recruitment of FADD and caspase-8 (Fig. 6.1). Preliminary studies to knockdown the transferrin receptor in Z138 cells were unsuccessful. However, similar experiments performed in the laboratory found that (a) the transferrin receptor associated with the TRAIL DISC in BJAB, Jurkat and Hela cells and (b) that its knockdown by RNAi decreased the sensitivity of cells to TRAIL but increased TRAIL-receptor surface expression levels (L. Dickens, unpublished results). These findings suggest that the transferrin receptor could modulate TRAIL-receptor signalling specifically through its interaction with TRAIL-receptor. In line with this, it has previously been shown that, similar to the transferrin receptor, the TRAIL-receptors are internalised by endocytosis in clathrin-coated vesicles (Fig. 1.6) although this is not paramount for successful TRAIL-signalling (Kohlhaas *et al*, 2007).

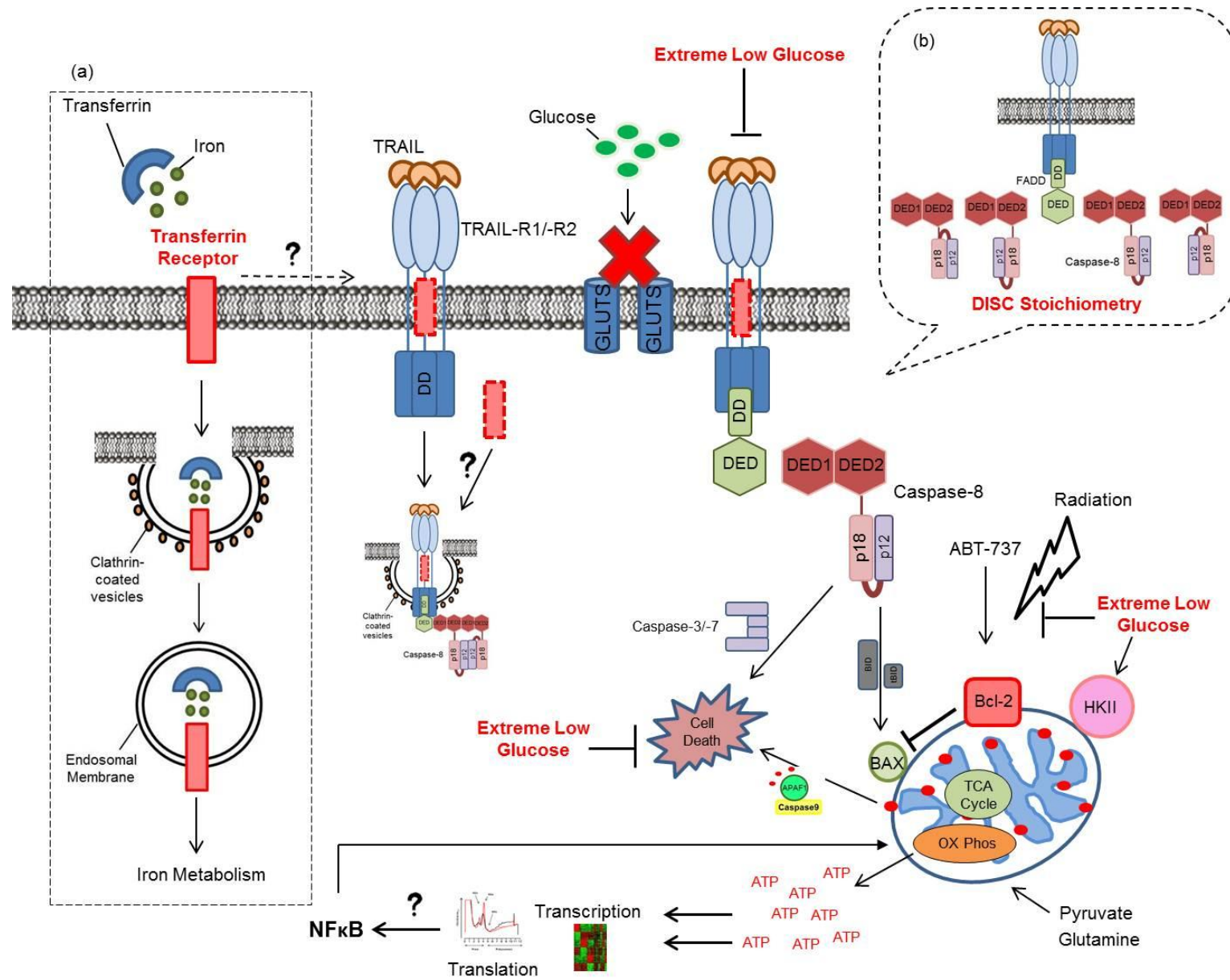


Figure 6.1 Scheme to show how the findings from the research performed in this thesis modulate extrinsic and intrinsic apoptotic signalling (a)

The transferrin receptor was identified as being present in a Z138 DISC. In normal cells, this receptor is involved in the internalisation of iron-laden transferrin by endocytosis. TRAIL, and other death receptor complexes, are also internalised by endocytosis in clathrin-coated vesicles and thus the transferrin receptor could potentially be involved in this process. (b) Using label-free quantitative analyses, FADD was found to be present in sub-stoichiometric amounts. A new structure of the DISC based on caspase-8 chain formation has been proposed (Dickens *et al*, 2011). This model takes into account the low levels of FADD and high levels of caspase-8 that are commonly observed in an isolated TRAIL DISC. (Remaining figure) The deprivation of glucose from culture media brought about a switch in bioenergetics reducing glycolysis and increasing mitochondrial respiration. This was in line with a decrease in sensitivity to apoptotic stimuli, specifically TRAIL, ABT-737 and radiation. Chronic glucose-deprivation also brought about key gene expression changes that correlate with an anti-apoptotic/pro-survival phenotype. Specifically, regulators of the NFκB transcription factor were found to be modulated and this signalling cascade has recently been implicated in inhibiting glycolysis and increasing mitochondrial respiration (Mauro *et al*, 2011). Taken together, this schematic shows how the findings from this thesis directly regulate apoptotic signalling.

Thus, the transferrin receptor could potentially modulate the internalisation or trafficking of the TRAIL-R1/-R2 and this needs to be investigated further.

Secondly, using the mass spectrometry data and label-free quantitative analyses, the known TRAIL DISC components were found to be present in a stoichiometry that did not match the currently accepted model of 1:1:1 for receptor:FADD:caspase-8. Instead, FADD was found to be present in sub-stoichiometric amounts and this led to the proposal of a new DISC structure based on caspase-8 chain formation (Fig. 1.6 – boxed (b)), which accounts for the low FADD:caspase-8 ratio at the DISC (Dickens, *et al*, 2011). The implications of these findings are currently being investigated further. Nevertheless, taken together, the discovery of a potential novel TRAIL DISC interactor and the proposal of an alternative DISC stoichiometry provide key information as to previously unidentified requirements for successful TRAIL-signalling. Both the knockdown of the TFR (L. Dickens, unpublished results) and the prevention of caspase-8 chain formation through mutations in the binding-domains (Dickens *et al*, 2011) reduced apoptotic cell death and TRAIL DISC activity, respectively. Thus, these findings are clearly key to understanding how TRAIL signals successfully to cell death.

6.3 Metabolic regulation of cancer

There are a number of changes that a tumour cell undergoes in order to survive the environment in which they reside and these appear to have implications in the successful signalling of these cells to apoptosis. The lack of oxygen available to the majority of tumours means that ATP generation through the electron transport chain is largely inhibited and therefore these cells must rely on glycolysis for their energy supplies. This alone can cause fluctuations in both the abundance of mitochondria and the up regulation of glycolytic enzymes due to the demands on the cell. However, how exactly these changes affect apoptosis are still unclear. The reliance of cancer cells on glycolysis could provide a weakness of the tumour to specific inhibitors of this pathway and thus conditions that prevent glycolysis could contribute to an increase in sensitivity to apoptotic stimuli. However, attempting to modulate glucose-deprivation *in vitro* is far simpler than trying to modulate this *in vivo*. Studies carried out to date largely modulate glucose metabolism in cell lines through the short-term deprivation of glucose from cell culture media or treatment of cells with anti-glycolytics, such as 2DG. However, the physiological relevance of these are unclear since it is unlikely that these situations would occur *in vivo* and, presumably, if they were to occur, then the damage caused to normal rapidly proliferating cells would likely be substantial. Similarly, initial research carried out in Chapter 4 of this thesis observed that acute glucose-deprivation, and

treatment with 2DG, caused a significant increase in the amount of necrotic cell death occurring both before and after treatment with TRAIL. This suggests that these cells are already stressed from the changes in culture conditions and thus appear to be 'primed' for death. Therefore, the potential of short-term glucose deprivation as a cancer therapeutic approach or as a combinational therapy requires more extensive study before its benefits in patients can be assessed.

The centres of solid tumours, as well as being hypoxic, have the potential to harbour areas of extreme low glucose. Similar to hypoxia, this would presumably be a direct result of the lack of vascularisation during early tumourigenesis and it has been suggested that the changes associated with cancer cell metabolism, i.e. the Warburg effect, occur as a direct result of this stage of proliferation. It has long been known that, in addition to glucose, cancer cells can utilise other nutrients for growth and survival (DeBerardinis and Cheng, 2010). However, the ability of these to substitute for glucose is unclear. The research carried out in Chapter 4 of this thesis suggests that cancer cells, specifically the mantle cell lymphoma cell line Z138, can proliferate and survive in the absence of glucose through glutamine and pyruvate metabolism. In line with this, mitochondrial respiration is significantly increased and the cellular response to apoptotic stimuli are reduced (Fig. 6.1). Taken together, these data imply that under certain conditions glucose deprivation could promote cancer cell survival rather than sensitise such cells to apoptotic stimuli. These findings clearly contradict current studies into the potential of modulated glucose metabolism as a cancer treatment regime and thus signify a clear line of research that needs to be extensively tested before this treatment approach is taken any further.

Clearly, areas of extreme low glucose are only likely to be associated with the centres of solid tumours and rather, in the case of cancers of the blood cells, once the cancer enters the leukaemic phase then conditions of low glucose, or even low oxygen, are unlikely to occur. Interestingly, in line with this, leukaemia is extremely difficult to identify with FDG-PET unless it is present as a lymphoma in, for example, the lymph node (Weiler-Sagie *et al*, 2010). This suggests that once these cells enter the blood stream, mitochondrial respiration rather than glycolysis predominates although it should be noted that these cells are not proliferating. Thus, modulated glucose metabolism depending on the stage of tumourigenesis could provide a window of time at which the cancer would be sensitive to TRAIL and other anti-cancer therapies. Similarly, my data suggests that, under these conditions, depriving Z138 cells of glucose results in a loss in sensitivity to apoptotic stimuli both through the extrinsic

pathway (TRAIL) and intrinsic pathway (ABT-737 and radiation) (Fig. 6.1). Thus, depriving these cells of glucose as a way to sensitise them to apoptotic stimuli is clearly not recommended. Together, these findings provide a novel previously unreported role of modulated glucose metabolism in tumour cells.

6.4 Future Work

From the research performed in this thesis, I propose that the following experiments could be performed to provide further evidence as to the actual role of the novel interactors and modulators of TRAIL-induced apoptosis identified in this research.

From the proteomic analysis of the TRAIL DISC, the role of the transferrin receptor in other receptor-complexes that promote apoptosis could be investigated such as that of the CD95 DISC. Furthermore, its potential role in internalisation or trafficking of the TRAIL receptors could be investigated as could its presence in the TRAIL DISC from multiple cell lines/tumour models to determine if it's a constitutive component of the DISC. Further research into the stoichiometry of known DISC components could include determining its relevance in TRAIL-receptor signalling, determining the length of the caspase-8 chains and how these are modulated by, for example, cFLIP_S, cFLIP_L and caspase-10.

From the metabolic research performed in Chapter 4, the key follow-up experiment is to perform glucose-deprivation studies in other cancer cell lines to determine if these findings are evident in other cancer-models or, in line with this, if it is tumour-type specific. This should also include further examination in patient samples to determine the relevance of these findings in a physiological system. Furthermore, the role of glutamine and pyruvate in the metabolism of these cells should also be confirmed by tracking their breakdown to assess for their ability to substitute for glucose metabolism. In line with this, the data obtained from the transcriptional and translation studies of glucose-deprived cells needs to be followed-up to check that the gene changes correlate with a change in protein expression. These can also be confirmed from the extraction of RNA from polysome fractions to examine their translation. Inhibitors of the AKT pathway could also be employed to confirm the activation and effect of this pathway in glucose-free cells. Most importantly, the relevance of these findings in a clinical setting need to be assessed.

List of publications, talks and awards

Robinson, GL., Dinsdale, D., MacFarlane, M., Cain, K. 2011 '**Switching from aerobic glycolysis to oxidative phosphorylation modulates tumor cell sensitivity to TRAIL**'. (*Under review Oncogene*)

Dickens, L., Boyd, R., Robinson, GL., Jukes-Jones, R., Cain, K., MacFarlane, M 2011 '**Stoichiometry of the TRAIL Death-Inducing Signalling Complex (DISC):Structural modelling and *in vitro* reconstitution reveal a new DISC model based on caspase-8 chain formation**'. (*Under review Molecular Cell*).

Robinson, GL. July 2011 '**Daniel Turnberg Travel Fellowship Award**' Visiting Prof. Atan Gross at the Weizmann Institute of Science, Israel.

Robinson, GL., MacFarlane, M., Cain, K. July 2010 '**Switching from aerobic glycolysis to oxidative phosphorylation modulates tumor cell sensitivity to TRAIL**'. European Workshop on Cell Death (*Conference Seminar*).

Robinson, GL., Dickens, L., Boyd, R., Jukes-Jones, R., MacFarlane, M., Cain, K. June 2010 '**To die or not to die – a *TRAIL* of death**'. Festival of Postgraduate Research, University of Leicester (*Poster Presentation Finalist*).

Appendix 1 – Ethics Consent Form

University Hospitals of Leicester **NHS**
NHS Trust

DIRECTORATE OF RESEARCH & DEVELOPMENT

Research & Development Office
Leicester General Hospital
Gwendolen Road
Leicester
LE5 4PW

Director: Professor D Rowbotham

Assistant Director: David Hetmanski

R&D Manager: Carolyn Maloney

Direct Dial: (0116) 258 8351
Fax No: (0116) 258 4226

21/10/2009

Prof Martin JS Dyer
MRC Toxicology Unit
Hodgkin Building
Leicester University
Lancaster Rd
PO BOX 138
LE1 9HN
UK

Dear Prof Martin JS Dyer

Ref: UHL 10132
Title: Proteomic analysis of the B-cell surface membrane.
Project Status: Project Approved
End Date: 10/07/2026

Thank you for submitting documentation for Non-Substantial amendment for the above study.

I confirm that the amendment has the approval of the University Hospitals of Leicester NHS Trust R&D Department and may be implemented with immediate effect.

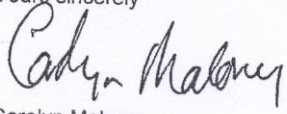
The documents received are as follows:

Document Name	Version Number	Date
CV and GCP for Ms Gemma Robinson		

Please be aware that any changes to these documents after approval may constitute an amendment. The process of approval for amendments should be followed. Failure to do so may invalidate the approval of the study at this trust.

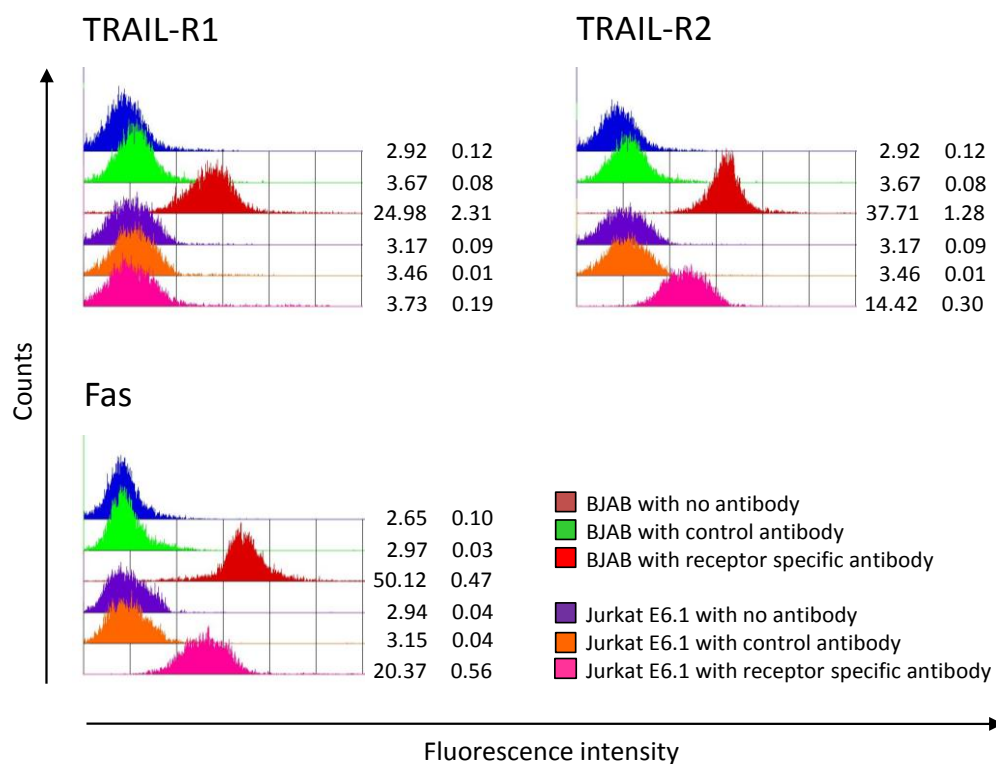
Please ensure that all documentation and correspondence relating to this amendment are filed appropriately in the relevant site file.

Yours sincerely



Carolyn Maloney
R&D Manager

Appendix 2



Appendix 1: Cell Surface expression of TRAIL-R1 and –R2 is higher in BJAB cells than in Jurkat Cells. BJAB and Jurkat cells were examined for TRAIL-receptor surface expression by Dr. Laura Dickens (MRC Toxicology Unit) essentially as previously described in Figure 3.5

References

- Acehan, D., Jiang, X., Morgan, D.G., Heuser, J.E., Wang, X., and Akey, C.W. (2002). Three-dimensional structure of the apoptosome: implications for assembly, procaspase-9 binding, and activation. *Mol. Cell* 9, 423-432.
- Adrain, C., and Martin, S.J. (2001). The mitochondrial apoptosome: a killer unleashed by the cytochrome seas. *Trends Biochem. Sci.* 26, 390-397.
- Aft, R.L., Zhang, F.W., and Gius, D. (2002). Evaluation of 2-deoxy-D-glucose as a chemotherapeutic agent: mechanism of cell death. *Br. J. Cancer* 87, 805-812.
- Aguirre, V., Uchida, T., Yenush, L., Davis, R., and White, M.F. (2000). The c-Jun NH(2)-terminal kinase promotes insulin resistance during association with insulin receptor substrate-1 and phosphorylation of Ser(307). *J. Biol. Chem.* 275, 9047-9054.
- Alao, J.P. (2007). The regulation of cyclin D1 degradation: roles in cancer development and the potential for therapeutic invention. *Mol. Cancer* 6, 24.
- Alberts, B., Johnson, A., Lewis, J., Raff, M., Roberts, K., Walter, P. (2002). *Molecular Biology of the Cell* (New York: Garland Science).
- Algeciras-Schimnich, A., Shen, L., Barnhart, B.C., Murmann, A.E., Burkhardt, J.K., and Peter, M.E. (2002). Molecular ordering of the initial signaling events of CD95. *Mol. Cell. Biol.* 22, 207-220.
- Alizadeh, A.A., Eisen, M.B., Davis, R.E., Ma, C., Lossos, I.S., Rosenwald, A., Boldrick, J.C., Sabet, H., Tran, T., Yu, X., *et al.* (2000). Distinct types of diffuse large B-cell lymphoma identified by gene expression profiling. *Nature* 403, 503-511.
- Alnemri, E.S., Livingston, D.J., Nicholson, D.W., Salvesen, G., Thornberry, N.A., Wong, W.W., and Yuan, J. (1996). Human ICE/CED-3 protease nomenclature. *Cell* 87, 171.
- Arcaro, A., and Guerreiro, A.S. (2007). The phosphoinositide 3-kinase pathway in human cancer: genetic alterations and therapeutic implications. *Curr. Genomics* 8, 271-306.
- Ashkenazi, A. (2002). Targeting death and decoy receptors of the tumour-necrosis factor superfamily. *Nat. Rev. Cancer* 2, 420-430.

- Ashkenazi, A. (2008). Directing cancer cells to self-destruct with pro-apoptotic receptor agonists. *Nat. Rev. Drug Discov.* 7, 1001-1012.
- Ashkenazi, A., and Dixit, V.M. (1998). Death receptors: signaling and modulation. *Science* 281, 1305-1308.
- Ashkenazi, A., Pai, R.C., Fong, S., Leung, S., Lawrence, D.A., Marsters, S.A., Blackie, C., Chang, L., McMurtrey, A.E., Hebert, A., *et al.* (1999). Safety and antitumor activity of recombinant soluble Apo2 ligand. *J. Clin. Invest.* 104, 155-162.
- Barnhart, B.C., Alappat, E.C., and Peter, M.E. (2003). The CD95 type I/type II model. *Semin. Immunol.* 15, 185-193.
- Beilharz, T.H., and Preiss, T. (2004). Translational profiling: the genome-wide measure of the nascent proteome. *Brief Funct. Genomic Proteomic* 3, 103-111.
- Bellail, A.C., Qi, L., Mulligan, P., Chhabra, V., and Hao, C. (2009). TRAIL agonists on clinical trials for cancer therapy: the promises and the challenges. *Rev. Recent. Clin. Trials* 4, 34-41.
- Benard, G., and Rossignol, R. (2008). Ultrastructure of the mitochondrion and its bearing on function and bioenergetics. *Antioxid. Redox Signal.* 10, 1313-1342.
- Benn, D.E., Richardson, A.L., Marsh, D.J., and Robinson, B.G. (2006). Genetic testing in pheochromocytoma- and paraganglioma-associated syndromes. *Ann. N. Y. Acad. Sci.* 1073, 104-111.
- Bensaad, K., Tsuruta, A., Selak, M.A., Vidal, M.N., Nakano, K., Bartrons, R., Gottlieb, E., and Vousden, K.H. (2006). TIGAR, a p53-inducible regulator of glycolysis and apoptosis. *Cell* 126, 107-120.
- Bensaad, K., and Vousden, K.H. (2007). P53: New Roles in Metabolism. *Trends Cell Biol.* 17, 286-291.
- Berger, T., and Kretzler, M. (2002). TRAIL-induced apoptosis is independent of the mitochondrial apoptosis mediator DAP3. *Biochem. Biophys. Res. Commun.* 297, 880-884.

- Boatright, K.M., Renatus, M., Scott, F.L., Sperandio, S., Shin, H., Pedersen, I.M., Ricci, J.E., Edris, W.A., Sutherlin, D.P., Green, D.R., and Salvesen, G.S. (2003). A unified model for apical caspase activation. *Mol. Cell* 11, 529-541.
- Boatright, K.M., and Salvesen, G.S. (2003). Mechanisms of caspase activation. *Curr. Opin. Cell Biol.* 15, 725-731.
- Bossy-Wetzel, E., Newmeyer, D.D., and Green, D.R. (1998). Mitochondrial cytochrome c release in apoptosis occurs upstream of DEVD-specific caspase activation and independently of mitochondrial transmembrane depolarization. *EMBO J.* 17, 37-49.
- Boyd, R.S., Jukes-Jones, R., Walewska, R., Brown, D., Dyer, M.J., and Cain, K. (2009). Protein profiling of plasma membranes defines aberrant signaling pathways in mantle cell lymphoma. *Mol. Cell. Proteomics* 8, 1501-1515.
- Bradford, M.M. (1976). A rapid and sensitive method for the quantitation of microgram quantities of protein utilizing the principle of protein-dye binding. *Anal. Biochem.* 72, 248-254.
- Bradley, J.R., and Pober, J.S. (2001). Tumor necrosis factor receptor-associated factors (TRAFs). *Oncogene* 20, 6482-6491.
- Brancolini, C., Benedetti, M., and Schneider, C. (1995). Microfilament reorganization during apoptosis: the role of Gas2, a possible substrate for ICE-like proteases. *EMBO J.* 14, 5179-5190.
- Brill, A., Torchinsky, A., Carp, H., and Toder, V. (1999). The role of apoptosis in normal and abnormal embryonic development. *J. Assist. Reprod. Genet.* 16, 512-519.
- BROWN, J. (1962). Effects of 2-deoxyglucose on carbohydrate metabolism: review of the literature and studies in the rat. *Metabolism* 11, 1098-1112.
- Brown, P.O., and Botstein, D. (1999). Exploring the new world of the genome with DNA microarrays. *Nat. Genet.* 21, 33-37.
- Brumatti, G., Sheridan, C., and Martin, S.J. (2008). Expression and purification of recombinant annexin V for the detection of membrane alterations on apoptotic cells. *Methods* 44, 235-240.

- Cain, K., Bratton, S.B., and Cohen, G.M. (2002). The Apaf-1 apoptosome: a large caspase-activating complex. *Biochimie* 84, 203-214.
- Cairns, R.A., Harris, I.S., and Mak, T.W. (2011). Regulation of cancer cell metabolism. *Nat. Rev. Cancer*. 11, 85-95.
- Campos, C.B., Paim, B.A., Cosso, R.G., Castilho, R.F., Rottenberg, H., and Vercesi, A.E. (2006). Method for monitoring of mitochondrial cytochrome c release during cell death: Immunodetection of cytochrome c by flow cytometry after selective permeabilization of the plasma membrane. *Cytometry A*. 69, 515-523.
- Capasso, M., Bhamrah, M.K., Henley, T., Boyd, R.S., Langlais, C., Cain, K., Dinsdale, D., Pulford, K., Khan, M., Musset, B., *et al.* (2010). HVCN1 modulates BCR signal strength via regulation of BCR-dependent generation of reactive oxygen species. *Nat. Immunol.* 11, 265-272.
- Caro-Maldonado, A., Tait, S.W., Ramirez-Peinado, S., Ricci, J.E., Fabregat, I., Green, D.R., and Munoz-Pinedo, C. (2010). Glucose deprivation induces an atypical form of apoptosis mediated by caspase-8 in Bax-, Bak-deficient cells. *Cell Death Differ.* 17, 1335-1344.
- Cerretti, D.P., Kozlosky, C.J., Mosley, B., Nelson, N., Van Ness, K., Greenstreet, T.A., March, C.J., Kronheim, S.R., Druck, T., and Cannizzaro, L.A. (1992). Molecular cloning of the interleukin-1 beta converting enzyme. *Science* 256, 97-100.
- Chai, J., Wu, Q., Shiozaki, E., Srinivasula, S.M., Alnemri, E.S., and Shi, Y. (2001). Crystal structure of a procaspase-7 zymogen: mechanisms of activation and substrate binding. *Cell* 107, 399-407.
- Chang, D.W., Xing, Z., Pan, Y., Algeciras-Schimnich, A., Barnhart, B.C., Yaish-Ohad, S., Peter, M.E., and Yang, X. (2002). c-FLIP(L) is a dual function regulator for caspase-8 activation and CD95-mediated apoptosis. *EMBO J.* 21, 3704-3714.
- Chao, D.T., and Korsmeyer, S.J. (1998). BCL-2 family: regulators of cell death. *Annu. Rev. Immunol.* 16, 395-419.
- Chaturvedi, M.M., Sung, B., Yadav, V.R., Kannappan, R., and Aggarwal, B.B. (2011). NF-kappaB addiction and its role in cancer: 'one size does not fit all'. *Oncogene* 30, 1615-1630.

- Christofk, H.R., Vander Heiden, M.G., Harris, M.H., Ramanathan, A., Gerszten, R.E., Wei, R., Fleming, M.D., Schreiber, S.L., and Cantley, L.C. (2008). The M2 splice isoform of pyruvate kinase is important for cancer metabolism and tumour growth. *Nature* **452**, 230-233.
- Christofk, H.R., Vander Heiden, M.G., Wu, N., Asara, J.M., and Cantley, L.C. (2008). Pyruvate kinase M2 is a phosphotyrosine-binding protein. *Nature* **452**, 181-186.
- Chun, H.J., Zheng, L., Ahmad, M., Wang, J., Speirs, C.K., Siegel, R.M., Dale, J.K., Puck, J., Davis, J., Hall, C.G., *et al.* (2002). Pleiotropic defects in lymphocyte activation caused by caspase-8 mutations lead to human immunodeficiency. *Nature* **419**, 395-399.
- Cohen, G.M. (1997). Caspases: the executioners of apoptosis. *Biochem. J.* **326** (Pt 1), 1-16.
- Cohen, P.T. (2002). Protein phosphatase 1--targeted in many directions. *J. Cell. Sci.* **115**, 241-256.
- Cole, K.A., Krizman, D.B., and Emmert-Buck, M.R. (1999). The genetics of cancer--a 3D model. *Nat. Genet.* **21**, 38-41.
- Coleman, M.C., Asbury, C.R., Daniels, D., Du, J., Aykin-Burns, N., Smith, B.J., Li, L., Spitz, D.R., and Cullen, J.J. (2008). 2-deoxy-D-glucose causes cytotoxicity, oxidative stress, and radiosensitization in pancreatic cancer. *Free Radic. Biol. Med.* **44**, 322-331.
- Conradt, B., and Horvitz, H.R. (1998). The *C. elegans* protein EGL-1 is required for programmed cell death and interacts with the Bcl-2-like protein CED-9. *Cell* **93**, 519-529.
- Creagh, E.M., Conroy, H., and Martin, S.J. (2003). Caspase-activation pathways in apoptosis and immunity. *Immunol. Rev.* **193**, 10-21.
- Cretney, E., Takeda, K., Yagita, H., Glaccum, M., Peschon, J.J., and Smyth, M.J. (2002). Increased susceptibility to tumor initiation and metastasis in TNF-related apoptosis-inducing ligand-deficient mice. *J. Immunol.* **168**, 1356-1361.
- Cui, H., Darmanin, S., Natsuisaka, M., Kondo, T., Asaka, M., Shindoh, M., Higashino, F., Hamuro, J., Okada, F., Kobayashi, M., *et al.* (2007). Enhanced expression of

asparagine synthetase under glucose-deprived conditions protects pancreatic cancer cells from apoptosis induced by glucose deprivation and cisplatin. *Cancer Res.* 67, 3345-3355.

DAJANI, R.M., DANIELSKI, J., GAMBLE, W., and ORTEN, J.M. (1961). A study of the citric acid cycle in certain tumour tissue. *Biochem. J.* 81, 494-503.

Dang, C.V., and Semenza, G.L. (1999). Oncogenic alterations of metabolism. *Trends Biochem. Sci.* 24, 68-72.

Dang, L., White, D.W., Gross, S., Bennett, B.D., Bittinger, M.A., Driggers, E.M., Fantin, V.R., Jang, H.G., Jin, S., Keenan, M.C., *et al.* (2009). Cancer-associated IDH1 mutations produce 2-hydroxyglutarate. *Nature* 462, 739-744.

Danial, N.N., Gramm, C.F., Scorrano, L., Zhang, C.Y., Krauss, S., Ranger, A.M., Datta, S.R., Greenberg, M.E., Licklider, L.J., Lowell, B.B., Gygi, S.P., and Korsmeyer, S.J. (2003). BAD and glucokinase reside in a mitochondrial complex that integrates glycolysis and apoptosis. *Nature* 424, 952-956.

Danial, N.N., and Korsmeyer, S.J. (2004). Cell death: critical control points. *Cell* 116, 205-219.

da-Silva, W.S., Gomez-Puyou, A., de Gomez-Puyou, M.T., Moreno-Sanchez, R., De Felice, F.G., de Meis, L., Oliveira, M.F., and Galina, A. (2004). Mitochondrial bound hexokinase activity as a preventive antioxidant defense: steady-state ADP formation as a regulatory mechanism of membrane potential and reactive oxygen species generation in mitochondria. *J. Biol. Chem.* 279, 39846-39855.

Datta, S.R., Dudek, H., Tao, X., Masters, S., Fu, H., Gotoh, Y., and Greenberg, M.E. (1997). Akt phosphorylation of BAD couples survival signals to the cell-intrinsic death machinery. *Cell* 91, 231-241.

Davis, R.J. (2000). Signal transduction by the JNK group of MAP kinases. *Cell* 103, 239-252.

DeBerardinis, R.J., and Cheng, T. (2010). Q's next: the diverse functions of glutamine in metabolism, cell biology and cancer. *Oncogene* 29, 313-324.

- Deberardinis, R.J., Sayed, N., Ditsworth, D., and Thompson, C.B. (2008). Brick by brick: metabolism and tumor cell growth. *Curr. Opin. Genet. Dev.* 18, 54-61.
- Debouck, C., and Goodfellow, P.N. (1999). DNA microarrays in drug discovery and development. *Nat. Genet.* 21, 48-50.
- Degli-Esposti, M. (1999). To die or not to die--the quest of the TRAIL receptors. *J. Leukoc. Biol.* 65, 535-542.
- DeRisi, J., Penland, L., Brown, P.O., Bittner, M.L., Meltzer, P.S., Ray, M., Chen, Y., Su, Y.A., and Trent, J.M. (1996). Use of a cDNA microarray to analyse gene expression patterns in human cancer. *Nat. Genet.* 14, 457-460.
- Desagher, S., Osen-Sand, A., Nichols, A., Eskes, R., Montessuit, S., Lauper, S., Maundrell, K., Antonsson, B., and Martinou, J.C. (1999). Bid-induced conformational change of Bax is responsible for mitochondrial cytochrome c release during apoptosis. *J. Cell Biol.* 144, 891-901.
- Devenish, R.J., Prescott, M., Boyle, G.M., and Nagley, P. (2000). The oligomycin axis of mitochondrial ATP synthase: OSCP and the proton channel. *J. Bioenerg. Biomembr.* 32, 507-515.
- Deveraux, Q.L., and Reed, J.C. (1999). IAP family proteins--suppressors of apoptosis. *Genes Dev.* 13, 239-252.
- Dickens, LS., Boyd, R., Robinson, GL., Jukes-Jones, R., Cain, K., MacFarlane, M. (2011). Stoichiometry of the TRAIL Death-Inducing Signalling Complex: Structural modelling and *in vitro* reconstitution reveal a new DISC model based on capase-8 chain formation. Under Review Molecular Cell
- Drakas, R., Prisco, M., and Baserga, R. (2005). A modified tandem affinity purification tag technique for the purification of protein complexes in mammalian cells. *Proteomics* 5, 132-137.
- Drexler, H.G., and MacLeod, R.A. (2002). Malignant hematopoietic cell lines: in vitro models for the study of mantle cell lymphoma. *Leuk. Res.* 26, 781-787.

- Duan, H., Orth, K., Chinnaiyan, A.M., Poirier, G.G., Froelich, C.J., He, W.W., and Dixit, V.M. (1996). ICE-LAP6, a novel member of the ICE/Ced-3 gene family, is activated by the cytotoxic T cell protease granzyme B. *J. Biol. Chem.* 271, 16720-16724.
- Duggan, D.J., Bittner, M., Chen, Y., Meltzer, P., and Trent, J.M. (1999). Expression profiling using cDNA microarrays. *Nat. Genet.* 21, 10-14.
- Dwarakanath, B.S. (2009). Cytotoxicity, radiosensitization, and chemosensitization of tumor cells by 2-deoxy-D-glucose in vitro. *J. Cancer. Res. Ther.* 5 *Suppl* 1, S27-31.
- Dyer, M.J., MacFarlane, M., and Cohen, G.M. (2007). Barriers to effective TRAIL-targeted therapy of malignancy. *J. Clin. Oncol.* 25, 4505-4506.
- Ea, C.K., Sun, L., Inoue, J., and Chen, Z.J. (2004). TIFA activates IkappaB kinase (IKK) by promoting oligomerization and ubiquitination of TRAF6. *Proc. Natl. Acad. Sci. U. S. A.* 101, 15318-15323.
- Edinger, A.L., and Thompson, C.B. (2002). Akt maintains cell size and survival by increasing mTOR-dependent nutrient uptake. *Mol. Biol. Cell* 13, 2276-2288.
- Eisen, M.B., Spellman, P.T., Brown, P.O., and Botstein, D. (1998). Cluster analysis and display of genome-wide expression patterns. *Proc. Natl. Acad. Sci. U. S. A.* 95, 14863-14868.
- El Mjiyad, N., Caro-Maldonado, A., Ramirez-Peinado, S., and Munoz-Pinedo, C. (2011). Sugar-free approaches to cancer cell killing. *Oncogene* 30, 253-264.
- Ellis, H.M., and Horvitz, H.R. (1986). Genetic control of programmed cell death in the nematode *C. elegans*. *Cell* 44, 817-829.
- Ellis, R.E., Yuan, J.Y., and Horvitz, H.R. (1991). Mechanisms and functions of cell death. *Annu. Rev. Cell Biol.* 7, 663-698.
- Emdad, L., Sarkar, D., Su, Z.Z., Lee, S.G., Kang, D.C., Bruce, J.N., Volsky, D.J., and Fisher, P.B. (2007). Astrocyte elevated gene-1: recent insights into a novel gene involved in tumor progression, metastasis and neurodegeneration. *Pharmacol. Ther.* 114, 155-170.

- Emdad, L., Sarkar, D., Su, Z.Z., Randolph, A., Boukerche, H., Valerie, K., and Fisher, P.B. (2006). Activation of the nuclear factor kappaB pathway by astrocyte elevated gene-1: implications for tumor progression and metastasis. *Cancer Res.* 66, 1509-1516.
- Emery, J.G., McDonnell, P., Burke, M.B., Deen, K.C., Lyn, S., Silverman, C., Dul, E., Appelbaum, E.R., Eichman, C., DiPrinzio, R., *et al.* (1998). Osteoprotegerin is a receptor for the cytotoxic ligand TRAIL. *J. Biol. Chem.* 273, 14363-14367.
- Erecinska, M., and Wilson, D.F. (1982). Regulation of cellular energy metabolism. *J. Membr. Biol.* 70, 1-14.
- Estrov, Z., Talpaz, M., Ku, S., Harris, D., Van, Q., Beran, M., Hirsch-Ginsberg, C., Huh, Y., Yee, G., and Kurzrock, R. (1998). Z-138: a new mature B-cell acute lymphoblastic leukemia cell line from a patient with transformed chronic lymphocytic leukemia. *Leuk. Res.* 22, 341-353.
- Fadok, V.A., Voelker, D.R., Campbell, P.A., Cohen, J.J., Bratton, D.L., and Henson, P.M. (1992). Exposure of phosphatidylserine on the surface of apoptotic lymphocytes triggers specific recognition and removal by macrophages. *J. Immunol.* 148, 2207-2216.
- Falschlehner, C., Emmerich, C.H., Gerlach, B., and Walczak, H. (2007). TRAIL signalling: decisions between life and death. *Int. J. Biochem. Cell Biol.* 39, 1462-1475.
- Falschlehner, C., Schaefer, U., and Walczak, H. (2009). Following TRAIL's path in the immune system. *Immunology* 127, 145-154.
- Fantin, V.R., St-Pierre, J., and Leder, P. (2006). Attenuation of LDH-A expression uncovers a link between glycolysis, mitochondrial physiology, and tumor maintenance. *Cancer. Cell.* 9, 425-434.
- Feig, C., and Peter, M.E. (2007). How apoptosis got the immune system in shape. *Eur. J. Immunol.* 37 Suppl 1, S61-70.
- Fenton, T.R., and Gout, I.T. (2011). Functions and regulation of the 70kDa ribosomal S6 kinases. *Int. J. Biochem. Cell Biol.* 43, 47-59.

- Fernandes-Alnemri, T., Armstrong, R.C., Krebs, J., Srinivasula, S.M., Wang, L., Bullrich, F., Fritz, L.C., Trapani, J.A., Tomaselli, K.J., Litwack, G., and Alnemri, E.S. (1996). In vitro activation of CPP32 and Mch3 by Mch4, a novel human apoptotic cysteine protease containing two FADD-like domains. *Proc. Natl. Acad. Sci. U. S. A.* 93, 7464-7469.
- Fernandes-Alnemri, T., Litwack, G., and Alnemri, E.S. (1995). Mch2, a new member of the apoptotic Ced-3/Ice cysteine protease gene family. *Cancer Res.* 55, 2737-2742.
- Fernandes-Alnemri, T., Litwack, G., and Alnemri, E.S. (1994). CPP32, a novel human apoptotic protein with homology to *Caenorhabditis elegans* cell death protein Ced-3 and mammalian interleukin-1 beta-converting enzyme. *J. Biol. Chem.* 269, 30761-30764.
- Feron, O. (2009). Pyruvate into lactate and back: from the Warburg effect to symbiotic energy fuel exchange in cancer cells. *Radiother. Oncol.* 92, 329-333.
- Ferrari, D., Stepczynska, A., Los, M., Wesselborg, S., and Schulze-Osthoff, K. (1998). Differential regulation and ATP requirement for caspase-8 and caspase-3 activation during CD95- and anticancer drug-induced apoptosis. *J. Exp. Med.* 188, 979-984.
- Fingrut, O., and Flescher, E. (2002). Plant stress hormones suppress the proliferation and induce apoptosis in human cancer cells. *Leukemia* 16, 608-616.
- Flescher, E. (2005). Jasmonates--a new family of anti-cancer agents. *Anticancer Drugs* 16, 911-916.
- Frezza, C., Tennant, D.A., and Gottlieb, E. (2010). IDH1 mutations in gliomas: when an enzyme loses its grip. *Cancer. Cell.* 17, 7-9.
- Frezza, C., Zheng, L., Tennant, D.A., Papkovsky, D.B., Hedley, B.A., Kalna, G., Watson, D.G., and Gottlieb, E. (2011). Metabolic profiling of hypoxic cells revealed a catabolic signature required for cell survival. *PLoS One* 6, e24411.
- Fricker, N., Beaudouin, J., Richter, P., Eils, R., Krammer, P.H., and Lavrik, I.N. (2010). Model-based dissection of CD95 signaling dynamics reveals both a pro- and antiapoptotic role of c-FLIPL. *J. Cell Biol.* 190, 377-389.

- Fuentes-Prior, P., and Salvesen, G.S. (2004). The protein structures that shape caspase activity, specificity, activation and inhibition. *Biochem. J.* 384, 201-232.
- Fulda, S., and Debatin, K.M. (2007). HIF-1-regulated glucose metabolism: a key to apoptosis resistance? *Cell. Cycle* 6, 790-792.
- Gagliardini, V., Fernandez, P.A., Lee, R.K., Drexler, H.C., Rotello, R.J., Fishman, M.C., and Yuan, J. (1994). Prevention of vertebrate neuronal death by the crmA gene. *Science* 263, 826-828.
- Gambhir, S.S. (2002). Molecular imaging of cancer with positron emission tomography. *Nat. Rev. Cancer.* 2, 683-693.
- Gatenby, R.A., and Gillies, R.J. (2004). Why do cancers have high aerobic glycolysis? *Nat. Rev. Cancer.* 4, 891-899.
- Gatter, K.C., Brown, G., Trowbridge, I.S., Woolston, R.E., and Mason, D.Y. (1983). Transferrin receptors in human tissues: their distribution and possible clinical relevance. *J. Clin. Pathol.* 36, 539-545.
- Georgakis, G.V., Li, Y., Humphreys, R., Andreeff, M., O'Brien, S., Younes, M., Carbone, A., Albert, V., and Younes, A. (2005). Activity of selective fully human agonistic antibodies to the TRAIL death receptors TRAIL-R1 and TRAIL-R2 in primary and cultured lymphoma cells: induction of apoptosis and enhancement of doxorubicin- and bortezomib-induced cell death. *Br. J. Haematol.* 130, 501-510.
- Ghosh, S., and Karin, M. (2002). Missing pieces in the NF-kappaB puzzle. *Cell* 109 *Suppl*, S81-96.
- Gibson, E.M., Henson, E.S., Villanueva, J., and Gibson, S.B. (2002). MEK kinase 1 induces mitochondrial permeability transition leading to apoptosis independent of cytochrome c release. *J. Biol. Chem.* 277, 10573-10580.
- Gillissen, B., Wendt, J., Richter, A., Richter, A., Muer, A., Overkamp, T., Gebhardt, N., Preissner, R., Belka, C., Dorken, B., and Daniel, P.T. (2010). Endogenous Bak inhibitors Mcl-1 and Bcl-xL: differential impact on TRAIL resistance in Bax-deficient carcinoma. *J. Cell Biol.* 188, 851-862.

- Goldin, N., Arzoin, L., Heyfets, A., Israelson, A., Zaslavsky, Z., Bravman, T., Bronner, V., Notcovich, A., Shoshan-Barmatz, V., and Flescher, E. (2008). Methyl jasmonate binds to and detaches mitochondria-bound hexokinase. *Oncogene* 27, 4636-4643.
- Gonzalez, F., and Ashkenazi, A. (2010). New insights into apoptosis signaling by Apo2L/TRAIL. *Oncogene* 29, 4752-4765.
- Gonzalez, F., and Gottlieb, E. (2007). Cardiolipin: setting the beat of apoptosis. *Apoptosis* 12, 877-885.
- Gonzalez, F., Schug, Z.T., Houtkooper, R.H., MacKenzie, E.D., Brooks, D.G., Wanders, R.J., Petit, P.X., Vaz, F.M., and Gottlieb, E. (2008). Cardiolipin provides an essential activating platform for caspase-8 on mitochondria. *J. Cell Biol.* 183, 681-696.
- Gottlieb, E., Armour, S.M., Harris, M.H., and Thompson, C.B. (2003). Mitochondrial membrane potential regulates matrix configuration and cytochrome c release during apoptosis. *Cell Death Differ.* 10, 709-717.
- Gottlob, K., Majewski, N., Kennedy, S., Kandel, E., Robey, R.B., and Hay, N. (2001). Inhibition of early apoptotic events by Akt/PKB is dependent on the first committed step of glycolysis and mitochondrial hexokinase. *Genes Dev.* 15, 1406-1418.
- Gough, D.J., Corlett, A., Schlessinger, K., Wegrzyn, J., Lerner, A.C., and Levy, D.E. (2009). Mitochondrial STAT3 supports Ras-dependent oncogenic transformation. *Science* 324, 1713-1716.
- Goy, A., and Kahl, B. (2010). Mantle cell lymphoma: The promise of new treatment options. *Crit. Rev. Oncol. Hematol.*
- Greig, K.T., Antonchuk, J., Metcalf, D., Morgan, P.O., Krebs, D.L., Zhang, J.G., Hacking, D.F., Bode, L., Robb, L., Kranz, C., *et al.* (2007). Agm1/Pgm3-mediated sugar nucleotide synthesis is essential for hematopoiesis and development. *Mol. Cell. Biol.* 27, 5849-5859.
- Gupta, V., and Bamezai, R.N. (2010). Human pyruvate kinase M2: a multifunctional protein. *Protein Sci.* 19, 2031-2044.
- Gyrd-Hansen, M., and Meier, P. (2010). IAPs: from caspase inhibitors to modulators of NF-kappaB, inflammation and cancer. *Nat. Rev. Cancer.* 10, 561-574.

- Haas, T.L., Emmerich, C.H., Gerlach, B., Schmukle, A.C., Cordier, S.M., Rieser, E., Feltham, R., Vince, J., Warnken, U., Wenger, T., *et al.* (2009). Recruitment of the linear ubiquitin chain assembly complex stabilizes the TNF-R1 signaling complex and is required for TNF-mediated gene induction. *Mol. Cell* 36, 831-844.
- Hackenbrock, C.R. (1966). Ultrastructural bases for metabolically linked mechanical activity in mitochondria. I. Reversible ultrastructural changes with change in metabolic steady state in isolated liver mitochondria. *J. Cell Biol.* 30, 269-297.
- Hale, A.J., Smith, C.A., Sutherland, L.C., Stoneman, V.E., Longthorne, V., Culhane, A.C., and Williams, G.T. (1996). Apoptosis: molecular regulation of cell death. *Eur. J. Biochem.* 237, 884.
- Halicka, H.D., Ardelt, B., Li, X., Melamed, M.M., and Darzynkiewicz, Z. (1995). 2-Deoxy-D-glucose enhances sensitivity of human histiocytic lymphoma U937 cells to apoptosis induced by tumor necrosis factor. *Cancer Res.* 55, 444-449.
- Hames, D and Hooper, N. (2005). *Biochemistry* (New York: Taylor and Francis).
- Hanahan, D., and Weinberg, R.A. (2000). The hallmarks of cancer. *Cell* 100, 57-70.
- Hao, C., Song, J.H., Hsi, B., Lewis, J., Song, D.K., Petruk, K.C., Tyrrell, D.L., and Kneteman, N.M. (2004). TRAIL inhibits tumor growth but is nontoxic to human hepatocytes in chimeric mice. *Cancer Res.* 64, 8502-8506.
- Hardie, D.G. (2011). Signal transduction: How cells sense energy. *Nature* 472, 176-177.
- Harper, N., Farrow, S.N., Kaptein, A., Cohen, G.M., and MacFarlane, M. (2001). Modulation of tumor necrosis factor apoptosis-inducing ligand- induced NF-kappa B activation by inhibition of apical caspases. *J. Biol. Chem.* 276, 34743-34752.
- Harper, N., and MacFarlane, M. (2008). Recombinant TRAIL and TRAIL receptor analysis. *Methods Enzymol.* 446, 293-313.
- Hartl, P., Gottesfeld, J., and Forbes, D.J. (1993). Mitotic repression of transcription in vitro. *J. Cell Biol.* 120, 613-624.

- Hawkins, R.A., and Phelps, M.E. (1988). PET in clinical oncology. *Cancer Metastasis Rev.* 7, 119-142.
- Heiskanen, K.M., Bhat, M.B., Wang, H.W., Ma, J., and Nieminen, A.L. (1999). Mitochondrial depolarization accompanies cytochrome c release during apoptosis in PC6 cells. *J. Biol. Chem.* 274, 5654-5658.
- Heller, R.A., Schena, M., Chai, A., Shalon, D., Bedilion, T., Gilmore, J., Woolley, D.E., and Davis, R.W. (1997). Discovery and analysis of inflammatory disease-related genes using cDNA microarrays. *Proc. Natl. Acad. Sci. U. S. A.* 94, 2150-2155.
- Hirawake, H., Wang, H., Kuramochi, T., Kojima, S., and Kita, K. (1994). Human complex II (succinate-ubiquinone oxidoreductase): cDNA cloning of the flavoprotein (Fp) subunit of liver mitochondria. *J. Biochem.* 116, 221-227.
- Hitosugi, T., Kang, S., Vander Heiden, M.G., Chung, T.W., Elf, S., Lythgoe, K., Dong, S., Lonial, S., Wang, X., Chen, G.Z., *et al.* (2009). Tyrosine phosphorylation inhibits PKM2 to promote the Warburg effect and tumor growth. *Sci. Signal.* 2, ra73.
- Hopkins-Donaldson, S., Bodmer, J.L., Bours, K.B., Brognara, C.B., Tschopp, J., and Gross, N. (2000). Loss of caspase-8 expression in highly malignant human neuroblastoma cells correlates with resistance to tumor necrosis factor-related apoptosis-inducing ligand-induced apoptosis. *Cancer Res.* 60, 4315-4319.
- Hossler, P., Khattak, S.F., and Li, Z.J. (2009). Optimal and consistent protein glycosylation in mammalian cell culture. *Glycobiology* 19, 936-949.
- Hsu, H., Huang, J., Shu, H.B., Baichwal, V., and Goeddel, D.V. (1996). TNF-dependent recruitment of the protein kinase RIP to the TNF receptor-1 signaling complex. *Immunity* 4, 387-396.
- Hsu, H., Shu, H.B., Pan, M.G., and Goeddel, D.V. (1996). TRADD-TRAF2 and TRADD-FADD interactions define two distinct TNF receptor 1 signal transduction pathways. *Cell* 84, 299-308.
- Hughes, M.A., Harper, N., Butterworth, M., Cain, K., Cohen, G.M., and MacFarlane, M. (2009). Reconstitution of the death-inducing signaling complex reveals a substrate switch that determines CD95-mediated death or survival. *Mol. Cell* 35, 265-279.

- Huttemann, M., Pecina, P., Rainbolt, M., Sanderson, T.H., Kagan, V.E., Samavati, L., Doan, J.W., and Lee, I. (2011). The multiple functions of cytochrome c and their regulation in life and death decisions of the mammalian cell: From respiration to apoptosis. *Mitochondrion* 11, 369-381.
- Imai, Y., Kimura, T., Murakami, A., Yajima, N., Sakamaki, K., and Yonehara, S. (1999). The CED-4-homologous protein FLASH is involved in Fas-mediated activation of caspase-8 during apoptosis. *Nature* 398, 777-785.
- Ip, Y.T., and Davis, R.J. (1998). Signal transduction by the c-Jun N-terminal kinase (JNK)--from inflammation to development. *Curr. Opin. Cell Biol.* 10, 205-219.
- Israel, M., and Schwartz, L. (2011). The metabolic advantage of tumor cells. *Mol. Cancer.* 10, 70.
- Izumi, H., Torigoe, T., Ishiguchi, H., Uramoto, H., Yoshida, Y., Tanabe, M., Ise, T., Murakami, T., Yoshida, T., Nomoto, M., and Kohno, K. (2003). Cellular pH regulators: potentially promising molecular targets for cancer chemotherapy. *Cancer Treat. Rev.* 29, 541-549.
- Jain, V.K., Kalia, V.K., Sharma, R., Maharajan, V., and Menon, M. (1985). Effects of 2-deoxy-D-glucose on glycolysis, proliferation kinetics and radiation response of human cancer cells. *Int. J. Radiat. Oncol. Biol. Phys.* 11, 943-950.
- Jares, P., Colomer, D., and Campo, E. (2007). Genetic and molecular pathogenesis of mantle cell lymphoma: perspectives for new targeted therapeutics. *Nat. Rev. Cancer.* 7, 750-762.
- Jeffers, J.R., Parganas, E., Lee, Y., Yang, C., Wang, J., Brennan, J., MacLean, K.H., Han, J., Chittenden, T., Ihle, J.N., *et al.* (2003). Puma is an essential mediator of p53-dependent and -independent apoptotic pathways. *Cancer. Cell.* 4, 321-328.
- Jemal, A., Bray, F., Center, M.M., Ferlay, J., Ward, E., and Forman, D. (2011). Global cancer statistics. *CA Cancer. J. Clin.* 61, 69-90.
- Jiang, L., Luo, X., Shi, J., Sun, H., Sun, Q., Sheikh, M.S., and Huang, Y. (2011). PDRG1, a novel tumor marker for multiple malignancies that is selectively regulated by genotoxic stress. *Cancer. Biol. Ther.* 11, 567-573.

- Jin, Z., Li, Y., Pitti, R., Lawrence, D., Pham, V.C., Lill, J.R., and Ashkenazi, A. (2009). Cullin3-based polyubiquitination and p62-dependent aggregation of caspase-8 mediate extrinsic apoptosis signaling. *Cell* 137, 721-735.
- Johannes, G., and Sarnow, P. (1998). Cap-independent polysomal association of natural mRNAs encoding c-myc, BiP, and eIF4G conferred by internal ribosome entry sites. *RNA* 4, 1500-1513.
- Jones, D.T., Trowbridge, I.S., and Harris, A.L. (2006). Effects of transferrin receptor blockade on cancer cell proliferation and hypoxia-inducible factor function and their differential regulation by ascorbate. *Cancer Res.* 66, 2749-2756.
- Jones, R.G., Plas, D.R., Kubek, S., Buzzai, M., Mu, J., Xu, Y., Birnbaum, M.J., and Thompson, C.B. (2005). AMP-activated protein kinase induces a p53-dependent metabolic checkpoint. *Mol. Cell* 18, 283-293.
- Jones, R.G., and Thompson, C.B. (2009). Tumor suppressors and cell metabolism: a recipe for cancer growth. *Genes Dev.* 23, 537-548.
- Jonscher, K. (2005). Validating sequence assignments for peptide fragmentation patterns: A primer in ms/ms sequence identification. *Proteome Software*
- Kanamori, M., Suzuki, H., Saito, R., Muramatsu, M., and Hayashizaki, Y. (2002). T2BP, a novel TRAF2 binding protein, can activate NF-kappaB and AP-1 without TNF stimulation. *Biochem. Biophys. Res. Commun.* 290, 1108-1113.
- Kang, H.T., and Hwang, E.S. (2006). 2-Deoxyglucose: an anticancer and antiviral therapeutic, but not any more a low glucose mimetic. *Life Sci.* 78, 1392-1399.
- Kaplan, O., Navon, G., Lyon, R.C., Faustino, P.J., Straka, E.J., and Cohen, J.S. (1990). Effects of 2-deoxyglucose on drug-sensitive and drug-resistant human breast cancer cells: toxicity and magnetic resonance spectroscopy studies of metabolism. *Cancer Res.* 50, 544-551.
- Karin, M. (2006). Nuclear factor-kappaB in cancer development and progression. *Nature* 441, 431-436.
- Karin, M., Cao, Y., Greten, F.R., and Li, Z.W. (2002). NF-kappaB in cancer: from innocent bystander to major culprit. *Nat. Rev. Cancer.* 2, 301-310.

- Kasibhatla, S., Jessen, K.A., Maliartchouk, S., Wang, J.Y., English, N.M., Drewe, J., Qiu, L., Archer, S.P., Ponce, A.E., Sirisoma, N., *et al.* (2005). A role for transferrin receptor in triggering apoptosis when targeted with gambogic acid. *Proc. Natl. Acad. Sci. U. S. A.* *102*, 12095-12100.
- Kaufmann, S.H., and Earnshaw, W.C. (2000). Induction of apoptosis by cancer chemotherapy. *Exp. Cell Res.* *256*, 42-49.
- Kennedy, K.M., and Dewhirst, M.W. (2010). Tumor metabolism of lactate: the influence and therapeutic potential for MCT and CD147 regulation. *Future Oncol.* *6*, 127-148.
- Kern, K.A., and Norton, J.A. (1987). Inhibition of established rat fibrosarcoma growth by the glucose antagonist 2-deoxy-D-glucose. *Surgery* *102*, 380-385.
- Kerr, J.F., Wyllie, A.H., and Currie, A.R. (1972). Apoptosis: a basic biological phenomenon with wide-ranging implications in tissue kinetics. *Br. J. Cancer* *26*, 239-257.
- Kim, J., Gardner, L., Dang, C. (2005). Oncogenic alterations of metabolism and the warburg effect. *Drug Discovery Today* *2*,
- Kimberley, F.C., and Screaton, G.R. (2004). Following a TRAIL: update on a ligand and its five receptors. *Cell Res.* *14*, 359-372.
- Kimble, J., and Hirsh, D. (1979). The postembryonic cell lineages of the hermaphrodite and male gonads in *Caenorhabditis elegans*. *Dev. Biol.* *70*, 396-417.
- King, D., Pringle, J.H., Hutchinson, M., and Cohen, G.M. (1998). Processing/activation of caspases, -3 and -7 and -8 but not caspase-2, in the induction of apoptosis in B-chronic lymphocytic leukemia cells. *Leukemia* *12*, 1553-1560.
- Kischkel, F.C., Hellbardt, S., Behrmann, I., Germer, M., Pawlita, M., Krammer, P.H., and Peter, M.E. (1995). Cytotoxicity-dependent APO-1 (Fas/CD95)-associated proteins form a death-inducing signaling complex (DISC) with the receptor. *EMBO J.* *14*, 5579-5588.
- Kischkel, F.C., Lawrence, D.A., Chuntharapai, A., Schow, P., Kim, K.J., and Ashkenazi, A. (2000). Apo2L/TRAIL-dependent recruitment of endogenous FADD and caspase-8 to death receptors 4 and 5. *Immunity* *12*, 611-620.

- Kischkel, F.C., Lawrence, D.A., Tinel, A., LeBlanc, H., Virmani, A., Schow, P., Gazdar, A., Blenis, J., Arnott, D., and Ashkenazi, A. (2001). Death receptor recruitment of endogenous caspase-10 and apoptosis initiation in the absence of caspase-8. *J. Biol. Chem.* 276, 46639-46646.
- Ko, Y.H., Pedersen, P.L., and Geschwind, J.F. (2001). Glucose catabolism in the rabbit VX2 tumor model for liver cancer: characterization and targeting hexokinase. *Cancer Lett.* 173, 83-91.
- Kohlhaas, S.L., Craxton, A., Sun, X.M., Pinkoski, M.J., and Cohen, G.M. (2007). Receptor-mediated endocytosis is not required for tumor necrosis factor-related apoptosis-inducing ligand (TRAIL)-induced apoptosis. *J. Biol. Chem.* 282, 12831-12841.
- Kondoh, H., Lleontart, M.E., Gil, J., Wang, J., Degan, P., Peters, G., Martinez, D., Carnero, A., and Beach, D. (2005). Glycolytic enzymes can modulate cellular life span. *Cancer Res.* 65, 177-185.
- Kondoh, N., Wakatsuki, T., Ryo, A., Hada, A., Aihara, T., Horiuchi, S., Goseki, N., Matsubara, O., Takenaka, K., Shichita, M., *et al.* (1999). Identification and characterization of genes associated with human hepatocellular carcinogenesis. *Cancer Res.* 59, 4990-4996.
- Koonin, E.V., Aravind, L., Hofmann, K., Tschopp, J., and Dixit, V.M. (1999). Apoptosis. Searching for FLASH domains. *Nature* 401, 662; discussion 662-3.
- Krueger, A., Schmitz, I., Baumann, S., Krammer, P.H., and Kirchhoff, S. (2001). Cellular FLICE-inhibitory protein splice variants inhibit different steps of caspase-8 activation at the CD95 death-inducing signaling complex. *J. Biol. Chem.* 276, 20633-20640.
- Kumar, S. (1997). The apoptotic cysteine protease CPP32. *Int. J. Biochem. Cell Biol.* 29, 393-396.
- Kuo, M., Zilberfarb, V., Gangneux, N., Christeff, N., and Issad, T. (2008). O-glycosylation of FoxO1 increases its transcriptional activity towards the glucose 6-phosphatase gene. *FEBS Lett.* 582, 829-834.

- Kurtoglu, M., Gao, N., Shang, J., Maher, J.C., Lehrman, M.A., Wangpaichitr, M., Savaraj, N., Lane, A.N., and Lampidis, T.J. (2007). Under normoxia, 2-deoxy-D-glucose elicits cell death in select tumor types not by inhibition of glycolysis but by interfering with N-linked glycosylation. *Mol. Cancer. Ther.* 6, 3049-3058.
- Lacronique, V., Mignon, A., Fabre, M., Viollet, B., Rouquet, N., Molina, T., Porteu, A., Henrion, A., Bouscary, D., Varlet, P., Joulin, V., and Kahn, A. (1996). Bcl-2 protects from lethal hepatic apoptosis induced by an anti-Fas antibody in mice. *Nat. Med.* 2, 80-86.
- Lamkanfi, M., and Kanneganti, T.D. (2010). Caspase-7: a protease involved in apoptosis and inflammation. *Int. J. Biochem. Cell Biol.* 42, 21-24.
- Lanquar, V., Lelievre, F., Bolte, S., Hames, C., Alcon, C., Neumann, D., Vansuyt, G., Curie, C., Schroder, A., Kramer, U., Barbier-Brygoo, H., and Thomine, S. (2005). Mobilization of vacuolar iron by AtNRAMP3 and AtNRAMP4 is essential for seed germination on low iron. *EMBO J.* 24, 4041-4051.
- Lapointe, J., Li, C., Higgins, J.P., van de Rijn, M., Bair, E., Montgomery, K., Ferrari, M., Egevad, L., Rayford, W., Bergerheim, U., *et al.* (2004). Gene expression profiling identifies clinically relevant subtypes of prostate cancer. *Proc. Natl. Acad. Sci. U. S. A.* 101, 811-816.
- Lavrik, I.N., Golks, A., Baumann, S., and Krammer, P.H. (2006). Caspase-2 is activated at the CD95 death-inducing signaling complex in the course of CD95-induced apoptosis. *Blood* 108, 559-565.
- Lavrik, I.N., Mock, T., Golks, A., Hoffmann, J.C., Baumann, S., and Krammer, P.H. (2008). CD95 stimulation results in the formation of a novel death effector domain protein-containing complex. *J. Biol. Chem.* 283, 26401-26408.
- Lawrence, D., Shahrokh, Z., Marsters, S., Achilles, K., Shih, D., Mounho, B., Hillan, K., Totpal, K., DeForge, L., Schow, P., *et al.* (2001). Differential hepatocyte toxicity of recombinant Apo2L/TRAIL versions. *Nat. Med.* 7, 383-385.
- Le, A., Cooper, C.R., Gouw, A.M., Dinavahi, R., Maitra, A., Deck, L.M., Royer, R.E., Vander Jagt, D.L., Semenza, G.L., and Dang, C.V. (2010). Inhibition of lactate dehydrogenase A induces oxidative stress and inhibits tumor progression. *Proc. Natl. Acad. Sci. U. S. A.* 107, 2037-2042.

- Lee, F.S., Hagler, J., Chen, Z.J., and Maniatis, T. (1997). Activation of the IkappaB alpha kinase complex by MEKK1, a kinase of the JNK pathway. *Cell* 88, 213-222.
- Lee, Y.H., Giraud, J., Davis, R.J., and White, M.F. (2003). c-Jun N-terminal kinase (JNK) mediates feedback inhibition of the insulin signaling cascade. *J. Biol. Chem.* 278, 2896-2902.
- Leist, M., Single, B., Castoldi, A.F., Kuhnle, S., and Nicotera, P. (1997). Intracellular adenosine triphosphate (ATP) concentration: a switch in the decision between apoptosis and necrosis. *J. Exp. Med.* 185, 1481-1486.
- Lettre, G., and Hengartner, M.O. (2006). Developmental apoptosis in *C. elegans*: a complex CEDnario. *Nat. Rev. Mol. Cell Biol.* 7, 97-108.
- Li, H., Zhu, H., Xu, C.J., and Yuan, J. (1998). Cleavage of BID by caspase 8 mediates the mitochondrial damage in the Fas pathway of apoptosis. *Cell* 94, 491-501.
- Li, Y.C., Tzeng, C.C., Song, J.H., Tsia, F.J., Hsieh, L.J., Liao, S.J., Tsai, C.H., Van Meir, E.G., Hao, C., and Lin, C.C. (2006). Genomic alterations in human malignant glioma cells associate with the cell resistance to the combination treatment with tumor necrosis factor-related apoptosis-inducing ligand and chemotherapy. *Clin. Cancer Res.* 12, 2716-2729.
- Lippke, J.A., Gu, Y., Sarnecki, C., Caron, P.R., and Su, M.S. (1996). Identification and characterization of CPP32/Mch2 homolog 1, a novel cysteine protease similar to CPP32. *J. Biol. Chem.* 271, 1825-1828.
- Liu, H., Jiang, C.C., Lavis, C.J., Croft, A., Dong, L., Tseng, H.Y., Yang, F., Tay, K.H., Hersey, P., and Zhang, X.D. (2009). 2-Deoxy-D-glucose enhances TRAIL-induced apoptosis in human melanoma cells through XBP-1-mediated up-regulation of TRAIL-R2. *Mol. Cancer.* 8, 122.
- Liu, H., Jiang, C.C., Lavis, C.J., Croft, A., Dong, L., Tseng, H.Y., Yang, F., Tay, K.H., Hersey, P., and Zhang, X.D. (2009). 2-Deoxy-D-glucose enhances TRAIL-induced apoptosis in human melanoma cells through XBP-1-mediated up-regulation of TRAIL-R2. *Mol. Cancer.* 8, 122.
- Liu, P., Cheng, H., Roberts, T.M., and Zhao, J.J. (2009). Targeting the phosphoinositide 3-kinase pathway in cancer. *Nat. Rev. Drug Discov.* 8, 627-644.

- Lockhart, D.J., and Winzeler, E.A. (2000). Genomics, gene expression and DNA arrays. *Nature* 405, 827-836.
- Locksley, R.M., Killeen, N., and Lenardo, M.J. (2001). The TNF and TNF receptor superfamilies: integrating mammalian biology. *Cell* 104, 487-501.
- LoPiccolo, J., Blumenthal, G.M., Bernstein, W.B., and Dennis, P.A. (2008). Targeting the PI3K/Akt/mTOR pathway: effective combinations and clinical considerations. *Drug Resist Updat* 11, 32-50.
- Lozano, G., and Zambetti, G.P. (2005). What have animal models taught us about the p53 pathway? *J. Pathol.* 205, 206-220.
- Lu, C.W., Lin, S.C., Chen, K.F., Lai, Y.Y., and Tsai, S.J. (2008). Induction of pyruvate dehydrogenase kinase-3 by hypoxia-inducible factor-1 promotes metabolic switch and drug resistance. *J. Biol. Chem.* 283, 28106-28114.
- Luo, X., Budihardjo, I., Zou, H., Slaughter, C., and Wang, X. (1998). Bid, a Bcl2 interacting protein, mediates cytochrome c release from mitochondria in response to activation of cell surface death receptors. *Cell* 94, 481-490.
- Luo, X., Huang, Y., and Sheikh, M.S. (2003). Cloning and characterization of a novel gene PDRG that is differentially regulated by p53 and ultraviolet radiation. *Oncogene* 22, 7247-7257.
- MacFarlane, M. (2003). TRAIL-induced signalling and apoptosis. *Toxicol. Lett.* 139, 89-97.
- MacFarlane, M., Ahmad, M., Srinivasula, S.M., Fernandes-Alnemri, T., Cohen, G.M., and Alnemri, E.S. (1997). Identification and molecular cloning of two novel receptors for the cytotoxic ligand TRAIL. *J. Biol. Chem.* 272, 25417-25420.
- MacFarlane, M., Harper, N., Snowden, R.T., Dyer, M.J., Barnett, G.A., Pringle, J.H., and Cohen, G.M. (2002). Mechanisms of resistance to TRAIL-induced apoptosis in primary B cell chronic lymphocytic leukaemia. *Oncogene* 21, 6809-6818.
- MacFarlane, M., Kohlhaas, S.L., Sutcliffe, M.J., Dyer, M.J., and Cohen, G.M. (2005). TRAIL receptor-selective mutants signal to apoptosis via TRAIL-R1 in primary lymphoid malignancies. *Cancer Res.* 65, 11265-11270.

- Macheda, M.L., Rogers, S., and Best, J.D. (2005). Molecular and cellular regulation of glucose transporter (GLUT) proteins in cancer. *J. Cell. Physiol.* 202, 654-662.
- Majewski, N., Nogueira, V., Bhaskar, P., Coy, P.E., Skeen, J.E., Gottlob, K., Chandel, N.S., Thompson, C.B., Robey, R.B., and Hay, N. (2004). Hexokinase-mitochondria interaction mediated by Akt is required to inhibit apoptosis in the presence or absence of Bax and Bak. *Mol. Cell* 16, 819-830.
- Majewski, N., Nogueira, V., Robey, R.B., and Hay, N. (2004). Akt inhibits apoptosis downstream of BID cleavage via a glucose-dependent mechanism involving mitochondrial hexokinases. *Mol. Cell. Biol.* 24, 730-740.
- Manning, B.D., and Cantley, L.C. (2007). AKT/PKB signaling: navigating downstream. *Cell* 129, 1261-1274.
- Marino, K., Bones, J., Kattla, J.J., and Rudd, P.M. (2010). A systematic approach to protein glycosylation analysis: a path through the maze. *Nat. Chem. Biol.* 6, 713-723.
- Marsters, S.A., Sheridan, J.P., Donahue, C.J., Pitti, R.M., Gray, C.L., Goddard, A.D., Bauer, K.D., and Ashkenazi, A. (1996). Apo-3, a new member of the tumor necrosis factor receptor family, contains a death domain and activates apoptosis and NF-kappa B. *Curr. Biol.* 6, 1669-1676.
- Martin, S.J., Finucane, D.M., Amarante-Mendes, G.P., O'Brien, G.A., and Green, D.R. (1996). Phosphatidylserine externalization during CD95-induced apoptosis of cells and cytoplasts requires ICE/CED-3 protease activity. *J. Biol. Chem.* 271, 28753-28756.
- Martins, L.M., Iaccarino, I., Tenev, T., Gschmeissner, S., Totty, N.F., Lemoine, N.R., Savopoulos, J., Gray, C.W., Creasy, C.L., Dingwall, C., and Downward, J. (2002). The serine protease Omi/HtrA2 regulates apoptosis by binding XIAP through a reaper-like motif. *J. Biol. Chem.* 277, 439-444.
- Marx, J. (2000). Tumor angiogenesis. Gene expression patterns identified. *Science* 289, 1121-1122.
- Mates, J.M., Segura, J.A., Alonso, F.J., and Marquez, J. (2006). Pathways from glutamine to apoptosis. *Front. Biosci.* 11, 3164-3180.

- Mathupala, S.P., Ko, Y.H., and Pedersen, P.L. (2009). Hexokinase-2 bound to mitochondria: cancer's stygian link to the "Warburg Effect" and a pivotal target for effective therapy. *Semin. Cancer Biol.* 19, 17-24.
- Matoba, S., Kang, J.G., Patino, W.D., Wragg, A., Boehm, M., Gavrilova, O., Hurley, P.J., Bunz, F., and Hwang, P.M. (2006). P53 Regulates Mitochondrial Respiration. *Science* 312, 1650-1653.
- Mauro, C., Leow, S., Anso, E et al. (2011). NFkB controls energy homeostasis and metabolic adaptation by upregulating mitochondrial respiration. *Nature Cell Biology*
- Medeiros, L.J., Estrov, Z., and Rassidakis, G.Z. (2006). Z-138 cell line was derived from a patient with blastoid variant mantle cell lymphoma. *Leuk. Res.* 30, 497-501.
- Medema, J.P., Scaffidi, C., Kischkel, F.C., Shevchenko, A., Mann, M., Krammer, P.H., and Peter, M.E. (1997). FLICE is activated by association with the CD95 death-inducing signaling complex (DISC). *EMBO J.* 16, 2794-2804.
- Medina, R.A., and Owen, G.I. (2002). Glucose transporters: expression, regulation and cancer. *Biol. Res.* 35, 9-26.
- Melamed, D., and Arava, Y. (2007). Genome-wide analysis of mRNA polysomal profiles with spotted DNA microarrays. *Methods Enzymol.* 431, 177-201.
- Micheau, O. (2003). Cellular FLICE-inhibitory protein: an attractive therapeutic target? *Expert Opin. Ther. Targets* 7, 559-573.
- Micheau, O., and Tschopp, J. (2003). Induction of TNF receptor I-mediated apoptosis via two sequential signaling complexes. *Cell* 114, 181-190.
- Miyazaki, T., and Reed, J.C. (2001). A GTP-binding adapter protein couples TRAIL receptors to apoptosis-inducing proteins. *Nat. Immunol.* 2, 493-500.
- Moreno-Aliaga, M.J., Marti, A., Garcia-Foncillas, J., and Alfredo Martinez, J. (2001). DNA hybridization arrays: a powerful technology for nutritional and obesity research. *Br. J. Nutr.* 86, 119-122.
- Munoz-Pinedo, C., Ruiz-Ruiz, C., Ruiz de Almodovar, C., Palacios, C., and Lopez-Rivas, A. (2003). Inhibition of glucose metabolism sensitizes tumor cells to death

receptor-triggered apoptosis through enhancement of death-inducing signaling complex formation and apical procaspase-8 processing. *J. Biol. Chem.* 278, 12759-12768.

Munoz-Pinedo, C., Ruiz-Ruiz, C., Ruiz de Almodovar, C., Palacios, C., and Lopez-Rivas, A. (2003). Inhibition of glucose metabolism sensitizes tumor cells to death receptor-triggered apoptosis through enhancement of death-inducing signaling complex formation and apical procaspase-8 processing. *J. Biol. Chem.* 278, 12759-12768.

Muppidi, J.R., Tschopp, J., and Siegel, R.M. (2004). Life and death decisions: secondary complexes and lipid rafts in TNF receptor family signal transduction. *Immunity* 21, 461-465.

Muzio, M., Chinnaiyan, A.M., Kischkel, F.C., O'Rourke, K., Shevchenko, A., Ni, J., Scaffidi, C., Bretz, J.D., Zhang, M., Gentz, R., *et al.* (1996). FLICE, a novel FADD-homologous ICE/CED-3-like protease, is recruited to the CD95 (Fas/APO-1) death-inducing signaling complex. *Cell* 85, 817-827.

Nagata, S. (2000). Steering anti-cancer drugs away from the TRAIL. *Nat. Med.* 6, 502-503.

Nakano, K., and Vousden, K.H. (2001). PUMA, a novel proapoptotic gene, is induced by p53. *Mol. Cell* 7, 683-694.

Nam, S.Y., Amoscato, A.A., and Lee, Y.J. (2002). Low glucose-enhanced TRAIL cytotoxicity is mediated through the ceramide-Akt-FLIP pathway. *Oncogene* 21, 337-346.

Newsholme, E.A., Crabtree, B., and Ardawi, M.S. (1985). The role of high rates of glycolysis and glutamine utilization in rapidly dividing cells. *Biosci. Rep.* 5, 393-400.

Nicholson, D.W., Ali, A., Thornberry, N.A., Vaillancourt, J.P., Ding, C.K., Gallant, M., Gareau, Y., Griffin, P.R., Labelle, M., and Lazebnik, Y.A. (1995). Identification and inhibition of the ICE/CED-3 protease necessary for mammalian apoptosis. *Nature* 376, 37-43.

Norbury, C.J., and Zivnotovsky, B. (2004). DNA damage-induced apoptosis. *Oncogene* 23, 2797-2808.

- Oda, E., Ohki, R., Murasawa, H., Nemoto, J., Shibue, T., Yamashita, T., Tokino, T., Taniguchi, T., and Tanaka, N. (2000). Noxa, a BH3-only member of the Bcl-2 family and candidate mediator of p53-induced apoptosis. *Science* 288, 1053-1058.
- Oehler, R., and Roth, E. (2003). Regulative capacity of glutamine. *Curr. Opin. Clin. Nutr. Metab. Care* 6, 277-282.
- Ogawara, Y., Kishishita, S., Obata, T., Isazawa, Y., Suzuki, T., Tanaka, K., Masuyama, N., and Gotoh, Y. (2002). Akt enhances Mdm2-mediated ubiquitination and degradation of p53. *J. Biol. Chem.* 277, 21843-21850.
- Ogura, M. (2010). Current treatment strategy and new agents in mantle cell lymphoma. *Int. J. Hematol.* 92, 25-32.
- Oltersdorf, T., Elmore, S.W., Shoemaker, A.R., Armstrong, R.C., Augeri, D.J., Belli, B.A., Bruncko, M., Deckwerth, T.L., Dinges, J., Hajduk, P.J., *et al.* (2005). An inhibitor of Bcl-2 family proteins induces regression of solid tumours. *Nature* 435, 677-681.
- Pan, G., O'Rourke, K., Chinnaiyan, A.M., Gentz, R., Ebner, R., Ni, J., and Dixit, V.M. (1997). The receptor for the cytotoxic ligand TRAIL. *Science* 276, 111-113.
- Pang, H., Koda, Y., Soejima, M., and Kimura, H. (2002). Identification of human phosphoglucomutase 3 (PGM3) as N-acetylglucosamine-phosphate mutase (AGM1). *Ann. Hum. Genet.* 66, 139-144.
- Paoletti, A.C., Parmely, T.J., Tomomori-Sato, C., Sato, S., Zhu, D., Conaway, R.C., Conaway, J.W., Florens, L., and Washburn, M.P. (2006). Quantitative proteomic analysis of distinct mammalian Mediator complexes using normalized spectral abundance factors. *Proc. Natl. Acad. Sci. U. S. A.* 103, 18928-18933.
- Park, H.R., Ryoo, I.J., Choo, S.J., Hwang, J.H., Kim, J.Y., Cha, M.R., Shin-Ya, K., and Yoo, I.D. (2007). Glucose-deprived HT-29 human colon carcinoma cells are sensitive to verrucosidin as a GRP78 down-regulator. *Toxicology* 229, 253-261.
- Park, W.R., and Nakamura, Y. (2005). p53CSV, a novel p53-inducible gene involved in the p53-dependent cell-survival pathway. *Cancer Res.* 65, 1197-1206.

- Parniak, M.A., and Kalant, N. (1988). Enhancement of glycogen concentrations in primary cultures of rat hepatocytes exposed to glucose and fructose. *Biochem. J.* 251, 795-802.
- Parsons, D.W., Jones, S., Zhang, X., Lin, J.C., Leary, R.J., Angenendt, P., Mankoo, P., Carter, H., Siu, I.M., Gallia, G.L., *et al.* (2008). An integrated genomic analysis of human glioblastoma multiforme. *Science* 321, 1807-1812.
- Pasquini, L., Petrucci, E., Riccioni, R., Petronelli, A., Tesa, U. (2006). Sensitivity and resistance of human cancer cells to TRAIL: mechanisms and therapeutical perspectives. *Cancer Therapy* 4, 47.
- Pastorino, J.G., Shulga, N., and Hoek, J.B. (2002). Mitochondrial binding of hexokinase II inhibits Bax-induced cytochrome c release and apoptosis. *J. Biol. Chem.* 277, 7610-7618.
- Pedersen, P.L., Mathupala, S., Rempel, A., Geschwind, J.F., and Ko, Y.H. (2002). Mitochondrial bound type II hexokinase: a key player in the growth and survival of many cancers and an ideal prospect for therapeutic intervention. *Biochim. Biophys. Acta* 1555, 14-20.
- Pelicano, H., Martin, D.S., Xu, R.H., and Huang, P. (2006). Glycolysis inhibition for anticancer treatment. *Oncogene* 25, 4633-4646.
- Perez-Galan, P., Dreyling, M., and Wiestner, A. (2011). Mantle cell lymphoma: biology, pathogenesis, and the molecular basis of treatment in the genomic era. *Blood* 117, 26-38.
- Peter, M.E., Kischkel, F.C., Hellbardt, S., Chinnaiyan, A.M., Krammer, P.H., and Dixit, V.M. (1996). CD95 (APO-1/Fas)-associating signalling proteins. *Cell Death Differ.* 3, 161-170.
- Peter, M.E., Kischkel, F.C., Scheuerpflug, C.G., Medema, J.P., Debatin, K.M., and Krammer, P.H. (1997). Resistance of cultured peripheral T cells towards activation-induced cell death involves a lack of recruitment of FLICE (MACH/caspase 8) to the CD95 death-inducing signaling complex. *Eur. J. Immunol.* 27, 1207-1212.
- Peter, M.E., and Krammer, P.H. (2003). The CD95(APO-1/Fas) DISC and beyond. *Cell Death Differ.* 10, 26-35.

- Pike, L.S., Smift, A.L., Croteau, N.J., Ferrick, D.A., and Wu, M. (2011). Inhibition of fatty acid oxidation by etomoxir impairs NADPH production and increases reactive oxygen species resulting in ATP depletion and cell death in human glioblastoma cells. *Biochim. Biophys. Acta* 1807, 726-734.
- Pitti, R.M., Marsters, S.A., Ruppert, S., Donahue, C.J., Moore, A., and Ashkenazi, A. (1996). Induction of apoptosis by Apo-2 ligand, a new member of the tumor necrosis factor cytokine family. *J. Biol. Chem.* 271, 12687-12690.
- Pluskal, M.G., Bogdanova, A., Lopez, M., Gutierrez, S., and Pitt, A.M. (2002). Multiwell in-gel protein digestion and microscale sample preparation for protein identification by mass spectrometry. *Proteomics* 2, 145-150.
- Pointon, A.V., Walker, T.M., Phillips, K.M., Luo, J., Riley, J., Zhang, S.D., Parry, J.D., Lyon, J.J., Marczylo, E.L., and Gant, T.W. (2010). Doxorubicin in vivo rapidly alters expression and translation of myocardial electron transport chain genes, leads to ATP loss and caspase 3 activation. *PLoS One* 5, e12733.
- Pomerantz, J.L., and Baltimore, D. (1999). NF-kappaB activation by a signaling complex containing TRAF2, TANK and TBK1, a novel IKK-related kinase. *EMBO J.* 18, 6694-6704.
- Pop, C., and Salvesen, G.S. (2009). Human caspases: activation, specificity, and regulation. *J. Biol. Chem.* 284, 21777-21781.
- Powley, I.R., Kondrashov, A., Young, L.A., Dobbyn, H.C., Hill, K., Cannell, I.G., Stoneley, M., Kong, Y.W., Cotes, J.A., Smith, G.C., *et al.* (2009). Translational reprogramming following UVB irradiation is mediated by DNA-PKcs and allows selective recruitment to the polysomes of mRNAs encoding DNA repair enzymes. *Genes Dev.* 23, 1207-1220.
- Pradelli, L.A., Beneteau, M., Chauvin, C., Jacquin, M.A., Marchetti, S., Munoz-Pinedo, C., Auberger, P., Pende, M., and Ricci, J.E. (2010). Glycolysis inhibition sensitizes tumor cells to death receptors-induced apoptosis by AMP kinase activation leading to Mcl-1 block in translation. *Oncogene* 29, 1641-1652.
- Pradelli, L.A., Beneteau, M., Chauvin, C., Jacquin, M.A., Marchetti, S., Munoz-Pinedo, C., Auberger, P., Pende, M., and Ricci, J.E. (2010). Glycolysis inhibition sensitizes

tumor cells to death receptors-induced apoptosis by AMP kinase activation leading to Mcl-1 block in translation. *Oncogene* 29, 1641-1652.

Pradelli, L.A., Beneteau, M., and Ricci, J.E. (2010). Mitochondrial control of caspase-dependent and -independent cell death. *Cell Mol. Life Sci.* 67, 1589-1597.

PRESCOTT, D.M., and BENDER, M.A. (1962). Synthesis of RNA and protein during mitosis in mammalian tissue culture cells. *Exp. Cell Res.* 26, 260-268.

Presek, P., Reinacher, M., and Eigenbrodt, E. (1988). Pyruvate kinase type M2 is phosphorylated at tyrosine residues in cells transformed by Rous sarcoma virus. *FEBS Lett.* 242, 194-198.

Privette Vinnedge, L.M., McClaine, R., Wagh, P.K., Wikenheiser-Brokamp, K.A., Waltz, S.E., and Wells, S.I. (2011). The human DEK oncogene stimulates beta-catenin signaling, invasion and mammosphere formation in breast cancer. *Oncogene* 30, 2741-2752.

Ramanathan, A., Wang, C., and Schreiber, S.L. (2005). Perturbational profiling of a cell-line model of tumorigenesis by using metabolic measurements. *Proc. Natl. Acad. Sci. U. S. A.* 102, 5992-5997.

Rayasam, G.V., Tulasi, V.K., Sodhi, R., Davis, J.A., and Ray, A. (2009). Glycogen synthase kinase 3: more than a namesake. *Br. J. Pharmacol.* 156, 885-898.

Renatus, M., Stennicke, H.R., Scott, F.L., Liddington, R.C., and Salvesen, G.S. (2001). Dimer formation drives the activation of the cell death protease caspase 9. *Proc. Natl. Acad. Sci. U. S. A.* 98, 14250-14255.

Riedl, S.J., Fuentes-Prior, P., Renatus, M., Kairies, N., Krapp, S., Huber, R., Salvesen, G.S., and Bode, W. (2001). Structural basis for the activation of human procaspase-7. *Proc. Natl. Acad. Sci. U. S. A.* 98, 14790-14795.

Riedl, S.J., and Shi, Y. (2004). Molecular mechanisms of caspase regulation during apoptosis. *Nat. Rev. Mol. Cell Biol.* 5, 897-907.

Rotem, R., Heyfets, A., Fingrut, O., Blickstein, D., Shaklai, M., and Flescher, E. (2005). Jasmonates: novel anticancer agents acting directly and selectively on human cancer cell mitochondria. *Cancer Res.* 65, 1984-1993.

- Rothe, M., Xiong, J., Shu, H.B., Williamson, K., Goddard, A., and Goeddel, D.V. (1996). I-TRAF is a novel TRAF-interacting protein that regulates TRAF-mediated signal transduction. *Proc. Natl. Acad. Sci. U. S. A.* 93, 8241-8246.
- Roue, G., Perez-Galan, P., Lopez-Guerra, M., Villamor, N., Campo, E., and Colomer, D. (2007). Selective inhibition of I κ B kinase sensitizes mantle cell lymphoma B cells to TRAIL by decreasing cellular FLIP level. *J. Immunol.* 178, 1923-1930.
- Rudner, J., Jendrossek, V., Lauber, K., Daniel, P.T., Wesselborg, S., and Belka, C. (2005). Type I and type II reactions in TRAIL-induced apoptosis -- results from dose-response studies. *Oncogene* 24, 130-140.
- Ryoo, H.D., and Baehrecke, E.H. (2010). Distinct death mechanisms in *Drosophila* development. *Curr. Opin. Cell Biol.* 22, 889-895.
- Ryu, S.W., Lee, S.J., Park, M.Y., Jun, J.I., Jung, Y.K., and Kim, E. (2003). Fas-associated factor 1, FAF1, is a member of Fas death-inducing signaling complex. *J. Biol. Chem.* 278, 24003-24010.
- Sallinen, S.L., Sallinen, P.K., Haapasalo, H.K., Helin, H.J., Helen, P.T., Schraml, P., Kallioniemi, O.P., and Kononen, J. (2000). Identification of differentially expressed genes in human gliomas by DNA microarray and tissue chip techniques. *Cancer Res.* 60, 6617-6622.
- Samanta, A.K., Huang, H.J., Bast, R.C., Jr, and Liao, W.S. (2004). Overexpression of MEKK3 confers resistance to apoptosis through activation of NF κ B. *J. Biol. Chem.* 279, 7576-7583.
- Scaffidi, C., Fulda, S., Srinivasan, A., Friesen, C., Li, F., Tomaselli, K.J., Debatin, K.M., Krammer, P.H., and Peter, M.E. (1998). Two CD95 (APO-1/Fas) signaling pathways. *EMBO J.* 17, 1675-1687.
- Scaffidi, C., Medema, J.P., Krammer, P.H., and Peter, M.E. (1997). FLICE is predominantly expressed as two functionally active isoforms, caspase-8/a and caspase-8/b. *J. Biol. Chem.* 272, 26953-26958.
- Scaffidi, C., Schmitz, I., Zha, J., Korsmeyer, S.J., Krammer, P.H., and Peter, M.E. (1999). Differential modulation of apoptosis sensitivity in CD95 type I and type II cells. *J. Biol. Chem.* 274, 22532-22538.

- Schena, M., Shalon, D., Davis, R.W., and Brown, P.O. (1995). Quantitative monitoring of gene expression patterns with a complementary DNA microarray. *Science* 270, 467-470.
- Schena, M., Shalon, D., Heller, R., Chai, A., Brown, P.O., and Davis, R.W. (1996). Parallel human genome analysis: microarray-based expression monitoring of 1000 genes. *Proc. Natl. Acad. Sci. U. S. A.* 93, 10614-10619.
- Schenk, G., Duggleby, R.G., and Nixon, P.F. (1998). Properties and functions of the thiamin diphosphate dependent enzyme transketolase. *Int. J. Biochem. Cell Biol.* 30, 1297-1318.
- Schenk, G., Layfield, R., Candy, J.M., Duggleby, R.G., and Nixon, P.F. (1997). Molecular evolutionary analysis of the thiamine-diphosphate-dependent enzyme, transketolase. *J. Mol. Evol.* 44, 552-572.
- Schlesinger, T.K., Bonvin, C., Jarpe, M.B., Fanger, G.R., Cardinaux, J.R., Johnson, G.L., and Widmann, C. (2002). Apoptosis stimulated by the 91-kDa caspase cleavage MEKK1 fragment requires translocation to soluble cellular compartments. *J. Biol. Chem.* 277, 10283-10291.
- Schneider, C., King, R.M., and Philipson, L. (1988). Genes specifically expressed at growth arrest of mammalian cells. *Cell* 54, 787-793.
- Schug, Z.T., Gonzalez, F., Houtkooper, R.H., Vaz, F.M., and Gottlieb, E. (2011). BID is cleaved by caspase-8 within a native complex on the mitochondrial membrane. *Cell Death Differ.* 18, 538-548.
- Screaton, G.R., Mongkolsapaya, J., Xu, X.N., Cowper, A.E., McMichael, A.J., and Bell, J.I. (1997). TRICK2, a new alternatively spliced receptor that transduces the cytotoxic signal from TRAIL. *Curr. Biol.* 7, 693-696.
- Sedger, L.M., Glaccum, M.B., Schuh, J.C., Kanaly, S.T., Williamson, E., Kayagaki, N., Yun, T., Smolak, P., Le, T., Goodwin, R., and Gliniak, B. (2002). Characterization of the in vivo function of TNF-alpha-related apoptosis-inducing ligand, TRAIL/Apo2L, using TRAIL/Apo2L gene-deficient mice. *Eur. J. Immunol.* 32, 2246-2254.
- Semenza, G.L. (2010). HIF-1: upstream and downstream of cancer metabolism. *Curr. Opin. Genet. Dev.* 20, 51-56.

- Sgorbissa, A., Benetti, R., Marzinotto, S., Schneider, C., and Brancolini, C. (1999). Caspase-3 and caspase-7 but not caspase-6 cleave Gas2 in vitro: implications for microfilament reorganization during apoptosis. *J. Cell. Sci.* 112 (Pt 23), 4475-4482.
- Shaw, R.J. (2006). Glucose metabolism and cancer. *Curr. Opin. Cell Biol.* 18, 598-608.
- Shu, H.B., Takeuchi, M., and Goeddel, D.V. (1996). The tumor necrosis factor receptor 2 signal transducers TRAF2 and c-IAP1 are components of the tumor necrosis factor receptor 1 signaling complex. *Proc. Natl. Acad. Sci. U. S. A.* 93, 13973-13978.
- Skalka, M., Matyasova, J., and Cejkova, M. (1976). Dna in chromatin of irradiated lymphoid tissues degrades in vivo into regular fragments. *FEBS Lett.* 72, 271-274.
- Song, J.H., Tse, M.C., Bellail, A., Phuphanich, S., Khuri, F., Kneteman, N.M., and Hao, C. (2007). Lipid rafts and nonrafts mediate tumor necrosis factor related apoptosis-inducing ligand induced apoptotic and nonapoptotic signals in non small cell lung carcinoma cells. *Cancer Res.* 67, 6946-6955.
- Sprick, M.R., Rieser, E., Stahl, H., Grosse-Wilde, A., Weigand, M.A., and Walczak, H. (2002). Caspase-10 is recruited to and activated at the native TRAIL and CD95 death-inducing signalling complexes in a FADD-dependent manner but can not functionally substitute caspase-8. *EMBO J.* 21, 4520-4530.
- Sprick, M.R., Weigand, M.A., Rieser, E., Rauch, C.T., Juo, P., Blenis, J., Krammer, P.H., and Walczak, H. (2000). FADD/MORT1 and caspase-8 are recruited to TRAIL receptors 1 and 2 and are essential for apoptosis mediated by TRAIL receptor 2. *Immunity* 12, 599-609.
- Spriggs, K.A., Bushell, M., and Willis, A.E. (2010). Translational regulation of gene expression during conditions of cell stress. *Mol. Cell* 40, 228-237.
- Stadel, D., Mohr, A., Ref, C., MacFarlane, M., Zhou, S., Humphreys, R., Bachem, M., Cohen, G., Moller, P., Zwacka, R.M., Debatin, K.M., and Fulda, S. (2010). TRAIL-induced apoptosis is preferentially mediated via TRAIL receptor 1 in pancreatic carcinoma cells and profoundly enhanced by XIAP inhibitors. *Clin. Cancer Res.* 16, 5734-5749.
- Stalheim, L., and Johnson, G. (2007). MAPK kinase kinase regulation of SAPK/JNK pathway. *Topics in Current Genetics* 20,

- Stennicke, H.R., Renatus, M., Meldal, M., and Salvesen, G.S. (2000). Internally quenched fluorescent peptide substrates disclose the subsite preferences of human caspases 1, 3, 6, 7 and 8. *Biochem. J.* 350 Pt 2, 563-568.
- Sugden, M.C., and Holness, M.J. (1994). Interactive regulation of the pyruvate dehydrogenase complex and the carnitine palmitoyltransferase system. *FASEB J.* 8, 54-61.
- Sulston, J.E., and Horvitz, H.R. (1977). Post-embryonic cell lineages of the nematode, *Caenorhabditis elegans*. *Dev. Biol.* 56, 110-156.
- Sulston, J.E., Schierenberg, E., White, J.G., and Thomson, J.N. (1983). The embryonic cell lineage of the nematode *Caenorhabditis elegans*. *Dev. Biol.* 100, 64-119.
- Sun, X.J., Wang, L.M., Zhang, Y., Yenush, L., Myers, M.G., Jr, Glasheen, E., Lane, W.S., Pierce, J.H., and White, M.F. (1995). Role of IRS-2 in insulin and cytokine signalling. *Nature* 377, 173-177.
- Sun, X.M., MacFarlane, M., Zhuang, J., Wolf, B.B., Green, D.R., and Cohen, G.M. (1999). Distinct caspase cascades are initiated in receptor-mediated and chemical-induced apoptosis. *J. Biol. Chem.* 274, 5053-5060.
- Takeda, K., Smyth, M.J., Cretney, E., Hayakawa, Y., Kayagaki, N., Yagita, H., and Okumura, K. (2002). Critical role for tumor necrosis factor-related apoptosis-inducing ligand in immune surveillance against tumor development. *J. Exp. Med.* 195, 161-169.
- Talanian, R.V., Quinlan, C., Trautz, S., Hackett, M.C., Mankovich, J.A., Banach, D., Ghayur, T., Brady, K.D., and Wong, W.W. (1997). Substrate specificities of caspase family proteases. *J. Biol. Chem.* 272, 9677-9682.
- Taylor, R.C., Cullen, S.P., and Martin, S.J. (2008). Apoptosis: controlled demolition at the cellular level. *Nat. Rev. Mol. Cell Biol.* 9, 231-241.
- Tennant, D.A., Duran, R.V., Boulahbel, H., and Gottlieb, E. (2009). Metabolic transformation in cancer. *Carcinogenesis* 30, 1269-1280.
- Testa, U. (2010). TRAIL/TRAIL-R in hematologic malignancies. *J. Cell. Biochem.* 110, 21-34.

- Thakkar, N.S., and Potten, C.S. (1993). Inhibition of doxorubicin-induced apoptosis in vivo by 2-deoxy-D-glucose. *Cancer Res.* 53, 2057-2060.
- Thelander, E.F., and Rosenquist, R. (2008). Molecular genetic characterization reveals new subsets of mantle cell lymphoma. *Leuk. Lymphoma* 49, 1042-1049.
- Thomas, L.R., Johnson, R.L., Reed, J.C., and Thorburn, A. (2004). The C-terminal tails of tumor necrosis factor-related apoptosis-inducing ligand (TRAIL) and Fas receptors have opposing functions in Fas-associated death domain (FADD) recruitment and can regulate agonist-specific mechanisms of receptor activation. *J. Biol. Chem.* 279, 52479-52486.
- Thornberry, N.A., Bull, H.G., Calaycay, J.R., Chapman, K.T., Howard, A.D., Kostura, M.J., Miller, D.K., Molineaux, S.M., Weidner, J.R., and Aunins, J. (1992). A novel heterodimeric cysteine protease is required for interleukin-1 beta processing in monocytes. *Nature* 356, 768-774.
- Thornberry, N.A., Rano, T.A., Peterson, E.P., Rasper, D.M., Timkey, T., Garcia-Calvo, M., Houtzager, V.M., Nordstrom, P.A., Roy, S., Vaillancourt, J.P., Chapman, K.T., and Nicholson, D.W. (1997). A combinatorial approach defines specificities of members of the caspase family and granzyme B. Functional relationships established for key mediators of apoptosis. *J. Biol. Chem.* 272, 17907-17911.
- Thorstensen, K., and Romslo, I. (1990). The role of transferrin in the mechanism of cellular iron uptake. *Biochem. J.* 271, 1-9.
- Tournier, C., Hess, P., Yang, D.D., Xu, J., Turner, T.K., Nimnual, A., Bar-Sagi, D., Jones, S.N., Flavell, R.A., and Davis, R.J. (2000). Requirement of JNK for stress-induced activation of the cytochrome c-mediated death pathway. *Science* 288, 870-874.
- Touzeau, C., Dousset, C., Bodet, L., Gomez-Bougie, P., Bonnaud, S., Moreau, A., Moreau, P., Pellat-Deceunynk, C., Amiot, M., and Le Gouill, S. (2011). ABT-737 Induces Apoptosis in Mantle Cell Lymphoma Cells with a Bcl-2high/Mcl-1low Profile and Synergizes with Other Antineoplastic Agents. *Clin. Cancer Res.* 17, 5973-5981.
- Tsujimoto, Y., Finger, L.R., Yunis, J., Nowell, P.C., and Croce, C.M. (1984). Cloning of the chromosome breakpoint of neoplastic B cells with the t(14;18) chromosome translocation. *Science* 226, 1097-1099.

- Tucker, C.A., Kapanen, A.I., Chikh, G., Hoffman, B.G., Kyle, A.H., Wilson, I.M., Masin, D., Gascoyne, R.D., Bally, M., and Klasa, R.J. (2008). Silencing Bcl-2 in models of mantle cell lymphoma is associated with decreases in cyclin D1, nuclear factor-kappaB, p53, bax, and p27 levels. *Mol. Cancer. Ther.* 7, 749-758.
- Twiddy, D., Brown, D.G., Adrain, C., Jukes, R., Martin, S.J., Cohen, G.M., MacFarlane, M., and Cain, K. (2004). Pro-apoptotic proteins released from the mitochondria regulate the protein composition and caspase-processing activity of the native Apaf-1/caspase-9 apoptosome complex. *J. Biol. Chem.* 279, 19665-19682.
- Van Cruchten, S., and Van Den Broeck, W. (2002). Morphological and biochemical aspects of apoptosis, oncosis and necrosis. *Anat. Histol. Embryol.* 31, 214-223.
- Varfolomeev, E., Maecker, H., Sharp, D., Lawrence, D., Renz, M., Vucic, D., and Ashkenazi, A. (2005). Molecular determinants of kinase pathway activation by Apo2 ligand/tumor necrosis factor-related apoptosis-inducing ligand. *J. Biol. Chem.* 280, 40599-40608.
- Vaux, D.L., Cory, S., and Adams, J.M. (1988). Bcl-2 gene promotes haemopoietic cell survival and cooperates with c-myc to immortalize pre-B cells. *Nature* 335, 440-442.
- Villunger, A., Huang, D.C., Holler, N., Tschopp, J., and Strasser, A. (2000). Fas ligand-induced c-Jun kinase activation in lymphoid cells requires extensive receptor aggregation but is independent of DAXX, and Fas-mediated cell death does not involve DAXX, RIP, or RAIDD. *J. Immunol.* 165, 1337-1343.
- Vitovski, S., Phillips, J.S., Sayers, J., and Croucher, P.I. (2007). Investigating the interaction between osteoprotegerin and receptor activator of NF-kappaB or tumor necrosis factor-related apoptosis-inducing ligand: evidence for a pivotal role for osteoprotegerin in regulating two distinct pathways. *J. Biol. Chem.* 282, 31601-31609.
- Vivanco, I., and Sawyers, C.L. (2002). The phosphatidylinositol 3-Kinase AKT pathway in human cancer. *Nat. Rev. Cancer.* 2, 489-501.
- Vogelstein, B., Kinzler, K.W. (2002). *The genetic basis of human cancer (USA: The McGraw-Hill Companies).*
- Vogelstein, B., Lane, D., and Levine, A.J. (2000). Surfing the p53 network. *Nature* 408, 307-310.

- Vousden, K.H. (2005). Apoptosis. p53 and PUMA: a deadly duo. *Science* 309, 1685-1686.
- Vousden, K.H. (2002). Activation of the p53 tumor suppressor protein. *Biochim. Biophys. Acta* 1602, 47-59.
- Wagner, K.W., Punnoose, E.A., Januario, T., Lawrence, D.A., Pitti, R.M., Lancaster, K., Lee, D., von Goetz, M., Yee, S.F., Totpal, K., *et al.* (2007). Death-receptor O-glycosylation controls tumor-cell sensitivity to the proapoptotic ligand Apo2L/TRAIL. *Nat. Med.* 13, 1070-1077.
- Walczak, H., and Haas, T.L. (2008). Biochemical analysis of the native TRAIL death-inducing signaling complex. *Methods Mol. Biol.* 414, 221-239.
- Walczak, H., Miller, R.E., Ariail, K., Gliniak, B., Griffith, T.S., Kubin, M., Chin, W., Jones, J., Woodward, A., Le, T., *et al.* (1999). Tumoricidal activity of tumor necrosis factor-related apoptosis-inducing ligand in vivo. *Nat. Med.* 5, 157-163.
- Wang, J., and Pantopoulos, K. (2011). Regulation of cellular iron metabolism. *Biochem. J.* 434, 365-381.
- Wang, J., Zheng, L., Lobito, A., Chan, F.K., Dale, J., Sneller, M., Yao, X., Puck, J.M., Straus, S.E., and Lenardo, M.J. (1999). Inherited human Caspase 10 mutations underlie defective lymphocyte and dendritic cell apoptosis in autoimmune lymphoproliferative syndrome type II. *Cell* 98, 47-58.
- Wang, L., McDonnell, S.K., Hebring, S.J., Cunningham, J.M., St Sauver, J., Cerhan, J.R., Isaya, G., Schaid, D.J., and Thibodeau, S.N. (2008). Polymorphisms in mitochondrial genes and prostate cancer risk. *Cancer Epidemiol. Biomarkers Prev.* 17, 3558-3566.
- Wang, S., and El-Deiry, W.S. (2003). TRAIL and apoptosis induction by TNF-family death receptors. *Oncogene* 22, 8628-8633.
- Warburg, O. (1956). On the origin of cancer cells. *Science* 123, 309-314.
- Warburg, O., Wind, F., and Negelein, E. (1927). The Metabolism of Tumors in the Body. *J. Gen. Physiol.* 8, 519-530.

- WARNER, J., MADDEN, M.J., and DARNELL, J.E. (1963). The interaction of poliovirus RNA with *Escherichia coli* ribosomes. *Virology* 19, 393-399.
- Weber, W.A., Ziegler, S.I., Thodtman, R., Hanauske, A.R., and Schwaiger, M. (1999). Reproducibility of metabolic measurements in malignant tumors using FDG PET. *J. Nucl. Med.* 40, 1771-1777.
- Wei, M.C., Zong, W.X., Cheng, E.H., Lindsten, T., Panoutsakopoulou, V., Ross, A.J., Roth, K.A., MacGregor, G.R., Thompson, C.B., and Korsmeyer, S.J. (2001). Proapoptotic BAX and BAK: a requisite gateway to mitochondrial dysfunction and death. *Science* 292, 727-730.
- Weston, C.R., and Davis, R.J. (2007). The JNK signal transduction pathway. *Curr. Opin. Cell Biol.* 19, 142-149.
- Whitehouse, D.B., Tomkins, J., Lovegrove, J.U., Hopkinson, D.A., and McMillan, W.O. (1998). A phylogenetic approach to the identification of phosphoglucosyltransferase genes. *Mol. Biol. Evol.* 15, 456-462.
- WHO. (2008). Fight against cancer - strategies that prevent, cure and care.
- Wiley, S.R., Schooley, K., Smolak, P.J., Din, W.S., Huang, C.P., Nicholl, J.K., Sutherland, G.R., Smith, T.D., Rauch, C., and Smith, C.A. (1995). Identification and characterization of a new member of the TNF family that induces apoptosis. *Immunity* 3, 673-682.
- Wiley, S.R., Schooley, K., Smolak, P.J., Din, W.S., Huang, C.P., Nicholl, J.K., Sutherland, G.R., Smith, T.D., Rauch, C., and Smith, C.A. (1995). Identification and characterization of a new member of the TNF family that induces apoptosis. *Immunity* 3, 673-682.
- Williams, Me., Connors, JM., Dreyling, MH., et al. (2011). Mantle cell lymphoma: report of the 2010 mantle cell lymphoma consortium workshop. *Leukemia and Lymphoma* 52, 24.
- Wilson, J.E. (2003). Isozymes of mammalian hexokinase: structure, subcellular localization and metabolic function. *J. Exp. Biol.* 206, 2049-2057.

- Wilson, K.P., Black, J.A., Thomson, J.A., Kim, E.E., Griffith, J.P., Navia, M.A., Murcko, M.A., Chambers, S.P., Aldape, R.A., and Raybuck, S.A. (1994). Structure and mechanism of interleukin-1 beta converting enzyme. *Nature* 370, 270-275.
- Wilson, W.R., and Hay, M.P. (2011). Targeting hypoxia in cancer therapy. *Nat. Rev. Cancer*. 11, 393-410.
- Wood, T.E., Dalili, S., Simpson, C.D., Hurren, R., Mao, X., Saiz, F.S., Gronda, M., Eberhard, Y., Minden, M.D., Bilan, P.J., *et al.* (2008). A novel inhibitor of glucose uptake sensitizes cells to FAS-induced cell death. *Mol. Cancer. Ther.* 7, 3546-3555.
- Wu, G.S., Burns, T.F., Zhan, Y., Alnemri, E.S., and El-Deiry, W.S. (1999). Molecular cloning and functional analysis of the mouse homologue of the KILLER/DR5 tumor necrosis factor-related apoptosis-inducing ligand (TRAIL) death receptor. *Cancer Res.* 59, 2770-2775.
- Wu, M., Neilson, A., Swift, A.L., Moran, R., Tamagnine, J., Parslow, D., Armistead, S., Lemire, K., Orrell, J., Teich, J., Chomicz, S., and Ferrick, D.A. (2007). Multiparameter metabolic analysis reveals a close link between attenuated mitochondrial bioenergetic function and enhanced glycolysis dependency in human tumor cells. *Am. J. Physiol. Cell. Physiol.* 292, C125-36.
- Xiao, L., Gong, L.L., Yuan, D., Deng, M., Zeng, X.M., Chen, L.L., Zhang, L., Yan, Q., Liu, J.P., Hu, X.H., *et al.* (2010). Protein phosphatase-1 regulates Akt1 signal transduction pathway to control gene expression, cell survival and differentiation. *Cell Death Differ.* 17, 1448-1462.
- Yamada, K., and Noguchi, T. (1999). Nutrient and hormonal regulation of pyruvate kinase gene expression. *Biochem. J.* 337 (Pt 1), 1-11.
- Yan, N., and Shi, Y. (2005). Mechanisms of apoptosis through structural biology. *Annu. Rev. Cell Dev. Biol.* 21, 35-56.
- Yang, J., Li, J.H., Wang, J., and Zhang, C.Y. (2010). Molecular modeling of BAD complex resided in a mitochondrion integrating glycolysis and apoptosis. *J. Theor. Biol.* 266, 231-241.

- Yang, J., Lin, Y., Guo, Z., Cheng, J., Huang, J., Deng, L., Liao, W., Chen, Z., Liu, Z., and Su, B. (2001). The essential role of MEKK3 in TNF-induced NF-kappaB activation. *Nat. Immunol.* 2, 620-624.
- Yang, L., Liu, X., Hao, J., Yang, Y., Zhao, M., Zuo, J., and Liu, W. (2008). Glucose-regulated protein 75 suppresses apoptosis induced by glucose deprivation in PC12 cells through inhibition of Bax conformational change. *Acta Biochim. Biophys. Sin. (Shanghai)* 40, 339-348.
- Yang, X., Khosravi-Far, R., Chang, H.Y., and Baltimore, D. (1997). Daxx, a novel Fas-binding protein that activates JNK and apoptosis. *Cell* 89, 1067-1076.
- Yen, K.E., Bittinger, M.A., Su, S.M., and Fantin, V.R. (2010). Cancer-associated IDH mutations: biomarker and therapeutic opportunities. *Oncogene* 29, 6409-6417.
- Yuan, J., Shaham, S., Ledoux, S., Ellis, H.M., and Horvitz, H.R. (1993). The *C. elegans* cell death gene *ced-3* encodes a protein similar to mammalian interleukin-1 beta-converting enzyme. *Cell* 75, 641-652.
- Zamaraeva, M.V., Sabirov, R.Z., Maeno, E., Ando-Akatsuka, Y., Bessonova, S.V., and Okada, Y. (2005). Cells die with increased cytosolic ATP during apoptosis: a bioluminescence study with intracellular luciferase. *Cell Death Differ.* 12, 1390-1397.
- Zhang, H., Bosch-Marce, M., Shimoda, L.A., Tan, Y.S., Baek, J.H., Wesley, J.B., Gonzalez, F.J., and Semenza, G.L. (2008). Mitochondrial autophagy is an HIF-1-dependent adaptive metabolic response to hypoxia. *J. Biol. Chem.* 283, 10892-10903.
- Zhang, K., and Kaufman, R.J. (2004). Signaling the unfolded protein response from the endoplasmic reticulum. *J. Biol. Chem.* 279, 25935-25938.
- Zhang, L., and Fang, B. (2005). Mechanisms of resistance to TRAIL-induced apoptosis in cancer. *Cancer Gene Ther.* 12, 228-237.
- Zybailov, B., Mosley, A.L., Sardi, M.E., Coleman, M.K., Florens, L., and Washburn, M.P. (2006). Statistical analysis of membrane proteome expression changes in *Saccharomyces cerevisiae*. *J. Proteome Res.* 5, 2339-2347.